Validation of First Pass Magnetic Resonance Myocardial Perfusion Imaging using Fractional Flow Reserve

Dr Stuart Watkins

B.Sc (Med Sci) (Hons), MB ChB, MRCP(UK)

A thesis submitted for the degree of

Doctor of Medicine (MD)

University of Glasgow

Division of Cardiovascular and Medical Sciences

May 2009

Dedication

In memory of Leander Watkins (1917-2009), a thoughtful caring man and wonderful Papa who is sadly missed.

Acknowledgements

I am greatly indebted to Dr Keith Oldroyd, my supervisor for his encouragement, support, patience and teaching in the techniques of percutaneous coronary intervention. Keith provided multiple ideas for this study and without his enthusiasm and assistance this project would not have been started and certainly not completed. I am also greatly indebted to Professor Henry Dargie, my joint supervisor, for his help in the planning of this study, support and encouragement throughout. I am grateful to my advisor of studies Professor Stewart Hillis for his continued support throughout. I thank Dr Mitchell Lindsay and Dr Stephen Robb at the Western Infirmary for their encouragement to get this written and assistance at times in the cardiac catheterisation laboratory. I thank Professor Ian Ford and Dr Vladimir Beslyak for their help and advice with the statistical analysis of the huge amounts of data generated by this research. I am grateful to Dr Jonathan Lyne (Royal Brompton Hospital, London) and Dr Ross McGeoch (Western Infirmary, Glasgow) for their help in acting as second observers in the analysis of the MRI data. I am grateful to Mr Tony Cunningham for acting as a second observer in the analysis of the QCA data. I thank Miss Tracy Steedman for her help with the MRI scanning in this study and for her support throughout this research. I thank Dr Murdoch Norton (University of Aberdeen) for his teachings in the physics of quantifying myocardial perfusion, for developing the program used in the analysis of this study and also for acting as a second observer in the MPRI analysis. Murdoch has always been there for support on the analysis of MPRI and for multiple troubleshooting scenarios where my knowledge of computer programming let me down. I thank Mr Mark Hawthorne for ensuring we had plenty of pressure wires on the shelf and for sponsoring me to attend a pressure wire course prior to commencing this project. I thank Miss Jennifer Weightman of GE Healthcare for teaching me how to perform quantitative coronary angiography and for her support throughout this research.

I am grateful for Dr Stephen Frohwein and his staff at St Joseph's Hospital, Atlanta for teaching me whole body MRI scanning, including the heart. I thank Professor Dudley Pennell, Professor David Firmin, Dr Peter Gatehouse and Mrs Gillian Smith at the Royal Brompton Hospital, London for allowing me to visit regularly, for scanner troubleshooting and for teaching me the technique of perfusion MRI. I am indebted to my patients who attended for their scans, abstained from caffeine and held their breath for prolonged periods as I made them feel unwell with an adenosine infusion. I thank the staff of the cardiac catheterisation laboratories of the Western Infirmary and the Golden Jubilee National Hospital for their patience and staying late during the prolonged procedures as a result of this study. I am grateful to Mr Jim Christie for his help in designing a database to cope with the huge amounts of data collected. I am indebted to my parents Ian and Janice, my sister Lyndsay and my grandpa Leander for their encouragement to get this thesis finished and their support in my prolonged absence whilst writing this. I am grateful to the McLaughlin family for their support during this research. I thank my close friends for their patience while I have neglected them during the writing up of this research (Christophe & Stephanie Criaud, Colin Hunter, Zenya Kandyba, Ross & Judi McMath, Frankie Craig, Mike & Annette Love, Colin Fraser and members of the Royal Troon Young Team). I am grateful to my SpR colleagues especially Gillian Marshall and Margaret McEnteggart for their advice during the writing up of this research. I would also like to thank my long suffering fiancé who has had to put up with my absence from normal domestic functions, holidays, weekends and numerous social occasions while I have conducted this research. Mairi-Jean has helped with data analysis, reading of drafts and above all has kept me sane over the past couple of years when balancing a busy clinical job with writing a thesis was getting increasingly difficult. Finally I would like to thank the British Heart Foundation for funding this research.

Contents

List Of Figures

List of Tables

Publications Arising From Research

Papers

First Pass Myocardial Perfusion Magnetic Resonance Imaging (MPMRI) – A New Era in the Diagnosis of Reversible Myocardial Ischaemia

Stuart Watkins, Keith G. Oldroyd, Stephen Frohwein

Heart 2007;93(1):7-10

Papers directly related to this research are currently being peer reviewed by journals.

Abstracts

Magnetic Resonance Myocardial Perfusion Imaging (MRMPI) in Patients With Chest Pain – A Validation Study With Fractional Flow Reserve (FFR)

Stuart Watkins, Tracey Steedman, Jonathan Lyne, Ross J. McGeoch, Ian Ford, John Foster, Henry J. Dargie, Keith G. Oldroyd

Journal of the American College of Cardiology 2008; 51(10) Supp A: A161

Magnetic Resonance Myocardial Perfusion Imaging (MPMRI) for the Detection of Myocardial Ischaemia as Determined by Pressure Wire Derived Fractional Flow Reserve (FFR)

Stuart Watkins, Tracey Steedman, Jonathan Lyne, Ian Ford, John Foster, Henry J. Dargie, Keith G. Oldroyd

Scottish Medical Journal 2008; 53(2):56

Can False Positive and Negative First Pass Myocardial Perfusion MRI Scans be Explained by Coronary Physiological Measurements?

Stuart Watkins, Tracey Steedman, Jonathan Lyne, John Foster, Bjoern Groenning, Ian Ford, Henry J. Dargie, Keith G. Oldroyd

Heart 2007; 93:A21

Myocardial Perfusion Magnetic Resonance Imaging (MRI) for the Detection of Myocardial Ischaemia as Determined by Pressure Wire Derived Fractional Flow Reserve (FFR)

Stuart Watkins, Tracey Steedman, Jonathan Lyne, Stephen Frohwein, John Foster, Bjoern Groenning, Ian Ford, Henry J. Dargie, Keith G. Oldroyd

Heart 2006; 92(Supp 2):A102

First Pass Myocardial Perfusion Magnetic Resonance Imaging (MRI) for the Detection of Myocardial Ischaemia as Determined by Invasive Coronary Pressure Measurement – Fractional Flow Reserve (FFR)

Stuart Watkins, Tracey Steedman, Jonathan Lyne, Stephen Frohwein, John Foster, Bjoern Groenning, Ian Ford, Henry J. Dargie, Keith G. Oldroyd

Journal of Cardiovascular Magnetic Resonance 2006; 8(1):38

Can First Pass Myocardial Perfusion Magnetic Resonance Imaging be Used to Detect Isolated Microvascular Dysfunction?

Stuart Watkins, Tracey Steedman, Jonathan Lyne, John Foster, Bjoern Groenning, Ian Ford, Henry J. Dargie, Keith G. Oldroyd

European Heart Journal 2006, Vol. 27 (Abstract Supplement)

"One Stop" Cardiac Magnetic Resonance Imaging (CMR)

S. Watkins, T. Steedman, S. Frohwein, J. Foster, B. Groenning, I. Ford, H.J. Dargie, K.G. Oldroyd

Catheterization and Cardiovascular Interventions 2005; 65(1):150

Abbreviations

AHA – American Heart Association

AIF – Arterial Input Function

ATP – Adenosine Triphosphate

CABG – Coronary Artery Bypass Grafting

CAD – Coronary Artery Disease

CCS – Canadian Cardiovascular Study

CHD – Coronary Heart Disease

CFI –Collateral Flow Index

CFR – Coronary Flow Reserve

CFVR – Coronary Flow Velocity Reserve

CK – Creatine Kinase

CMRI – Cardiac Magnetic Resonance Imaging

CTA – Computerised Tomographic Angiography

CTO – Chronic Total Occlusion

D1 – 1st Diagonal Coronary Artery

DBP – Diastolic Blood Pressure

DF – Degrees of Freedom

DS – Diameter Stenosis

DSE – Dobutamine Stress Echocardiography

ECG – Electrocardiogram

EF – Ejection Fraction

EPI – Echo Planar Imaging

ETT – Exercise Tolerance Test

FFR – Fractional Flow Reserve

FFRmyo – Myocardial Fractional Flow Reserve

FLASH – Fast Low Angled Shot

GE – General Electric

IM – Intermediate Coronary Artery or Ramus

IMR – Index of Microcirculatory Resistance

IMRcorr – Corrected Index of Microcirculatory Resistance

IMRuncorr – Uncorrected Index of Microcirculatory Resistance

IVUS – Intravascular Ultrasound Examination

LAD – Left Anterior Descending Coronary Artery

LCx – Left Circumflex Coronary Artery

LGE – Late Gadolinium Enhancement

LPDA – Left Posterior Descending Coronary Artery

LV – Left Ventricle

LVEF – Left Ventricular Ejection Fraction

LVESV – Left Ventricular End Systolic Volume

MCE – Myocardial Contrast Echocardiography

MCE – Maximum Contrast Enhancement

MI – Myocardial Infarction

MPR – Myocardial Perfusion Reserve

MPRI – Myocardial Perfusion Reserve Index

MRI – Magnetic Resonance Imaging

MRMPI – Magnetic Resonance Myocardial Perfusion Imaging

MSCT – Multi-slice Computerised Tomography

MTT – Mean Transit Time

NSF – Nephrogenic Systemic Fibrosis

OM – Obtuse Marginal Coronary Artery

Pa – Aortic Pressure

PCI – Percutaneous Coronary Intervention

Pd – Distal Coronary Pressure

PET – Positron Emission Tomography

POBA – Plain Old Balloon Angioplasty

Pw – Coronary Wedge Pressure

QCA – Quantitative Coronary Angiography

Qcorr – Surrogate of Coronary Flow (1/Tmn)

RCA – Right Coronary Artery

R.micro – Microvascular Resistance

ROC – Receiver Operator Curves

RV – Right Ventricle

SBP – Systolic Blood Pressure

SD – Standard Deviation

SENSE – Sensitivity Encoding

SNR – Signal to Noise Ratio

SPECT – Single Photon Emission Computed Tomography

TE – Time to Echo

TGE – Turbo Gradient Echo

TIMI – Thrombolysis in Myocardial Infarction

TMPG – TIMI Myocardial Perfusion Grade

Tmn – Mean Transit Time

TMR – True Microcirculatory Resistance

TR – Repetition Time

Abstract of Thesis

Background

Magnetic Resonance Myocardial Perfusion Imaging (MRMPI) has been used for the detection of reversible myocardial ischaemia in humans since the early 1990's. This non-invasive method of diagnosing reversible myocardial ischaemia has a number of advantages over the other more commonly used non-invasive tests such as ETT, stress echocardiography and radionuclide single photon emission computerised tomography (SPECT). There is no need to perform physical exercise, no image orientation constraints, excellent spatial and temporal resolution, no photon scatter or attenuation artefacts and no exposure to ionising radiation. The use of MRMPI for the detection of reversible myocardial ischaemia has been extensively investigated in the past using other non-invasive tests as the gold standard namely PET and SPECT. Invasive comparisons have been made with visual coronary angiography and quantitative coronary angiography (QCA). This previous work has been summarised in a meta-analysis which estimated the sensitivity and specificity to be 84% and 85% respectively.(1) The majority of previous studies have used QCA or visual estimation of stenosis severity to determine the diameter of stenosis (DS). This however has been shown to correlate poorly with the functional significance of disease within a coronary artery.(2;3) Prior to the commencement of this study no comparison had been made with the invasive gold standard of FFR. This is measured using a coronary pressure wire at the time of coronary angiography and is regarded by many cardiologists to be the current invasive gold standard for determining if coronary artery disease (CAD) is physiologically significant. We therefore undertook the present study to determine the true accuracy of MRMPI for the diagnosis of physiologically significant CAD. We also assessed the ability of MRMPI to detect isolated microcirculatory disease as determined by thermodilution derived CFR. Our other aims included an analysis of troponin release

following PCI and its relation to QCA, pressure wire data and the occurrence of new late gadolinium enhancement (LGE). New LGE post CABG was also quantified and compared with that encountered post-PCI.

Methods

One hundred and three patients with chest pain were referred for coronary angiography and underwent MRMPI in the week prior to the angiogram. This was performed on a Siemens Sonata 1.5Tesla scanner (Erlangen, Germany). Scanning commenced with localisers and cine long and short axis scans (TrueFISP sequence) to provide left ventricular mass, volume and ejection fraction data. This was followed by perfusion imaging of 3 short axis slices using a turboFLASH sequence (TI 90ms, TE 0.99ms, TR 173ms, Flip Angle 8^{o}, Matrix 80 x 128). Thereafter long and short axis slices were acquired for the detection of LGE (turboFLASH). Maximal hyperaemia was achieved using intravenous adenosine (140μg/kg/min). The first pass bolus contained 0.1mmol/kg of gadolinium (Omniscan, Amersham Health, Oslo, Norway) power injected at 5ml/sec (Medrad, Pittsburgh, PA) followed by a 20ml saline bolus. Twenty minutes after the initial bolus of gadolinium a further bolus was administered to obtain rest perfusion images. During coronary angiography the FFR was recorded in all patent major epicardial coronary arteries using a coronary pressure wire (RADI Medical Systems Ltd, Uppsala, Sweden) with hyperaemia induced using intravenous adenosine as above. An FFR value of <0.75 was taken as the cut off for the diagnosis of significant CAD. CFR measurements were obtained at rest and during maximal hyperaemia by means of thermodilution using 3ml boluses of saline. Following coronary angiography those patients who underwent PCI returned for a repeat MRMPI scan at 24 hours and 4 weeks and CABG patients returned for a 4 week scan. PCI patients had a troponin I measurement performed at approximately 24 hours, just prior to their repeat MRMPI.

Qualitative MRMPI analysis, left ventricular mass, volume and ejection fraction analysis and QCA were all performed by two blinded independent experienced observers.

Results

Of the 103 enrolled patients, two were excluded from the final analysis. Seventy-six (74%) were male with a mean age of 60 years (SD = 9). 25 (24.8%) of 101 scans were normal, 40 (39.6%) had single-vessel disease, 26 (25.7%) had two-vessel disease and 10 (9.9%) had triple-vessel disease. 121 perfusion defects were reported in 300 coronary territories (3 patients had complete data for only 2 coronary territories) of which 110 had an FFR<0.75. 168 of 179 normally perfused territories were confirmed normal with an FFR≥0.75. The sensitivity, specificity, PPV and NPV of MRMPI for the detection of significant CAD were 91, 94, 91 and 94%. Cohen's kappa was 0.97 per patient and 0.76 per coronary territory indicating excellent and substantial agreement between observers. Twenty-eight coronary arteries were identified as having an FFR>0.8 and a CFR<2.0 indicative of isolated microcirculatory disease with no physiologically significant epicardial disease. No coronary territories were found to have a perfusion defect on MRMPI suggesting that by visual analysis MRMPI is unable to detect isolated microvascular disease. The median post PCI troponin level was 0.57µg/L (SD=2, Range undetected - 13.1). The only parameters found to correlate with troponin I levels post-PCI were increasing lesion length ($r=0.6$, $p<0.0001$) and increasing total stent length ($r=0.37$, $p=0.02$). We compared the increase in mass of LGE between the post-PCI scans and the pre-PCI scan and compared this with the troponin measurement. No significant correlation was found to exist between these parameters at 24 hours ($r=0.25$, $p=0.07$) or at 4 weeks ($r=-0.19$, $p=0.2$). The change in mass of LGE was calculated for the PCI and CABG patients. The mean difference in the PCI group was -0.12g

(Median=0, SD=0.8, Interquartile Range 0 – 0) and for the CABG group was 1.08g (Median=0.11, SD=2.3, Interquartile Range -0.11 – 1.38). There is a trend towards the development of more LGE following CABG than PCI however the difference between groups did not reach statistical significance (p=0.07).

Conclusion

MRMPI can accurately detect significant CHD with excellent results using FFR as the gold standard. Interobserver agreement is also very good even when examining individual coronary artery territories. Qualitative analysis of MRMPI is unable to detect isolated microcirculatory disease as defined by an FFR>0.8 and a CFR<2.0. Small troponin releases are common post-PCI and are related to the length of the lesion being treated and the length of stent deployed to treat the lesion. These small troponin releases do not accurately correlate with the occurrence of new LGE. CABG did result in a trend towards more new LGE compared to PCI.

1 Introduction

1.1 Background

Coronary heart disease (CHD) remains one of the leading causes of death in Europe and is especially prevalent in Scotland.(4) This is despite recent reductions in the incidence of acute MI. Between December 2005 and 2006 the incidence of patients diagnosed with CHD standardised by age and sex decreased by 8.4%, however remains high at 307.5 cases per 100,000 of the population.(4) The treatment of CHD and its consequences consumes the largest proportion of our healthcare budget here in the UK compared to other European countries.(5) CHD presents most commonly as either a MI or angina pectoris and is due to coronary atherosclerosis. Atherosclerotic plaques develop in the coronary arteries over many years and are present in the arteries of the majority of Western adults. Once a plaque reduces the luminal diameter by greater than 70%, blood flow to the myocardium can be reduced by such an extent to cause angina pectoris, depending on the site of the narrowing. Coronary artery plaques can rupture causing ulceration and thrombosis, which can lead to occlusion of the vessel and the subsequent development of a MI. Risk factors such as cigarette smoking, hypertension, diabetes, diet and genetics affect the progression of these atherosclerotic plaques.

The routine diagnosis of coronary artery disease at this time involves a combination of tests including: electrocardiography (ECG); ETT; myocardial perfusion imaging using single photon emission computed tomography (SPECT) and a study of the coronary artery anatomy by coronary angiography. PET is available in a few centres in the UK and is regarded by many to be the current non-invasive gold standard test for the diagnosis of significant coronary artery disease. Stress echocardiography is being performed in many centres with a specialist interest in echo imaging. Multislice

computerised tomography imaging (MSCT) is rapidly being developed and is also being utilised to a certain extent by some centres in the UK. Each of these techniques has its limitations such as false positive and false negative results and the exposure of patients to ionizing radiation. In patients with chest pain and a narrowing of a coronary artery on angiography, evaluation and treatment can be difficult. A narrowing within a coronary artery can be treated by either PCI with or without a stent or by CABG. It can often be difficult to tell if a narrowing within a coronary artery is the cause of a patient's symptoms and a considerable number of patients undergo coronary revascularisation without definite evidence that the coronary artery stenosis is significant. In addition to this, in patients with multiple narrowings, it can be difficult to tell which narrowing is the culprit lesion causing symptoms and requiring treatment. It is important to be sure that patients' symptoms are attributable to coronary artery disease as revascularisation techniques are invasive and there is a mortality associated with both PCI and CABG. Cardiac sounding chest pain may be caused by conditions not related to the heart at all, such as oesophagitis, oesophageal spasm, gastro-oesophageal reflux disease and costochondritis.

The currently employed tests for the detection of reversible myocardial ischaemia have a number of limitations. Exercise electrocardiography has only moderate sensitivity and specificity (68% and 77%).(6) Single photon emission computerised tomography (SPECT) has improved sensitivity of 86% and equivalent specificity of 74% but the radiation exposure is considerable at between 8 and 20 millisieverts depending on the radioisotope utilised and the images are frequently degraded by photon scatter and attenuation artefacts.(7). PET is widely regarded as the non-invasive gold standard but it is expensive, requires radioisotopes and has very limited availability in the UK. Stress echocardiography involves no radiation and can be utilised in conjunction with either

exercise or pharmacological stress. It has comparable sensitivity and specificity to SPECT but a proportion of patients have inadequate imaging windows.(8) Multidetector CT coronary angiography (CTA) is a relatively new imaging modality.(9) As with nuclear imaging techniques radiation exposure is not insignificant and like conventional coronary angiography it is not possible to confirm the functional significance of any stenoses identified.(2;3)

Magnetic resonance myocardial perfusion imaging (MRMPI) has multiple potential advantages over the above techniques. It provides superior spatial resolution compared to nuclear perfusion imaging, which allows the delineation of both sub-endocardial and transmural perfusion defects. The majority of currently employed perfusion pulse sequences provide a spatial resolution of 2-3mm^2 without any orientation constraints or problems with inadequate imaging windows. The currently used pulse sequences also provide excellent temporal resolution and 3-4 slices can usually be obtained per heartbeat at the heart rates achieved during pharmacological stress. During stress imaging, three short axis slices are obtained to cover the basal, mid and apical segments of the left ventricle. This protocol covers 16 of 17 segments of the AHA coronary arterial territory model.(10) The disadvantages of MRMPI are comapatively small compared to other techniques. However, scanning may not be possible in obese patients or patients with certain metallic implants. Claustrophobia is not infrequently encountered and can be particularly distressing for affected patients.

MRMPI is becoming increasing available for the non-invasive detection of myocardial ischaemia as the number of MRI scanners increase. MRMPI was first put to clinical use in the 1990's and since then a number of studies have been performed looking at its performance in the assessment of chest pain (Table 1.1).

Table 1.1 - Magnetic Resonance Myocardial Perfusion Imaging (MRMPI) Studies 1994 – 2007.

Author	Year	Patients	Sensitivity	Specificity	Comparison
Eichenberger AC(11)	1994	8	65	76	Thallium + QCA (>75%)
Keijer JT(12)	2000	13	71	71	Thallium SPECT
Al-Saadi N(13)	2000	54 (incl. 5 normals)	90	83	QCA (≥75%)
Schwitter J(14)	2001	66 (incl. 18 volunteers)	91 / 87	94 / 85	PET / QCA (≥50%)
Bertshinger KM(15)	2001	24 (incl. 10 volunteers)	85	81	QCA (≥50%)
Ibrahim T(16)	2002	59 (incl. 34 volunteers)	69 / 86	89 / 84	QCA (>75%) / PET
Nagel E(17)	2003	84	88	90	QCA (≥75%)
Ishida N(18)	2003	104	90	85	QCA (≥70%)+ SPECT
Plein S(19)	2004	68	88	83	Angiography (≥70%)
Paetsch I(20)	2004	79	91	62	QCA (>50%)
Takase B(21)	2004	102	93	85	Angiography (>50%)
Wolff SD(22)	2004	75	93 ± 0	75 ± 7%	QCA (≥70%)
Giang TH(23)	2004	80	94 / 91 / 94	25 / 78 / 71	QCA (≥50%)
Ishida M(24)	2005	49	79	87	QCA (≥70%)
Plein S(25)	2005	102 (incl. 10 volunteers)	88	82	Angiography (>70%)
Sakuma H(26)	2005	40	70	87	QCA (≥70%)
Fenchel M(27)	2005	22	81	89	SPECT
Klem I(28)	2006	92	84	58	Angiography (≥70%, LMS≥50%)
Cury RC(29)	2006	46	87	89	QCA (≥70%)
Rieber J(30)	2006	43	88	90	FFR(≤0.75) & QCA (>50%)
Futamatsu H(31)	2007	37	93	57	FFR≤0.75
Merkle N(32)	2007	228	96	72	Angiography (>70%)
Costa MA(33)	2007	37	93	57	FFR≤0.75
Barmeyer AA(34)	2007	35	84	67	Doppler CFR (<2)
Kühl HP(35)	2007	30	92	92	FFR≤0.75

It has a number of advantages over other tests used in the diagnosis of myocardial ischaemia. Patients are not required to exercise, as in the Bruce protocol ETT, which is

a frequently encountered stumbling block as the elderly population increases. There is no patient radiation exposure, as occurs with SPECT, PET and CT coronary angiography. In addition there are no attenuation or scatter artefacts that are also common with SPECT and PET. There are no image orientation constraints or inadequate windows as can occur during dobutamine stress (DSE) and myocardial contrast echocardiography (MCE). A complete assessment of myocardial viability including an assessment of left ventricular function, myocardial perfusion and late gadolinium enhancement can be performed in less than 1 hour with MRI. The gold standard test used to assess MRMPI in the previous studies (Table 1.1) have varied considerably with quantitative coronary angiography (QCA) and a visual assessment of the coronary angiogram being the most frequent test used with varying degrees of stenosis being chosen as the cut-off. QCA is employed in the majority of previous studies with 3 different cut-off's being commonly used: 50%;(14;15;20;23;30); 70%;(22;24;26;29) and 75%.(11;13;16-18) Visual assessment of the coronary angiograms has also been employed without using QCA.(19;21;25;28;32) Bearing in mind that degree of stenosis does not correlate with functional significance, we undertook the present study to determine the true sensitivity, specificity, positive and negative predictive values of MRMPI for the detection of significant CAD. Invasive assessment of a coronary stenosis using FFR has been widely accepted as a new gold standard in the cardiac catheterisation laboratory. Pressure wire derived FFR can reliably identify a flow limiting stenosis in an epicardial coronary artery and has been previously validated against what is probably the best current gold standard, PET.(36) It is independent of heart rate, blood pressure and contractility, and takes into account the contribution of collateral flow to myocardial perfusion.(37) At steady state hyperaemia, FFRmyo is calculated as the ratio of the mean distal intracoronary pressure (measured by the coronary pressure wire) to the mean arterial pressure (measured by the coronary

guide catheter). An FFR value < 0.75 confirms that the stenosis being interrogated has the potential to induce ischaemia at maximal hyperaemia.(38;39) In addition to determining the true sensitivity, specificity, positive and negative predictive values of MRMPI as determined by FFR, we will also compare MRMPI with QCA as has been utilised in the previous studies (Table 1.1).

1.2 Magnetic Resonance Myocardial Perfusion Imaging (MRMPI)

1.2.1 Magnetic Resonance Myocardial Perfusion Imaging (MRMPI) – Technique

A large number of studies have already been performed in an attempt to determine the diagnostic accuracy of MRMPI. The present study was not aimed at repeating old work but to determine the true accuracy of this relatively new method of diagnosing myocardial ischaemia. Our aim was to provide this information in normal clinical practice using the best present gold standard at our disposal, FFR. Table 1.1 lists the most relevant work in this field to date. In addition to the advances in the cardiac catheterisation laboratory which will be discussed later in this section, there have been major advances in scanner technology and sequence development. This has led to the rapid acquisition of multiple images at different positions to accurately diagnose regions of myocardial hypoperfusion. Improvements in temporal resolution and ECG synchronisation allow us to image up to 5 slices of myocardium within one second. Depending on heart rate this means we can image multiple slices per heartbeat within the R-R interval. This rapid acquisition of images enables us to follow a bolus of paramagnetic contrast agent, a chelation compound of gadolinium, as it passes through the heart. As the contrast reaches the myocardium perfusion defects emerge as areas of hypoenhancement. The pulse sequences we currently have available allow us to null the myocardium prior to the arrival of the gadolinium in order that the myocardium “lights

up" as it passes through. As shown in table 1.2 the majority of studies have chosen a fast gradient echo sequence such as turboFLASH (Fast Low Angled Shot) or an EPI (Echo Planar Imaging) sequence. The sequence used in this study is a fast gradient echo sequence which is T1 weighted. This means that the image generated shows differences in T1 times of the tissues scanned. The details of the sequence parameters can be found in appendix 2. This sequence has a short time to echo (TE) of 0.99msecs and a low flip angle of 8 degrees. This is the angle of the net magnetisation vector which is generated by the alignment of excess protons within the magnetic field of the scanner. Keeping the TE short and flip angle low and using a relatively short repetition time (TR - the time between each of the excitation pulses) allows for rapid image acquisition and imaging of multiple slice planes within each heartbeat. Multiple previous studies chose a gradient echo sequence for acquisition of their perfusion images as shown in table 1.2.(11-13;19;25;26;28;30;31;33;34). EPI on the other hand allows for rapid image acquisition as a result of a rapidly switching magnetic field gradient which follows the radiofrequency pulse generating many gradient echoes. Image acquisition using this technique is rapid however the signal to noise ratio (SNR) is reduced. Various techniques can be used to improve image quality including acquiring the data using a multi-shot technique. EPI has mainly tended to be used as a hybrid sequence along with gradient echo in studies using a General Electric (GE) or Philips scanner as highlighted in table 1.2.(14-18;20-24;29;35) Either of these pulse sequences can be utilised so long as scanning is fast and an in-plane resolution of 2-3mm can be achieved in order to visualise the endocardial and epicardial layers of the left ventricular myocardium.

Table 1.2 - MRI scanner make and sequence used in previous MRMPI studies 1994 – 2007. The myocardial coverage and method of analysing these scans is also presented.

Author	Year	Scanner	Sequence	Slices	Analysis
Eichenberger AC(11)	1994	GE 1.5T	Gradient Echo	3 per R-R	Normalised Upslope
Keijer JT(12)	2000	Siemens 1T	turboFLASH	2 per R-R	MCE, upslope, 1/MTT
Al-Saadi N(13)	2000	Philips 1.5T	TGE	1 per R-R	MPR linear fit
Schwitter J(14)	2001	GE 1.5T	Hybrid EPI	4 per 2 R-R	Upslope
Bertshinger KM(15)	2001	GE 1.5T	Gradient Echo / EPI	4 per 2 R-R	Upslope
Ibrahim T(16)	2002	Philips 1.5T	Fast hybrid sequence	3per R-R	Upslope index and peak SI
Nagel E(17)	2003	Philips 1.5T	TGE/EPI	5 per R-R	MPRI
Ishida N(18)	2003	GE 1.5T	Gradient Echo / EPI	7-8 per 2 R-R	Qualitative
Plein S(19)	2004	Philips 1.5T	Segmented K-space TGE	4 per R-R	Qualitative
Paetsch I(20)	2004	Philips 1.5T	TGE/EPI	3 per R-R	Qualitative
Takase B(21)	2004	GE 1.5T	TGE/EPI	8 per 2 R-R	Qualitative
Wolff SD(22)	2004	GE 1.5T	Segmented EPI	6-8 per 2 R-R	Qualitative
Giang TH(23)	2004	GE 1.5T	Hybrid EPI	6-8 per 2 R-R	Qualitative + Upslope data
Ishida M(24)	2005	GE 1.5T	TGE/EPI	7-8 per 2 R-R	Qualitative
Plein S(25)	2005	Philips 1.5T	TGE with SENSE	4 per R-R	MPRI
Sakuma H(26)	2005	Siemens 1.5T	turboFLASH	5-6 per 2 R-R	Qualitative
Fenchel M(27)	2005	Siemens 1.5T	True FISP	3 per R-R	Semiquatitative PMRS
Klem I(28)	2006	Siemens 1.5T	Gradient echo	4-5 per R-R	Qualitative
Cury RC(29)	2006	GE 1.5T	TGE/EPI	5-8 per 2 R-R	Qualitative
Rieber J(30)	2006	Siemens 1.5T	turboFLASH	3 per R-R	Upslope MPRI
Futamatsu H(31)	2007	Siemens 1.5T	Gradient echo	3 per R-R	Fermi MPR
Merkle N(32)	2007	Philips 1.5T	SSFP with SENSE	3 per R-R	Qualitative
Costa MA(33)	2007	Siemens 1.5T	Gradient echo	3 per R-R	Fermi MPR
Barmeyer AA(34)	2007	Siemens 1.5T	Gradient echo SSFP	3 per R-R	Upslope MPRI
Kühl HP(35)	2007	Philips 1.5T	TGE/EPI	3 per R-R	Upslope MPR

In addition to differences in pulse sequence used between studies the dose of gadolinium infused during these pulse sequences varies (Table 1.3). The lowest dose utilised was 0.025mmol/kg,(13;17;27) and the highest 1.5mmol/kg which was used in two optimal dose finding studies.(22;23) Other studies have used doses between these levels possibly due to local experience and expertise in interpreting images with the chosen concentration of gadolinium or possibly depending on the method chosen to analyse the images. For studies attempting to quantify absolute myocardial perfusion reserve a dose of gadolinium of less than 0.05mmol/kg would be best used when employing a T1 weighted gradient echo sequence.(31) Only at this lower dose of gadolinium is the relationship between signal intensity and gadolinium concentration in the left ventricle linear.(40) High doses of gadolinium result in full magnetisation recovery with a long saturation delay which can cause clipping of the AIF, which is the signal intensity / time curve for the bolus of gadolinium within the left ventricular blood pool.(41) Clipping leads to underestimation of the AIF which leads to inaccuracies in measuring the myocardial perfusion reserve (MPR). This will be discussed later as a method of quantifying myocardial blood flow.

Giang et al, in 2004 published a study using different doses of gadolinium in 94 patients with known or suspected coronary arterial disease from 3 different centres in Europe.(23) Three different doses of gadolinium were studied including 0.05, 0.1, 0.15mmol/kg body weight. Patients thereafter had coronary angiography performed and a DS on QCA ≥50% was considered significant. MRI scans were analysed using a 5 point linear fit to calculate the maximum upslope at stress (adenosine stress only protocol) using a semi-automatic program in a core laboratory. The study found that the area under the receiver operator curves (ROC) was significantly greater when either of

the higher doses of gadolinium were used (0.91 for 0.1mmol/kg, 0.86 for 0.15mmol/kg and 0.53 for 0.05mmol/kg).(23)

Another multicentre dose-ranging study was published in 2004 by Wolff et al.(22) This study was conducted at 3 international sites and recruited 99 patients. The same three doses of gadolinium were studied again using intravenous adenosine as the stress agent. On this occasion the MRI scans were interpreted visually by 4 independent blinded observers. The gold standard for the diagnosis of significant coronary artery disease was higher at ≥70% DS by QCA. In this study the low dose (0.05mmol/kg) of gadolinium performed best (area under the ROC curves - 0.9 for 0.05mmol/kg, 0.72 for 0.1mmol/kg and 0.83 for 0.15mmol/kg). The difference between the two lower doses was significant at p=0.02.(22) Taking these two studies together suggests that low dose gadolinium is best for visual assessment of MRMPI scans whereas semi-quantification using a semi-automated computer program works best at medium or high doses. We chose the intermediate dose of 0.1mmol/kg in this study as we planned to perform both visual and semi-quantitative assessments.

Table 1.3 - Stress agent, gadolinium dose and infusion rate used in previous MRMPI studies 1994 – 2007.

Author	Year	Stressor	Gadolinium Dose (mmol/kg)	Gd Injection Rate (ml/s)
Eichenberger AC(11)	1994	Dipyridamole	0.05	Over 5secs
Keijer JT(12)	2000	Dipyridamole	0.03	Hand-injection
Al-Saadi N(13)	2000	Dipyridamole	0.025	Hand-injection
Schwitter J(14)	2001	Dipyridamole	0.1	3
Bertshinger KM(15)	2001	Dipyridamole	0.1	3
Ibrahim T(16)	2002	Adenosine	0.05	3
Nagel E(17)	2003	Adenosine	0.025	8
Ishida N(18)	2003	Dipyridamole	0.075	4
Plein S(19)	2004	Adenosine	0.05	6
Paetsch I(20)	2004	Adenosine	0.05	4
Takase B(21)	2004	Dipyridamole	0.1	Not available
Wolff SD(22)	2004	Adenosine	0.05/0.1/0.15	5
Giang TH(23)	2004	Adenosine	0.05/0.1/0.15	Over <5 secs
Ishida M(24)	2005	Dipyridamole	0.075	4
Plein S(25)	2005	Adenosine	0.05	6
Sakuma H(26)	2005	Dipyridamole	0.03	Not available
Fenchel M(27)	2005	Dipyridamole	0.025	5
Klem I(28)	2006	Adenosine	0.065	3.5
Cury RC(29)	2006	Dipyridamole	0.1	5
Rieber J(30)	2006	Adenosine	0.05	5
Futamatsu H(31)	2007	Adenosine	0.04	Not available
Merkle N(32)	2007	Adenosine	0.1	6
Costa MA(33)	2007	Adenosine	0.1	10
Barmeyer AA(34)	2007	Adenosine	0.05	5
Kühl HP(35)	2007	Adenosine	0.025	5

Table 1.3 also demonstrates the rate of injection of gadolinium chosen in the previous studies. For the purposes of quantification of myocardial perfusion a rapid injection is preferred in order to achieve a sharp AIF curve which would not be achievable using a

hand injection as was used in some of the previous studies (table 1.3). The majority of previous studies have chosen an injection rate of ≥4ml/second using a power injector.

The stress agent used in the early studies of MRMPI imaging was almost exclusively dipyridamole, however this has been superseded by intravenous adenosine which gives a more controlled period of hyperaemia and a far shorter half life and therefore shorter duration of side effects.(42) Adenosine and dipyridamole will be discussed in greater detail later in this introduction.

1.2.2 Magnetic Resonance Myocardial Perfusion Imaging (MRMPI) – The Evidence So Far

The major findings of the largest studies in this field are presented in Table 1.1. The sensitivities and specificities of MRMPI for the detection of functionally significant coronary arterial disease not surprisingly vary with the differing scanners, pulse sequences, angiographic gold standards, gadolinium dose and method of analyzing the scans used. The data to date indicate that MRMPI scanning is a good test comparable to other non-invasive tests currently employed such as SPECT and stress echocardiography. Perhaps the pivotal study in this field to date was published by Schwitter et al in 2001.(14) In this study MRMPI scanning was compared with coronary angiography and PET which is widely considered to be the current non-invasive gold standard. Forty-eight unselected patients with suspected coronary disease were studied by MRMPI prior to coronary angiography, using dipyridamole as the vasodilating stress agent. A further 18 healthy volunteers were also studied by MR alone. ^{13}N-ammonia PET examination was performed prior to coronary angiography. The invasive gold standard for the diagnosis of significant coronary artery disease was QCA with a degree of stenosis ≥50% in any of the three coronary arteries. MRMPI scans were interpreted

using the relative upslope of the signal intensity / time curve for multiple sectors of myocardium corrected for the precontrast signal and also the AIF. Analysis of the subendocardial upslope data provided a sensitivity of 91% and specificity of 94% when compared with PET and a sensitivity of 87% and specificity of 85% when compared with QCA. The number of hypoperfused sectors on PET and MRMPI correlated well with r=0.76. This study concluded that MRMPI can reliably diagnose patients with significant coronary disease and also provide information of the amount of ischaemic myocardium under threat.(14)

During the course of this research project four studies were published in which FFR was used as one of the methods of assessing whether coronary arterial disease was significant in causing myocardial ischaemia.(30;31;33) As shown in table 1.1 two of these studies by Futamatsu et al and Costa et al produced the same results in the same number of patients and were from the same centre in Florida, USA. These studies recruited 37 patients however the comparison between FFR and MPR was only made in 44 coronary segments. These studies found an excellent sensitivity of 92.9% however specificity was lower at 56.7% when using absolute myocardial blood flow derived myocardial perfusion reserve (MPR) of the coronary sectors corresponding to the supplying coronary artery.(33) Rieber et al published a study of 43 patients with suspected or known coronary artery disease in 2006.(30) In this study, patients had upslope derived MPRI values calculated for coronary segments from the MRMPI scan and then had coronary angiography with QCA measurements and a FFR study performed. This study reported a sensitivity of 88% and specificity of 90% however again only 42 of 129 coronary territories had FFR measurements performed.(30) Kühl et al also published their study of 30 patients (20 patients with CAD and 10 without CAD) in 2007. In this study upslope derived MPR was calculated and compared with

FFR. An excellent sensitivity and specificity of 92% was found however FFR again was only estimated in 28 of 90 coronary artery territories.(35) These studies will be discussed in more detail in the results section where comparisons will be made with the present research study.

1.2.3 Myocardial Perfusion Reserve Index

Analysis of MRMPI scans can be performed by a qualitative, semi-quantitative or fully quantitative approach. Ideally all scans would be analysed by an automated system providing absolute myocardial flow in ml/g/min, however no commercially available software in current existence can perform this task in a non-labour intensive, non-time consuming and inexpensive way. As shown on table 1.2, almost half of the previous studies performed to date have chosen a qualitative approach to analysis. (18-24;26;28;29;32) Using this method blinded observers visualise both rest and stress scans together and diagnose perfusion defects on the basis of visual appearance. Some investigators advocate that a dark subendocardial rim must be present at stress for 5 or more cardiac cycles and be absent at rest in order to diagnose a reversible perfusion defect. Other studies allow perfusion defects to be diagnosed at the discretion of the experienced observers. Dark subendocardial defects at both stress and rest may represent infarction or may be due to dark rim artefact.(43) Artefacts caused by susceptibility are unfortunately common in perfusion imaging and are most common with gradient echo and EPI pulse sequences at the interface between tissues. This is important at the interface of the LV blood pool and the subendocardium where dark areas may be mistaken for perfusion defects.

Some of the MPRI studies have chosen a semi-quantitative method to analyse their scans as shown in table 1.2.(11-17;23;25;27;30;34) This method of analysis is model

free and uses the signal intensity / time curves generated for each of the myocardial segments of interest under conditions of stress and at rest and also the left ventricular blood pool.(10) Over the years multiple different approaches to this data have been utilised including: analysis of the peak signal intensity of the gadolinium in each of the myocardial segments during the first pass; upslope / rate of enhancement of myocardium calculated by analysing the initial increase in signal intensity during the first pass; time to peak signal intensity of the gadolinium bolus as it perfuses the myocardium; the mean transit time of the gadolinium bolus to pass through a myocardial segment and the area under the signal intensity / time curve for a segment of myocardium. The difficulty with the majority of these parameters is the large inter-individual variation of normal which makes it difficult to compare results between patients. The most common semi-quantitative parameter used in the previous literature is the upslope of the signal intensity / time curve for individual myocardial segments (table 1.2). This has been shown to correlate well with changes in blood flow when using radiolabelled microspheres in dogs.(44) In order to calculate the upslope of the curves at stress and rest they must first be smoothed by using a function to approximate the shape of the signal intensity / time curve. A gamma variate function can be applied to the curves for this purpose prior to determining the upslope.(45) A simpler method of performing this is to select a line of best fit between the signal intensity points on the upslope curve and determine the upslope value from this. This method was chosen in the previously described study by Schwitter et al in 2001 where excellent sensitivities and specificities were obtained in a comparison with PET imaging.(14) A signal intensity / time curve for the left ventricular blood pool should be calculated in addition to those curves for the myocardial sectors. This curve is known as the arterial input function (AIF) and must be taken into account when determining the myocardial upslope curves as these vary depending on the AIF. The upslopes of the myocardial

signal intensity / time curves are divided by the upslope of the AIF at both stress and rest. It is also useful to subtract baseline signal intensity prior to gadolinium injection from the curves in order that the upslope starts from a signal intensity measurement of zero. The myocardial perfusion reserve index (MPRI) is then calculated for each of the myocardial segments of the AHA model by dividing the stress upslope by the resting value. MPRI can also be calculated by using the maximum signal of each of the myocardial segments and dividing the stress by the rest value as described above. This was one of the parameters chosen in the present study. Another approach to dealing with the effects of the AIF on the myocardial signal intensity / time curve is by performing deconvolution of the signal intensity / time curves which more accurately accounts for the kinetics of the gadolinium bolus. This requires a low dose of gadolinium to be used as mentioned above (<0.05mmol/kg) so that the relationship between gadolinium concentration and the signal intensity is linear. As deconvolution is sensitive to noise a Fermi function is applied to the curves. This method has been mainly developed as a method of absolute quantification of myocardial flow and has been extensively validated.(46;47) It was used for the analysis of two of the previous studies listed in table 1.2.(31;33)

1.3 Coronary Pressure Wire

1.3.1 Fractional Flow Reserve (FFR)

The measurement of FFR in the cardiac catheterisation laboratory was developed in order to assess the functional significance of a moderate coronary artery stenosis in which it can be difficult to decide if the lesion is significant. RADI Medical Systems Ltd have developed a coronary guide wire which has a highly sensitive pressure and temperature sensor 3cm from the tip. This wire is passed into the distal third of a coronary artery where it can measure distal coronary pressure. Simultaneously aortic pressure is measured using the guide catheter. FFR is calculated by dividing distal coronary pressure by aortic pressure and the normal value for this index is 1.0 in arteries with no coronary disease. The measurements are made under conditions of maximal hyperaemia induced by intravenous adenosine at an infusion rate of 140 micrograms per kg per minute, as used in the present study, or using intra-coronary adenosine at far smaller doses, or also intra-coronary papaverine.(48) In a patient with normal coronary arteries with a mean distal coronary pressure (Pd) of 100 mmHg and a mean aortic pressure (Pa) of 100 mmHg, this would give a FFR of 1.0. In a patient with significant coronary disease and a distal coronary pressure of 60mmHg and an aortic pressure of 100mmHg this would provide a FFR of 0.6. Multiple studies have shown that a stenosis with a FFR of less than 0.75 is highly likely to cause reversible myocardial ischaemia. One of the first studies demonstrating this cut-off was published in 1995 by Pijls et al.(49) In this study 60 patients with single vessel coronary artery disease and a positive ETT had the FFR measured in the stenotic artery prior to and following percutaneous coronary angioplasty. These patients had a repeat ETT performed between 5 and 7 days post angioplasty and only if the ETT post angioplasty was normal was the FFR pre-angioplasty taken as being associated with reversible myocardial ischaemia. In all

patients a FFR of less than or equal to 0.74 was associated with reversible myocardial ischaemia.

Pjils et al published a landmark paper in the New England Journal of Medicine in 1996 describing the utility of FFR in a group of 45 patients who suffered from chest pain and had a coronary artery stenosis on coronary angiography of approximately 50% by visual estimation.(39) Each of these patients had a degree of clinical uncertainty as to whether their chest pain was related to reversible myocardial ischaemia. They all underwent a bicycle ETT, a thallium nuclear perfusion scan, dobutamine stress echocardiography (DSE) and a coronary angiogram with measurement of the FFR. Patients had PCI or bypass surgery performed based on a FFR with a cut off of 0.75. Those patients who were revascularised and had positive evidence of reversible myocardial ischaemia on the non-invasive tests had these tests repeated within 6 weeks of the revascularisation procedure. Twenty one patients had coronary disease with a FFR of less than 0.75. Each of these patients had evidence of reversible myocardial ischaemia on at least 1 of their non-invasive tests. Following revascularisation, these positive non invasive test results returned to normal. Of the 24 patients with an FFR of greater than or equal to 0.75, 21 had no evidence of reversible myocardial ischaemia on any of the non invasive tests performed. In this study FFR was determined to have a sensitivity of 88%, specificity 100%, positive predictive value 100% and a negative predictive value of 88%. The overall diagnostic accuracy was 93%.

The value of FFR was also assessed in patients with serial stenoses within a single coronary artery. Thirty two patients were included in this study. They had been referred for PCI of arteries which had greater than or equal to 2 stenoses with greater than or equal to 50% degree of stenosis by visual examination. These stenoses had to be

separated by a normal length of artery of greater than or equal to 2cm. During the pressure wire study the wire was passed into the distal coronary artery beyond the stenoses and then pulled back measuring the FFR during maximal hyperaemia at points prior to and proximal to the stenoses. The lesion with the largest pressure gradient was then dilated and stented and the FFR recorded again. If there continued to be a pressure gradient, the second stenosis was also angioplastied and stented. A repeat FFR was then performed with a pull back at the end of the procedure. A predicted FFR was calculated prior to PCI given the pressure gradient across each stenosis. In this study, the predicted FFR correlated very well with the measured FFR in all patients with an R value of 0.92. This study confirmed that the measurement of FFR in this manner helps identify those stenoses requiring PCI and provides a functional result of the angioplasty performed. This was postulated to minimise unnecessary procedures on stenoses that were not haemodynamically significant. This would therefore reduce the risk of complications during the procedure or the development of in-stent re-stenosis in the future.(50)

FFR has also been validated in patients who have had a prior MI. FFR is independent of LVEF.(51) It was however not known if a change in the mass of viable myocardium served by coronary artery would affect the 0.75 cut off value of FFR which had previously been used in patients without prior MI. Fifty-seven patients who had a documented MI without any akinetic segments on visual assessment of the LV angiogram were studied. They had normal contractility in other coronary territories and were scheduled for coronary angioplasty of the infarct related artery. Each of these patients also had an adenosine stress single photon emission scintigraphy (SPECT) scan performed prior to and following coronary intervention. The FFR was measured before and after PCI. The sensitivity, specificity, positive and negative predictive values of using the 0.75 cut-off of FFR in detecting flow mal-distribution on SPECT imaging was

82%, 87%, 81% and 91% respectively. As expected, patients with the lowest FFR values had positive SPECT imaging pre-angioplasty. These FFR values were significantly lower than those patients with negative SPECT scanning with p=0.0079. This study confirmed that an FFR cut-off of 0.75 distinguished those post MI patients with positive and negative SPECT imaging. Thus, FFR can still be used in patients undergoing pre-discharge coronary angiography following a MI.(52)

As well as determining the significance of a coronary artery stenosis in inducing myocardial ischaemia, FFR can also be used to predict the clinical outcome of percutaneous coronary angioplasty. In one study, 66 patients who had undergone balloon angioplasty to a single vessel were studied. They all had normal left ventricular function.(53) Each of these patients had a positive ETT within 24 hours of the balloon angioplasty. The FFR was measured prior to and following successful balloon angioplasty and the ETT was repeated between 5 to 7 days thereafter. Fifty eight patients of the sixty recruited had successful balloon angioplasty. Twenty four month follow up was obtained for all patients, during which time 16 adverse events occurred. These were defined as death, MI, unstable angina, coronary artery bypass surgery, repeat PCI or the recurrence of angina with a positive ETT. A multi-variant logistic regression analysis was performed and showed that the post-percutaneous coronary angioplasty FFR was the most significant independent predictor of adverse cardiac events. These data suggest that an FFR greater than or equal to 0.9 indicates an optimal functional PCI result, whereas values between 0.75 and 0.9 were felt to be initially successful, however overall suboptimal. The degree of stenosis following angioplasty was measured as a separate parameter in this study and the authors concluded that a degree of stenosis of less than or equal to 35% and an FFR greater than or equal to 0.9 provided excellent clinical outcome at 2 years.(53) Beck et al also examined the

usefulness of FFR in determining how appropriate angioplasty was in arteries with moderate coronary stenosis.(3) This study followed previous studies which suggested that patients who had a coronary stenosis with an FFR greater than 0.75 were safe to be deferred without coronary angioplasty with excellent clinical outcome.(39;54) Three hundred and twenty five patients referred for elective PCI of lesions greater than 50% diameter by visual assessment were recruited into the study. None of these patients had any evidence of reversible ischaemia by non invasive testing. Prior to percutaneous coronary angioplasty patients were randomised into a defer or a performance group. Following coronary angiography the FFR was measured in the artery of interest. In those patients who were randomised to deferral, angioplasty was only performed if the FFR was less than 0.75. Patients randomised to performance of PCI underwent the procedure regardless of whether the FFR was less than 0.75 or greater than or equal to 0.75. Those patients initially randomised to either deferral or performance of PCI who had an FFR of less than 0.75 were categorised as being in the reference group. Those patients in the performance group who had PCI performed despite an FFR greater than or equal to 0.75 were defined as the perform group. Clinical follow up of these patients was obtained at 1, 3, 6, 12 and 24 months. Interestingly, the event free survival is similar between the deferral and the performance group with 92% vs 89% at 12 month follow up and 89% vs 83% at 24 month follow up. The reference group had a significantly lower event free survival at 80% at 12 months and 78% at 24 months. The reference group however had a significantly higher percentage of patients free from angina at 67% at 12 months and 80% at 24 months compared to 49% in a deferral group and 50% in a performance group at 12 months and 70% in a deferral group and 51% in a performance group at 24 months. These 2 year follow up data conclude that in patients without non invasive evidence of reversible myocardial ischaemia, the measurement of FFR with a value less than 0.75 identifies patients in whom PCI is appropriate and

improves functional angina class. Patients with an FFR greater than 0.75 in this study did not benefit from PCI.(3) A 5 year follow up of these patients was published in the Journal of the American College of Cardiology in 2007.(55) Complete long term follow up was obtained in 313 patients at 5 years (97%). Again, there was no difference in event free survival between the defer and the perform groups (80% vs 73%). However, event free survival was significantly lower in the reference group at 63% despite having PCI performed. Patients with a significant stenosis with an FFR less than 0.75 which was treated by PCI had a 5 times greater chance of cardiac death or acute MI than patients with similar angiographic findings but a FFR greater than or equal to 0.75 that was treated by medical therapy ($p = 0.002$). The prognosis of a non significant stenosis (FFR greater than or equal to 0.75) was excellent with a rate of death or acute MI related to that stenosis of less than 1% per year. This rate was not reduced by PCI as demonstrated in the perform group. The composite rate of cardiac death and acute MI in the defer, perform and reference groups was 3.3%, 7.9% and 15.7% at 5 years follow up. There was no difference in the percentage of patients free of angina at 5 year follow up in defer or perform groups. These 5 year follow up data confirmed that patients treated by PCI did significantly worse than patients with a stenosis and an FFR greater than or equal to 0.75. This study did not include any patients with unstable coronary syndromes.(55)

Measurement of the FFR following stenting has been shown to be a strong independent predictor of clinical outcome at 6 months in 750 patients who all underwent coronary stenting in a multicentre study involving Europe, the United States and Asia.(56) Adverse events were recorded as death from any cause, acute MI or repeat target vessel revascularisation by PCI or CABG. Multi-variant analysis showed that FFR measured immediately following stenting was the most significant and dependent variable related

to all types of adverse events. In patients with a post stent FFR of 0.9 to 0.95 the adverse event rate was 6.2% compared to those patients with a post stent FFR less than 0.9 who had an adverse event rate of 20.3%. If the post stent FFR was less than 0.8 the adverse event rate was 29.5%. This study highlights the value of measuring FFR following angioplasty and stenting to predict adverse events at 6 months follow up.

Therefore FFR has been shown to be an extremely useful technique, not only in the determination of functionally significant coronary artery disease but also in the guiding of PCI.(57) As is the case with many biological measurements there is no exact cut off for the determination of a significant coronary stenosis. A grey area is known to exist between 0.75 and 0.8 in which a lesion may be capable of inducing myocardial ischaemia. This is taken into account in the results of this research study.

1.3.2 Coronary Flow Reserve (CFR)

Thermodilution derived (CFR) is another physiological parameter that can be measured using the RADI coronary guide wire. While FFR gives us information regarding the stenosis severity in the epicardial coronary artery, CFR on the other hand provides information on the microvascular resistance as well as epicardial coronary disease. Prior to the development of the coronary pressure wire with a temperature sensor, FFR and CFR had to be measured using 2 separate wires. The aforementioned RADI pressure wire has the capabilities of measuring thermodilution derived CFR. The shaft of the pressure wire which monitors temperature dependent electrical resistance acts as a proximal thermistor and the distal sensor, 3cm from the tip, has capabilities of measuring both pressure and temperature. Following the injection of a bolus of saline the shaft of the wire detects the start of the injection and the distal sensor detects the bolus as it passes the distal coronary artery. Thermodilution derived CFR can be

calculated by dividing the mean transit time of a 3ml bolus of room temperature saline at rest by the transit time at maximal hyperaemia induced by a continuous infusion of intravenous adenosine at 140 micrograms/kg/minute. This assumes that the epicardial volume remains unchanged between injections. Doppler derived CFR measurements have been available using a specific Doppler wire for some time. The new method by thermodilution has been validated using an in-vitro model and also an animal model (6 mongrel dogs). In the initial validation study 360 paired flow velocity measurements and thermodilution curves were obtained in the animal model. In this study 3 sets of measurements were obtained for each curve to provide the mean transit time of a bolus of saline. A significant correlation was found between the Doppler derived CFR measurements and the thermodilution derived measurements with an r value of 0.76. In the in-vitro model there was a significant correlation between absolute flow measurements and the mean transit time of a bolus of saline (r=-0.75). This study concluded that the mean transit time of a 3 ml hand injected bolus of saline at room temperature closely correlates with absolute flow using the in-vitro model and flow velocity recorded using the Doppler wire in mongrel dogs.(58) In 2002 the coronary thermodilution method of calculating CFR using the same wire as used to calculate the FFR was validated in humans. This was again performed using simultaneous recordings of the Doppler derived CFR. In this study 50 patients were included using 103 coronary arteries. These patients had all been referred for physiological assessment of at least 1 coronary stenosis. In the cardiac catheterisation laboratory both the RADI pressure wire and a Doppler wire were passed distal to the coronary stenosis. Maximal hyperaemia was achieved using either intravenous adenosine at a dose of 140 micrograms/kg/minute or by the administration of intracoronary papaverine at a dose of 50 to 20mg. The FFR, thermodilution derived CFR and Doppler derived CFR were all measured pre and post angioplasty. A significant correlation was found between thermodilution derived and

Doppler derived CFR with r=0.80 and p<0.0001.(59) Being able to measure thermodilution derived CFR in addition to FFR using the same wire allows the clinician determine to what extent microvascular disease is contributing to inducible ischaemia. Using the same wire means that there is no increase in cost compared to the measurement of FFR on its own.(59) In 2002 thermodilution derived CFR was validated in clinical practice in 8 hospitals within 5 countries in Europe. Eighty six patients who had been referred for physiological assessment +/– coronary angioplasty of at least 1 stenosis were included into the study. Both the thermodilution derived CFR and Doppler derived CFR were measured prior to angioplasty. The data from 27 patients were excluded due to sub-optimal Doppler tracings. Ninety seven percent of these patients had a thermodilution derived CFR measured. When these two methods were compared the r value was 0.79 with p<0.0001. CFR measurements obtained by the thermodilution method had a tendency to be higher than that recorded by Doppler flow velocity (2.2 vs 2.0). This study however, confirmed that thermodilution derived CFR measurements was both feasible and reliable in a multi-centre setting.(60) A further study also compared pressure derived CFR with flow derived CFR in an animal model and also velocity derived CFR in 30 patients. This study provided an r value of 0.92 in the animal model compared to 0.85 in humans. This was similar to those values obtained in previous studies.(61) Also in 2003 an open chest pig model was developed at the University of Stanford in order to compare thermodilution derived CFR with Doppler derived CFR and absolute flow derived CFR. Interestingly in this model the thermodilution derived method was found to correlate better with absolute flow derived CFR than the Doppler derived CFR.(62)

The ability of Doppler derived CFR to predict outcome following PCI was studied in 379 patients. Peri-procedural outcome was compared to CFVR results at the end of the

procedure and separated into those with a CFVR greater than or equal to 2.5 or a CFVR less than 2.5. In this study a low CFVR was associated with a worse peri-procedural outcome at 30 days. There was however, no difference between groups on late follow up at 1 year.(63) Thermodilution derived CFR using the RADI pressure wire was used to examine the effects of diabetes mellitus on collateral flow index (CFI) in patients with stable coronary heart disease. In this study, 100 patients with diabetes mellitus and 100 non diabetics had pressure wire derived coronary CFI or Doppler flow velocity derived CFI measured or both. Interestingly this was found not to differ between diabetic and non diabetic patients, even when angiographically normal arteries or chronic totally occluded arteries were studied.(64)

1.3.3 Index of Microcirculatory Resistance (IMR)

During the course of this project a novel method of assessing the coronary microcirculation invasively was developed. CFR reflects the epicardial coronary artery as well the microcirculation. Most previous studies noted that thermodilution derived CFR tended to overestimate CFR when compared to Doppler derived values with the differences ranging up to 20%.(59) In addition, CFR by thermodilution may be overestimated where large side branches originate proximal to a coronary stenosis. Thermodilution derived CFR required intravenous adenosine in order to maintain maximal hyperaemia for at least 30 seconds in order for the curves to be obtained. This is unlike Doppler derived CFR or FFR where bolus intra-coronary injections of adenosine or papaverine may be used. As IV adenosine results in a drop in systemic blood pressure by up to 15% this may cause an underestimation of CFR. In clinical practice trying to obtain 3 identical thermodilution curves, especially at rest, can be difficult depending on guide catheter engagement and the position of the distal sensor.

The index of microcirculatory resistance (IMR) is a novel parameter which provides information on the the coronary microcirculation independently of the status of the epicardial coronary artery. It is defined as distal coronary pressure multiplied by the mean transit time of a bolus of saline injected at room temperature during maximal hyperaemia. The calculation of IMR assumes that at maximal hyperaemia the variability of resting vascular tone and haemodynamics will be eliminated thus achieving the minimum microvascular resistance. In an open chest porcine model, using Yorkshire swine, the true microcirculatory resistance (TMR) defined as distal coronary pressure divided by absolute coronary flow at hyperaemia was compared with IMR in left anterior descending coronary arteries. The microcirculation was disrupted with micro-spheres and measurements repeated within a normal epicardial artery and after the creation of an epicardial coronary artery stenosis. Sixty one measurements of TMR and IMR were made and a significant correlation was found on linear regression analysis with $r=0.87$ and $p<0.001$. The mean IMR and TMR increased significantly to a similar degree after the coronary microcirculation was disrupted using micro-spheres. This study proved that IMR could be measured quantitatively using a coronary pressure wire.(65) In order to further validate the independency of the index of microcirculatory resistance over a range of epicardial coronary stenoses, a further study was conducted.(66) In this study an in-vitro model was developed to mimic the human heart with an external coronary occluder to provide a range or coronary stenoses. The inverse mean transit time of a bolus of saline correlated well with absolute blood flow ($R^2=0.93$) and an excellent correlation was again found between the index of microcirculatory resistance and the true myocardial resistance ($R^2=0.94$).(66) IMR was again confirmed to be independent of epicardial stenosis severity. Researchers then realised that the minimum achievable microvascular resistance actually increased as epicardial stenosis severity increased. Previous work had not taken into account the

contribution of collateral flow to myocardial resistance and therefore the open chest pig model was used again to look at the index of microcirculatory resistance, however on this occasion coronary wedge pressure (Pw), which is a measure of collateral flow, was incorporated into the equation. Bearing this in mind, the index of microcirculatory resistance can be calculated by multiplying aortic pressure by mean transit time of a bolus of saline at hyperaemia and multiplying this by coronary FFR, which is calculated by subtracting the wedge pressure from distal coronary pressure divided by aortic pressure minus wedge pressure. The equation is therefore as follows:-

$$IMR = Pa \times Tmn \times (Pd-Pw)/(Pa-Pw)$$

Using the open chest pig model, measurements of IMR were compared with the apparent minimal microvascular resistance calculated at peak hyperaemia using a flow probe and also a true microvascular resistance (R micro). Measurements were made with no stenosis present and also after the creation of a moderate and severe epicardial stenosis. When collateral flow was not taken into account in determining the index of microcirculatory resistance the IMR increased progressively and significantly with increasing stenosis severity. Once collateral flow was incorporated as in the above formula neither IMR or R micro increased as a result of increasing epicardial stenosis.(67) This finding was also confirmed in humans when 30 patients scheduled for coronary intervention had different degrees of coronary stenosis reproduced by inflating an intra-coronary balloon by different degrees to mimic stenoses of 10%, 50% and 75%. This was performed following stenting. At each of the 3 degrees of inducible coronary stenosis both the FFR and IMR were measured during an intravenous adenosine infusion. A total of 90 measurements were made and again when coronary wedge pressure was not taken into account there was an increase in the microvascular

resistance noted with increasing stenosis severity. However, when the wedge pressure was incorporated into equation there was no increase in IMR with increasing stenosis severity.(68) IMR is the most recent haemodynamic parameter provided by the pressure wire and to date there has been relatively little work performed. One study has looked at the predictive value of IMR in patients who undergo primary PCI for ST elevation MI. Twenty nine patients who presented with ST elevation MI within 12 hours of the onset of symptoms or after failed fibrinolytic therapy were included in this study. These patients had the IMR calculated and the CFR and FFR were also measured. This study showed that IMR significantly correlated with peak creatinine kinase (CK) with $r=0.61$ and $p=0.0005$. IMR also correlated with 3 month echo wall motion score with $r=0.59$ and $p=0.002$. Using a multi-variant analysis IMR was the strongest predictor of peak CK and 3 month wall motion scoring. In addition to this, IMR was found to be the only predictor of recovery of left ventricular function based on the change in wall motion score ($r=0.5$ with $p<0.01$). The authors of this study concluded that IMR was an independent predictor of acute and short term myocardial damage in the setting of primary PCI for acute ST elevation MI.(69)

1.4 Adenosine Pharmacological Stress

For the purpose of this study adenosine will be used as our intravenous pharmacological stress agent. This will be utilised in both the first pass magnetic resonance myocardial perfusion imaging (MRMPI) scan and also during the coronary artery pressure wire studies. Adenosine is a purine nucleoside and has many roles in the regulation of tissue function. Adenosine is produced by cells naturally when the tissue is under stress. This is a method of autoregulation increasing energy supply to cells under stress by means of vasodilation. In the case of myocardium, when the cardiac myocytes are put under strain by physical exertion in a patient with coronary disease, the myocardial ischaemia leads

to the release of adenosine which in turn causes the supplying coronary artery to vasodilate. Adenosine is also known to have a protective effect preventing cellular damage caused by ischaemia. Adenosine is also thought to have a role in ischaemic pre-conditioning where a short period of ischaemia followed by reperfusion prevents cell death during longer periods of ischaemia thereafter.(70) During the period of ischaemic preconditioning, adenosine in the cell interstitium accumulates and remains in higher concentrations even after reperfusion has occurred. Adenosine binds adenosine receptors within the sarcolemma of cardiac myocytes. There are 4 different types of adenosine receptor (A1, A2A, A2B and A3) each of which exist within cardiac myocytes. Adenosine A2 receptors are most common within the coronary arteries. The A1 and A3 receptors found in cardiac myocytes are involved in protecting these cells during periods of ischaemia preventing infarction. Adenosine is also known to suppress the effects of adrenaline which is increased due to sympathetic stimulation which occurs during myocardial ischaemia. Given these protective effects it is not surprising that intracoronary adenosine given during PCI for acute MI results in improved recovery of myocardial perfusion and also myocardial contractility with less no-reflow phenomenon.(71) This was also noted in the AMISTAD trial, which showed that adenosine administration along with thrombolysis for acute MI, resulted in a reduction in the size of anterior MIs.(72)

It is the effect of adenosine on the A2 receptors within coronary arteries which makes it useful as a pharmacological stress agent. In normal coronary arteries without endothelial dysfunction caused by coronary artery disease an intravenous infusion of adenosine will lead to coronary vasodilation and an increase in coronary flow by between 2 and 3 times baseline flow. During an intravenous infusion this vasodilation begins around 20 to 30 seconds after commencement and is at its maximum after 1 minute. This period of

maximum hyperaemia continues for the duration of the adenosine infusion which is mandatory as adenosine has a very short half life of less than 10 seconds.(42) The value of adenosine in stress testing is that it causes a disparity in flow between myocardium supplied by normal coronary arteries and that supplied by arteries with significant coronary disease. In an artery with significant coronary disease there will be little or no increase from baseline flow with an adenosine infusion, increasing the difference in flow between the 2 areas at stress. Therefore the CFR in abnormal arteries is significantly less than in normal arteries. During the adenosine infusion there is an increase in the heart rate and simultaneous drop in the blood pressure. The most common side effects experienced by patients are those of chest pain, breathlessness, flushing, headache and abdominal pain. Rarely patients may develop atrio-ventricular block due to the effects of adenosine on the adenosine A1 receptors within the atrio-ventricular node. Due to the very short half life of adenosine, any symptoms quickly resolve on stopping the infusion. In the event of prolonged AV block, this may be reversed by administration of intravenous aminophylline. Adenosine is contra-indicated in patients with significant reversible airways disease as this may lead to bronchospasm. Patients taking theophylline should also avoid adenosine. Adenosine is also contra-indicated in patients who have second or third degree heart block as there is a risk of developing higher degrees of prolonged atrio-ventricular block.

In the case of cardiac MRI adenosine is an ideal agent as exercise testing within the magnetic field of the scanner is difficult. In addition, due to the time it takes to set up a perfusion sequence following localisers, it would be impossible to physically stress a patient outwith the scanner room and quickly transfer them into the room and commence the perfusion sequence. Some centres have developed an exercise bike fixed to the scanner, however, this will not be appropriate for all patients.(73) When a bolus

of gadolinium is administered during steady state maximum hyperaemia induced by the adenosine, the gadolinium will perfuse the myocardium supplied by normal coronary arteries faster than the myocardium supplied by abnormal coronary arteries. This difference in first pass delivery of gadolinium is detectable using cardiac magnetic resonance.

An alternative to intravenous adenosine is intravenous dipyridamole, which also causes coronary vasodilation. Dipyridamole's mechanism of action is by increasing levels of natural adenosine by preventing its re-uptake and metabolism. However it is more expensive than adenosine and has a longer half life. This results in longer duration of side effects for patients and also the need for longer monitoring.(48)

New pharmacological stress agents are in the process of being developed. These have been designed to selectively stimulate the adenosine A2a sub-type of receptor which is mainly found in vascular smooth muscle cells and results in vasodilation. The closest of these agents to routine clinical use is regadenoson which is a selective agonist of the adenosine A2a receptor with a relatively low affinity. This low affinity leads to a rapid onset of coronary vasodilation and also a rapid termination. Regadenoson causes a dose dependent increase in coronary blood flow which is more sustained than that achieved with intravenous adenosine.(74) Pre-clinical studies have shown no evidence of AV block as one would expect with selective A2a receptor agonism. There has been no evidence of bronchoconstriction with regadenoson which is an effect mediated through the adenosine A2b receptor. Side effects with regadenoson have so far been infrequent, with the most common being chest discomfort in 4 of 34 patients and increased awareness of rapid heartbeat, also in 4 of 34 patients. A small number of patients also complained of vasodilation, dizziness, cough, nausea and shortness of breath.(75) Less

shortness of breath is an excellent advantage for improving image quality in magnetic resonance myocardial perfusion imaging as breathing during the breath hold can result in artefact leading to the misinterpretation of perfusion defects. Having a still image from a good breathold is also advantageous if semi quantitative or fully quantitative measurements are required as image registration can be time consuming.

1.5 Caffeine

Exogenous caffeine can inhibit the vasodilation produced by adenosine and therefore patients are asked to abstain from caffeine for 24 hours prior to MRMPI scanning and pressure wire studies in the cardiac catheterisation laboratory. Caffeine belongs to a family of methylxanthines which also include theophylline and theobromine. All these methylxanthines antagonise adenosine receptors. Caffeine is mainly consumed in coffee, tea, fizzy drinks and chocolate. It is also present in a common UK over the counter analgesic called Anadin. Theophylline is found in high concentrations in tea and theobromines are found in chocolate and coca cola. Following consumption of caffeine peak levels are found in the circulation within 15 to 45 minutes. It has a half life between 2 and 12 hours, depending on individual variation in activity of the cytochrome P450 reductase system. Drugs which interact with this enzyme system such as rifampicin and phenytoin reduce the half life of caffeine. An increase in half life is seen in patients with alcoholic liver disease and in those taking cimetidine. Caffeine increases heart rate and blood pressure in normal individuals and can cause supraventricular arrhythmias. Caffeine antagonises adenosine by 2 mechanisms; firstly an increase in intra-cellular cyclic adenosine monophosphate (cAMP) due to inhibition of phosphodiesterase and secondly competitive binding to adenosine receptors. This has a significant impact in reducing the level of hyperaemia achieved and thus may cause false negative perfusion scan results. This has been shown with both adenosine and

dipyridamole stress perfusion scans, mainly performed by nuclear perfusion techniques. In a case report from 1989 a patient developed down sloping ST depression and evidence of reversible ischaemia on a dipyridamole thallium nuclear perfusion scan. This initial scan had been done during caffeine abstinence. One week following this initial test the patient re-attended and had an infusion of caffeine and a repeat ECG and thallium scan. The ECG showed no ST depression and there was a reduction in the signs of ischaemia on the thallium scan. It was postulated that coffee may be responsible for false negative dipyridamole thallium scanning.(76) In order to quantify the effects of caffeine on hyperaemic blood flow 12 healthy volunteers had myocardial blood flow measured at rest and following intravenous dipyridamole at baseline and also after the consumption of caffeine. Myocardial blood flow was quantified using intravenous ^{13}N-ammonia dynamic positron imaging tomography (PET). Caffeine was found to increase the rate pressure product at rest from 6873 to 7566, which was mainly due to a statistically significant increase in SBP (from 112 to 121 mmHg). Prior to caffeine consumption dipyridamole led to an increase in the rate pressure product by 59%, however following caffeine consumption the increase was only 26% ($p<0.05$). The heart rate response to dipyridamole was inversely related to serum caffeine levels ($r=0.68$). Blood flow at maximum hyperaemia was 2.01ml/g/min prior to caffeine consumption, however following caffeine consumption this was only 1.31ml/g/min ($p<0.001$). CFR was also blunted, measuring 3.4 at baseline and 2.3 following caffeine consumption ($p<0.001$). Both hyperaemic blood flow and flow reserve were inversely related to caffeine dose. Caffeine reduced the hyperaemic blood flow and CFR in a dose dependent fashion when using dipyridamole as the stress agent. This study emphasised the importance of giving patients dietary advice prior to pharmacological stress testing.(77) A similar PET study was performed in 10 healthy volunteers using ^{15}O-labelled water and using ATP as well as dipyridamole as a stress agent. Patients were

asked to abstain from caffeine for 24 hours while a baseline evaluation of hyperaemic blood flow was performed and then within 2 weeks a further PET study was performed 1½ hours after the consumption of oral caffeine at a dose of 3mg/kg. This was an equivalent to 2 to 3 cups of coffee. Interestingly, on this occasion myocardial blood flow at rest in the baseline and the caffeine groups were not significantly different. At baseline myocardial blood flow was significantly higher in the ATP group compared to those who received dipyridamole ($p=0.003$). The myocardial flow reserve however in this comparison was not statistically significantly different ($p=0.07$). Following caffeine myocardial blood flow during the ATP infusion and following dipyridamole was significantly lower than it had been at baseline ($p<0.0001$). In addition, myocardial flow reserve was also significantly reduced ($p<0.005$). The degree by which these hyperaemic responses was reduced was similar in both the dipyridamole and ATP groups further emphasising the importance of refraining from caffeine prior to nuclear perfusion imaging.(78)

There is however some controversy in this area as 2 recent studies have failed to show that caffeine administration prior to tests looking for reversible myocardial ischaemia affects the results. The first of these studies was published in 2004.(79) In this study 10 veterans who had clinical indications for coronary angiography and who had abstained from caffeine for 24 hours had a coronary pressure wire placed distal to a stenosis in order to measure distal coronary pressure. The FFR was recorded using the intracoronary administration of adenosine. Each of these patients had at least one stenosis of greater than 50% diameter. The FFR was recorded at baseline and then repeated after administration of 4mg/kg of caffeine which was injected intravenously. This is an equivalent to approximately 2 to 3 cups of coffee. The FFR was then repeated again with an intracoronary adenosine bolus. Venous blood measurements of caffeine

levels were made thereafter using high performance liquid chromatography. There was a significant increase in resting mean systolic and diastolic pressures and a significant increase in aortic and mean distal coronary pressures, as well as a decrease in heart rate at 5 minutes following the administration of caffeine compared to pressures and heart rate at rest. Unexpectedly intravenous caffeine did not alter the FFR in the diseased coronary arteries. If the caffeine did reduce maximal hyperaemia during adenosine infusion FFR should have increased. The authors concluded that the intravenous caffeine increased aortic pressure and also decreased heart rate, however there was no attenuation of the hyperaemic effects of intracoronary adenosine. The authors felt that the caffeine effect may not be relevant for adenosine stress testing as interaction between caffeine and adenosine is competitive and interstitial levels of adenosine are far greater with exogenous adenosine administration than following dipyridamole.(79)

A second study was performed by a group who noted the number of perfusion scans being cancelled or changed to dobutamine stress testing because patients had consumed caffeine prior to their proposed adenosine stress SPECT scan.(80) Therefore this study aimed to assess the effects of an 8 ounce cup of coffee 1 hour prior to adenosine SPECT scanning. Thirty patients with known or high likelihood of coronary artery disease who had already undergone a SPECT perfusion scan and had evidence of a reversible defect in one or more vascular territories were recruited. A repeat SPECT scan was performed 1 hour after an 8 ounce cup of brewed caffeinated coffee and pharmacological stress was repeated using intravenous adenosine. Blood caffeine levels were checked after 1 hour of ingestion. Technetium sestamibi or tetrafosmin were the radioactive tracers used. A sum stress score using the 17 segment model was employed. There was no significant difference in the summed stress score (extent of stress perfusion defect), summed difference score (extent of reversible perfusion defect) or the quantitative

perfusion defect size with or without caffeine ingestion. No difference in perfusion defect size was seen with or without caffeine corrected for caffeine blood levels. No patients with a positive perfusion defect converted to a negative study after caffeine. This study concluded that an 8 ounce cup of coffee 1 hour before adenosine stress had no effect on the extent and severity of adenosine SPECT myocardial perfusion imaging reversible perfusion defects. Interestingly, 50% of these patients had caffeine levels less than or equal to 3mg/L. Thus a more strict conclusion is that a cup of coffee producing a mean caffeine level of 3.1 +/– 1.6 mg/L does not attenuate the results of adenosine myocardial perfusion imaging. A practical recommendation of this study was that having 1 cup of coffee should not be a reason to cancel an adenosine SPECT study or change to dobutamine stress.(80)

A number of other studies have looked at the issue of abstaining from caffeine prior to nuclear perfusion imaging. In 1994, 86 patients underwent myocardial perfusion scintigraphy using thallium-201. Seventy-five of these patients had pharmacological stress induced by dipyridamole and 11 by intravenous adenosine. All patients abstained from caffeine containing products for 24 hours prior to their scan and blood was taken prior to initiation of adenosine or dipyridamole for serum caffeine levels. These were measured using an enzyme immunoassay technique. Haemodynamic parameters for pulse and blood pressure were measured during and following the adenosine or dipyridamole infusion. Detectable caffeine was found in 34 (40%) patients and the levels of caffeine encountered ranged between 0.1 and 5 mg/L. The decrease in mean SBP and the increase in mean pulse was not significantly different between those patients with caffeine levels greater than 1.0 mg/L and those with lower or no detectable caffeine levels. Results of the thallium scans were also similar in these groups.(81) A study on the haemodynamic effects of caffeine during adenosine myocardial perfusion

scans was published in 2000.(82) Seventy patients undergoing tetrafosmin myocardial perfusion scintigraphy were asked to abstain from caffeine for a minimum of 12 hours. Venous blood was collected prior to pharmacological stress and each patient was questioned on their drinking habits and consumption of caffeine-containing products. Pulse and blood pressure were monitored every 2 minutes during an adenosine infusion of 140μg/kg/min for 6 minutes. Symptoms were recorded and patients were categorised into 4 groups depending on the severity of their symptoms. Caffeine levels were measured using high performance liquid chromatography. Fifty two (74%) patients had a measurable serum caffeine level. Thirty five patients (50%) had levels ≤1mg/L and greater than 0mg/L. No correlation was found between tea or coffee drinking habits and a measured serum caffeine level. No correlation was found between serum caffeine levels and maximum change in pulse, SBP or DBP. In addition, no difference was seen in mean maximum change in pulse, SBP or DBP between those patients with caffeine levels less than 2.9mg/L and those with levels ≥2.9mg/L. The mean pulse rate increase in the group with caffeine levels ≥2.9mg/L was 29.9 beats per minute, compared to 19.9 beats per minute in those with levels less than 2.9mg/L. The difference in SBP was -11.25mmHg in the high caffeine group, compared to -17.27mmHg in the low caffeine group. The difference in DBP was -5.1mmHg in the high caffeine group, compared to -6.8mmHg in the low group. A significant difference in the occurrence of symptoms with the adenosine infusion was found between the group with low caffeine levels (less than 2.9mg/L) and those with high caffeine levels (≥2.9mg/L). In the high caffeine group 6 patients (75%) had no symptoms, compared to 20 of the 62 patients in the low caffeine group (32%), which was statistically significant (p=0.04). Unfortunately the number of patients in the high caffeine group was low, which is a limitation of this study. No analysis of perfusion imaging was performed in this study, however the authors concluded that in view of the symptoms experienced by patients a 12 hour

abstention from caffeine containing products may be insufficient and could potentially lead to false negative myocardial perfusion scans. The authors of this study propose a 24 hour abstention may be safer for the purpose of myocardial perfusion imaging.(82) The caffeine level at which adenosine induced vasodilation is inhibited varies in the current literature. Smits et al, 1990 demonstrated that a caffeine plasma level of 2.3 to 5.5mg/L inhibited vasodilation.(83) Bottcher et al, 1995 noted a reduction in hyperaemic blood flow and flow reserve at serum caffeine levels less than 8μg/L.(77)

A study of serum caffeine levels after 24 hours of abstention was published in the Journal of Nuclear Medicine Technology in 2002.(84) In this study 36 patients were recruited and had blood taken for caffeine levels measured by high performance liquid chromatography prior to stress with dipyridamole at a dose of 0.56mg/kg over 3½ minutes. During this time blood pressure and heart rate were recorded at 0 and 4 minutes. Sixty six percent of patients had detectable caffeine levels in the range of 0.1 to 0.8mg/L. There was no statistically significant change in the average DBP and SBP after the dipyridamole infusion and there was no correlation between measured serum caffeine levels and blood pressure. Heart rate increase was inversely correlated with serum caffeine levels, however the r value was only -0.22 and p=0.19. Interestingly in this study all patients had levels of caffeine less than 0.8 mg/L. This is a higher proportion than that noted in the aforementioned study by Jacobson et al. This study concluded that as the caffeine levels were all less than 1mg/L a 24 hour period of abstention from caffeine containing products should be sufficient for pharmacological stress testing.(84) A potential solution to the problem of caffeine in adenosine stress testing has been developed by Hurwitz et al in 1999. An adenosine challenge and boost protocol was used, whereby patients who had consumed caffeine within 24 hours of stress testing had a 6mg bolus of adenosine given and if there was a physiological

response the patient could go ahead and have this stress test performed. This was known as the adenosine challenge test. In patients, during a pharmacological stress test, who don't exhibit any symptoms a similar bolus of 6mg can be given to help validate the test. In this study 98 patients received the challenge test as they had inadvertently ingested caffeine prior to their perfusion scan. Using the challenge test 96% of these patients were able to proceed and have the standard stress infusion. Fifteen patients received an adenosine boost due to a lack of symptoms, of whom 14 were felt to have had a valid result of their nuclear perfusion scan. The authors conclude that these 2 protocols were useful and cost efficient adjuncts to pharmacological stress testing in the setting of myocardial perfusion imaging. This was felt to preserve health care resources and ensured more patients undergo appropriate stress testing.(85) In the UK, to our knowledge, this protocol has not been adopted by many centres. Interestingly recent research has closed the debate of whether long term habitual coffee consumption is associated with an increased risk of coronary heart disease. A prospective cohort study of 44005 men and 84488 women has concluded that there is no evidence that coffee consumption increases the risk of coronary heart disease.(86)

In the present research project we plan to examine the haemodynamic effects of adenosine during first pass magnetic resonance myocardial perfusion imaging and also assess the symptoms produced. Caffeine levels will also be recorded and correlated with symptoms and haemodynamic response. This has not previously been looked at in the setting of magnetic resonance myocardial perfusion imaging (MRMPI).

1.6 Late Gadolinium Enhancement Following PCI and CABG

Gadolinium is an extra cellular T1 enhancing contrast agent that is commonly used in contrast enhanced MRI examinations and is not specific to the heart. It has 7 unpaired

electrons and a large magnetic moment and when placed in a magnetic field the T1 relaxation time of hydrogen ions and water are reduced producing high signal intensity on T1 weighted images. Gadolinium is a rare earth metal and is present in the composition of most clinically approved contrast agents. It is included in ionic complexes with a chelation compound, such as diethylenetriaminepentaacetic acid as it cannot be excreted by the body in its unbound form. During first pass myocardial perfusion imaging the gadolinium perfuses into the interstitium of the myocardium in a rapid homogenous fashion in segments supplied by normal coronary arteries. Three minutes after gadolinium injection, late gadolinium enhancement images can be obtained. During this time an equilibrium exists between the blood and interstitium. If there has been any myocyte damage as in the case of myocardial necrosis following a MI, gadolinium can enter the intracellular space providing a differential enhancement. Over a period of several minutes the gadolinium which has penetrated the intracellular space will diffuse back into the blood pool and is eventually excreted by the kidneys. Whilst the gadolinium is present within the intracellular area of damaged cardiac myocytes, imaging can be performed in order to delineate abnormal from normal myocardium. Unfortunately scar tissue and viable myocardium do not have different T1 or T2 relaxation times and therefore it is essential to administer a freely diffusible contrast agent. In the initial phase after cell death enhancement is thought to be due to an increase in distribution volume, whereas in the chronic setting there is an increase in the interstitial space due to cell loss and scar formation. In a canine model the pattern of gadolinium enhancement accurately reflects infarct size as measured by triphenyltetrazolium chloride (TTC) staining on histology.(87;88) Bearing in mind that magnetic resonance imaging has very high spatial resolution, we can accurately measure the volume and transmurality of late gadolinium enhancement which reflects scar tissue which is useful in the clinical setting in determining which patients have viable

myocardium and therefore a probability of functional recovery following revascularisation. Greater than 50% transmurality of late gadolinium enhancement is one cut-off used to identify potentially irreversible myocardial dysfunction.(89) Late gadolinium enhancement is specific for myocardial damage, however this may not necessarily be due to coronary artery disease as it can also be caused by hypertrophic cardiomyopathy, infiltrative conditions such as cardiac sarcoidosis, arrhythmogenic right ventricular dysplasia, and myopericarditis. Gadolinium at a dose of 0.1 to 0.2mmol/kg is used for this type of imaging. Following a few minutes the dose of gadolinium in the blood pool should have dropped significantly to allow for late gadolinium enhancement imaging. During the period when the dose of gadolinium in the blood pool is high imaging can be performed to look for microvascular obstruction. These are areas of hypo-enhancement which commonly occur after an acute MI. In order to detect late gadolinium enhancement it is essential to null normal myocardium so that this appears black and that areas of myocardial necrosis appear bright. This is done using an optimal pre-pulse delay by applying a 2D inversion recovery sequence with differing inversion times selecting the one which provides the best suppression of normal myocardium. This is performed in both long and short axis planes covering the entire left ventricle.

Gadolinium can cause some mild side effects, including nausea, vomiting, mild headache, rash and GI upset. Mild hypotension and a slight increase in bilirubin and blood iron has also been reported. Contra-indications to the administration of gadolinium include haematological disorders, such as haemolytic anaemia and sickle cell anaemia. Pregnancy is also a contra-indication. More recently renal failure with an estimated glomerular filtration rate of less than 30 ml/min/1.73m^2 have been accepted as a contraindication following reports of nephrogenic systemic fibrosis (NSF).

In recent years there has been some interest in the use of late gadolinium enhancement following coronary revascularisation by either PCI or CABG. Minor elevations in creatinine kinase (CK) MB isoenzyme following PCI is a common finding.(90-92) A previous study in 2001 has shown that CK-MB elevation following stent placement is a result of myocardial necrosis.(93) Choi et al aimed to assess if impaired or declining tissue level perfusion measured using the TIMI myocardial perfusion grade was associated with any degree of myocardial necrosis using the late gadolinium enhancement technique.(94) The study recruited 14 patients who had gadolinium enhanced MRI performed soon after successful elective PCI. Nine patients (64%) had elevated CK-MB levels. The remaining 5 patients served as controls with no release of CK-MB. Late gadolinium enhancement images were performed after 0.1mmol/kg of gadolinium and wall motion and contrast enhancement were assessed by 2 observers. The coronary angiograms were analysed offline and TIMI flow grade was recorded along with TIMI myocardial perfusion grade (TMPG). All patients had TIMI 3 flow before and after stent deployment and had no angiographic evidence of acute vessel closure or distal embolisation. No major side branches were occluded in addition. The median CK-MB was 21ng/ml in those patients with elevated CK-MB. Each of these patients had evidence of hyper-enhancement by CMRI within the target vessel perfusion territory. Three patients with minor side branch occlusion had late gadolinium enhancement adjacent to the implanted stent and the remaining 6 patients had late gadolinium enhancement further down stream in the myocardium supplied by the stented artery. A TMPG score of ≤ 1 indicating minimal dye entry into the myocardium or minor side branch occlusion was significantly higher in the group with elevated CK-MB levels ($p=0.02$). A reduction in TMPG score was seen in 5 patients within the elevated CK-MB group whom had significantly greater CK-MB elevations and larger

mass of late gadolinium enhancement. Reduction in TMPG score was noted in those patients with the most extensive myonecrosis with CKMB levels greater than 3 times normal and a hyperenhancement mass greater than 3 grams (p=0.03). This study provides an understanding of the mechanism of myonecrosis following stenting as a decline in the TIMI myocardial perfusion grade score indicates the presence of microvascular obstruction.(94) This may be clinically relevant as microvascular obstruction in the setting of an acute MI is associated with increased mortality independent of the restoration of TIMI grade 3 blood flow down the coronary artery. It has been postulated that disruption of the fibrous cap of coronary atheroma can lead to platelet emboli. The contents of an atheromatus plaque, including lipids, matrix, endothelial cells and platelets can embolise down a vessel and cause obstruction of the microvasculature. In 2004 a study was published in the European Heart Journal looking at peri-operative MI in patients undergoing coronary artery bypass surgery.(95) This again was performed using contrast enhanced magnetic resonance imaging. A number of previous studies had shown that coronary artery bypass was associated with an elevation in cardiac enzymes.(96-98) Following bypass surgery elevated CK-MB is associated with a risk of long term mortality.(99) It was uncertain whether elevated cardiac enzymes were due to surgical trauma, ischaemia due to inadequate revascularisation or graft occlusion causing infarction. From an original group of 60 patients, there were 23 with no previous history of MI and normal pre-operative ECG and left ventricular function. All patients underwent on pump CABG and patients were selected for the study on the basis of day 1 post-operative CK-MB concentrations. Patients were selected in order to have a scattering of levels. After including 15 patients with a CK-MB <20μg/L, patients were thereafter only selected if their CK-MB was ≥20μg/L. Plasma CK-MB and troponin I levels were measured at days 1, 2 and 4 and cardiac MRI was performed between days 4 and 9 post-operatively. A gadolinium dose

of 0.2mmol/kg was used in order to detect late gadolinium enhancement. Evidence of MI was found in 18/23 (78%) patients. The median mass of necrosis was 4.4 grams. A moderate correlation was found between CK-MB and infarct mass on day 1 post-CABG ($r=0.54$, $p<0.01$). There were also correlations between troponin I levels and infarct mass with the r values varying between 0.46 and 0.53 when measured on days 1, 2 and 4 and for troponin T, r values varied between 0.38 and 0.5 for the same time intervals. The authors conclude that peri-operative elevations in CK-MB, troponin I and troponin T correspond with peri-operative MI. This corresponded to a consensus report suggesting increases in CK-MB to 5 times above the upper limit led to peri-procedural myocardial injury.(100) One of the limitations of this study was that no dedicated cardiac coil was used and the images acquired were only in 2 dimensions. This may have underestimated infarct sizes. However, despite this, good inter-observer agreement was achieved between the 2 radiologists. Another important consideration is that of infarction of the right ventricle which is not reliably detected unless right ventricular hypertrophy is present. This study did not examine infarctions of the right ventricle.(95)

A number of studies have shown evidence of myocardial injury following PCI by measuring levels of troponin T, troponin I and CK-MB.(101-104) Selvanayagam et al in 2005 examined troponin elevations following PCI and also performed late gadolinium enhancement MRI imaging to measure the extent of myocardial necrosis.(105) Fifty patients were included in a study who were either due to have: 2 vessel PCI; insertion of greater than 30mm of stent to a single vessel; or planned treatment involving a side branch of greater than 2mm diameter. MRI imaging was performed within 24 hours of PCI and 24 hours post procedure. Twenty four patients had a third MRI 7 to 8 months post PCI. All patients received aspirin, clopidogrel, heparin and intravenous abciximab. Cardiac magnetic resonance (CMR) images were analysed off-line by a single observer

and areas of late gadolinium enhancement were quantified using computer assisted planimetry. Troponin I levels were measured before and at 24 hours post-PCI. CMR and troponin results were available for 48 of the 50 patients recruited. The average stent length was 24mm +/- 13mms and the average lesion length was 15mms +/- 6mms. Post PCI, 14 patients had evidence of new late gadolinium enhancement (29%) with a mean mass of 6.0 +/- 5.8grams. Each of these patients had raised troponin levels. In 6 of the 14 patients (43%) with new late gadolinium enhancement this was located adjacent to the stent indicative of side branch occlusion and in the remaining 8 (57%) this was located in the apical myocardium distal to the stent. All 14 patients with late gadolinium enhancement had troponin elevations with a mean of 3.7 +/- 3.0μg/l. A strong correlation existed between the increased troponin I measurements at 24 hours and the mean mass of new late gadolinium enhancement (r=0.84 at 24 hours and r=0.71 after late scanning). Eleven patients who had post PCI troponin elevation and late gadolinium enhancement underwent a repeat scan at a median of 240 days post PCI. There was a strong trend for the mass of late gadolinium enhancement to decrease from 5.4 +/- 4.8grams in the acute post PCI scan to 3.8 +/- 5.0 grams in a later scan (p=0.07). There were no changes in the control group who had no new late gadolinium enhancement post PCI. Stent length was significantly associated with post-PCI late gadolinium enhancement (p=0.04). However, interestingly lesion length was not associated with new late gadolinium enhancement. In conclusion, 30% of patients developed irreversible myocardial injury following complex PCI. The magnitude of late gadolinium enhancement correlated well with the magnitude of troponin I elevation. These events occurred despite optimal use of anti-platelet therapy including abciximab and heparin.(105) A similar study was performed by the same group from Oxford, England in 2006.(106) Fifty-two patients had PCI performed, however on this occasion an intravascular ultrasound examination (IVUS) was performed on each of the arteries

studied. CMR was performed pre and 24 hours post PCI as in the previous study and the pattern of late gadolinium enhancement was defined as being distal or adjacent. Angiograms were analysed for TIMI myocardial perfusion grade and TIMI corrected frame count. Fifteen coronary territories (23%) had evidence of new late gadolinium enhancement on the post PCI scan. Eight of these (53%) demonstrated distal late gadolinium enhancement and 47% had adjacent late gadolinium enhancement. There was no difference in the mean mass of late gadolinium enhancement between the 2 distributions of necrosis with a mean mass of 7.6 +/- 6.2 grams (p=0.6). There was a greater reduction in plaque volume in a distal late gadolinium enhancement group compared to those patients with adjacent late gadolinium enhancement or no new late gadolinium enhancement ($p<0.001$). A significant correlation was reported between change in plaque volume post PCI and the mass of new late gadolinium enhancement ($p<0.001$). Closed microvasculature after PCI predicted recurrence of new late gadolinium enhancement with an odds ratio of 8.0 (95% confidence intervals were 1.4 to 46.1 and p=0.02). Side branch occlusion had an odds ratio of 16.2 (95% confidence interval was 2.6 to 102.5, p=0.03) for occurrence of new late gadolinium enhancement. This study suggested that impaired flow in the side branches of coronary arteries and distal embolisation of plaque material contribute to myocardial necrosis found during PCI. Side branch occlusion was associated with adjacent myocardial necrosis to the implanted stent, whereas distal necrosis was a result of embolisation of atheromatous plaque. Interestingly the volume of embolised material was directly proportional to the measured amount of late gadolinium enhancement indicative of myocardial necrosis. The relevance of this new late gadolinium enhancement was highlighted in a study by Kwong et al Circulation 2006 where small areas of late gadolinium enhancement (1.4% of LV mass) noted in patients without previous MI led to a greater than 7 fold increase risk of major cardiovascular events, possibly as a result of increased substrate to life

threatening arrhythmia and also the greater associated burden of atherosclerosis.(107) This may be clinically relevant bearing in mind greater than 900,000 procedures are performed annually in North America.(108) In addition, increasing numbers of percutaneous coronary procedures are being performed in the United Kingdom with a reduction in the incidence of coronary artery bypass surgery.

Selvanayagam et al, with a similar study population, went on to look at myocardial perfusion reserve index following PCI.(109) In this study 40 patients had pre-PCI and 24 hour post-PCI late gadolinium enhancement imaging and first pass myocardial perfusion imaging at rest and stress. These patients had either 1 or 2 vessel coronary disease scheduled for complex PCI with insertion of greater than 30mm of stent to a single vessel or treatment involved at least 1 major side branch or 2 vessel PCI. Myocardial blood flow was determined using deconvolution of the signal intensity over time curves with the blood pool AIF. The myocardial perfusion reserve index (MPRI) was calculated as a ratio of hyperaemic to resting myocardial blood flow. Twenty one patients (53%) had evidence of new distal late gadolinium enhancement post-PCI. The MPRI in these segments of late gadolinium enhancement measured 2.16 pre-PCI and 2.00 post-PCI ($p<0.001$). The mean MPRI in those segments without new late gadolinium enhancement significantly increased post procedure from 2.06 to a mean of 2.52 post-PCI ($p<0.001$). There was a significant increase in myocardial blood flow in those areas with late gadolinium enhancement late after PCI compared to 24 hour post PCI ($p=0.03$). This study showed that in segments of new late gadolinium enhancement post PCI there is a transient reduction in myocardial perfusion reserve index at 24 hours, which improves by 6 months. The study also showed that a reduction in MPRI is confined to the segments of myocardial injury and doesn't affect the entire area of myocardium supplied by the vessel which underwent PCI. It is thought that the

reduction in hyperaemic flow at 24 hours post-PCI is due to myocardial necrosis and extensive macrovascular and microvascular plugging of the distal vascular bed.(109)

In our current study we have looked at the presence of late gadolinium enhancement pre and post-PCI and CABG. In those patients who had PCI performed troponin I measurements were made at 12 hours post procedure and correlated with mass of late gadolinium enhancement measured at 24 hours and 4 weeks. Myocardial perfusion reserve index (MPRI) measurements have also been made from the MRMPI scans in the PCI group prior to, at 24 hours and at 4 weeks following PCI and in the coronary artery bypass group prior to surgery and at 4 weeks post surgery.

2 Research Aims

The main aim of this research is to determine the true sensitivity, specificity, positive and negative predictive values of qualitative and semi-quantitative magnetic resonance myocardial perfusion imaging (MRMPI) for the diagnosis of haemodynamically significant coronary disease as defined by FFR.

Measure the inter-observer variability in the qualitative assessment of MRMPI and the semiquantitive measurement of MPRI.

Determine if false positive MRMPI scans are due to microvascular coronary disease as assessed by CFR and IMR and if MRMPI can detect isolated microvascular disease.

Determine the rate of occurrence of troponin release post-PCI and compare this with the development of new late gadolinium enhancement (LGE).

Assess the frequency and extent of new LGE following PCI and CABG.

Investigate the symptomatic and haemodynamic effects of intravenous adenosine on patients during perfusion imaging and the influence serum caffeine levels has on these parameters.

3 Methods

3.1 Patients

We recruited 103 patients between November 2004 and April 2006. All patients had chest pain suspected to be angina with initial investigations leading to them being referred for coronary angiography +/- PCI. A flow diagram of the course of the study is shown on Figure 3.1. We recruited all patients aged between 18 and 80 with chest pain referred for angiography for standard clinical indications to one consultant cardiologist and in whom we were able to obtain fully informed written consent. Exclusion criteria included patients who had suffered a MI with evidence of ongoing ischaemia in the 48 hours preceding the study; pregnancy and atrial fibrillation. Standard contraindications to MRI were also excluded including pacemakers, cochlear implants, certain metal surgical prostheses, certain aneurysm and vascular clips, metal intraocular foreign bodies and certain prosthetic heart valves. Patients with contraindications to the use of adenosine which was the agent employed to induce maximal hyperaemia during both perfusion imaging and pressure wire studies were excluded including asthma, 2^{nd} or 3^{rd} degree atrio-ventricular block, sick sinus syndrome and patients taking dipyridamole. Patients with contraindications to gadolinium such as sickle cell and haemolytic anaemia were also excluded. During the course of this research study concern arose regarding the safety of gadolinium compounds in patients who suffer from renal failure with cases of nephrogenic systemic fibrosis (NSF) being reported. Thus, gadolinium is no longer administered to patients with an estimated glomerular filtration rate of $<30ml/min/1.73m^2$.(110-114)

Figure 3.1 - Study Flow Chart and Design

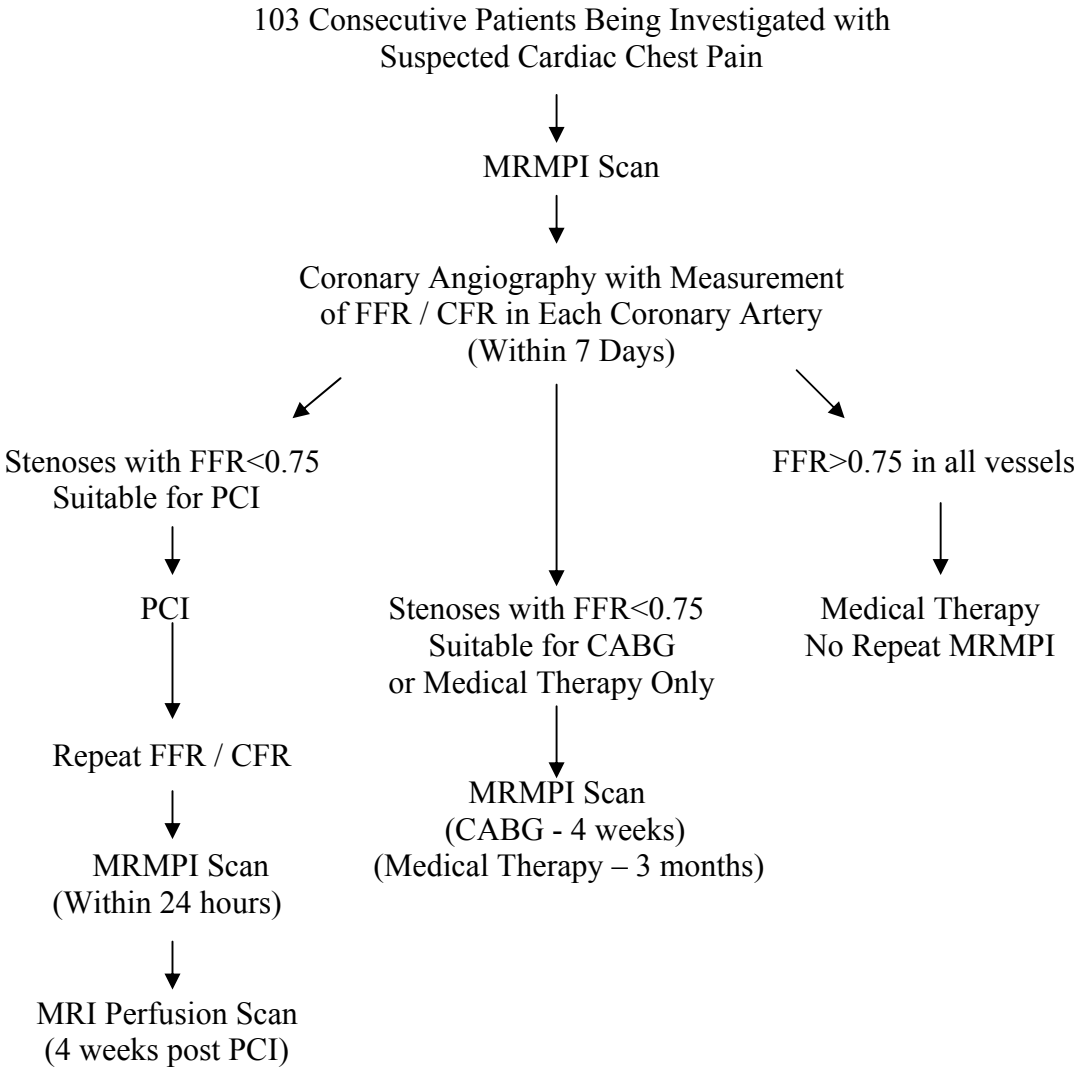

Patients selected for entry into the study would initially attend for an MRMPI scan. At this time a risk factor profile for coronary disease was obtained as well as weight and height measurements and a Canadian Cardiovascular Study angina grade was determined. A venous blood sample was taken for a biochemical and haematological profile including urea and electrolytes, liver function tests, random glucose and lipids, full blood count and coagulation screen. An MRMPI scan was then performed as documented in section 3.2. Within one week in the majority of cases the patients would then have a diagnostic coronary angiogram with fractional and CFR measurements and

the index of microcirculatory resistance made in each of the coronary arteries, excluding small non-dominant vessels. The details of this are contained in section 3.3. Those arteries with evidence of significant coronary artery disease would then go on to have PCI performed if this was felt to be both feasible and if bypass surgery was not indicated. PCI would be performed using standard techniques and following stent deployment further invasive haemodynamic measurements would be made (FFR and CFR) ensuring that the post-PCI FFR is greater than 0.9. Those patients who had PCI performed were invited to return for a repeat MPMRI scan at both 24 hours and 4 weeks following the procedure. Prior to the 24 hour scan venous blood was taken for a troponin I level and urea and electrolytes. The same scanning protocol was adhered to for each of the scans. Patients who were found to have significant multi-vessel coronary artery disease or left main stem disease which was felt to be best managed by coronary artery bypass surgery (CABG) were referred to a cardiothoracic surgeon. Following CABG patients were invited to return for a MRMPI scan at 4 weeks. Patients who were found to have significant coronary artery disease but were managed medically were invited to return for repeat scanning at 3 months following their coronary angiogram. Those patients with no significant coronary artery disease took no further part in the study. At the time of each MRMPI scan, CCS angina grade was recorded and a note of medication taken. A 12 lead ECG was also taken to ensure there was no high degree of AV block prior to MRMPI scanning and adenosine stress.

3.2 First Pass Magnetic Resonance Myocardial Perfusion Imaging (MRMPI)

In the week preceding the MRMPI scan patients were sent details of which caffeinated products to avoid prior to the scan and also their coronary angiogram (See appendix 8.1). Prior to scanning a MRI safety checklist was completed for each patient. Two 18G venous cannulae were inserted (one into each antecubital fossa). ECG electrodes were

positioned to achieve the best possible signal within the magnetic field of the scanner and a blood pressure cuff was secured to the non-adenosine arm. Scanning was performed using a Siemens Sonata 1.5T (Erlangen, Germany) scanner using a six channel anterior chest coil and spinal coils within the gantry table. Following the acquisition of localising images and a HASTE block of the thorax we obtained long and short axis cine images using a retrospectively gated TrueFISP sequence. Details of the scanning sequences used are documented in Appendix 8.2. The short axis cine scans were used to determine left ventricular mass, volume and function. Patients were then stressed using intravenous adenosine (140mcg/kg/min) which ran for 2 minutes prior to acquisition of stress perfusion images. Appendix 8.3 shows the infusion rate chart used for the study. A bolus of contrast medium, gadolinium-diethylenetriamine pentaacetic acid bismethylamide (Omniscan, Amersham Health, Oslo, Norway), was then injected at a rate of 5ml/sec using a power injector (Medrad, Pittsburgh, PA). The gadolinium dose used was 0.1mmol/kg. The three short axis slices were imaged during the first pass of the bolus of gadolinium using a TurboFLASH sequence (TE 0.99; TR 173; TI 90; Flip Angle 8^{o}; Slice Thickness 8mm; Slices 3; FOV 213x340; Matrix 80x128; Spatial Resolution 2.7x2.7mm^2; Bandwidth 780Hz/pixel). This pulse sequence was chosen as we had previous experience in its use and was able to get 3 slices per R-R interval in all patients. The turboFLASH sequence also produces excellent myocardial contrast during the first pass and has been used in many previous studies especially those using the same make of scanner (table 1.2). The three slices were chosen in order to include a section of the basal, mid and apical LV and therefore covering 16 of the 17 segements of the AHA coronary arterial territory model.(10) This pulse sequence was only slightly modified from that provided with the Siemens Sonata scanner in order to create a square pixel as opposed to a rectangular pixel. This allowed acquisition of three slices within 519ms and comfortably within a single R-R interval in all patients. Heart rate and blood

pressure were recorded prior to adenosine stress, during peak stress and 2 minutes following termination of the adenosine infusion (Schiller, Switzerland), in order to determine if patients were adequately stressed. Following the first pass, early gadolinium enhancement images were obtained using a segmented TrueFISP sequence looking for evidence of microvascular obstruction up to 5 mins following the bolus. We then collected a series of images during end-expiratory breathold in both the long and short axis planes looking for late gadolinium enhancement using a turboFLASH sequence. An inversion time of 320msecs was initially chosen for the vertical long axis slice and depending on the degree of myocardial nulling this figure was altered accordingly. Once twenty minutes had elapsed since the initial bolus of gadolinium, we repeated the first pass perfusion sequence at rest using a further bolus of gadolinium (0.1mmol/kg).

3.2.1 Qualitative Analysis of MRMPI Scans

The perfusion imaging analysis was performed by two blinded observers. The oberservers had received extensive training at different centres (Royal Brompton Hospital, London and St. Joseph's Hospital, Atlanta) and were experienced in the qualitative analysis of clinical and research MRMPI scans with approximately 2 years experience. Both observers viewed the three stress and rest slices simultaneously using a commercially available viewing package (CMR tools, Imperial College, London). In order to ensure that the observers were blinded to patient identity details, patient name was omitted from the casing and replaced by a number following the completion of the scan. In addition the scans were loaded onto the viewing software by an independent party and the patient's name and date of birth was removed prior to analysis of the scan. Both observers scored each of the 16 AHA segments as normal perfusion or hypoperfusion and then decided if they felt the patients were likely to have one, two or

three vessel coronary artery disease or had normal coronary perfusion. Dark rim artefacts were identified if they occurred at the interface between the LV blood pool and the endocardium typically affecting the interventricular septum and lateral walls. These artefacts tended to be one pixel in diameter and commonly when the LV blood pool reached its peak signal intensity and lasting less than 5 cardiac cycles. We viewed the stress and rest scans together which aided the identification of these artefacts and they tend to occur at both states. Coronary artery territories were scored as per the AHA model shown in Figure 3.2. If there was disagreement between observers then a third observer was used to adjudicate.

Figure 3.2 - Coronary Artery Territory Model(10)

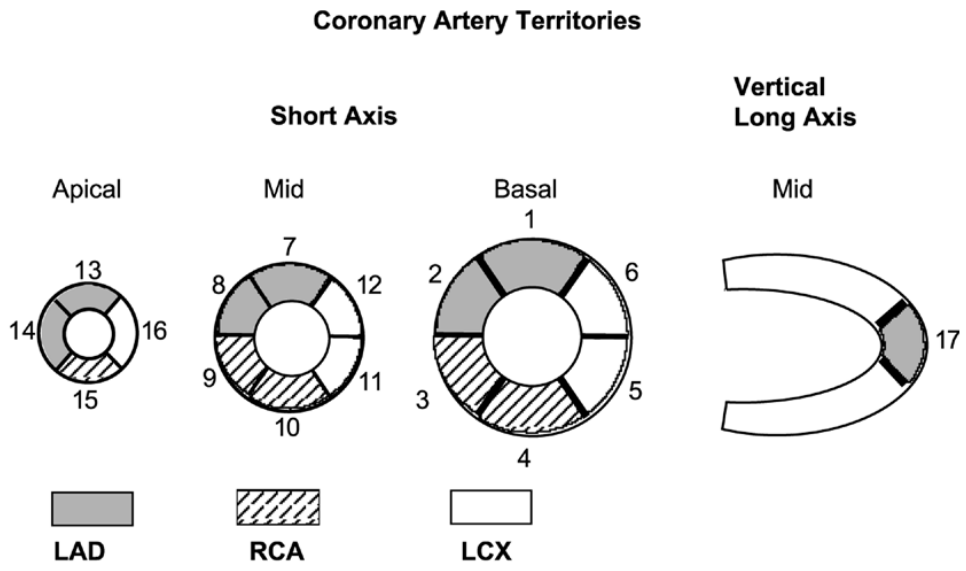

3.2.2 Myocardial Perfusion Reserve Index (MPRI)

Semi-quantitative measurements of MPRI were made using three different methods. Each of these methods used data from the signal intensity time curve of the different sectors of left ventricular myocardium as defined by Cerqueria in 2002.(10) The software used for this analysis was developed by Dr Murdoch Norton, Department of Physics, University of Aberdeen at Aberdeen Royal Infirmary. There are few commercially available software packages for this purpose, none are widely used and

they all have technical problems. Our program is relatively simple to use and incorporates all the steps of analysis that would be provided by a commercial software package.

To begin the analysis the program searches through the scan file and highlights the sequence DICOM headers from which we select the stress perfusion sequence. This scan is then viewed as a movie. Movements due to breathing and cardiac motion are then aligned such that the left ventricular images in each of the 50 images per slice are precisely aligned on top of one another. This process is performed by a program called ImageJ which is a Java based image processing program widely used in radiological studies which use DICOM files.(115) For extreme movements which are not corrected for by ImageJ manual correction is then performed image by image by the observer. If a good breath hold has been achieved this is not too time consuming for resting images however it is usually worse for the stress images where patients feel short of breath due to the adenosine infusion. Once all the images (50 images for each of the 3 slices of myocardium) are aligned we then manually select a single subendocardial region of interest around the left ventricle starting at the right ventricular insertion point with the left ventricle for each of the three slices. Using a computer mouse the operator would draw a freehand region of interest excluding the border between the LV blood pool and the endocardium where artefact is common. This region of interest would be confined to the subendocardium and no sub-epicardial contour was drawn. An example of the analysis screen at this point is shown in figure 3.3. The program would then divide the basal and mid LV slices into 6 myocardial segments and the apical slice into 4 slices as shown in the coronary artery territory model (Figure 3.2). The average signal intensity for the pixels within each of the myocardial segments is calculated for all 50 images which is plotted to give signal intensity / time curves for each myocardial segment so

that we have 16 stress curves. The baseline signal intensity of the myocardium at both stress and rest prior to the gadolinium bolus is recorded and subtracted from the signal intensity / time curves in order that the curves start with a signal intensity of zero units. Figure 3.4 provides an example of a normal signal intensity curve for a myocardial segment compared to figure 3.4 which is an example of a segment with significant coronary disease.

Figure 3.3 – Perfusion analysis software showing the selected subendocardial region of interest.

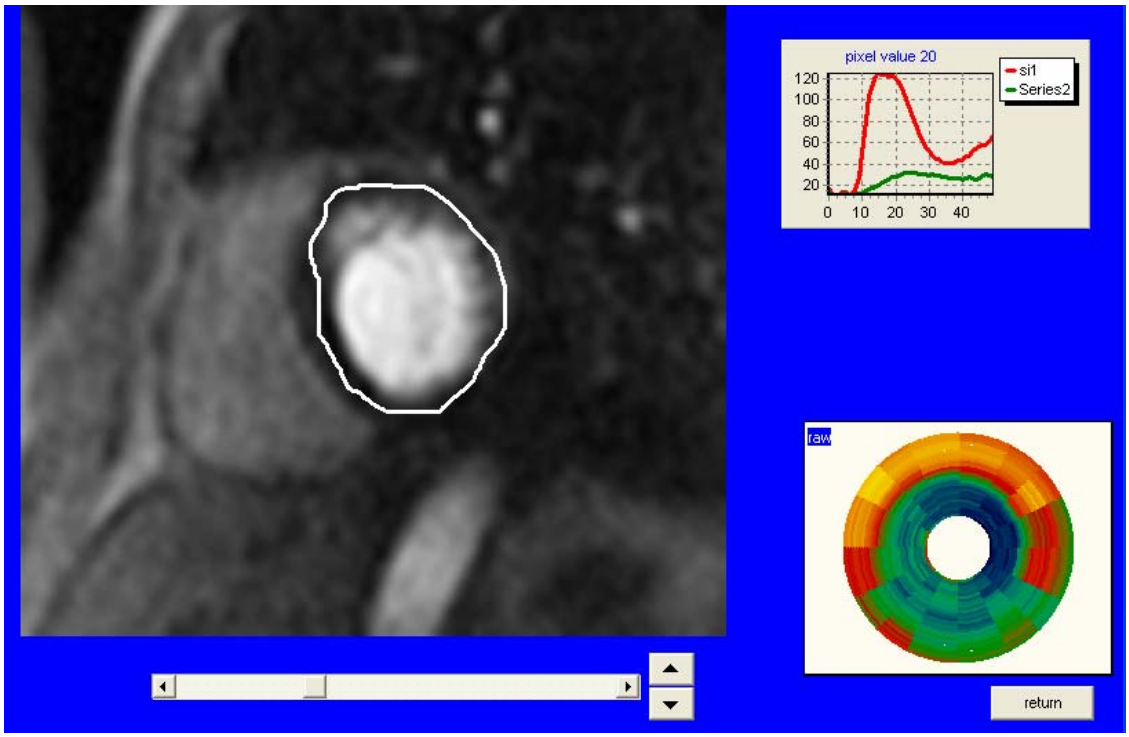

Figure 3.4 - Signal intensity v time curve of a myocardial segment supplied by a physiologically normal coronary artery (FFR=0.98, CFR=4.7). The signal intensity is plotted on the y axis and image number is plotted on the x axis which is a function of time. The red line shows the brisk up slope of the gadolinium as it perfuses the myocardium and then washes out.

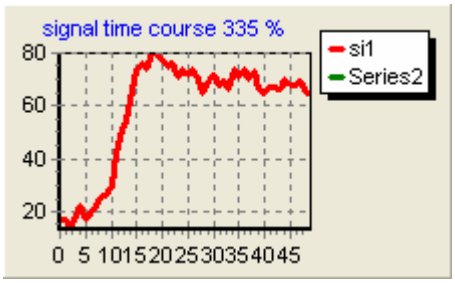

Figure 3.5 - Signal intensity v time curve of a myocardial segment supplied a physiologically abnormal coronary artery (FFR=0.56, CFR=1.4).The red line takes longer to reach its peak and does not achieve as high a signal intensity as the normal segment in figure 3.4.

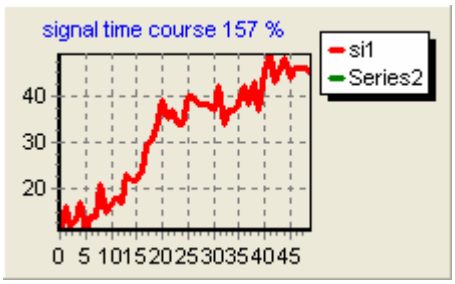

This process is then repeated for the rest images to give our 16 rest curves and the data saved for analysis. A signal intensity / time curve is also obtained at stress and rest for the LV blood pool which provides our AIF. An example of the signal intensity v time curve for the AIF is provided in figure 3.6. The analysis of these curves is then performed by IDL (Interactive Data Language) which is a software program commonly used for processing large amounts of image data using a unique data analysis language.

We start the analysis with the stress curves. The first method of calculating MPRI we performed was the measurement of the upslope of the signal intensity curve as the gadolinium perfuses through the myocardium. This is performed by manually selecting the base and peak points of the upslope from which the program looks for the maximum upward gradient in the selected data region. These data are then stored for each of the myocardial segments and for each slice. The maximum signal intensity of the gadolinium bolus within the myocardial segments is then selected and again these data are stored.

Figure 3.6 - Signal intensity v time curve of the AIF. Note the curve is clipped at its peak due to the dose of gadolinium being too high for the range of pixel intensities of the scanner.

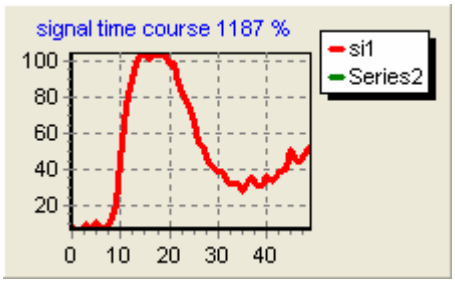

The Fermi method is a more automated process which the IDL program performs with very little observer interaction. The Fermi method assumes that if we convolve the function describing the delivery of the gadolinium i.e. the AIF, with a Fermi function, we will generate a response function which looks like the time course of the signal obtained from a region of myocardium.(116) The correct Fermi function is identified which generates the actual myocardial signal time course. The analysis program then generates multiple Fermi functions and convolves them with the measured AIF to find which best fits the signal uptake curve for each of the myocardial segments. This is performed using a non linear method of least squares fitting. The defining parameters of

the best fitting Fermi function provide the expected flow to that myocardial segment. The principal benefit of the Fermi method is that it uses all the measured data maximising the amount of information experimentally measured from the study. It also takes into account the bolus variation (AIF) in different studies.

This entire process is then repeated for the rest signal intensity / time curves. The program then automatically divides the stress values for all three methods by the rest values for each of the myocardial segments per scan. This provides MPRI values for 16 segments per scan by the three methods. Therefore 48 data points are collected per scan. Two observers analysed each of the scans in the study. For analysis of this data the mean MPRI value was calculated for each of the coronary arteries by dividing the sum of MPRI's for all the segments within the coronary territory by the total number of segments as defined by the AHA model.(10) We also used the lowest MPRI value within each of the coronary territories in the statistical analysis. This process was repeated by both observers for the three different methods of calculating MPRI. A schematic of the functions of this analysis program is highlighted in figure 3.7. In the final analysis the data for each territory was averaged between observers to provide an overall mean MPRI. The MPRI data by each observer was compared to assess interobserver variability using Bland-Altman plots.

Figure 3.7 - Schematic of MPRI analysis software functions

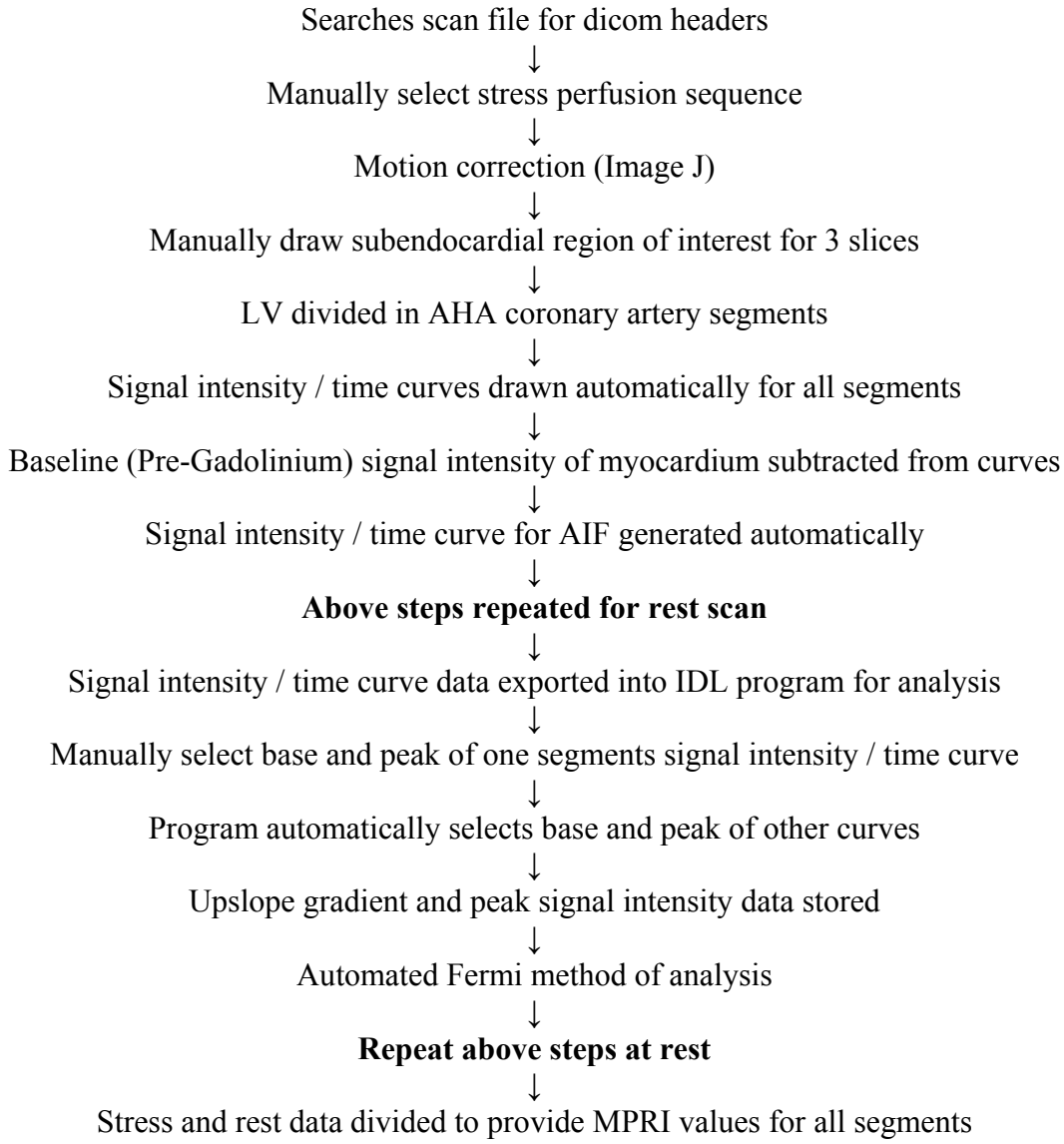

3.2.3 Left Ventricular Mass and Volume Analysis

LV mass, volume and ejection fraction analysis was performed by two observers blinded to patient details and the results of the perfusion MRI and pressure wire study. Results were obtained using Argus Dynamic Signal (Siemens, Erlangen, Germany) by drawing endo and epicardial contours using the short axis cine images at both end diastole and end systole. This provided us with left ventricular end-diastolic volume and end-systolic volume from which we were also able to calculate the ejection fraction and

the stroke volume. Using the patient's heart rate we were also able to calculate cardiac output. At end-diastole we also drew an epicardial border which allowed us to calculate LV mass in grams.

3.2.4 Late Gadolinium Enhancement Mass Analysis

By using the same software as to calculate LV mass, volume and ejection fraction (Argus Dynamic Signal) we were also able to draw around regions of late gadolinium enhancement pre and post PCI and CABG. No automated signal intensity based software was used in this analysis which was purely planimtery based. Both observers were instructed not to alter the windowing of the images prior to drawing around the areas of LGE. The volume of these regions was calculated for each slice of myocardium and collated to give a total volume. This value was multiplied by 1.06g/ml – the specific gravity of myocardium to provide us with the mass of infarcted myocardial tissue.

3.3 Coronary Angiography

On the day of the coronary angiogram patients had an 18G venous cannula inserted into the left antecubital fossa for the intravenous adenosine infusion during the pressure wire study. Patients had been instructed to abstain from caffeine containing products for the preceding 24 hours. Fully informed written consent for the coronary angiogram +/- PCI was obtained prior to entering the cardiac catheterisation laboratory. Patients were pre-treated with clopidogrel prior to the day of the angiogram in case PCI was indicated. Angiography was performed at either the Western Infirmary or the Golden Jubilee National Hospital in Glasgow using a General Electric (GE) Innova 2100 catheterisation laboratory. Arterial access was obtained in the vast majority of patients from the right radial artery using a 6F sheath. A sterile field was then created around the patient. Guide

catheters were used for the purposes of our diagnostic images and in the vast majority of patients we used an EBU3.5 (Medtronic, Launcher) for cannulation of the left coronary ostium and a JR4 (Medtronic, Launcher) for the right coronary ostium. Intracoronary glyceryl trinitrate (200µg) was injected following cannulation of the coronary arteries to reduce the occurrence of coronary artery spasm. We obtained cine coronary angiogram images in the standard planes for offline quantitative coronary angiographic (QCA) analysis. All patients had left and right anterior oblique images in both the cranial and caudal positions. Depending on the coronary anatomy other appropriate views were acquired.

3.3.1 Quantitative Coronary Angiography (QCA)

QCA was performed using GE automated edge detection software which calibrates using the coronary guide catheter as its reference diameter (Centricity Cardiology CA1000, GE). This method of analysis was validated in 2004.(117) Two observers blinded to all patient demographic and clinical details analysed each of the coronary angiograms. Both observers (the author of this thesis and a cardiac technician with over 10 years of clinical trial and core laboratory experience) had been trained by a GE representative and had clinical and research experience of this software and older software packages. Both observers would mark the region of interest within a coronary artery which they felt was the most severe region of coronary arterial disease. The software would then calibrate the minimal luminal diameter, reference vessel diameter (prior to a stenosis), lesion length and ideal vessel diameter at stenosis. From these figures the % DS and area of stenosis were calculated. No manual override of the generated contours was possible with this software package, however should the reference vessel diameter or minimal luminal diameter be affected by a side branch then the position of these measurements could be altered as appropriate. In the event of an

ostial stenosis then the reference vessel diameter was selected from the closest section of normal appearing artery distal to the stenosis. The two observers performed this for at least 3 coronary arteries per patient depending on circulatory dominance and number of occluded arteries. For occluded arteries only the reference vessel diameter was recorded where possible. Both observers were blinded to patient details, the pressure wire results and patient outcome.

3.4 Troponin I Measurement

This was performed in all patients who underwent PCI. Serum samples were collected at approximately 24 hours following PCI and transferred immediately to the biochemistry laboratory Samples were analysed by an immunoassay technique on a biochemistry analyser (Abbott Diagnostic Instruments Ltd, Architect ci8200, Berkshire, England). The lowest limit of quantification in our laboratory was 0.04µg/L. The coefficient of variation for a mean value of 0.137 was 5.8%, for 0.528 was 7.2% and for 13.591 was 6.8%.

3.5 Coronary Pressure Wire

Following the acquisition of the diagnostic coronary angiogram images patients would then have a coronary pressure wire study performed. The coronary pressure wire used in this study is a 0.0014 inch high fidelity wire with a sensitive temperature and pressure sensor 3 cm from its tip (Pressure Wire 5, RADI Medical Systems Ltd, Uppsala, Sweden). Figure 3.8 shows a RADI pressure wire which was used to provide us with the data required for the calculation of the FFR, CFR and the index of microcirculatory resistance (IMR). In addition to this the pressure wire also serves as a high performance guidewire for the delivery of balloons and stents for PCI. The 3cm tip of the wire is

made of platinum and can be easily shaped depending on the tortuosity of the artery to be interrogated. In addition the tip is radio-opaque which helps in deciding the length of stent or balloon to use. The wire comes in a plastic tube casing which is initially flushed with heparinised saline and unclipped from its attachments. The connecting electrical wire is then connected to the RADI Analyser® where measurements are displayed and recorded. The pressure wire is then calibrated prior to insertion into the guide catheter. It is then advanced to the coronary ostium where the needle introducer is removed and the pressure wire recorded pressure tracing is equalised with the aortic pressure trace obtained from the guide catheter. The pressure wire is then passed to the distal third of the coronary artery where possible and safe to do so. Once in position the measurements of FFR, CFR and IMR can be made.

Figure 3.8 - The RADI pressure wire, with its temperature and pressure sensor 3cm from the tip.

3.5.1 Fractional Flow Reserve

Once the wire is in a satisfactory position an intravenous adenosine infusion is given (140μg/kg/min) through the 18G cannula in the left antecubital fossa. The patient is warned beforehand to expect symptoms of chest pain, breathlessness, headache, facial flushing and dizziness and to let the operator know when these symptoms are experienced. The operator watches for the development of tachycardia and a blood pressure drop indicative of the achievement of maximal hyperaemia. Once steady state hyperaemia is achieved the mean distal pressure (Pd) mean aortic pressure (Pa) are recorded and divided to give us the FFR (Pd/Pa). This value is recorded for each of the coronary arteries.

For the purpose of comparisons with MPRI and other areas of analysis as highlighted in the results section, chronic totally occluded (CTO) arteries have been given the FFR value of 0.4. This was decided at the end of the study following a review of the previous literature in the field and some of our own findings. Often the coronary pressure wire is not suitable to pass down CTO's and other wires are designed specifically for this purpose. In the present study we were only able to pass the pressure wire across one occluded artery out of 35. The FFR distal to the occlusion in this artery was 0.3 and this is a reflection of the collateral supply to the myocardium distal to the coronary occlusion. We know that collateral perfusion varies widely between arteries from only minimal collateral flow up to 60% of maximal perfusion if the artery was not occluded and functioning normally.(118) In a study be Werner et al in 2006 of 107 patients with chronic total occlusion and no prior Q wave MI the collateral FFR was 0.32.(119) A further study of patients with CTO was published in 2006 in which patients who did not develop coronary steal had an average collateral FFR of 0.41.(120) The recently published FAME study in the New England Journal of Medicine assigned an FFR of 0.5

to CTO's however no justification of this value was made in the manuscript.(121) We measured coronary wedge pressure during balloon inflation in 46 patients with severe CAD requiring PCI (FFR<0.75). Using this value to calculate collateral FFR provided a mean of 0.24 (SD=0.11). In CTO's we would hope for better collaterals depending on how long the vessel was occluded for and how acutely the vessel occluded. However we know that collaterals will only provide up to 60% of normal maximal perfusion. Taking these factors together we have chosen an FFR of 0.4 for our CTO's.

3.5.2 Coronary Flow Reserve

Whilst the pressure wire is in the distal third of the coronary artery and prior to the adenosine infusion the resting thermodilution curves are obtained for the measurement of the CFR. The shaft of the pressure wire acts as a proximal thermistor as it can measure temperature dependent electrical resistance. It is therefore able to detect the start of an injection of saline into the coronary artery. The distal sensor also detects the bolus of saline as it passes through the distal third of the coronary artery. From the proximal and distal curve we are able to determine the length of time it has taken for the bolus of saline to pass down the artery. This transit time (Tmn) is actually the time taken for half the saline injection to exit the tip of the coronary guide catheter and for half to pass the distal coronary sensor. During the study we give three 3ml boluses of room temperature saline down the coronary guide catheter measuring the Tmn after each injection. The mean of this value is automatically stored on the RADI Analyser. We try to ensure the than Tmn values are all within 10% of each other to ensure an accurate result. We then commence an adenosine infusion (140μg/kg/min) and once we are happy that maximal hyperaemia has been achieved we repeat the three 3ml boluses of saline to give us a mean Tmn at stress. The CFR is then calculated automatically on

the RADI Analyser by dividing the mean rest Tmn by the mean stress Tmn. This value is also calculated for all three coronary arteries where possible per patient.

3.5.3 Index of Microcirculatory Resistance (IMR)

Using the aforementioned results we are also able to calculate the index of microcirculatory resistance (IMR) which is a new measure of the function of the microvasculature which received recognition during the course of this research study. The IMR is calculated by multiplying mean distal coronary pressure (Pd) by the hyperaemic transit time (Tmn). This is also known as the uncorrected IMR (IMRuncorr) where the contribution of collateral vessels is ignored. This calculation holds true in arteries in which there is no epicardial stenosis. In the event of significant coronary arterial disease the coronary wedge pressure (Pw) is necessary for the accurate calculation of the IMR. This is obtained when a balloon or stent is inflated in the coronary artery with the distal pressure wire sensor distal to the balloon or stent. Once antegrade flow is blocked by the stent or balloon the distal pressure sensor measures only the collateral flow to the distal coronary artery. This is measured on the RADI Analyser and stored for calculation of the corrected IMR (IMRcorr). The equation for the calculation of IMRcorr then becomes:-

$$IMRcorr = Pa \times Tmn \times [(Pd-Pw)/(Pa-Pw)]$$

Pa is the aortic pressure as measured by the guide catheter in the coronary ostium and Tmn is the mean transit time at hyperaemia as used in the equation to calculate the CFR. IMR only became established as a method of assessing the microcirculation after our study had commenced. As such no measurements were recorded in this regard until after the 8th patient was recruited into the study. In coronary arteries with an FFR<0.75

which were treated by PCI, a coronary wedge pressure (distal coronary pressure when a balloon is inflated proximal to the distal pressure sensor) was recorded in order that we were able to calculate the corrected index of microcirculatory resistance. In the presence of coronary artery disease where collateral vessels have been formed, antegrade coronary flow does not equal myocardial flow and we therefore must take the contribution of collateral flow into account when calculating IMR.(68)

The Tmn can also be used to calculate Qcorr which is 1/Tmn at maximal hyperaemia and is a surrogate of coronary flow.

3.6 Adenosine

Adenosine was chosen as our agent to induce pharmacological stress in both the MRMPI scans and the pressure wire studies. We used a continuous peripheral intravenous infusion at a dose of 140μg/kg/min using a large antecubital fossa vein. Adenosine solution was prepared and distributed from St Bartholomew's in London containing 1mg/ml in a 120ml bag which was adequate for both the MRMPI and the coronary angiogram. Occasionally where no haemodynamic or symptomatic response to the adenosine infusion was seen during the angiogram or MRMPI, the operator would increase the rate of the infusion by 50% and if required 100% (provided the infusion device would allow) in order to achieve maximal hyperaemia. Increasing the rate of the adenosine infusion was at the discretion of the primary operator in the cardiac catheterisation laboratory and the doctor supervising / performing the MRMPI scan if no typical symptoms were experienced and if there was no increase in heart rate or fall in blood pressure. Patients who failed to demonstrate any haemodynamic or symptomatic response are hightlighted in later sections as "non-responders".

3.7 Caffeine

Prior to the MRMPI scans and the coronary angiogram each patient had venous blood taken for caffeine levels. This was repeated after the MRMPI and following the angiogram to act as a control. Caffeine levels were compared with the clinical response to adenosine (heart rate, blood pressure and symptoms) to see if there was any correlation, and were also compared with the results of the perfusion MRI scans and measurements of coronary and FFR.

A recent review in the journal of nuclear cardiology recommends that until the potential problem of false negative results in stress perfusion studies is further clarified then simple measures should be implemented.(122) As such patients were advised to abstain from consuming dietary and drug sources of caffeine for the 24hrs prior to MRI scanning and the coronary angiogram. Appendix 8.1 was given to the patients as a guide as to what to avoid. Due to individual variations in the half life of caffeine certain subgroups of patients were asked to abstain from caffeine for 48 hours such as those suffering from liver disease, oral contraceptive pill users and patients taking cimetidine.

3.8 Caffeine Analysis

Clotted blood samples were obtained from patients prior to the MRMPI scans and the pressure wire studies. These samples were rapidly transferred to the biochemistry laboratory where the serum was extracted and stored between 2 – 8^{o}C. Analysis of the samples was performed in the Biochemistry Department of Gartnavel General Hospital in Glasgow. Samples were batched for analysis of caffeine levels. This was performed using the Emit® caffeine assay which is a homogenous enzyme immunoassay technique (Dade Behring Inc, Cupertino, CA). This assay works by competition between caffeine in the serum of the sample and caffeine labelled with bacterial glucose-6-phospate

dehydrogenase which compete for sheep antibody binding sites. A reduction in enzyme activity occurs with antibody binding. By this method caffeine levels can be calculated in terms of enzyme activity. The results are produced automatically by a biochemistry analyser (Abbott Diagnostic Instruments Ltd, Architect ci8200, Berkshire, England). This method has been extensively validated and is commercially available for use.(123-125) The coefficient of variance for our caffeine analysis over 7 measurement time points was 8.2%.

3.9 Power Calculation and Statistical Analysis

To maximize information, abnormality will be assessed on an artery rather than a patient basis. Since we plan to assess three arteries per patient, there is a possibility of a loss of information associated with any correlation in the correctness of the assessment of arteries in the same patient. The study will recruit sufficient subjects to generate 90 normal arteries and at least 150 abnormal arteries. Assuming underlying sensitivity and specificity of 80% and no loss of information due to correlation of results from the same subjects, this will allow sensitivity to be estimated with a standard error of 3.3% and specificity with a standard error of 4.2%. Even with an information loss equivalent to a 33% reduction (one third of arteries) in sample size, these standard errors will only increase to 4.0% and 5.2%.

Sensitivity, specificity, positive and negative predictive values will be calculated with 95% confidence intervals (CI) taking into account both within- and between-subject components of variance. Results will be presented as mean or median depending on the distribution of the data with standard deviation and ranges as appropriate. 95% confidence intervals are presented where appropriate. Students t-test, Mann-Whitney test, Pearson's correlation coefficient, Wilcoxon rank sum test, analysis of variance

(ANOVA) with and without Tukey 95% simultaneous confidence intervals, Kruskal-Wallis test and Cohen's kappa statistics are used where indicated in the results. In order to determine if data were skewed we performed tests of skewness and kurtosis. Logarithmic and square transformations are used in cases of skewed data in order to produce data with a normal distribution so we can use the t-test for further statistical analysis. When transformation is not possible non-parametric tests are used instead such as when the data set contained zero. Boxplots illustrating results are frequently used throughout the Results section. Outliers are highlighted however are included in the subsequent statistical analyses. The author was observer 1 for each of the methods of analysis and various other research fellows / cardiac technicians acted as second observer as noted in the acknowledgements section. Both observers 1 and 2 were completely blinded from any patient demographics or clinical data prior to and during image analysis. Angiograms and MRMPI scans were set up for analysis by an external party familiar with the use of the analysis software.

4 Results

4.1 Patient Baseline Characteristics

Of the one hundred and three patients recruited into the study, 2 patients were excluded following the initial MRI scan with one patient refusing his coronary angiogram due to mental health problems and the other having to delay her angiogram due to unexplained iron deficiency anaemia which required investigation.

The mean age as indicated in table 4.1 was 60 years with 74% of those patients being male in keeping with the male preponderance to developing coronary artery disease. The mean BMI for the patients was 30.1 which falls into the obese category. As shown in figure 4.1 only 10 patients had a normal BMI at less than 25. Forty-four patients fell into the obese categories with 12 patients being clinically obese and 2 patients being morbidly obese with a BMI of greater than 40. Fifty-nine patients were current or previous smokers and a substantial number were also known to have systemic hypertension and hyperlipidaemia (table 4.1). Two patients with severe chronic kidney disease were recruited into the study prior to the concern regarding nephrogenic systemic fibrosis (NSF) following exposure to gadolinium based MRI contrast agents. In addition over 50% of patients had a family history of premature coronary artery disease. On entry into the study the majority of patients were already taking aspirin, beta-blocker and statin (HMG CoA reductase inhibitors) medications. Fifty percent of patients were taking an angiotensin converting enzyme (ACE) inhibitor and 5% were taking an angiotensin receptor blocker (ARB). Calcium channel blockers, nitrates and nicorandil had also been prescribed as indicated in table 4.1. Clopidogrel had been prescribed in 44% of patients.

Table 4.1 - Risk factor profile for recruited patients.

Risk Factor	
Mean Age (Years ± SD)	60 ± 9
Male : Female	76 : 27
Mean BMI ± SD	30.1 ± 4.3
Current smoker	18 (17%)
Ex-smoker	41 (40%)
Type 1 diabetes mellitus	3 (3%)
Type 2 diabetes mellitus	14 (14%)
Hypertension	65 (63%)
Hypercholesterolaemia	81 (79%)
Previous MI	24 (23%)
Family history of IHD	53 (51%)
Stroke	2 (2%)
Peripheral vascular disease	2 (2%)
Renal failure:-	
Grade 3 CKD	18 (17%)
Grade 5 CKD	2 (2%)
Medication:-	
Aspirin	91 (88%)
Clopidogrel	45 (44%)
Beta blocker	86 (83%)
ACE inhibitor	52 (50%)
Statin	91 (88%)
Calcium channel blocker	35 (34%)
Nitrate	31 (30%)
Nicorandil	35 (34%)
ARB	5 (5%)

Figure 4.1 - Patient BMI by category.

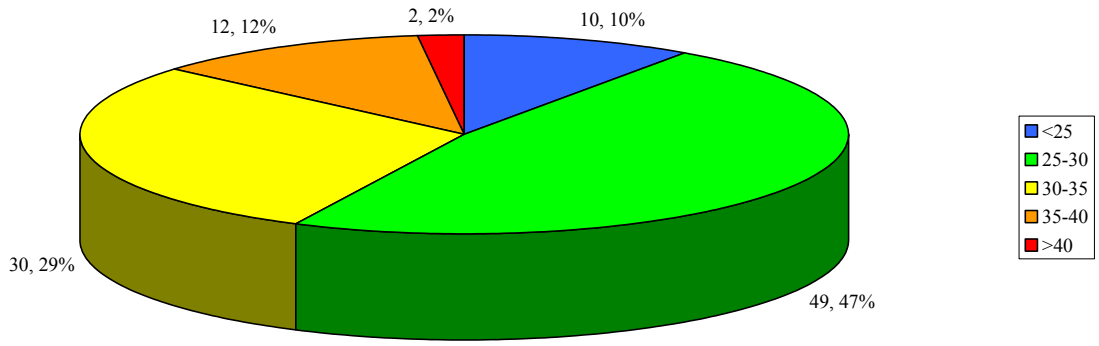

Baseline electrocardiographic changes are documented in table 4.2. All patients prior to entry into the study were in sinus rhythm. One patient of 57 (2%) developed atrial fibrillation following PCI and 9 of 15 (60%) CABG patients developed atrial fibrillation post-operatively. They all subsequently cardioverted prior to repeat MRI scanning. Nine patients had pathological Q waves indicative of previous transmural MI at the time of the initial MRI scan. Seventeen patients had resting ST depression raising the possibility of myocardial ischaemia and 3 patients had ST elevation, which was probably due to high take-off of the ST segment and not infarction. Twelve patients had either T wave inversion or biphasic T waves which is also potentially indicative of previous non-ST elevation acute coronary syndromes. A further twelve patients had voltage criteria for left ventricular hypertrophy (S wave in V1 or V2 + R wave in V5 or V6 =>35mV).

Table 4.2 - Baseline electrocardiograph findings.

ECG Findings	**Patients n(%)**
1st Degree AV block	5 (5%)
Pathological Q waves	9 (9%)
Bundle branch block	4 (4%)
ST depression	17 (17%)
ST elevation	3 (3%)
T wave inversion	8 (8%)
Biphasic T waves	4 (4%)
Left ventricular hypertrophy	12 (12%)

4.2 Patient Outcome

Figure 4.2 shows the distribution of coronary disease as determined by the FFR measurements. Patient outcome is shown in figure 4.3. The majority of patients had PCI, 57 (56%). Fifteen patients (15%) underwent CABG whereas 9 patients were found to have significant coronary artery disease however the pattern of disease and symptoms were felt to be best treated by medical therapy. Twenty (20%) patients had no significant CAD.

Figure 4.2 - Pattern of coronary artery disease as determined by FFR.

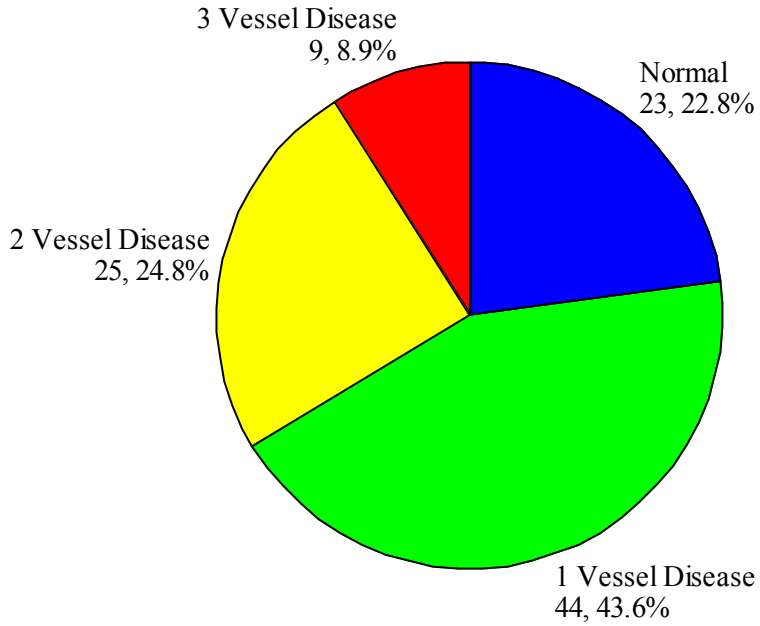

Figure 4.3 - Patient outcome following diagnostic angiography and pressure wire study.

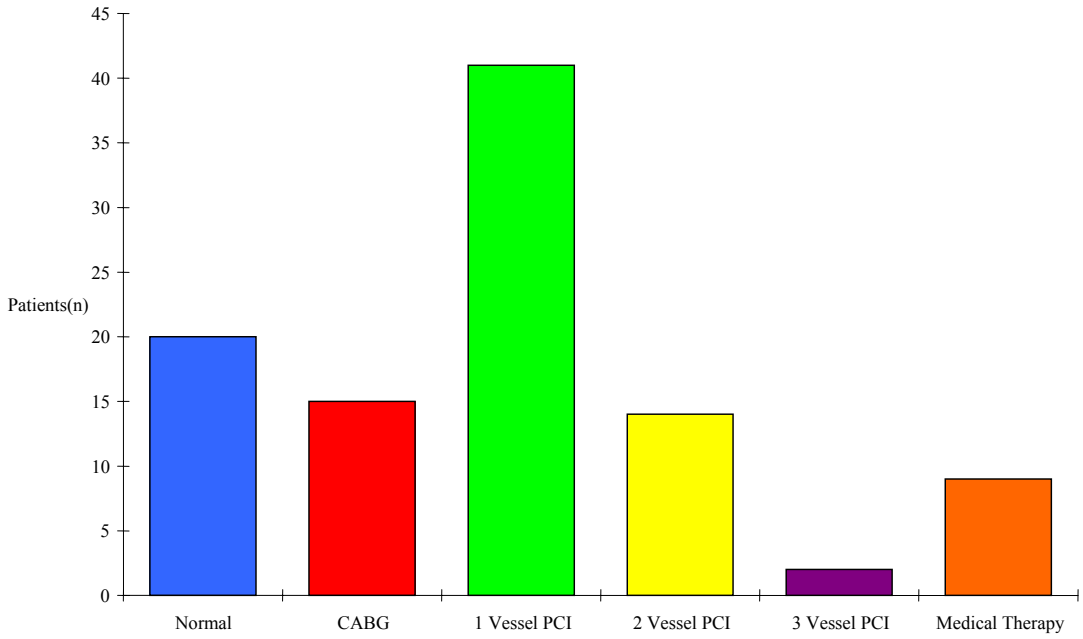

4.2.1 Post -PCI Results

The pre and post PCI pressure wire derived haemodynamic descriptive data are displayed in table 4.3. More data points are recorded post PCI as the pressure wire is sometimes unable to cross occluded vessels and a more flexible wire is required for this purpose. The pressure wire can usually be passed into the distal artery post PCI.

Table 4.3 - Pressure wire data pre and post-PCI for all recorded arteries. Note that the number of arteries varies between pre and post-PCI depending on technical factors and whether the pressure wire was able to pass down the diseased artery.

	Pre-PCI					**Post-PCI**				
	n	Mean	Med	SD	Range	n	Mean	Med	SD	Range
Qcorr	49	2.30	1.89	1.59	0.47-7.14	57	4.99	4.76	2.56	1.47-10.0
Pd/Pa	52	0.65	0.64	0.19	0.32-0.95	57	0.96	0.97	0.04	0.86-1.0
FFR	64	0.54	0.52	0.15	0.17-0.78	68	0.90	0.90	0.06	0.73-1.0
CFR	58	1.49	1.29	0.75	0.6-4.39	66	2.86	2.5	1.52	0.88-9.8
IMR uncorr	49	28.0	23.2	15.8	8.9-70.0	55	19.4	16.5	11.8	6.2-61.9
IMR corr	43	15.5	13.5	8.9	1.3-39.2	41	17.3	15.7	9.3	5.7-47.9

There was a significant increase in the resting Pd/Pa following revascularisation and a significant increase in the FFR as expected. The CFR and Qcorr also significantly increased following PCI as shown in table 4.4. Uncorrected IMR significantly dropped following PCI however there was no difference in the corrected IMR. The change in corrected IMR for those patients who had this recorded pre and post PCI are presented in figure 4.4, showing no significant difference despite treatment of the epicardial

stenosis. Table 4.4 only contains data for those patients where pre and post PCI data are available as opposed to all measured data in table 4.3.

Figure 4.4 - Line plot of corrected IMR pre and post PCI.

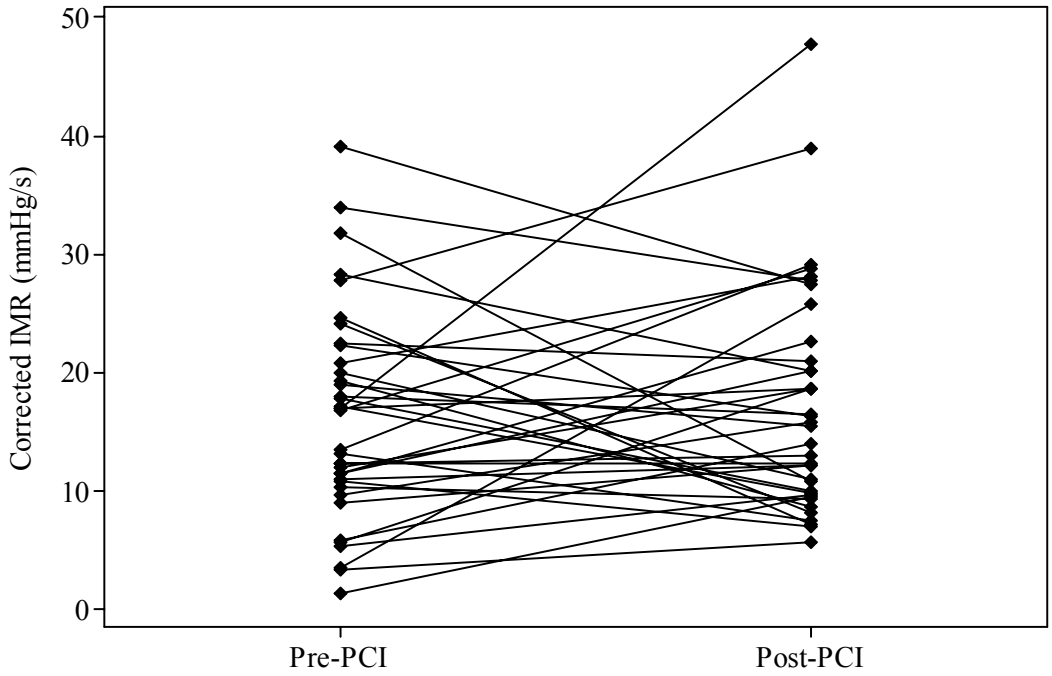

Table 4.4 - Paired pressure wire data for those arteries in which both a pre and post-PCI result was available with the results of the paired t-test. Due to skewed data all values required transformation prior to analysis.

		Pre-PCI			**Post-PCI**			**Paired T-Test**	
Parameter	n	Mean	Median	SD	Mean	Median	SD	T-value	P-value
Pd/Pa	47	0.65	0.64	0.19	0.95	0.96	0.04	10.03	<0.0001
FFR	59	0.54	0.52	0.15	0.89	0.90	0.06	14.8	<0.0001
CFR	52	1.52	1.29	0.77	2.76	2.50	1.55	6.91	<0.0001
IMRuncorr	42	28.62	22.90	15.7	19.35	16.50	11.6	3.66	0.001
IMRcorr	37	16.19	16.82	8.86	17.18	15.47	9.46	0.96	0.35
Qcorr	44	2.36	1.94	1.64	4.98	4.65	2.6	6.73	<0.0001

In total 81 arteries in 57 patients were treated by PCI. Forty-two patients (74%) underwent single vessel PCI, 13 (23%) had 2 vessel PCI and 2 (3%) had 3 vessel PCI as shown in figure 4.3. One hundred and twenty-eight stents were inserted in 74 vessels with a further 7 arteries treated by plain old balloon angioplasty (POBA). Of the stents, 100 (78%) were drug eluting and 28 (22%) were bare metal. Of the 100 drug eluting stents 95 were Taxus (paclitaxel eluting) and 5 were Cypher (sirolimus eluting). 14 (50%) of the inserted bare metal stents were Driver stents, 9 (32.1%) were Liberte stents, 2 (7.1%) were Minivision stents, and there was one (3.6%) Vision, one Yukon and one Microdriver stent. Data relating to the number of stents inserted per artery, maximum stent diameter, stent length, DS, area stenosis, lesion length and reference vessel diameter in the 74 arteries treated by PCI and stenting are displayed in table 4.5.

Table 4.5 - Number of stents, maximum stent diameter, stent length, DS, area stenosis, lesion length and reference vessel diameter for the 74 arteries treated by PCI and stenting.

	Arteries	**Mean**	**Median**	**SD**	**Min**	**Max**
Stent No	74	1.73	1.0	0.93	1.0	5.0
Stent Diameter	74	3.06	3.0	0.45	2.25	5.0
Stent Length	74	34.9	28.0	24.5	8.0	136.0
Degree of Stenosis %	74	71.1	70.5	18.0	29.9	100
Area of Stenosis %	74	88.1	91.1	10.8	50.9	100
Lesion Length (mm)	63	16.9	15.2	7.5	7.1	43.3
Ref Vessel Diameter (mm)	74	2.9	3.0	0.6	1.9	4.8

4.2.2 Post CABG Results

Fifteen patients underwent CABG. Of these, 4 patients had 4 grafts, 8 patients had 3 grafts and 3 patients had 2 grafts. Arterial revascularisation with the left internal mammary artery to the left anterior descending artery was performed in all 15 patients. The left radial artery was used to graft the posterior descending artery in 2 patients. Saphenous vein was used to graft the posterior descending artery in 8 patients, first obtuse marginal artery in 11 patients, second obtuse marginal artery in 2 patients, first diagonal artery in 2 patients, distal right coronary artery in 2 patients, left circumflex artery in 2 patients, and intermediate artery in 2 patients.

Table 4.6 - Complications of coronary artery bypass surgery.

Complication	**Number of Patients**
Atrial fibrillation	9
Required prolonged CPAP	3
Post-op bleeding requiring re-opening	2
Prolonged inotropic support	2
Transient ischaemic attack	1
Psychosis	1
Confusional state	1
Pneumonia	1
Sternal wound leak	1
Leg wound infection	1

The mean ischaemic time for these patients during surgery was 34.8 minutes (standard deviation 9.9, range 16-54 minutes). Mean bypass time was 59.6 minutes (standard

deviation 15.3, range 28-87 minutes). Mean theatre time was 174.2 minutes (standard deviation 29.4, range 130-210 minutes).

Only 3 (20%) patients had no listed post-operative complications. The complications encountered by the remaining 12 patients are listed in Table 4.6.

4.2.3 Follow-up MRMPI Scans

PCI treated patients: of those who attended for their 24 hour post-PCI follow up MRMPI scan, 50/54 (93%) had a reduction in the number of segmental perfusion defects with 24 (44%) having normal perfusion at this time (table 4.7). At 4 weeks 24/52 patients (46%) had normal perfusion. Nine patients had untreated occluded coronary arteries which accounts for some of the residual perfusion abnormalities. The reduction in perfusion defects from MRI1 to MRI2 was statistically significant ($p<0.0001$) however from MRI2 to MRI3 was not ($p=0.26$).

CABG treated patients: this group had significantly more perfusion defects on the presenting MRMPI compared to the PCI group ($p=0.004$). Of the 14 CABG patients who attended for follow-up MRMPI, 12 (86%) had a reduction in the number of hypoperfused segments with 5/14 (36%) having normal perfusion. There was no statistically significant difference in the number of residual perfusion defects between those treated by PCI or CABG (table 4.7) however, there was a trend towards fewer segments in the PCI group ($p=0.1$).

Medically treated patients: 4/9 patients (44%) who received optimisation of their medical therapy refused to attend for a second scan. It is difficult to draw any conclusions from this small group however 4 of the remaining 5 patients (80%) did

have a reduction in the number of hypoperfused territories on their second MRMPI scan.

Table 4.7 - Perfusion MRI data showing the number of scans performed at each stage with the median number of perfusion defects and their standard deviation and ranges for each of the three MRI scans per patient in the PCI group and the two scans in the CABG and medical therapy groups. These data are the mean of the results from the two independent observers.

	N(%)	Median (± SD)	Range
Pre-PCI MRI	57 (100%)	5 ± 2.9	0 – 13.5
24 Hours Post-PCI MRI	54 (95%)	1 ± 2.3	0 – 7.5
4 Week Post-PCI MRI	52 (91%)	0 ± 1.9	0 – 6.5
Pre-CABG MRI	15 (100%)	9 ± 3.5	0 – 11.5
4 Week Post-CABG MRI	14 (93%)	2.5 ± 3.6	0 – 12
Pre-Medical Rx MRI	9 (100%)	4 ± 2.1	0 – 5.5
3 Month Post Medical Rx MRI	5 (56%)	1 ± 2.0	0 – 4.5

4.2.4 Perfusion Defect Normalisation Post-Revascularisation

A total of 16 coronary territories demonstrated hypoperfusion on the baseline MRMPI but were not revascularised and 11 hypoperfused coronary territories had FFR values greater than or equal to 0.75 (false positives). This left 94 hypoperfused coronary artery territories on the baseline MRMPI which were revascularised and had at least one follow-up scan. Of these 64 (68%) were revascularised by PCI and 30 (32%) by CABG. 51/64 (80%) territories treated by PCI and 19/30 (63%) treated by CABG showed complete resolution of the perfusion defect on follow-up MRMPI scanning. An additional 10/64 (16%) treated by PCI and 8/30 (27%) treated by CABG had partial

resolution of the perfusion defect on follow-up MRMPI. Six (6%) coronary territories showed persistent abnormal perfusion despite revascularisation (3 had PCI and 3 had CABG).

In those patients with available FFR data the mean FFR pre-revascularisation was 0.51 (median – 0.47, SD=0.15, Interquartile Range 0.4 – 0.65) in those territories with complete resolution of perfusion defects following revascularisation. This is compared to 0.44 (median – 0.4, SD=0.08, Interquartile Range 0.4 – 0.5) in the territories with partial resolution of hypoperfusion and 0.45 (median – 0.4, SD=0.08, Interquartile Range 0.4 – 0.52) in the territories with no resolution of hypoperfusion post-revascularisation. The higher pre-revascularisation FFR in those patients with complete resolution of the perfusion defect was statistically significant compared to the partial resolution group (p=0.01). There was no difference between the complete resolution and no resolution groups (p=0.15) and the partial resolution and no resolution groups (p=0.84) however there were only 6 data points in the no resolution group making meaningful conclusions difficult. These data are presented on figure 4.5.

Figure 4.5 - Boxplot of FFR values pre-revascularisation in the group of patients who had complete, partial and no resolution of their perfusion defects on MRMPI post PCI and CABG. This demonstrates the median FFR, the interquartile range and spread of data for each group.

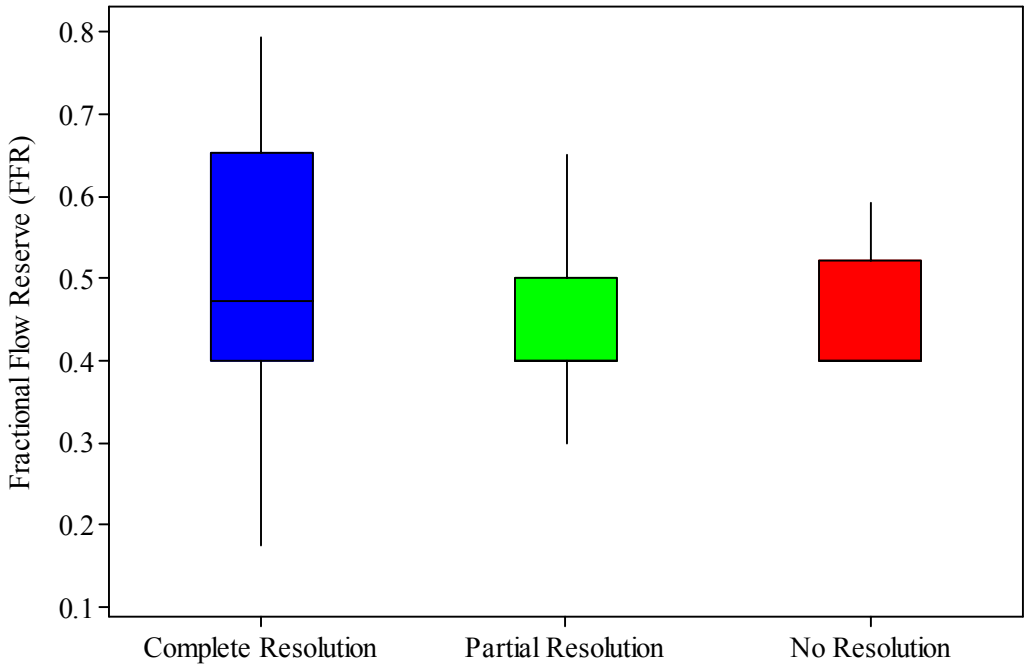

The pre-revascularisation diameter of stenosis (DS) was also analysed and compared between the complete resolution, partial resolution and no resolution groups. The mean DS in the complete resolution group was 72.9% (median – 70.2%, SD=17.4, Interquartile Range 59.5 – 86.9%) compared to 79.8% (median – 76.2%, SD=17.1, Interquartile Range 66.6 – 100%) in the partial resolution group and 82.8% (median – 85.6%, SD=19.5, Interquartile Range 66.5 – 100) in the no resolution group. These data are presented on figure 4.6. The trend towards milder coronary disease in the complete resolution group was not statistically significant when compared with the partial resolution group (p=0.14) and the no resolution group (p=0.29). Bearing in mind that DS has little bearing on the functional significance of coronary disease, the FFR data are probably of greater significance here.

Figure 4.6 - Boxplot of DS (%) in the coronary arteries pre-revascularisation in the group of patients who had complete, partial and no resolution of their perfusion defects on MRMPI post PCI and CABG. This demonstrates the median DS, the interquartile range and spread of data for each group.

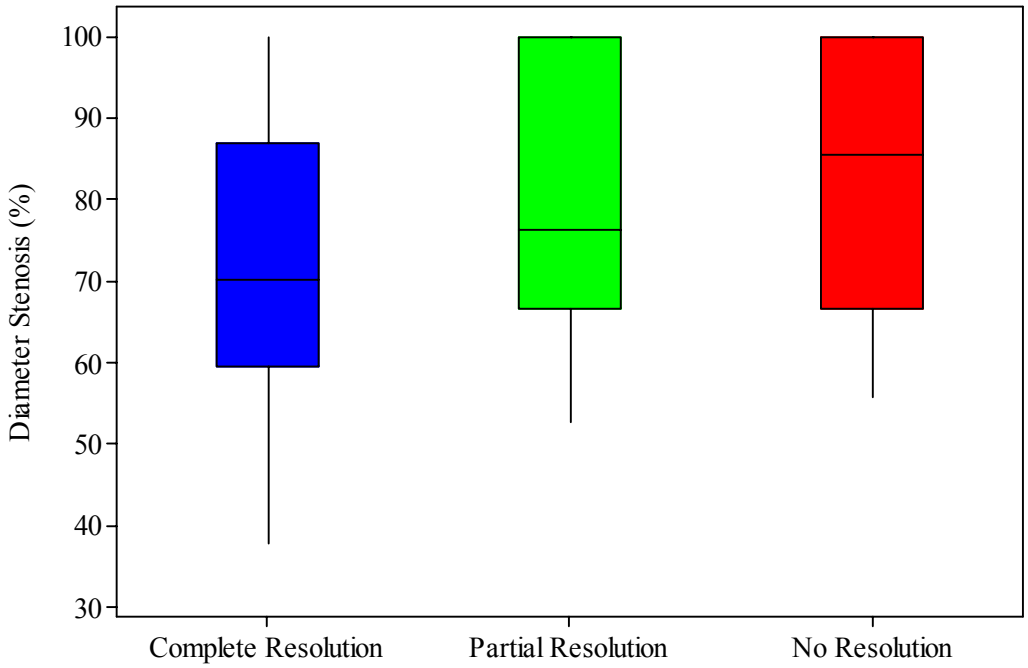

PCI patients who had FFR data post revascularisation had a mean FFR of 0.90 (median 0.91, SD=0.06, Interquartile Range 0.86 – 0.95) in the complete resolution group. This is compared to a mean FFR of 0.92 (median – 0.93, SD=0.05, Interquartile Range 0.9 – 0.96) in the partial resolution group and 0.88 (median – 0.9, SD=0.05, Interquartile Range 0.82 – 0.92) in the no resolution group. As these data were skewed to the left a square transformation was performed prior to comparing the groups however no statistically significant differences were found between each of the groups. This is an interesting observation and raises the possibility that the persistence of a perfusion defect within a territory may be caused by plaque embolisation into the microcirculation as opposed to any residual epicardial disease.

4.3 First Pass Magnetic Resonance Myocardial Perfusion Imaging (MRMPI)

4.3.1 Qualitative Analysis of MRMPI Scans

The technical quality of all MRMPI scans was felt to be adequate for visual diagnostic purposes. Figure 4.7 gives an example of the quality of our imaging with one of the cases from the study with a left anterior descending coronary artery perfusion defect. Of the 101 perfusion scans undertaken 25 (24.8%) were reported as normal, 40 (39.6%) demonstrated 1 vessel disease, 26 (25.7%) 2 vessel disease and 10 (9.9%) 3 vessel disease. 122 perfusion defects were reported of which 49 (40.2%) were in the territory of the left anterior descending coronary artery, 32 (26.2%) in the territory of the left circumflex / obtuse marginal artery and 41 (33.6%) in the territory of the right coronary artery. In the final statistical analysis one perfusion defect was omitted as we had no FFR data for the diseased artery supplying that territory. Therefore, where comparisons have been made with FFR, only 121 perfusion defects are quoted. Interobserver variability between the two observers was assessed on the identification of abnormal myocardial perfusion per patient which produced a κ of 0.97 indicating excellent agreement between the two observers. The interobserver variability for the extent of CHD (normal, 1, 2 or 3 vessel disease) was 0.76. Both observers agreed on the pattern of CHD in 84 (83.2%) scans and the 3rd observer adjudicated on the remaining 17 (16.8%). Interestingly the 3rd observer agreed with observer 1 on 47% of occasions and observer 2 on the remaining 53%.

Figure 4.7 - An anteroseptal subendocardial perfusion defect in a mid-ventricular slice following the injection of gadolinium at maximal hyperaemia (A). A stenosis in the proximal left anterior descending coronary artery in the LAO caudal projection (B). The FFR (yellow). The aortic and distal coronary pressure tracings are widely separated at maximal hyperaemia with an FFR of 0.5.

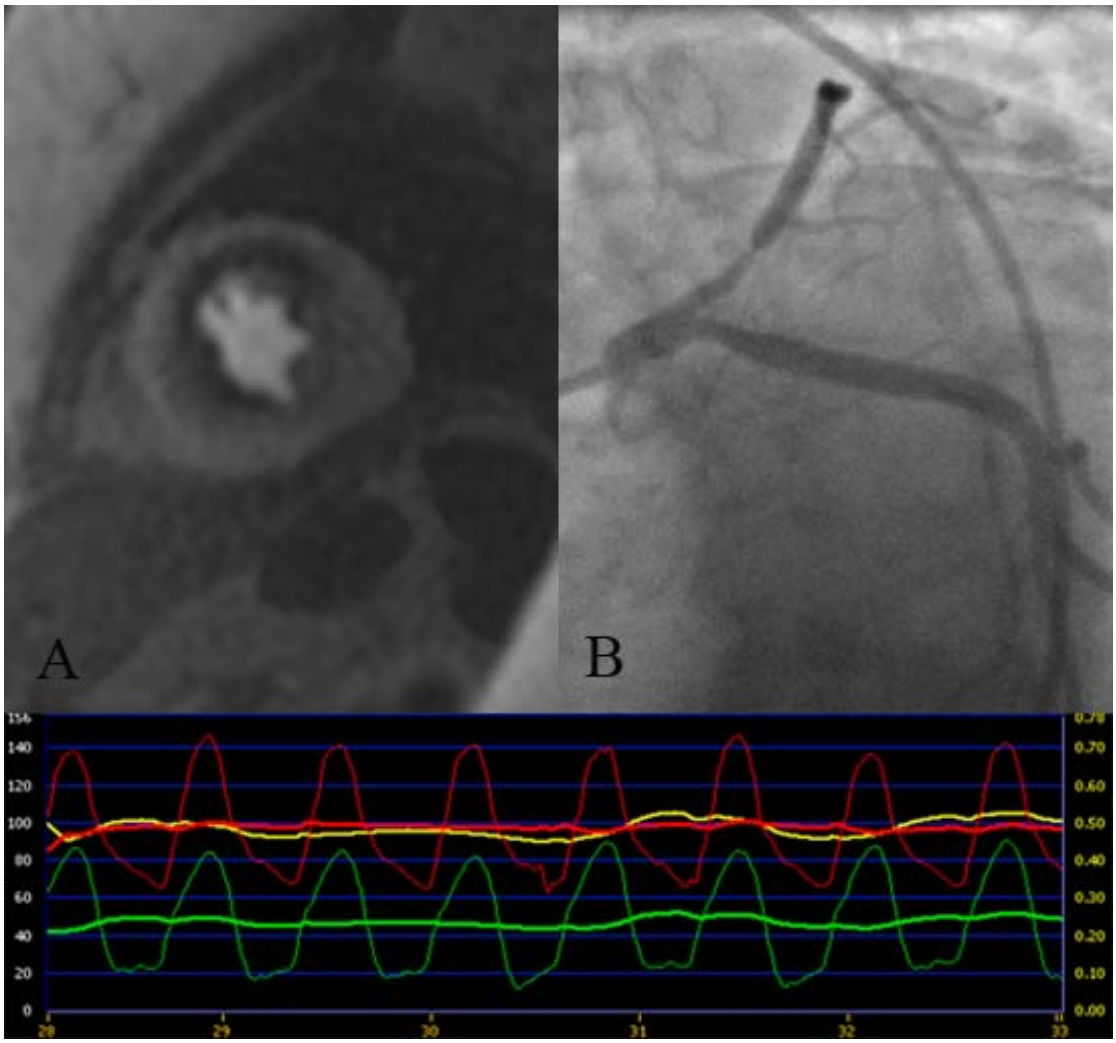

4.3.1.1 Magnetic Resonance Myocardial Perfusion Imaging (MRMPI) versus FFR.

The results are summarised in Table 4.8. Data are presented using the conventional FFR cut-off of <0.75 and also the more conservative FFR cut-off of ≤0.8 as was used in the FAME study which reported its findings this year.(126) Arteries which were chronic total occlusions (CTO) were given an FFR value of 0.4 as the pressure wire was not

able to cross these lesions. This takes into account the contribution to coronary territories of collateral blood flow. 110 coronary territories demonstrated a perfusion defect and a FFR <0.75 (true positive). There were 11 coronary territories with a perfusion defect but an FFR ≥0.75 (false positive). When the higher FFR cut-off of 0.8 is used the number of false positive results falls to 3. 168 coronary territories showed no perfusion defect and a FFR ≥0.75 (true negative). 11 coronary territories showed no perfusion defect but were subtended by an artery with FFR <0.75 (false negative).

Table 4.8 - MRMPI compared to FFR at 2 cut-off values. Results are expressed per coronary artery territory.

	FFR<0.75	**FFR≥0.75**	**Total**	**FFR≤0.8**	**FFR>0.8**	**Total**
Positive MRMPI	110	11	**121**	118	3	**121**
Negative MPMRI	11	168	**179**	26	153	**179**
Total	121	179	**300**	144	156	**300**
	Excluding non-responders to adenosine (5)					
	FFR<0.75	**FFR≥0.75**	**Total**	**FFR≤0.8**	**FFR>0.8**	**Total**
Positive MRMPI	109	10	**119**	116	3	**118**
Negative MPMRI	6	160	**166**	21	145	**167**
Total	115	170	**285**	137	148	**285**

There was a large increase in false negative results when the 0.8 cut-off was used with 26 territories without perfusion defects having an FFR ≤0.8. The sensitivity and specificity and positive and negative predictive values of MRMPI for the detecting of physiologically significant coronary artery disease using either FFR cut-off are shown in table 4.9. Five patients showed no haemodynamic or symptomatic response to the intravenous adenosine infusion during perfusion imaging. This was despite an increase

in the dose above the standard 140µg/kg/min. Tables 4.8 and 4.9 demonstrate the results when the data from these 5 patients are removed.

Table 4.9 - Sensitivity and specificity and positive and negative predictive values of MRMPI for the detection of significant coronary artery disease as defined using FFR.

	FFR<0.75		**FFR≤0.8**	
	All Patients	Excluding Non-Responders	All Patients	Excluding Non-Responders
Sensitivity (%) (95% CI)	90.9 (84.2-97.6)	94.8 (89.6-99.9)	81.9 (73.5-90.4)	84.7 (76.7-92.7)
Specificity (%) (95% CI)	93.9 (88.9-98.8)	94.1 (89.1-99.2)	98.1 (95.0-101.2)	97.9 (94.7-101.3)
PPV (%) (95% CI)	90.9 (84.3-97.5)	91.6 (85.2-98.0)	97.5 (94.0-101.0)	97.5 (93.9-101.1)
NPV (%) (95% CI)	93.9 (88.9-98.9)	96.4 (92.4-100.4)	85.5 (78.2-92.8)	87.4 (80.2-94.5)
Diagnostic Accuracy (%)	92.7	94.4	90.3	91.6

4.3.1.2 Per-Patient Analysis of MRMPI for the Detection of Significant CAD

Using qualitative analysis of the MRMPI scans we also assessed the diagnostic accuracy of this method of assessing myocardial perfusion on a per-patient basis. For this analysis we chose an FFR<0.75 as our cut-off for the diagnosis of physiologically significant coronary artery disease. Of the 76 patients with a perfusion defect on their MRMPI scan, 74 (97%) had an FFR<0.75 in at least one coronary artery. There were 2

false positive scans with FFR≥0.75 in all coronaries. Of the 25 patients with no perfusion defects on MRMPI, 21 (84%) had FFR values ≥0.75 in all coronaries and there were 4 false negative patients. These data are presented in table 4.10. Therefore, of 101 patients there was a false positive rate per patient of 2% and a false negative rate of 4%. On a per patient analysis MRMPI has a sensitivity, specificity, positive and negative predictive value of 95%, 91%, 97% and 84% respectively. The diagnostic accuracy was 94.1%.

Table 4.10 - Per-patient analysis of qualitative MRMPI versus FFR<0.75 cut-off.

	FFR<0.75	**FFR≥0.75**	**Total**
Positive MRMPI	74	2	76
Negative MRMPI	4	21	25
Total	78	23	101

4.3.1.3 Magnetic Resonance Myocardial Perfusion Imaging (MRMPI) versus CFR.

The CFR was recorded in 250 coronary arteries not including the 35 total occlusions. Four patients (4%) had CFR measured in 4 arteries, 57 (56%) in three arteries, 27 (27%) in two arteries, 9 (9%) in one artery and 4 (4%) had no CFR measurements (three left main stem stenoses and one patient with poor guide catheter engagement). CFR measurements were taken from 86 (85%) LAD coronary arteries, 62 (61%) RCA's, 44 (44%) LCx arteries, 36 (36%) OM arteries, 9 (9%) LPDA arteries, 7 (7%) IM arteries and 6 (6%) D1 arteries. The median CFR was 2.2 (SD=1.32; Range 0.45–8.21). Analysis of sensitivity, specificity and predictive values was undertaken including occluded vessels and limiting the number of major coronary arteries per patient to three. This provided data for 275 of 303 (91%) coronary arteries. When CFR with a cut-off of <2.5 is taken as the gold standard for the diagnosis of significant epicardial /

microvascular disease there were 94 (34%) coronary artery territories with a perfusion defect on MRMPI and a CFR in the corresponding coronary artery of <2.5. There were 12 (4%) false positives with perfusion defect and a normal CFR≥2.5. Eighty-nine (32%) territories demonstrated normal perfusion on MRMPI and had a normal CFR however 80 (29%) territories failed to show any perfusion defect and had a CFR<2.5. These are therefore false negatives using CFR as the gold standard. This provided a sensitivity, specificity, positive and negative predictive value of 54%, 88%, 89% and 53% respectively. The diagnostic accuracy was 66.5%.

Looking specifically at 10 of the 11 cases (1 excluded as had no CFR measurement) with a false positive perfusion MRI territory (table 4.8) as defined with an FFR≥0.75 as the gold standard, 6 (60%) had a CFR<2.5 raising the possibility that these perfusion defects were attributable to microvascular disease. However, 8 of 10 (80%) of these false positives had an FFR within the FFR grey zone 0.75-0.8. We also looked at those patients with a FFR>0.8 with a CFR<2.5 who are out with the FFR grey zone and may have microvascular disease in isolation. Sixty-seven coronary arteries in 50 patients were identified to have these physiological parameters however 12 territories were excluded from further analysis due to the presence of late gadolinium enhancement indicating previous MI. Of the remaining 55 coronary arteries 16(29%) were LAD arteries, 15 (27%) LCx arteries, 14 (25%) OM arteries, 8 (15%) RCA, 1 (2%) LPDA and 1 (2%) D1 artery. Only one (2%) coronary territory was identified to have a perfusion defect on MRMPI suggesting that by visual analysis MRMPI is unable to detect isolated microvascular disease. We then looked at those arteries with an FFR>0.8 and CFR<2.0 who would be more likely to have isolated microcirculatory disease. Twenty eight arteries were identified which fit this criteria and had no evidence of late gadolinium enhancement on MRI. None of these patients had any visually apparent

perfusion defect again confirming that qualitative MRMPI cannot diagnose isolated microvascular disease. The mean Fermi deconvolution derived MPRI for 26 of the 28 (93%) coronary territories that had this analysis performed was 2.2 which is below the MPRI cut-off of 2.41 documented in chapter 4.3.2.2. Sixteen of these 26 (62%) coronary territories had a MPRI of less than 2.41. We didn't perform sub-epicardial MPRI for comparison with the subendocardium and therefore we are unable to make any more meaningful conclusions from this data.

4.3.1.4 Magnetic Resonance Myocardial Perfusion Imaging (MRMPI) versus Index of Microcirculatory Resistance (IMR)

There is no distinct cut-off in IMR value to discriminate coronary arteries with normal microvascular function and abnormal microvascular function. The relationship between uncorrected IMR and FFR suggests as shown in Figure 4.8 that as FFR improves uncorrected IMR falls. This probably reflects that vessels with normal epicardial function are likely not to have significant microvascular disease. The r value was -0.3 which was a significant negative correlation ($p<0.001$).

Figure 4.8 - Scatterplot of uncorrected index of microcirculatory resistance (IMR) ($mmHgs^{-1}$) and FFR. Pearson's correlation coefficient r=-0.3, p<0.0001.

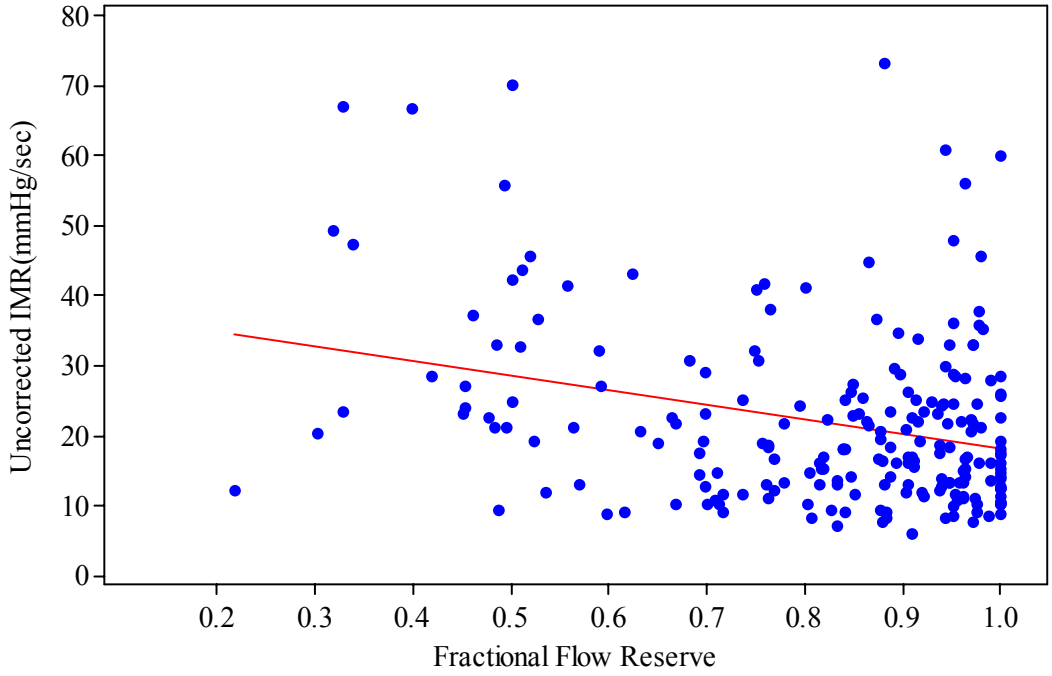

The relationship between corrected IMR where the coronary wedge pressure has been recorded and the FFR is more complex. As shown on figure 4.9 corrected IMR increases with increasing FFR with r=0.32 which was a significant correlation. Clearly the patients in this analysis all had significant epicardial disease on the basis of their FFR measurement triggering PCI. However within this group the measured microvascular resistance increases as FFR increases. The mean IMR in this group was 14.4±8.5$mmHgs^{-1}$ which is relatively low given the severity of the epicardial disease and probably reflects the development of a good supply of collaterals to the ischaemic myocardium. The reduction in IMR with increasing epicardial disease severity may reflect the amount of collateral supply which has developed in the most ischaemic areas.

Figure 4.9 - Scatterplot of corrected index of microcirculatory resistance (IMR) (mmHgs-^{1}) and FFR. Pearson's correlation coefficient r=0.32, p=0.03.

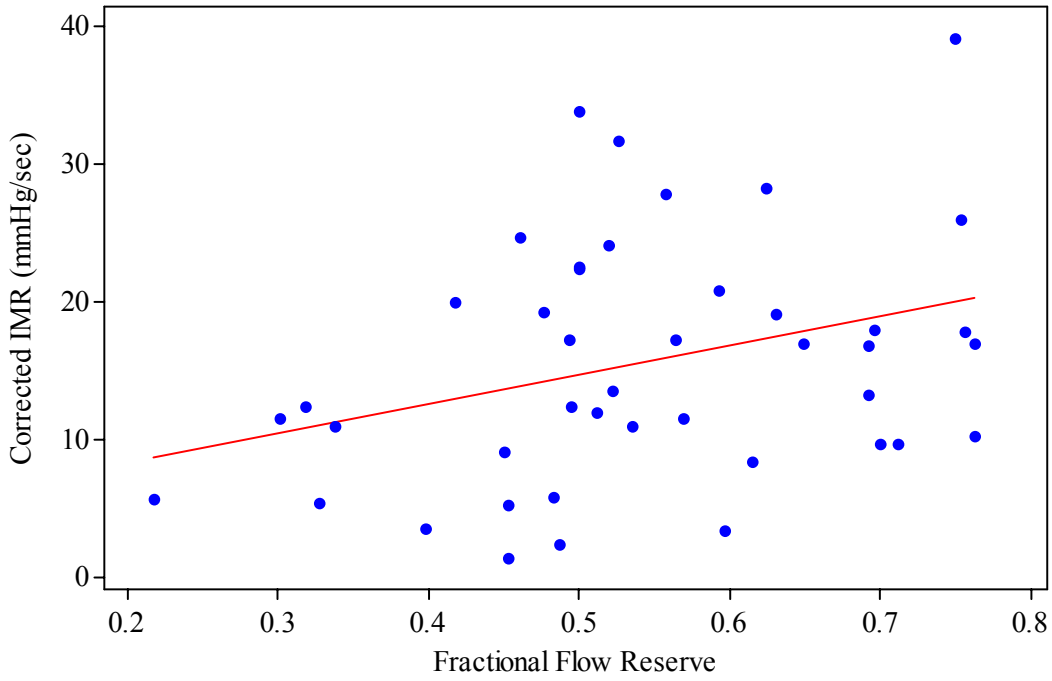

One of the questions we set out to answer was does microvasular disease account for perfusion defects in arteries with no significant epicardial coronary disease (FFR≥0.75). In our study we had 11 false positive MRMPI scans and we compared these patients' microvascular function results of CFR and IMR to those patients with perfusion defects and a significant FFR (<0.75) and patients with completely normal arteries i.e. no perfusion defect on MRMPI and FFR≥0.75. These results are presented in table 4.11. The differences between CFR, uncorrected IMR and corrected IMR between the false positives (column 1) and the true positives (column 2) were not significant (p values were 0.07, 0.65 and 0.45 respectively). The FFR was significantly lower in the true positives (p<0.0001). There were no significant differences when comparing the false positives with the true negatives (p=0.17, 0.31 and 0.77). The false positives did however have a significantly lower FFR (p<0.0001) and 8 of the 11 patients had FFR values in the "grey zone" between 0.75 and 0.8. So in this population, false positive MRMPI scans do not appear to be due to microvascular disease.

The final area of microvascular disease we examined was the relationship between CFR and uncorrected and corrected IMR. The scatterplot on figure 4.10 shows the relationship between uncorrected IMR and CFR. The r value was -0.3 indicating that as CFR increases IMR decreases as one would expect.

Figure 4.10 - Scatterplot of CFR versus uncorrected index of microcirculatory resistance (IMRuncorr). Pearson's correlation coefficient r=-0.3, p<0.0001.

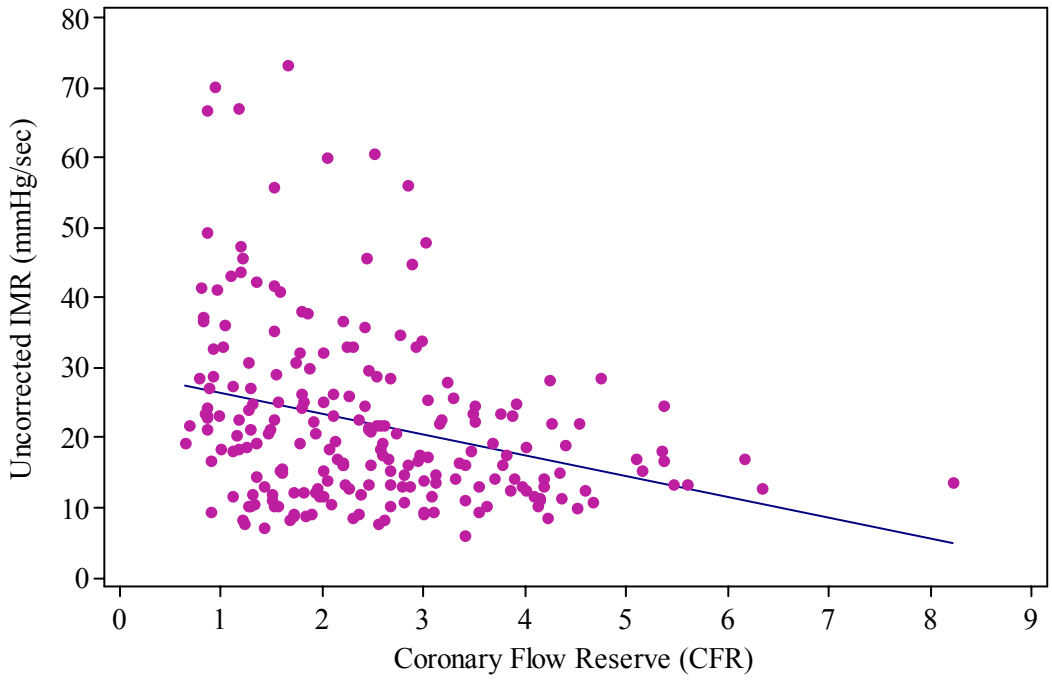

There was no correlation when the corrected IMR was compared with CFR in figure 4.11 (r=-0.02, p=0.9) suggesting that when collaterals are taken into account, there is no difference in microvascular function with increasing CFR.

Figure 4.11 - Scatterplot of CFR versus corrected index of microcirculatory resistance (IMRuncorr). Pearson's correlation coefficient r=-0.02, p=0.91.

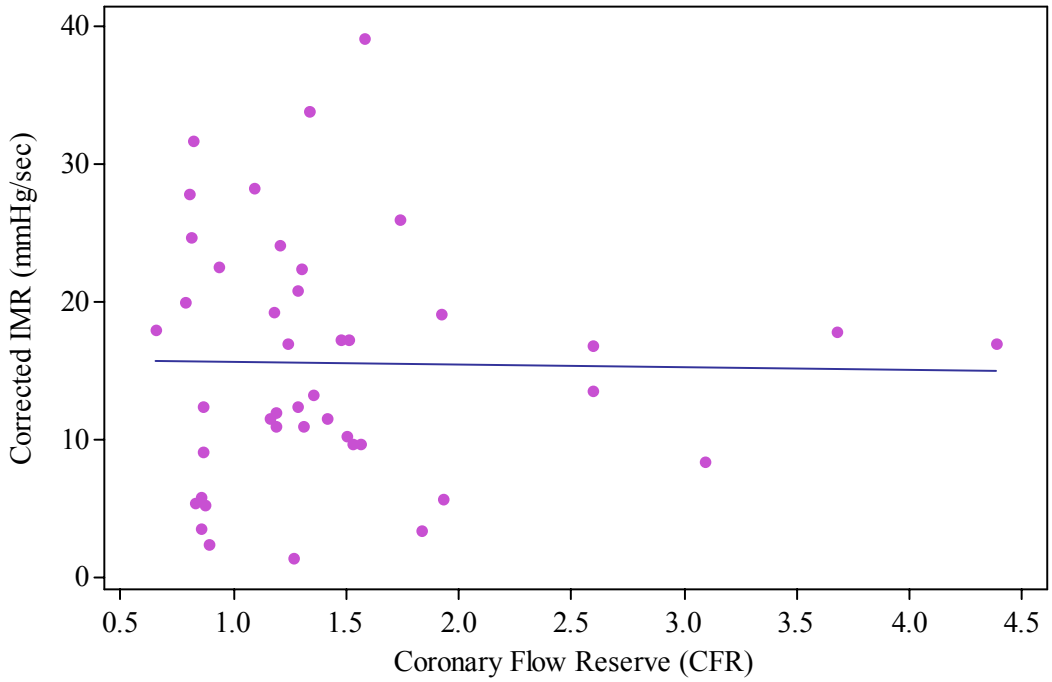

Table 4.11 - A comparison of haemodynamic and QCA parameters in patients with false positive (column 1), true positive (column 2) and true negative (column 3) MRMPI scans.

	Perfusion Defect / FFR≥0.75				**Perfusion Defect / FFR<0.75**				**No Perfusion Defect / FFR≥0.75**			
	Number	Mean	Median	SD	Number	Mean	Median	SD	Number	Mean	Median	SD
FFR	11	0.79	0.77	0.04	60	0.52	0.50	0.14	164	0.92	0.94	0.07
CFR	10	2.42	1.78	1.66	54	1.52	1.28	0.84	164	2.84	2.67	1.26
IMRuncorr	9	22.6	21.8	9.68	48	26.9	22.9	16.08	153	20.2	17.0	11.21
IMRcorr	3	18.0	17.81	7.84	34	14.4	12.8	8.45	2	28.1	28.1	15.7
Qcorr	9	3.57	2.78	1.96	48	2.40	1.94	1.71	154	4.65	4.17	2.26
%stenosis	11	52.6	51.9	18.7	61	67.54	68.0	13.8	164	25.0	24.7	20.9
Lesion length	11	14.5	15.0	7.7	60	17.9	15.8	8.7	135	12.5	12.6	8.2

4.3.1.5 Magnetic Resonance Myocardial Perfusion Imaging (MRMPI) versus Quantitative Coronary Angiography (QCA)

Table 4.12 outlines the results when MRMPI findings are compared with a QCA cut-off of 70% DS as has been done in multiple previous studies.(18;19;22;24;25) There were 72 territories with perfusion defects and a DS in the corresponding artery ≥70%. There were 50 territories with abnormal perfusion and a DS <70%. 178 territories had no perfusion defect and a DS <70%. Only 2 territories failed to show a perfusion defect on MRMPI with a DS ≥70% on QCA. Using a DS cut-off of 70% as the gold standard resulted in a sensitivity, specificity, positive and negative predictive value of 97%, 78%, 59% and 99% respectively as shown on table 4.13 along with the 95% confidence intervals. As documented previously there were 5 patients who failed to develop either symptoms or a haemodynamic response during the adenosine infusion. These patients were labelled as non-responders and the data excluding them from the analysis is included in table 4.12. The effect this has on the diagnostic accuracy of MRMPI is shown on table 4.13. This data shows that the number of false negative scans drops to zero leading to further improvements in sensitivity and negative predictive value. Figure 4.12 shows a comparison of %DS with FFR. We confirmed a previously described finding that degree of stenosis correlates poorly with functional significance (Figure 4.13). The majority of coronary arteries with an FFR<0.75 had a degree of stenosis (DS) less than 70% (39/68). Occluded arteries have been excluded from this analysis. The mean degree of stenosis for those arteries with a significant FFR was 65.2% (SD=14.9, range 29.9–96.3). For comparison, figure 4.14 shows the DS for those arteries with FFR>0.75. Excluding those arteries which are angiographically completely normal the mean degree of stenosis was 27.2% (SD=21.5, Range 0-84.8). The degree of stenosis was significantly higher in the group with physiologically significant disease as expected (T=16, p<0.0001, DF= 169). The mean area of stenosis for arteries with an

FFR<0.75 was 85.3% (SD=10.9, Range 50.9 – 99.8) compared to 42.2% (SD=30.7, Range 0 – 95.8) in those arteries with an FFR≥0.75 (T=17, p<0.0001). This analysis also excludes totally occluded vessels.

Table 4.12 - MRMPI compared to quantitative coronary angiography (QCA).

	% DS ≥70%	**% DS <70%**	**Totals**
Positive MRMPI	72	50	**122**
Negative MRMPI	2	178	**180**
Totals	74	228	**302**
	Excluding non-responders to adenosine (5)		
Positive MRMPI	71	49	**120**
Negative MRMPI	0	167	**167**
Totals	71	216	**287**

Table 4.13 - Sensitivity, specificity, positive and negative predictive values of MRMPI in the diagnosis of significant coronary disease as defined by a DS≥70%.

	All Patients (95% CI)	**Excluding Non-Responders (95% CI)**
Sensitivity (%)	97.3 (92.8-101.8)	100 (100-100)
Specificity (%)	78.1 (70.5-85.6)	77.3 (69.4-85.2)
PPV (%)	59.0 (47.5-70.6)	59.2 (47.5-70.9)
NPV (%)	98.9 (96.9-100.9)	100 (100-100)
Diagnostic Accuracy (%)	82.8	82.9

Figure 4.12 - A comparison of DS by QCA with FFR measurements with a line of best fit. R = -0.84 indicating a strong degree of correlation (Pearson Correlation Coefficient). CTO's are included with an FFR of 0.4 to take into account collateral flow.

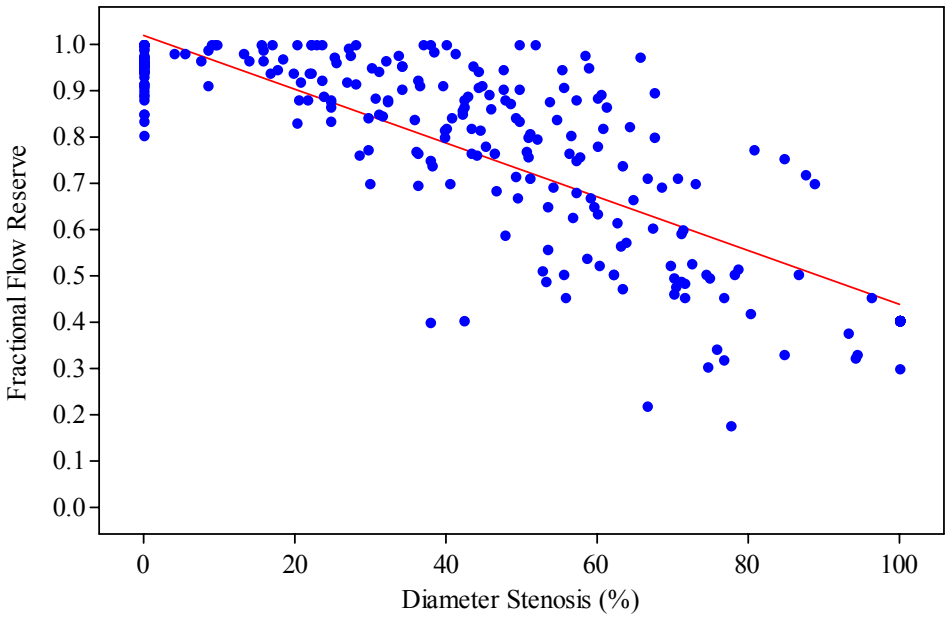

Figure 4.13 - Dot plot showing the degree of stenosis for those arteries with a significant FFR<0.75. A 70% cut-off has been accepted in many of the previous studies to represent an artery with haemodynamically significant disease. The majority of arteries in our study with physiologically significant disease have stenoses beneath 70% severity. No occluded coronary arteries are included in this figure.

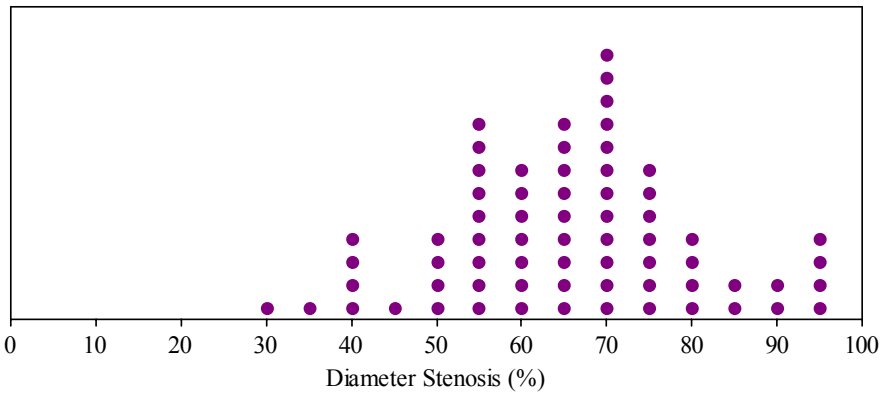

Figure 4.14 - Dot plot showing the degree of stenosis for those arteries with no physiologically significant disease (FFR≥0.75). Excluding 49 arteries with no evidence of luminal narrowing (0% stenosis).

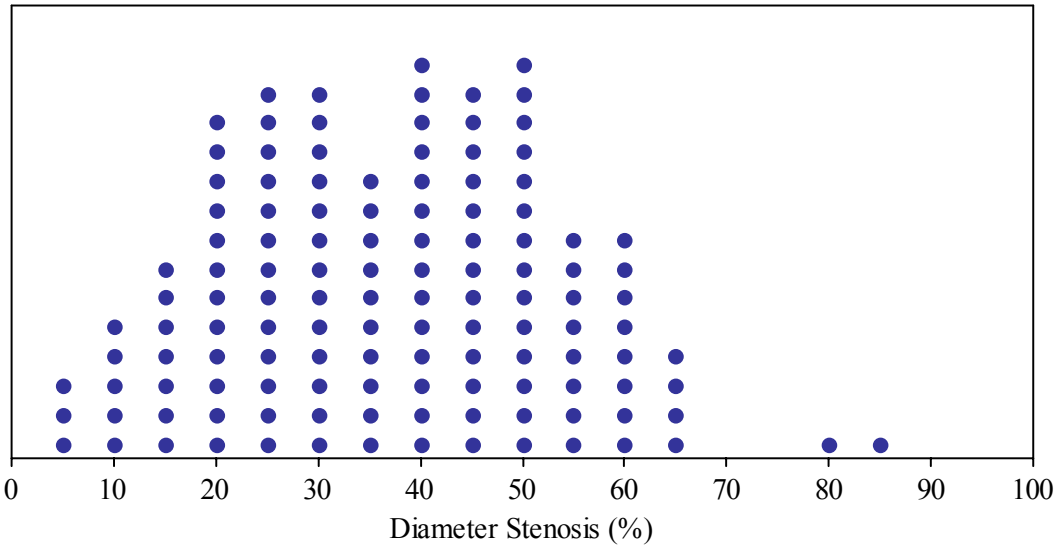

4.3.2 Myocardial Perfusion Reserve Index (MPRI)

4.3.2.1 MPRI Interobserver Variability For All Myocardial Segments Using Fermi Deconvolution Method

MPRI data using fermi deconvolution was calculated by two observers in 212 (94%) of 226 scans analysed. Of the 14 scans not analysed by both observers: 4 were felt to be uninterpretable by both observers due to image artefact; 3 were felt to be uninterpretable by observer 1 due to artefact; 4 were felt to be uninterpretable by observer 2 due to artefact and there were missing data in 3 of the scans.

In order to assess interobserver variability for the huge amounts of data produced from the MPRI analysis, we first looked at the mean MPRI for the complete myocardium (all 16 segments) per patient scan. This analysis included all available scans including all

pre and post revascularisation and pre and post medical therapy as well as those patients with normal coronary arteries. The mean MPRI for the 212 scans analysed by observer 1 was 2.37 (Median=2.32, SD=0.81, Range 0.70-4.92) and observer 2 was 2.20 (Median=2.18, SD=0.75, Range 0.79-4.92). The Pearson Correlation Coefficient for obsrever 1 versus observer 2 was $r=0.9$ with $p<0.0001$.

In order to examine the level of agreement between observers a Bland-Altman plot was created showing the difference between observers against their mean (Figure 4.15). This shows no relationship between measurement error and the mean values which we take to be the true mean MPRI for 16 segments per scan. In order to examine the measurement bias we calculated the mean difference between observers which was 0.18 with a standard deviation of 0.36. As shown in figure 4.15 most of the differences between observers lie between 0.18 and ±1.96xSD. Examining the limits of agreement between observers showed that observer 2 may be 0.53 below or 0.89 above observer 1.

Figure 4.15 - Difference in mean MPRI for all 16 segments per scan against the mean MPRI with reference lines showing the mean±1.96SD within which 95% of the differences lie.

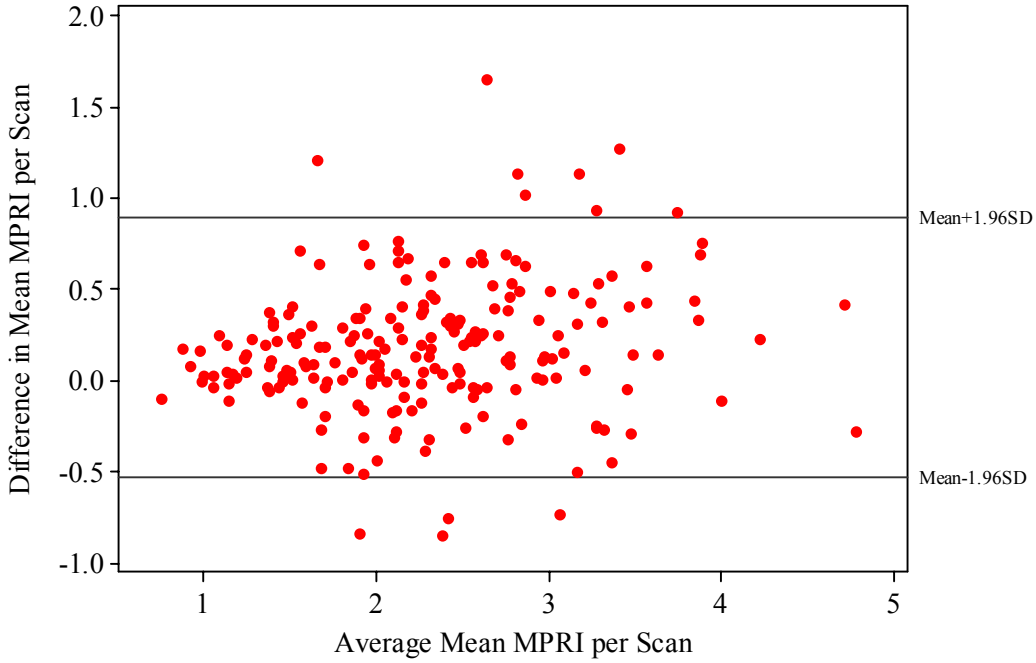

Examining the precision of the estimated limits of agreement the standard error of the mean difference was calculated to be 0.025 with 211 degrees of freedom (DF) and a t=1.97. The 95% confidence interval of the bias was 0.13 to 0.23. The standard error of the 95% limits of agreement was 0.043, therefore the 95% confidence intervals for the lower limit of agreement were narrow at -0.62 to -0.45 and for the upper limit of agreement were 0.81 to 0.98.

We then assessed the interobserver variability of Fermi deconvolution derived MPRI per coronary artery territory, where a mean MPRI per artery according to the myocardial segment as AHA model was taken from the data of each of the 2 observers. The mean MPRI for the 621 coronary artery segments analysed by observer 1 was 2.35 (Median=2.27, SD=0.89, Range 0.32-5.62) and observer 2 was 2.19 (Median=2.13,

SD=0.82, Range 0.39-5.24). The Pearson Correlation Coefficient for obsrever 1 versus observer 2 was r=0.85 with p<0.0001.

The Bland-Altman plot to assess the limits of agreement between the two observers is presented in Figure 4.16. This shows no relationship between measurement error and the mean values which we take to be the true mean MPRI for each of the coronary artery territories. Examining the measurement bias revealed a mean difference between observers of 0.17 with a standard deviation of 0.47. Figure 4.16 shows that most of the differences between observers lie between 0.17 and ±1.96xSD. Examining the limits of agreement between observers showed that observer 2 may be 0.75 below or 1.1 above observer 1.

Figure 4.16 - Difference in mean Fermi deconvolution derived MPRI for each coronary artery territory per scan against the mean MPRI with reference lines showing the mean±1.96SD within which 95% of the differences lie.

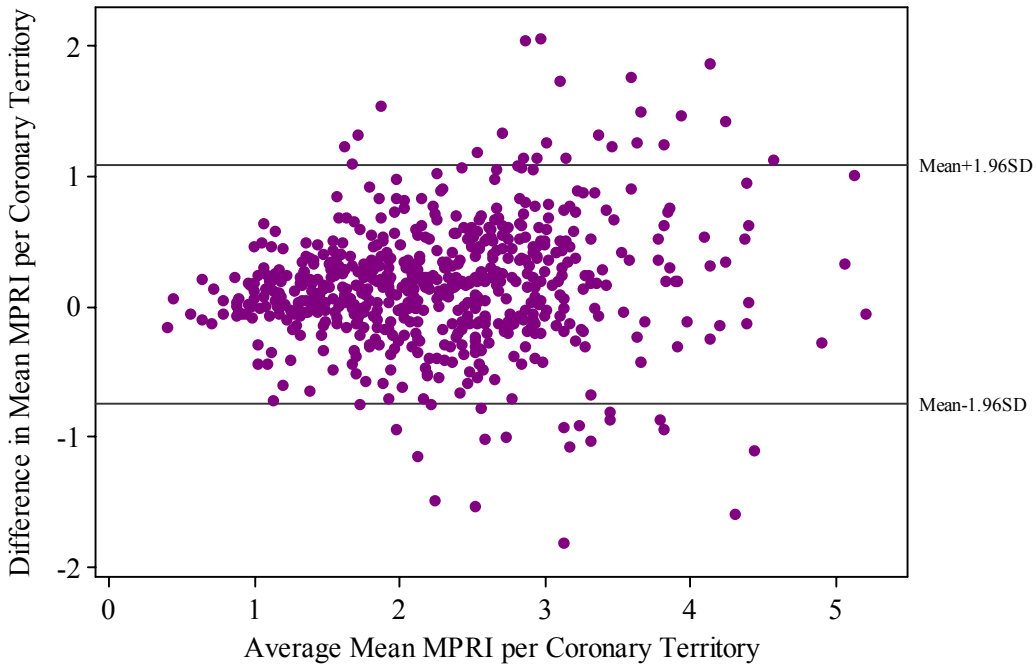

We then examined the precision of the estimated limits of agreement. The standard error of the mean difference was calculated to be 0.019 with 620 DF and a t=1.97. The 95% confidence interval of the bias was 0.14 to 0.19. The standard error of the 95% limits of agreement was 0.032, therefore the 95% confidence intervals for the lower limit of agreement were narrow at -0.81 to -0.69 and for the upper limit of agreement were 1.03 to 1.15.

The lowest mean MPRI for each coronary artery territory was also used in the analysis in case the mean MPRI diluted out a low MPRI from a small perfusion defect only affecting one or two of the myocardial segments of a coronary artery. The lowest mean Fermi deconvolution derived MPRI of the 621 coronary artery territories analysed by observer 1 was 1.6 (Median=1.57, SD=0.75, Range 0.001-4.19) and observer 2 was 1.49 (Median=1.44, SD=0.72, Range 0.12-4.8). The Pearson Correlation Coefficient for obsrever 1 versus observer 2 was r=0.74 with $p<0.0001$.

Assessing the limits of agreement using a Bland-Altman plot (Figure 4.17) show that spread of differences between observers is greater than that found when taking the mean MPRI per coronary artery territory. The mean difference between observers was 0.11 with a standard deviation of 0.53. Figure 4.17 shows that most of the differences between observers lie between 0.11 and ±1.96xSD. Examining the limits of agreement between observers showed that observer 2 may be 0.93 below or 1.15 above observer 1.

Figure 4.17 - Difference in lowest mean Fermi deconvolution derived MPRI for each coronary artery territory per scan against the mean MPRI with reference lines showing the mean±1.96SD within which 95% of the differences lie.

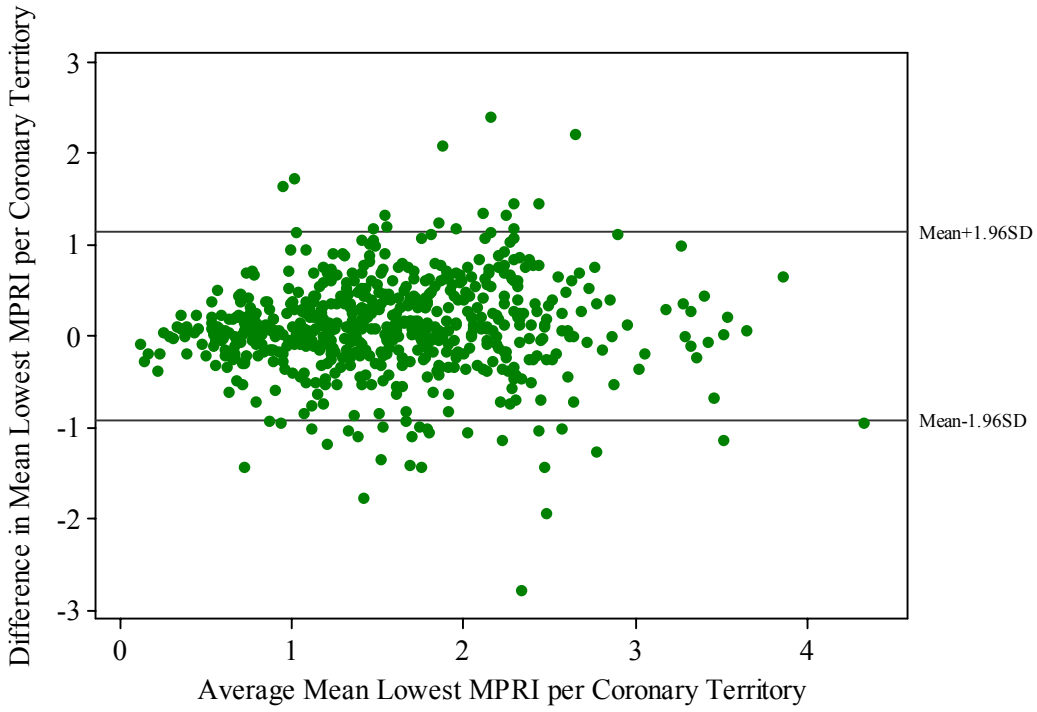

We then examined the precision of the estimated limits of agreement. The standard error of the mean difference was calculated to be 0.021 with 620 DF and a t=1.97. The 95% confidence interval of the bias was 0.07 to 0.15. The standard error of the 95% limits of agreement was 0.036, therefore the 95% confidence intervals for the lower limit of agreement were narrow at -1.0 to -0.86 and for the upper limit of agreement were 1.08 to 1.22.

4.3.2.2 Fermi Deconvolution Derived MPRI versus FFR.

Figure 4.18 shows a scatter plot of the Fermi Deconvolution derived lowest MPRI values for individual coronary artery territories along with the pressure wire measured FFR for that corresponding artery. Data from 95 of the 101 patients (94%) were included in this analysis. Artefact was the main reason for not including the MPRI data

from the 6 patients whose data was excluded. Occluded arteries were again given a FFR value of 0.4 to represent collateral flow. The Pearson's correlation coefficient on this occasion was higher at 0.48 ($p<0.0001$) indicating a more linear incremental relationship than that encountered when taking the mean MPRI for each of the segments per coronary artery territory.

Figure 4.18 - Scatterplot of Fermi deconvolution derived lowest mean MPRI for each coronary artery territory against the measured FFR for the corresponding coronary artery with a line of best fit.

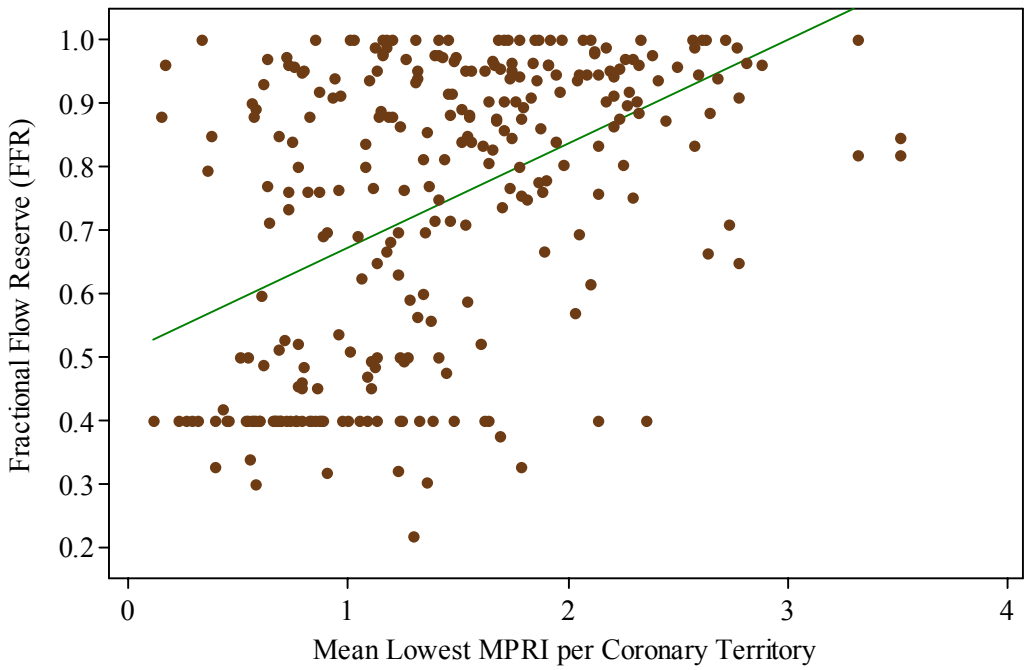

Bearing in mind that the majority of previous studies compared MPRI with degree of stenosis as the gold standard, Figures 4.19 and 4.20 show scatterplots of degree of stenosis versus mean and lowest Fermi deconvolution derived MPRI with line of best fit. The Pearson's correlation coefficient for this data was -0.38 using the mean MPRI and -0.47 for the lowest MPRI again indicating that as the degree of stenosis increases the MPRI falls.

Figure 4.19 - Scatterplot of Fermi deconvolution derived mean MPRI for each coronary artery territory against the QCA measured degree of stenosis (%) for the corresponding coronary artery with a line of best fit.

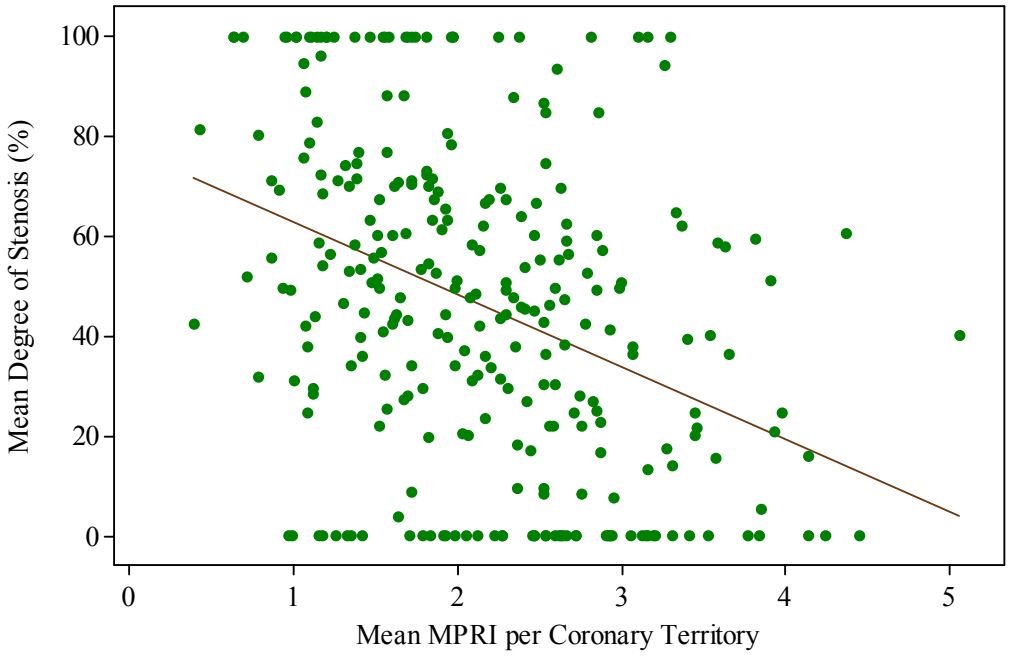

Figure 4.20 - Scatterplot of Fermi deconvolution derived lowest mean MPRI for each coronary artery territory against the QCA measured degree of stenosis (%) for the corresponding coronary artery with a line of best fit.

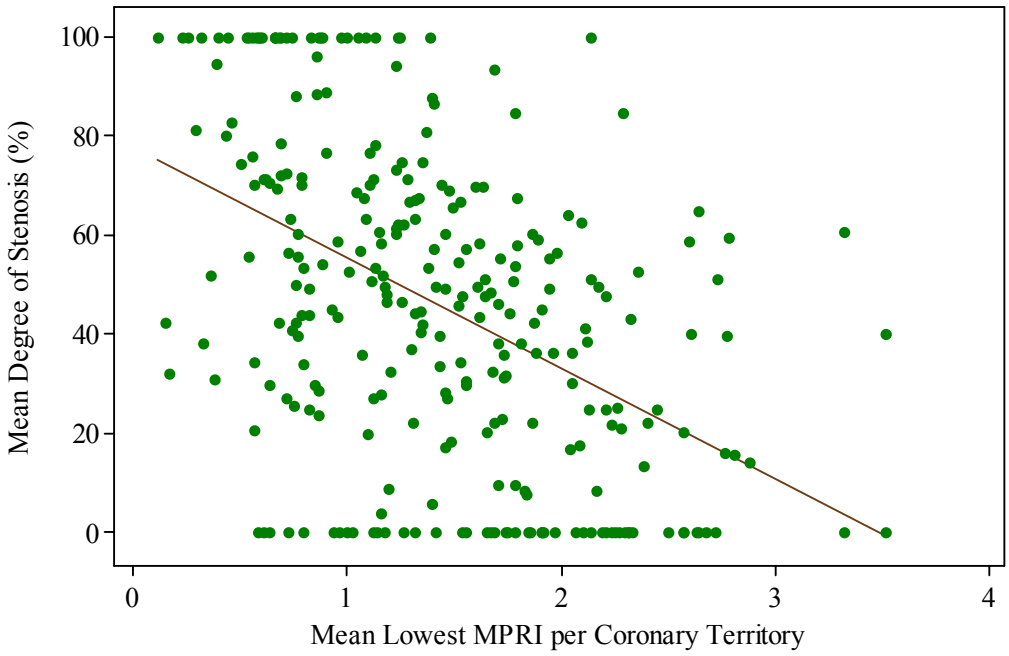

Correlations with other pressure wire derived haemodynamic parameters were made as for the maximum signal derived MPRI and are presented in table 4.14. Lowest MPRI per coronary territory has the best correlation coefficient of any these measurements.

Table 4.14 - Pearson's correlation coefficients for each of the pressure wire measured haemodynamic variables compared with Fermi deconvolution derived MPRI.

	Mean MPRI Per Coronary Territory	Lowest MPRI Per Coronary Territory
Fractional Flow Reserve (FFR)	0.4	0.48
Coronary Flow Reserve (CFR)	0.41	0.34
Uncorrected Index of Microcirculatory Resistance (IMRuncorr)	-0.15	-0.2
Corrected Index of Microcirculatory Resistance (IMRcorr)	0.22	0.10
Coronary Flow (Qcorr)	0.17	0.18

The receiver operator characteristic curve for Fermi deconvolution derived MPRI using both the mean MPRI for coronary artery territories and the lowest MPRI is shown in Figure 4.21. This provides a plot of sensitivity versus 1-specificity and allows us to select an optimum cut-off value of MPRI using an FFR of 0.75 as our gold standard cut off. The area under the curve for the mean MPRI per coronary territory was 0.73 compared to 0.77 for the lowest MPRI per coronary territory. This indicates that the probability of a randomly chosen ischaemic coronary territory having a lower MPRI than a normally perfused territory is higher when we take the lowest MPRI per territory. The low MPRI curve is closest to the y-axis for the majority of its course again indicating using the low value is the most accurate. The asymptotic 95% confidence

intervals however overlap to a large extent (Mean MPRI – 0.67 to 0.79 and Lowest MPRI – 0.72 to 0.83) indicating that the real difference between these tests is small. Taking a mean MPRI cutoff of 2.41 gave a sensitivity of 83% and 1-specificity of 50% (Specificity = 50%). Using a cut-off value for the low MPRI of 1.70 gave a sensitivity of 90% and 1-specificity of 52% (Specificity = 48%).

Figure 4.21 - Receiver Operator Characteristic (ROC) curve of mean Fermi deconvolution derived MPRI per coronary artery territory and lowest MPRI per coronary artery territory using an FFR cut-off of 0.75 as the gold standard for the diagnosis of coronary artery disease.

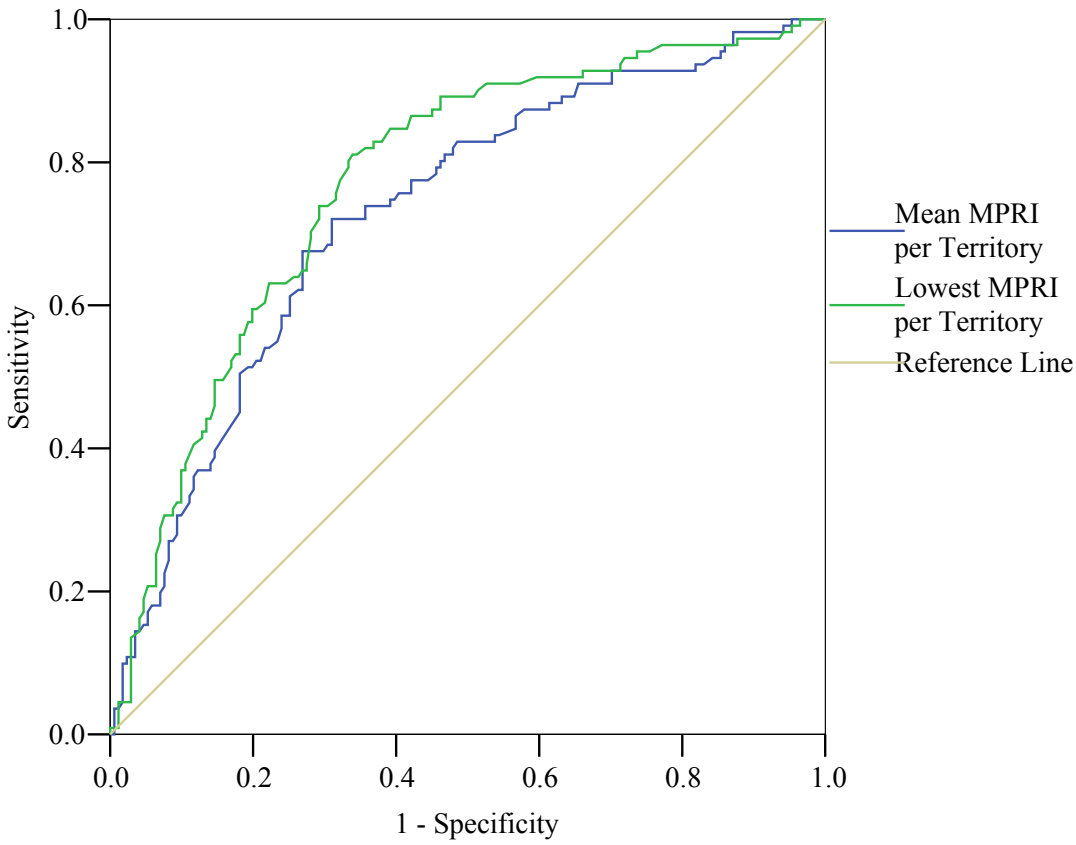

The distribution of Fermi deconvolution derived MPRI data are presented on Figure 4.22. This shows that the degree of overlap of MPRI values between arteries with significant (FFR<0.75) and non-significant (FFR≥0.75) disease is less using the lowest MPRI value as opposed to the mean MPRI value per coronary artery territory.

Figure 4.22 - Boxplot comparing mean and lowest Fermi deconvolution derived MPRI values in patients with and without significant coronary artery disease defined as an FFR<0.75 highlighting the median MPRI, the interquartile range, spread of data excluding outliers and the outliers.

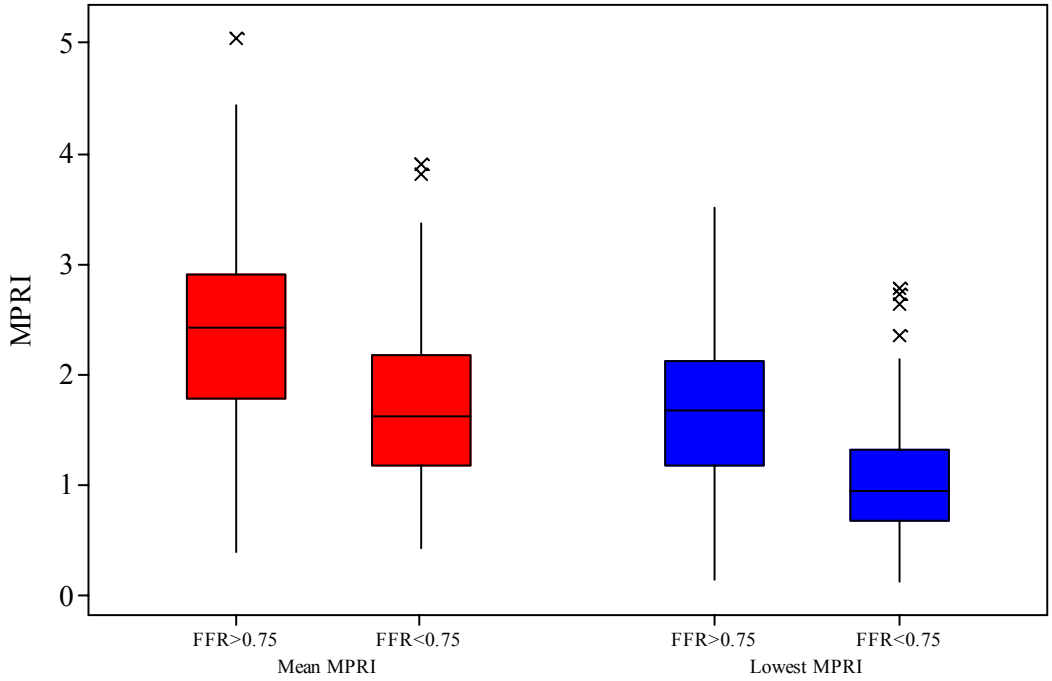

4.3.2.3 MPRI Interobserver Variability For All Myocardial Segments Using Maximum Signal Method

In order to assess interobserver variability for the data produced from the MPRI analysis, we first looked at the mean MPRI for the complete myocardium (all 16 segments) per patient scan. This analysis included all available scans including all pre and post revascularisation and pre and post medical therapy as well as those patients with normal coronary arteries. The mean MPRI for the 211 scans analysed by observer 1 was 1.56 (Median=1.55, SD=0.30, Range 0.83-2.76) and observer 2 was 1.52 (Median=1.50, SD=0.32, Range 0.84-2.67). The Pearson correlation coefficient for observer 1 versus observer 2 was r=0.87 with p<0.0001.

In order to examine the level of agreement between observers a Bland-Altman plot was created showing the difference between observers against their mean (Figure 4.23). This shows no relationship between measurement error and the mean values which we take to be the true mean MPRI for 16 segments per scan. In order to examine the measurement bias we calculated the mean difference between observers which was 0.043 with a standard deviation of 0.16. As shown in figure 4.23 most of the differences between observers lie between 0.043 and ±1.96xSD. Examining the limits of agreement between observers showed that observer 2 may be 0.31 below or 0.36 above observer 1.

Figure 4.23 - Difference in mean maximum signal derived MPRI for all 16 segments per scan against the mean MPRI with reference lines showing the mean±1.96SD within which 95% of the differences lie.

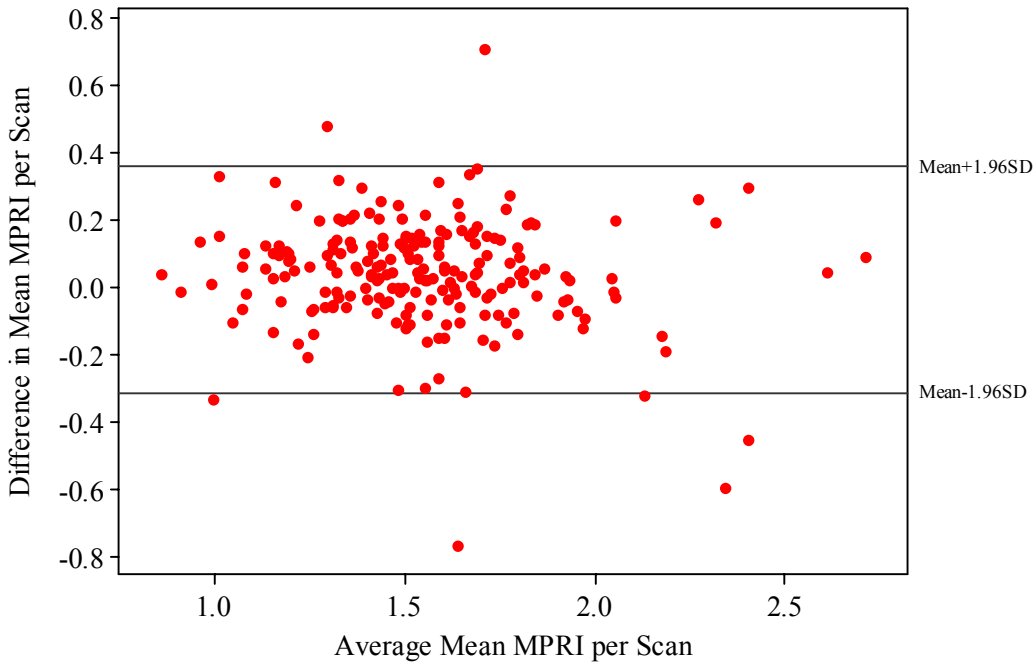

Examining the precision of the estimated limits of agreement the standard error of the mean difference was calculated to be 0.011 with 210 DF and a t=1.97. The 95% confidence interval of the bias was 0.021 to 0.065. The standard error of the 95% limits

of agreement was 0.019, therefore the 95% confidence intervals for the lower limit of agreement were -0.35 to -0.27 and for the upper limit of agreement were 0.32 to 0.40. The mean MPRI for the 633 coronary artery territories analysed by observer 1 was 1.56 (Median=1.56, SD=0.36, Range 0.42-3.15) and observer 2 was 1.52 (Median=1.51, SD=0.38, Range 0.39-3.62). The Pearson correlation coefficient for observer 1 versus observer 2 was $r=0.79$ with $p<0.0001$.

On the Bland-Altman plot for each coronary territory per scan there is no relationship between measurement error and the mean values which we take to be the true mean MPRI. In order to examine the measurement bias we calculated the mean difference between observers which was 0.043 with a standard deviation of 0.24. As shown in figure 4.24 most of the differences between observers lie between 0.043 and ±1.96xSD. Examining the limits of agreement between observers showed that observer 2 may be 0.43 below or 0.51 above observer 1.

Figure 4.24 - Difference in mean maximum signal derived MPRI for each coronary artery territory per scan against the mean MPRI with reference lines showing the mean±1.96SD within which 95% of the differences lie.

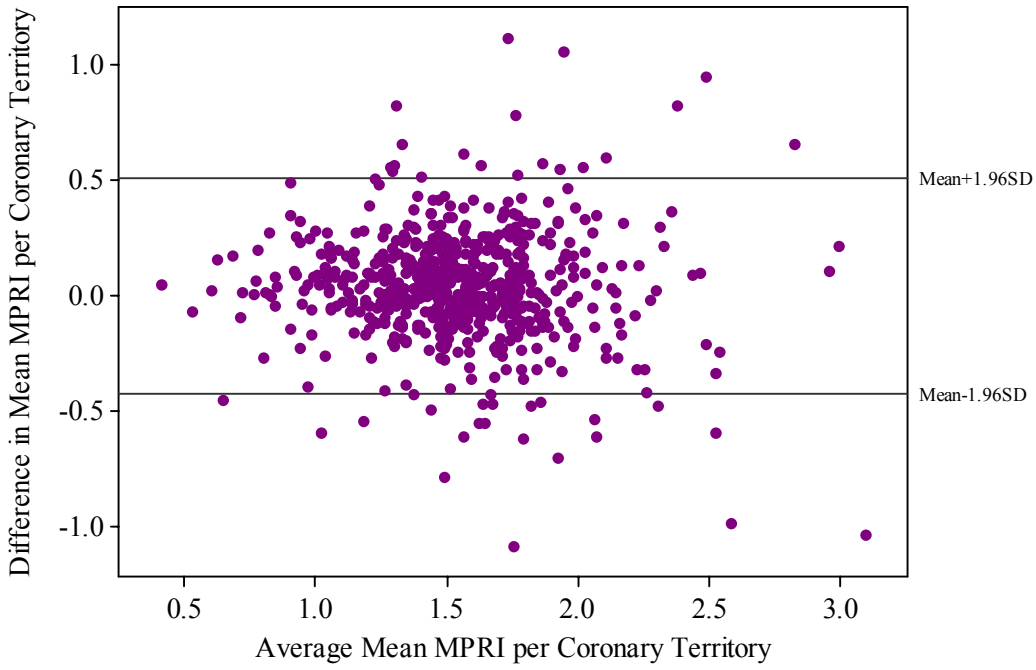

Examining the precision of the estimated limits of agreement the standard error of the mean difference was calculated to be 0.009 with 632 DF and a t=1.97. The 95% confidence interval of the bias was 0.025 to 0.061. The standard error of the 95% limits of agreement was 0.015, therefore the 95% confidence intervals for the lower limit of agreement were -0.46 to -0.4 and for the upper limit of agreement were 0.48 to 0.54.

The lowest mean MPRI within each of the coronary artery territories for the 633 coronary artery territories analysed by observer 1 was 1.16 (Median=1.23, SD=0.40, Range 0-2.47) and observer 2 was 1.14 (Median=1.19, SD=0.39, Range 0-2.65). The Pearson correlation coefficient for observer 1 versus observer 2 was r=0.71 with $p<0.0001$.

A Bland-Altman plot of the mean lowest MPRI for each coronary territory per scan is presented in figure 4.25 showing no relationship between measurement error and the mean values which we take to be the true mean MPRI. In order to examine the measurement bias we calculated the mean difference between observers which was 0.019 with a standard deviation of 0.3. As shown in figure 4.25 most of the differences between observers lie between 0.019 and ±1.96xSD. Examining the limits of agreement between observers showed that observer 2 may be 0.57 below or 0.61 above observer 1.

Figure 4.25 - Difference in lowest mean maximum signal derived MPRI for each coronary artery territory per scan against the mean MPRI with reference lines showing the mean±1.96SD within which 95% of the differences lie.

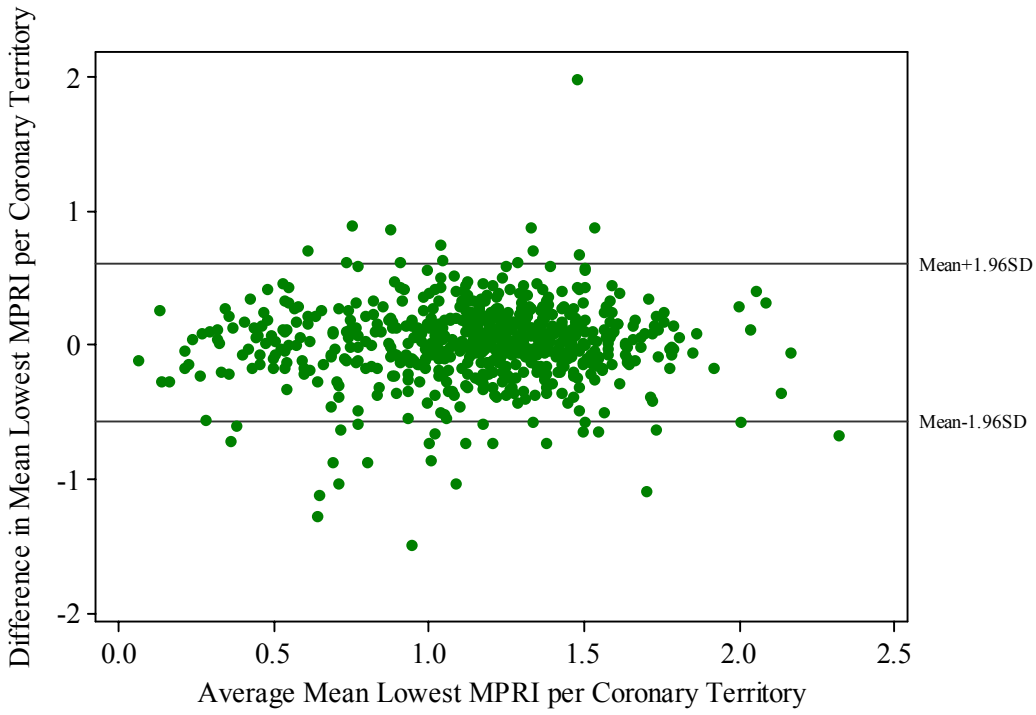

Examining the precision of the estimated limits of agreement the standard error of the mean difference was calculated to be 0.012 with 632 DF and a t=1.97. The 95% confidence interval of the bias was -0.005 to 0.043. The standard error of the 95% limits of agreement was 0.021, therefore the 95% confidence intervals for the lower limit of agreement were -0.61 to -0.53 and for the upper limit of agreement were 0.57 to 0.65.

4.3.2.4 Maximum Signal Derived MPRI versus FFR.

Figure 4.26 shows a scatter plot of the maximum signal derived MPRI values for individual coronary artery territories along with the FFR for that corresponding artery. The MPRI value for this analysis was obtained by taking the mean MPRI of those coronary segments for each of the coronary arteries and thereafter taking the mean of these values for the two observers. This provided us with three measurements per patient as we only used the initial MRI scan from each patient. Data from 97 of the 101 patients (96%) was included in this analysis. Artefact was the main reason for not including the MPRI data from the 4 patients whose data was excluded. Occluded arteries were given a FFR value of 0.4 taking into account that there will be a degree of collateral flow to the myocardium supplied by occluded arteries. As shown in Figure 4.26 there is no accurate straight line of plots comparing MPRI and FFR. The Pearson's correlation coefficient r is 0.36 with $p<0.0001$. The direction of the line indicates that MPRI increases with increasing FFR as one would expect.

Figure 4.26 - Scatterplot of maximum signal derived mean MPRI against measured FFR for the corresponding coronary artery with a line of best fit.

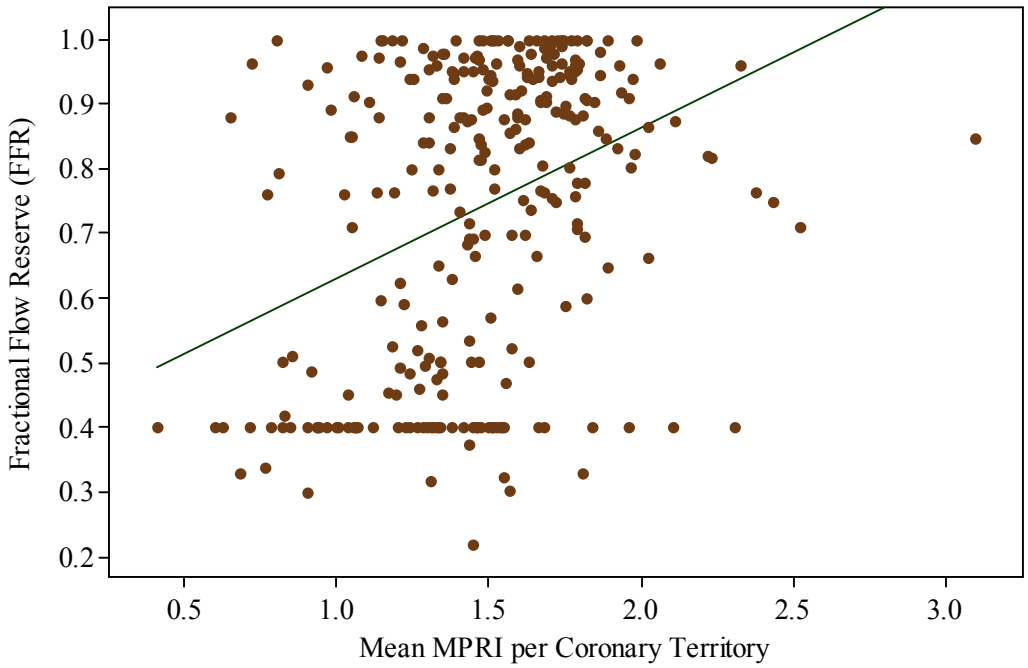

We also examined the lowest recorded MPRI for each of the segments within a coronary artery territory and compared these values with the recorded FFR for the corresponding coronary artery. Figure 4.27 shows a further scatterplot of the lowest MPRI for each coronary territory with the corresponding FFR. The Pearson's correlation coefficient on this occasion was higher at 0.45 ($p<0.0001$) indicating a more linear relationship than that encountered when taking the mean MPRI for each of the segments per coronary artery territory. Again as in Figure 4.26, as FFR increases so does the MPRI as expected.

Figure 4.27 - Scatterplot of maximum signal derived lowest mean MPRI for each coronary artery territory against the measured FFR for the corresponding coronary artery with a line of best fit.

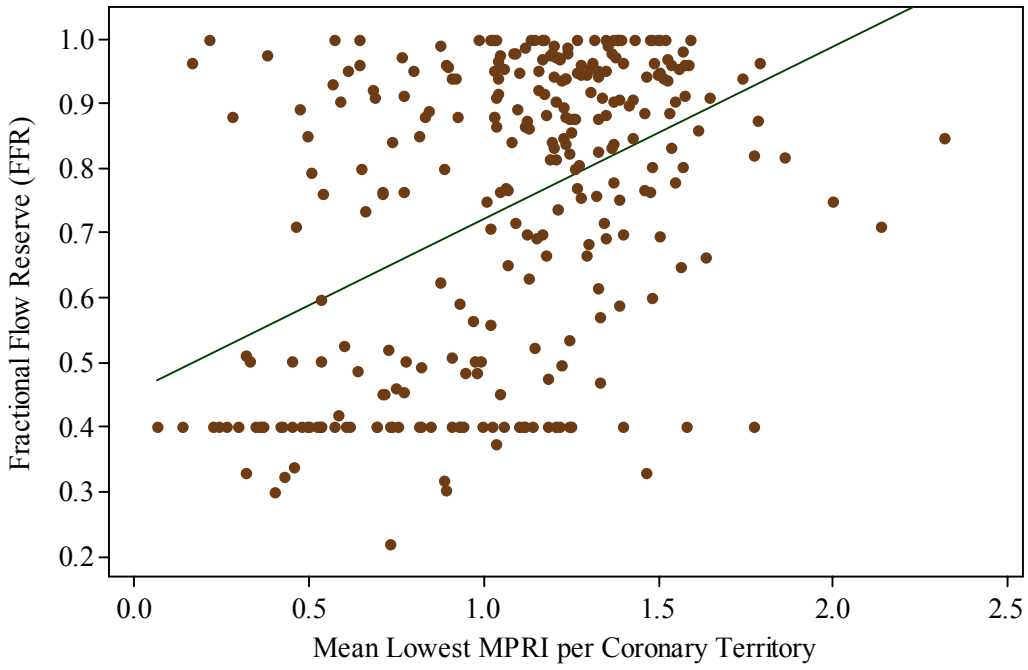

Accepting that taking the lowest MPRI value provides the best degree of correlation with FFR we also plotted the mean %DS as measured by QCA with the mean lowest obtained FFR for each of the coronary artery territories. These data are shown on Figure 4.28 again with a line of best fit. The Pearson's correlation coefficient for these data was the same as that obtained for FFR at -0.45 indicating that as the degree of stenosis increases the MPRI falls as one would expect.

Figure 4.28 - Scatterplot of maximum signal derived lowest mean MPRI for each coronary artery territory against the QCA measured degree of stenosis (%) for the corresponding coronary artery with a line of best fit.

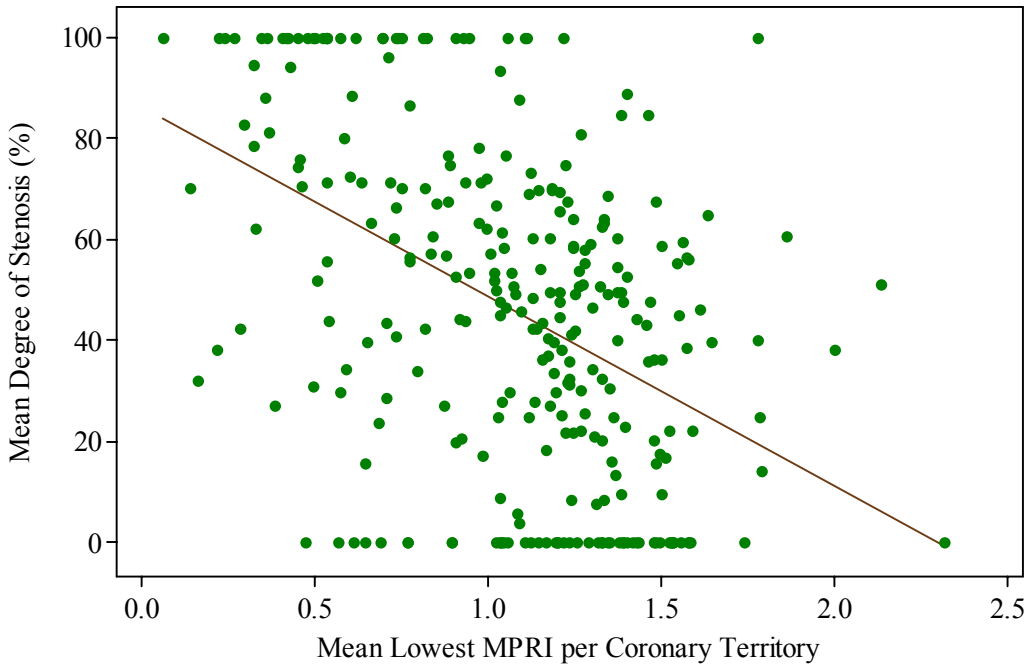

We made a number of comparisons with the other pressure wire derived measurements with the maximum signal derived MPRI. No parameter correlated better with MPRI than FFR. These data are presented in table 4.15.

Table 4.15 - Pearson's correlation coefficients for each of the pressure wire measured haemodynamic variables compared with maximum signal derived MPRI.

	Mean MPRI Per Coronary Territory	Lowest MPRI Per Coronary Territory
Fractional Flow Reserve (FFR)	0.36	0.45
Coronary Flow Reserve (CFR)	0.3	0.2
Uncorrected Index of Microcirculatory Resistance (IMRuncorr)	-0.29	-0.27
Corrected Index of Microcirculatory Resistance (IMRcorr)	0.15	0.07
Coronary Flow (Qcorr)	0.22	0.19

A receiver operator characteristic curve has been drawn for the maximum signal derived MPRI using both the mean MPRI for coronary artery territories and the lowest MPRI as shown in Figure 4.29. This provides a plot of sensitivity versus 1-specificity and allows us to select an optimum cut-off value of MPRI using an FFR of 0.75 as our gold standard cut off. The area under the curve for the mean MPRI per coronary territory was 0.71 compared to 0.74 for the lowest MPRI per coronary territory. The low MPRI curve is further away from the reference line for the majority of its course again indicating using the low value is more accurate which is similar to that encountered with the Fermi deconvolution method.. The asymptotic 95% confidence intervals however overlap to a large extent (Mean MPRI – 0.648 to 0.771 and Lowest MPRI – 0.676 to 0.796) therefore the difference between the tests is marginal. Taking a mean MPRI cutoff of 1.57 gave a sensitivity of 82% and 1-specificity of 47% (Specificity = 53%). Using a cut-off value for the low MPRI of 1.22 gave a sensitivity of 82% and 1-specificity of 48% (Specificity = 52%).

Figure 4.29 - Receiver Operator Characteristic (ROC) curve of mean MPRI per coronary artery territory and lowest MPRI per coronary artery territory using an FFR cut-off of 0.75 as the gold standard for the diagnosis of coronary artery disease.

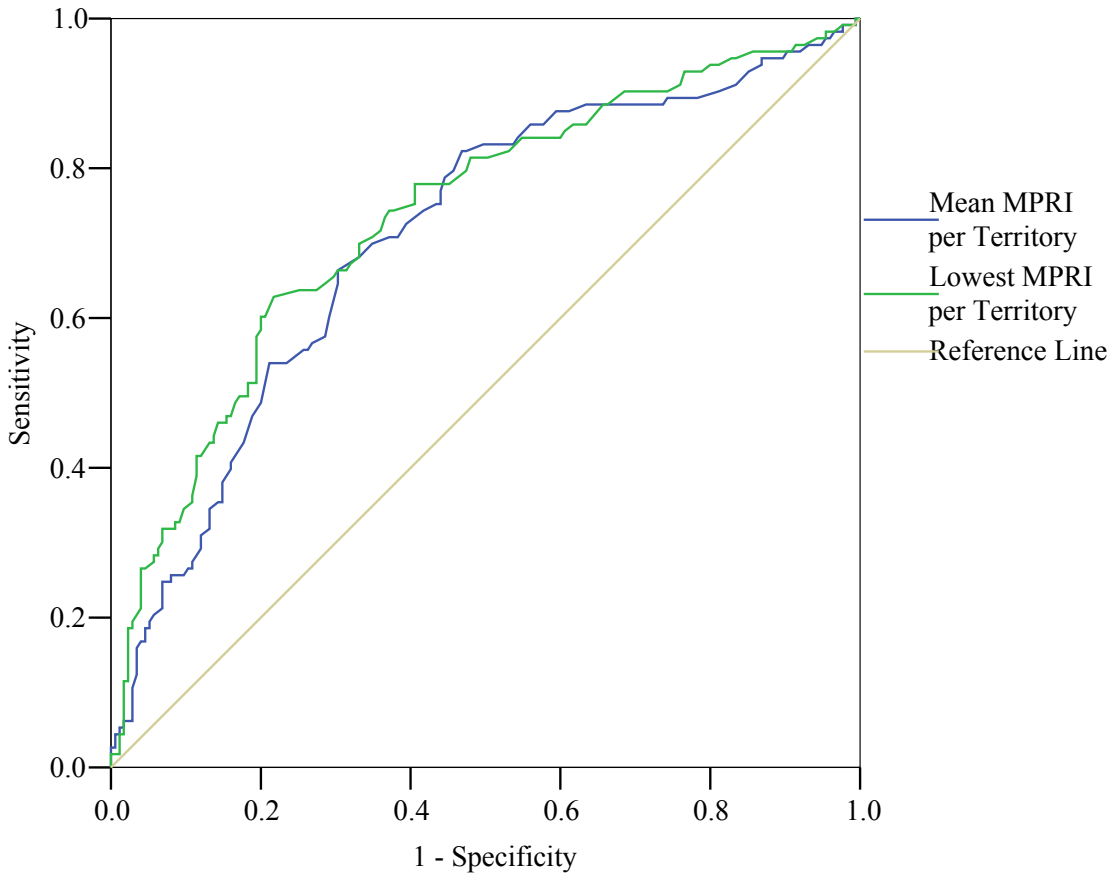

The distribution of the maximum signal derived MPRI data are presented on Figure 4.30 showing considerable overlap between the MPRI values in those arteries with significant coronary artery disease (FFR<0.75) and those with non-significant disease (FFR≥0.75). The considerable overlap exists when you take either the mean MPRI per coronary artery territory or the lowest MPRI per territory.

Figure 4.30 - Boxplot comparing mean and lowest MPRI values in patients with and without significant coronary artery disease defined as an FFR<0.75 highlighting the median MPRI, the interquartile range, spread of data excluding outliers and the outliers.

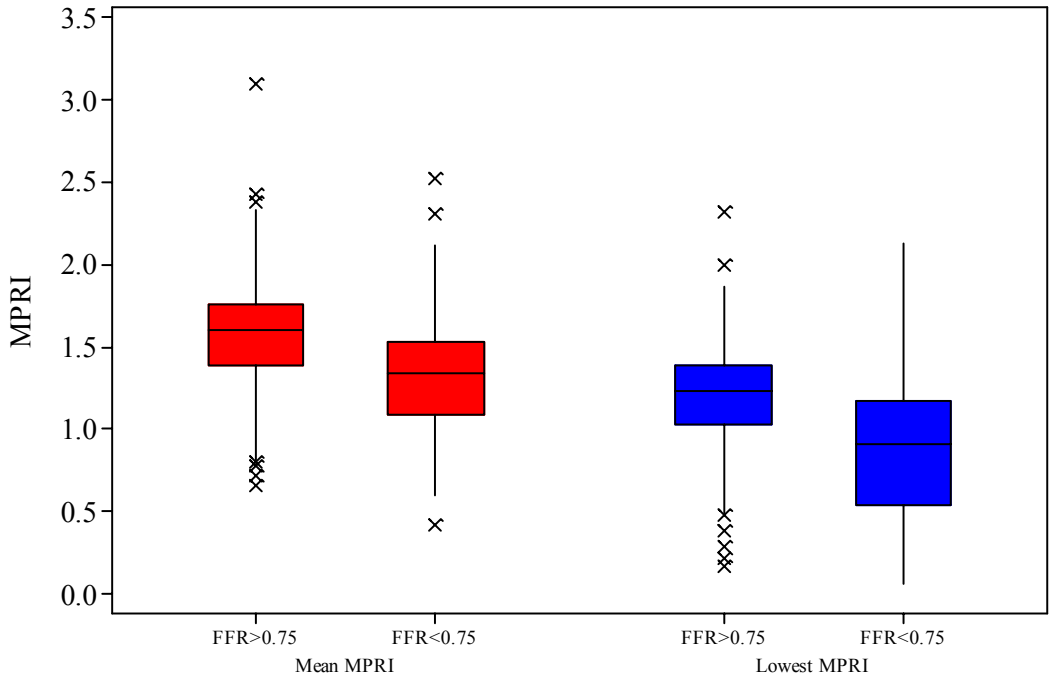

4.3.2.5 MPRI Interobserver Variability For All Myocardial Segments Using Upslope Gradient Method

Interobserver variability was first assessed by calculating MPRI by taking the mean of all myocardial segments. The mean MPRI for the 200 scans analysed by observer 1 was 2.21 (Median=2.09, SD=0.71, Range 0.72-4.41) and for observer 2 was 2.26 (Median=2.14, SD=0.8, Range 0.76-4.71). The Pearson correlation coefficient for observer 1 versus observer 2 was r=0.88 with p<0.0001.

We assessed the level of agreement between observers using a Bland-Altman plot (Figure 4.31). This confirms no relationship between measurement error and the mean values which we take to be the true mean MPRI for 16 segments per scan. The mean

difference between observers was -0.058 with a standard deviation of 0.38. As shown in figure 4.31, most of the differences between observers lie between -0.058 and ±1.96xSD. The limits of agreement between observers showed that observer 2 may be -0.80 below or 0.69 above observer 1.

Figure 4.31 - Difference in upslope gradient derived MPRI for all 16 segments per scan against the mean MPRI with reference lines showing the mean±1.96SD within which 95% of the differences lie.

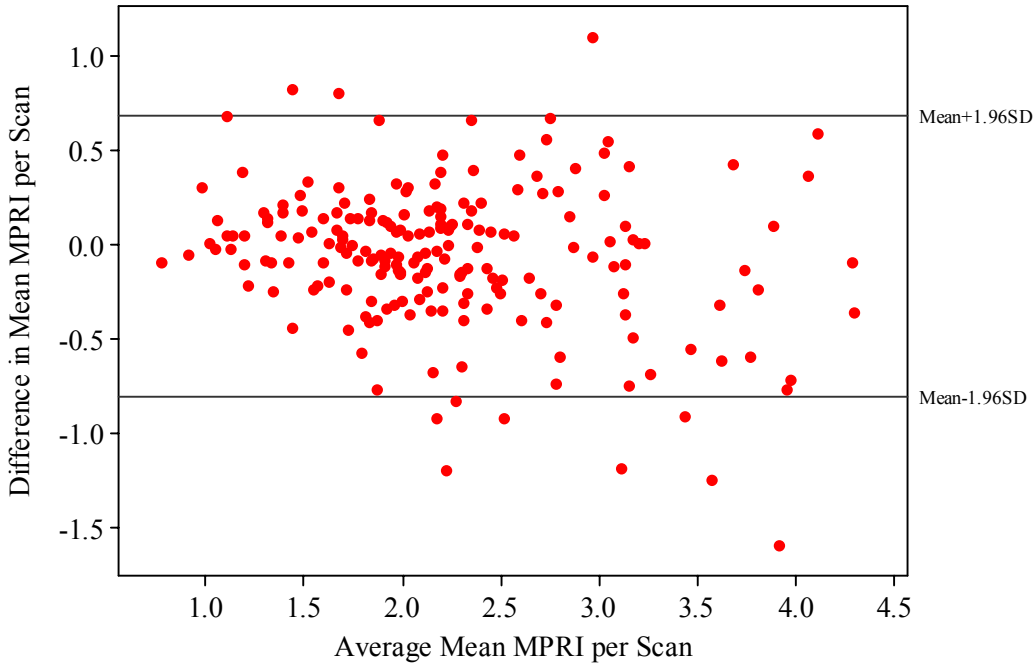

The precision of the estimated limits of agreement gave a standard error of the mean difference of 0.027 with 199 DF and t=1.97. The 95% confidence interval of the bias was -0.111 to -0.005. The standard error of the 95% limits of agreement was 0.046, therefore the 95% confidence intervals for the lower limit of agreement were -0.89 to -0.71 and for the upper limit of agreement were 0.59 to 0.78.

The mean MPRI for the 600 coronary artery territories analysed by observer 1 was 2.2 (Median=2.08, SD=0.78, Range 0.24-4.63) and observer 2 was 2.26 (Median=2.17,

SD=0.87, Range 0.39-5.79). The Pearson correlation coefficient for observer 1 versus observer 2 was r=0.83 with p<0.0001.

The Bland-Altman plot for each coronary territory per scan shows no relationship between measurement error and the mean values which we take to be the true mean MPRI. Looking at the measurement bias we calculated the mean difference between observers of -0.061 with a standard deviation of 0.48. As shown in figure 4.32 most of the differences between observers lie between -0.061 and ±1.96xSD. Examining the limits of agreement between observers showed that observer 2 may be -1.00 below or 0.88 above observer 1.

Figure 4.32 - Difference in mean upslope gradient derived MPRI for each coronary artery territory per scan against the mean MPRI with reference lines showing the mean±1.96SD within which 95% of the differences lie.

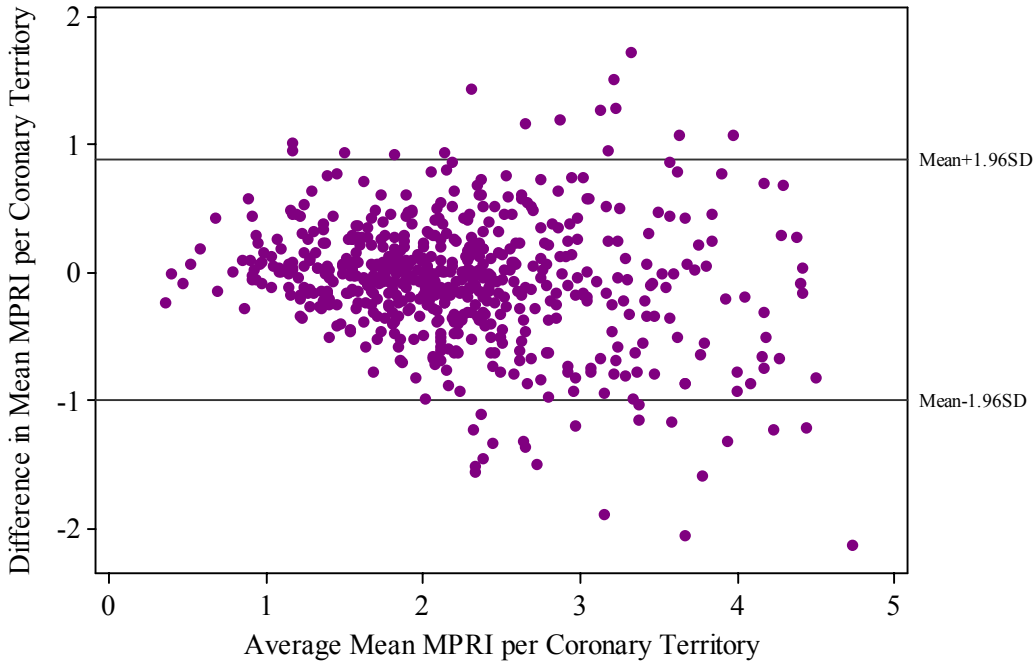

Examining the precision of the estimated limits of agreement, the standard error of the mean difference was 0.019 with DF=599 and t=1.97. The 95% confidence interval of

the bias was -0.098 to -0.061. The standard error of the 95% limits of agreement was 0.032, therefore the 95% confidence intervals for the lower limit of agreement were -1.06 to -0.94 and for the upper limit of agreement were 0.82 to 0.94.

The lowest mean MPRI of the segments within each of the coronary artery analysed by observer 1 was 1.56 (Median=1.55, SD=0.71, Range 0-4.24) and observer 2 was 1.62 (Median=1.58, SD=0.80, Range 0.02-4.30). The Pearson correlation coefficient for observer 1 versus observer 2 was $r=0.77$ with $p<0.0001$.

A Bland-Altman plot of the mean lowest MPRI for each coronary territory per scan is presented in figure 4.33 showing no relationship between measurement error and the mean values which we take to be the true mean MPRI. The mean difference between observers was -0.053 with a standard deviation of 0.53. As shown in figure 4.33, most of the differences between observers lie between -0.053 and ±1.96xSD. Examining the limits of agreement between observers showed that observer 2 may be -1.08 below or 0.98 above observer 1.

Figure 4.33 - Difference in lowest mean upslope gradient derived MPRI for each coronary artery territory per scan against the mean MPRI with reference lines showing the mean±1.96SD within which 95% of the differences lie.

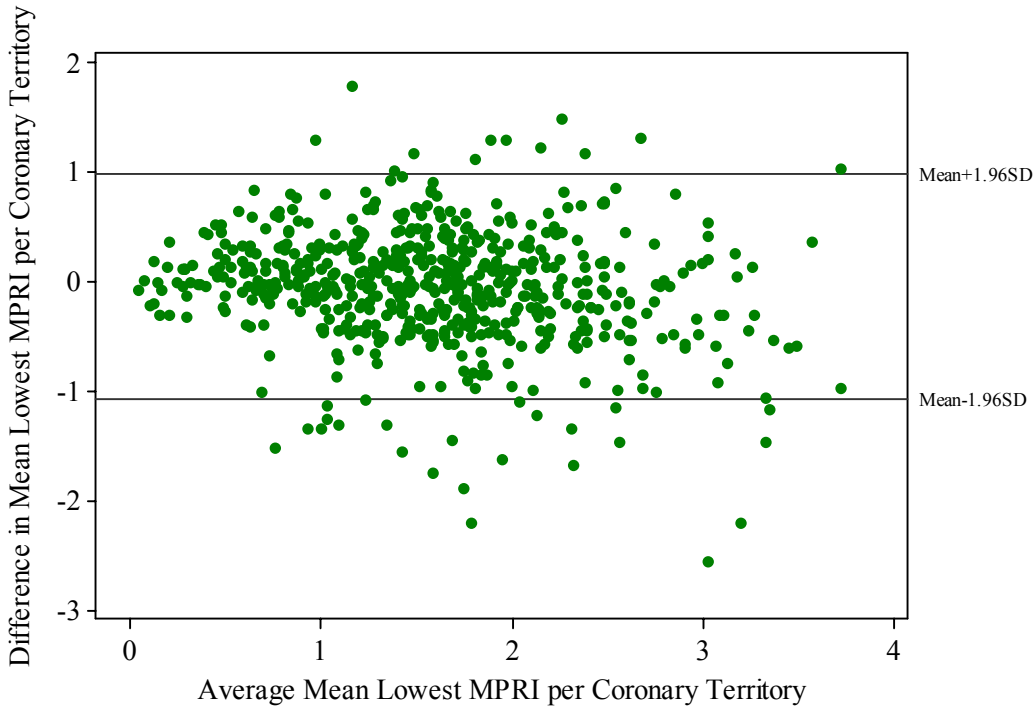

Examining the precision of the estimated limits of agreement, the standard error of the mean difference was 0.021 with DF=599 and t=1.97. The 95% confidence interval of the bias was -0.094 to -0.012. The standard error of the 95% limits of agreement was 0.036, therefore the 95% confidence intervals for the lower limit of agreement were -1.15 to -1.01 and for the upper limit of agreement were 0.91 to 1.05.

4.3.2.6 Upslope Gradient Derived MPRI versus FFR.

The mean MPRI per coronary artery territory from the two observers with corresponding FFR is shown on figure 4.34. The data from 273 arteries is included in this figure from 92 (91%) patients. Scan artefact was the main reason for not including the MPRI data from the 9 patients whose data was excluded. As in the preceding analyses occluded arteries were given a FFR value of 0.4. As with the other methods of

assessing MPRI, increasing MPRI does correlate with increasing FFR with a Pearson's correlation coefficient r of 0.34 with $p<0.0001$.

Figure 4.34 - Scatterplot of upslope gradient derived mean MPRI against FFR for the corresponding coronary artery with a line of best fit.

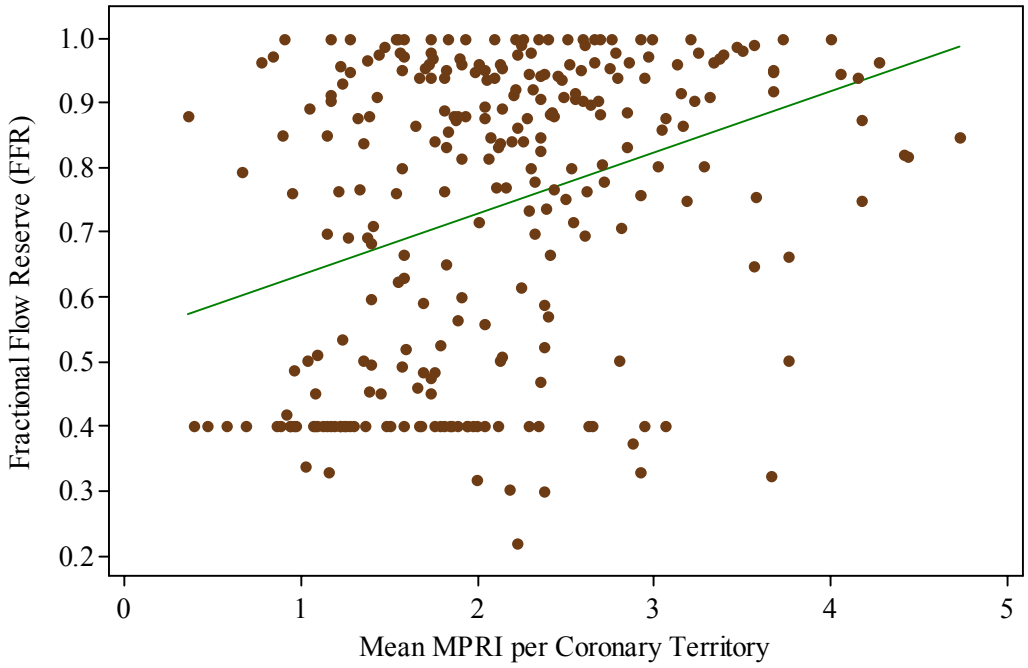

The lowest MPRI for each coronary territory was then compared with the FFR as shown on figure 4.35. The Pearson's correlation coefficient was better at 0.47 ($p<0.0001$) indicating a more linear relationship than that encountered when taking the mean MPRI. Upslope gradient derived MPRI again increases with FFR.

Figure 4.35 - Scatterplot of upslope gradient derived lowest mean MPRI for each coronary artery territory against the measured FFR for the corresponding coronary artery with a line of best fit.

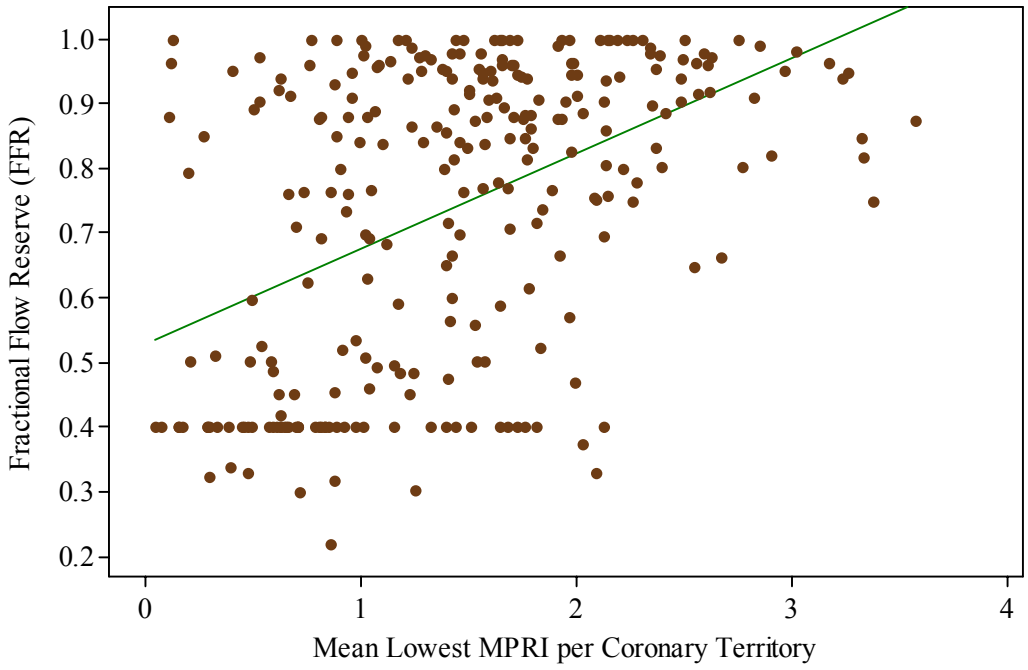

As for the other two methods of assessing MPRI we also plotted the mean degree of stenosis as measured by QCA with the mean and the lowest obtained FFR for each of the coronary artery territories. These data are shown on Figure 4.36 and 4.37 again with a line of best fit. The Pearson's correlation coefficient when using the mean MPRI in the correlation was -0.33 and using the lowest MPRI was -0.46 indicating that with increasing degrees of stenosis the MPRI falls as was shown using the other two methods.

Figure 4.36 - Scatterplot of upslope gradient derived mean MPRI for each coronary artery territory against the QCA measured degree of stenosis (%) for the corresponding coronary artery with a line of best fit.

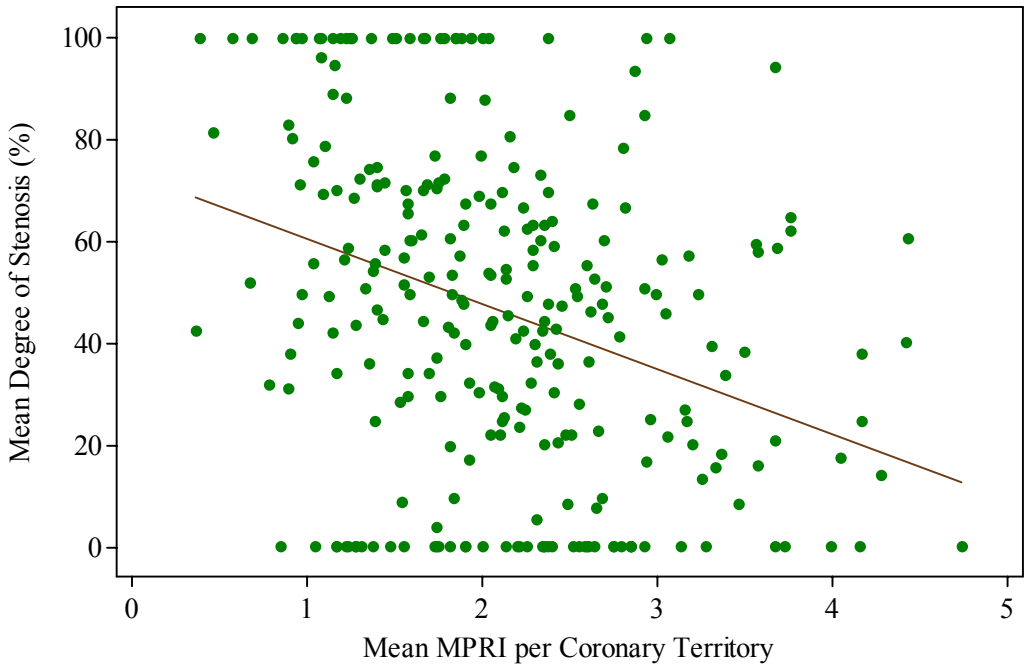

Figure 4.37 - Scatterplot of upslope gradient derived mean lowest MPRI for each coronary artery territory against the QCA measured degree of stenosis (%) for the corresponding coronary artery with a line of best fit.

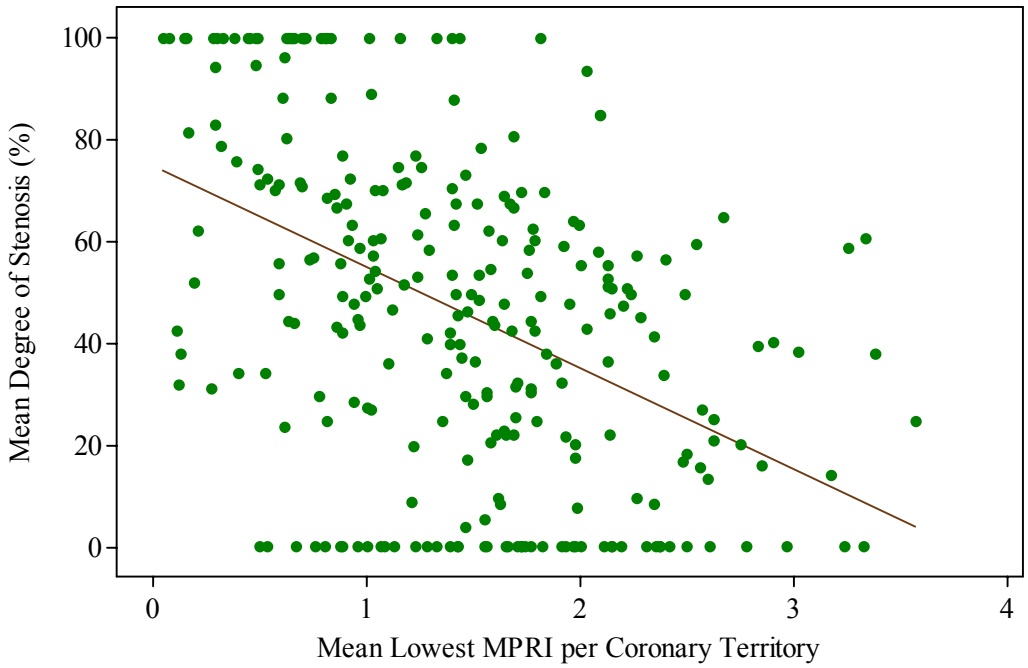

Correlation data with the other haemodynamic parameters measured with the coronary pressure wire are shown in table 4.16. Lowest MPRI per coronary territory again appears to have the highest degree of correlation with FFR as has been shown with the other data.

Table 4.16 - Pearson's correlation coefficients for each of the pressure wire measured haemodynamic variables compared with upslope gradient derived MPRI.

	Mean MPRI Per Coronary Territory	Lowest MPRI Per Coronary Territory
Fractional Flow Reserve (FFR)	0.34	0.47
Coronary Flow Reserve (CFR)	0.31	0.25
Uncorrected Index of Microcirculatory Resistance (IMRuncorr)	-0.09	-0.15
Corrected Index of Microcirculatory Resistance (IMRcorr)	0.32	0.27
Coronary Flow (Qcorr)	0.09	0.13

The receiver operator characteristic curve for upslope derived MPRI using both the mean MPRI for coronary artery territories and the lowest MPRI is shown in figure 4.38. The area under the curve for the mean MPRI per coronary territory was 0.71 compared to 0.77 for the lowest MPRI per coronary territory. As have been demonstrated using the aforementioned methods of assessing MPRI the lowest MPRI curve is further away from the reference line indicating using the low value is a more accurate test. The asymptotic 95% confidence intervals do partially overlap (Mean MPRI – 0.642 to 0.768 and Lowest MPRI – 0.712 to 0.825) therefore the difference between the tests is not large. Taking a mean MPRI cutoff of 2.35 gave a sensitivity of 80% and 1-specificity of 54% (Specificity = 46%). Using a cut-off value for the low MPRI of 1.68 gave a sensitivity of 84% and 1-specificity of 51% (Specificity = 49%).

Figure 4.38 - Receiver Operator Characteristic (ROC) curve of mean MPRI per coronary artery territory and lowest MPRI per coronary artery territory using an FFR cut-off of 0.75 as the gold standard for the diagnosis of coronary artery disease.

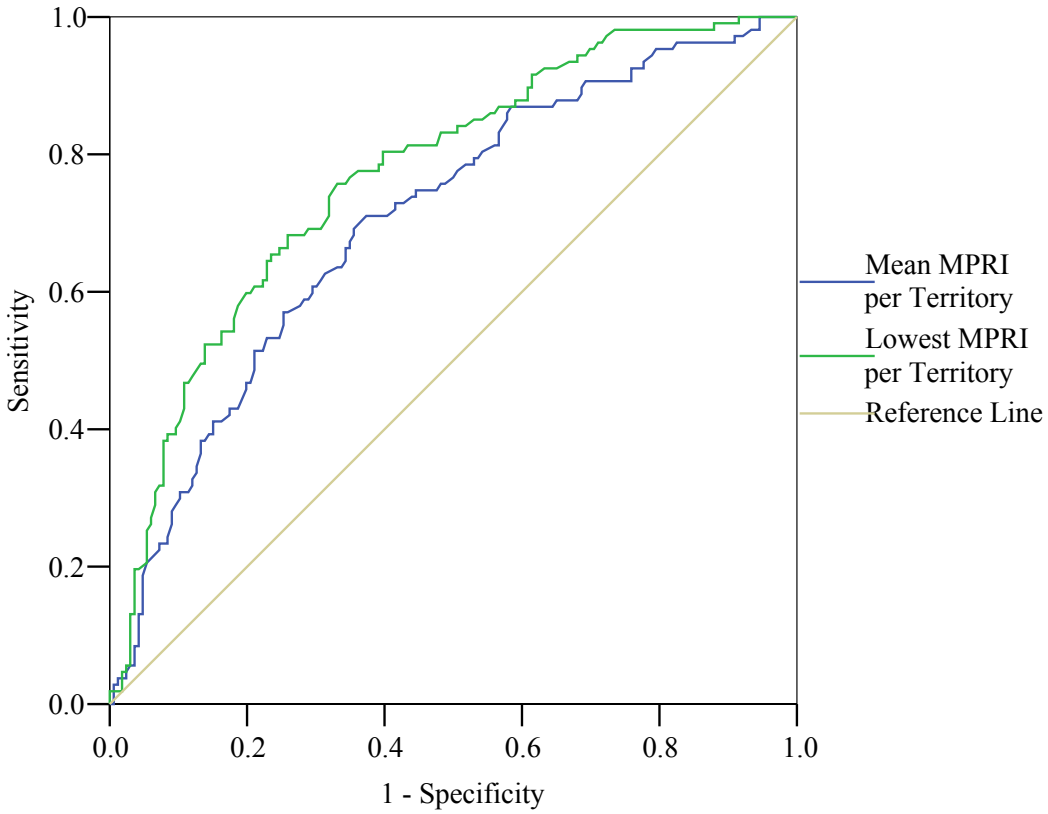

Boxplots of upslope gradient derived MPRI data are presented on Figure 4.39 showing the degree of overlap between the MPRI values in those arteries with significant coronary disease (FFR<0.75) and those with non-significant disease (FFR≥0.75). There is a lesser degree of overlap encountered when you take the lowest MPRI per coronary artery territory compared to the mean MPRI per territory.

Figure 4.39 - Boxplot comparing mean and lowest MPRI values in patients with and without significant coronary artery disease defined as an FFR<0.75 highlighting the median MPRI, the interquartile range, spread of data excluding outliers and the outliers.

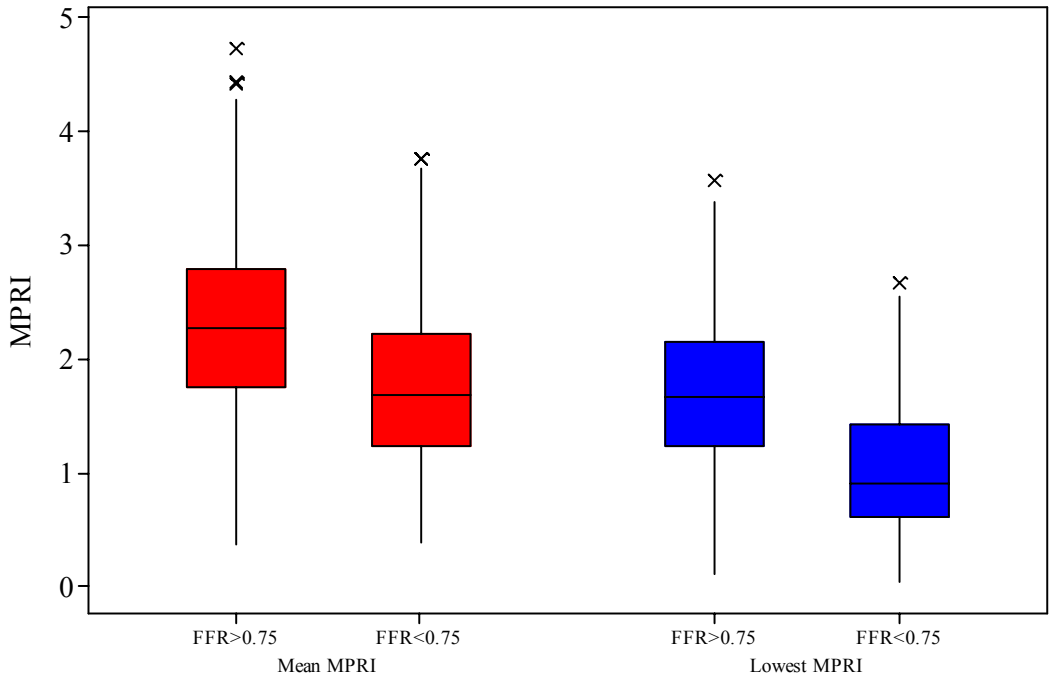

4.3.2.7 Comparison of Maximum Signal, Fermi Deconvolution and Upslope Gradient Derived MPRI in the Diagnosis of Significant Coronary Artery Disease

A comparison of the three methods of assessing MPRI was made using the data from those patients in whom measurement of the MPRI was obtainable using all of these methods and where FFR data was available for each of the coronary arteries where the MPRI was assessed. Data included in this analysis were provided from 92 of the 101 (91%) patients in the study. From these patients, 273 arteries had a FFR measured and the MPRI calculated using the aforementioned three methods. In three patients only 2 data points were obtained due to missing FFR measurements. Figure 4.40 shows receiver operator characteristic curves (ROC) for the mean MPRI calculated using each of the three methods. Of these three methods the mean Fermi deconvolution derived MPRI is farthest away from the reference line and therefore the best test. This is also

confirmed on table 4.17 where of these three methods, Fermi deconvolution derived MPRI has the largest area under the curve. However as shown on table 4.17 there is a large degree of overlap in the asymptotic 95% confidence intervals indicating that the differences between each of these tests is not substantial.

Figure 4.40 - Receiver Operator Characteristic (ROC) curves for mean upslope gradient derived MPRI (Gradient Mean MPRI), maximum signal derived MPRI (Max Signal MPRI) and Fermi deconvolution derived MPRI (Fermi Mean MPRI) for the diagnosis of significant coronary artery disease as defined by a FFR cut-off of <0.75.

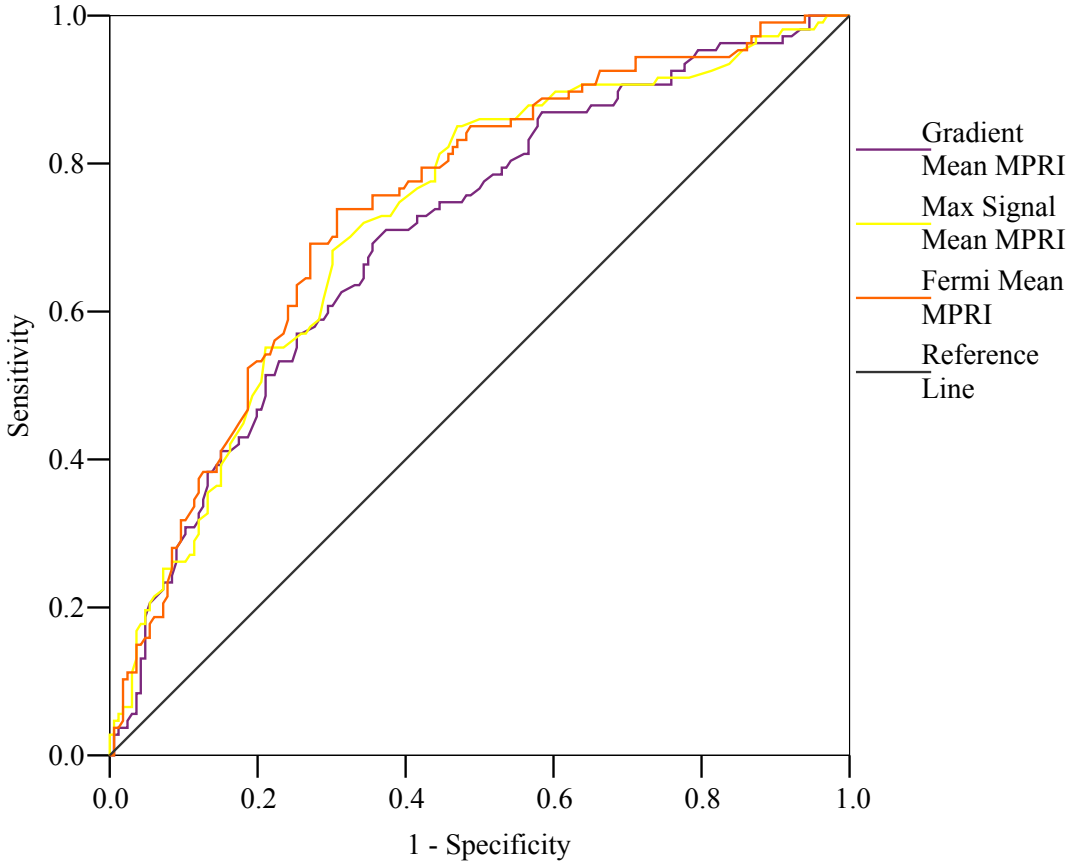

Table 4.17 - The area under the receiver operator characteristic (ROC) curves and the asymptotic 95% confidence intervals for each of the methods of assessing MPRI using either the mean MPRI or the lowest MPRI per coronary artery territory.

MPRI Method	Area Under Curve	Asymptotic 95% Confidence Interval	
		Lower Bound	Upper Bound
Gradient Mean MPRI	0.705	0.642	0.768
Max Signal Mean MPRI	0.726	0.665	0.788
Fermi Mean MPRI	0.741	0.681	0.801
Gradient Lowest MPRI	0.769	0.712	0.825
Max Signal Lowest MPRI	0.757	0.699	0.816
Fermi Lowest MPRI	0.784	0.729	0.839

A similar series of ROC curves is presented in figure 4.41 using the lowest MPRI value for each of the coronary artery territories using the 3 methods of assessing MPRI as shown above. As with the mean values of MPRI, Fermi deconvolution appears to be the best test when taking the lowest value of MPRI per coronary artery territory which is farthest away from the line of reference. This is again confirmed in table 4.17 where the lowest Fermi deconvolution MPRI has the largest area under the curve of the three methods assessed. As in the case of mean MPRI, there is a large degree of overlap in the asymptotic 95% confidence intervals again indicating a non-substantial difference between each of the three methods.

Figure 4.41 - Receiver Operator Characteristic (ROC) curves for mean lowest upslope gradient derived MPRI (Gradient Mean MPRI), maximum signal derived MPRI (Max Signal MPRI) and Fermi deconvolution derived MPRI (Fermi Mean MPRI) for the diagnosis of significant coronary artery disease as defined by a FFR cut-off of <0.75.

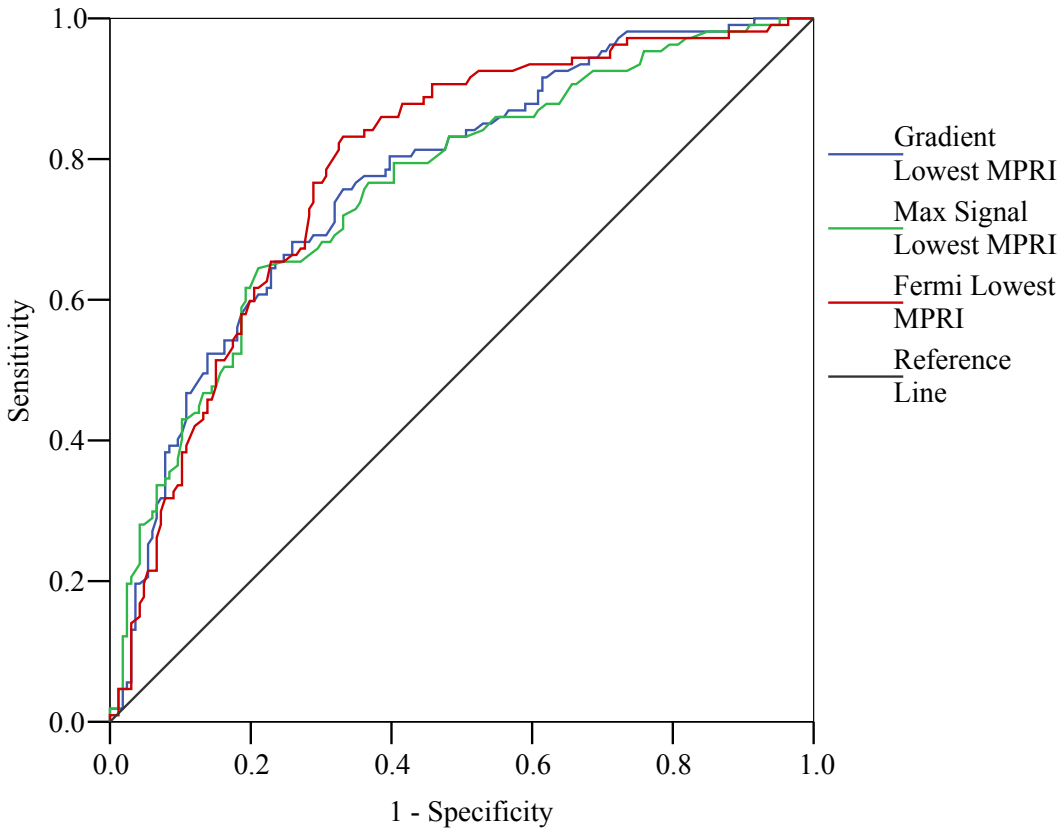

All 6 ROC curves of the methods of calculating MPRI are presented on the same graph for comparison in order to determine the best method overall (Figure 4.42). As shown the lowest Fermi deconvolution derived MPRI is farthest away from the line of reference whereas mean upslope gradient derived MPRI is the least accurate being closest to the reference line. This is confirmed by the areas under the ROC curves as presented in table 4.17.

Figure 4.42 - Receiver Operator Characteristic (ROC) curves for both the mean and lowest upslope gradient derived MPRI (Gradient Mean MPRI), maximum signal derived MPRI (Max Signal MPRI) and Fermi deconvolution derived MPRI (Fermi Mean MPRI) for the diagnosis of significant coronary artery disease as defined by a FFR cut-off of <0.75.

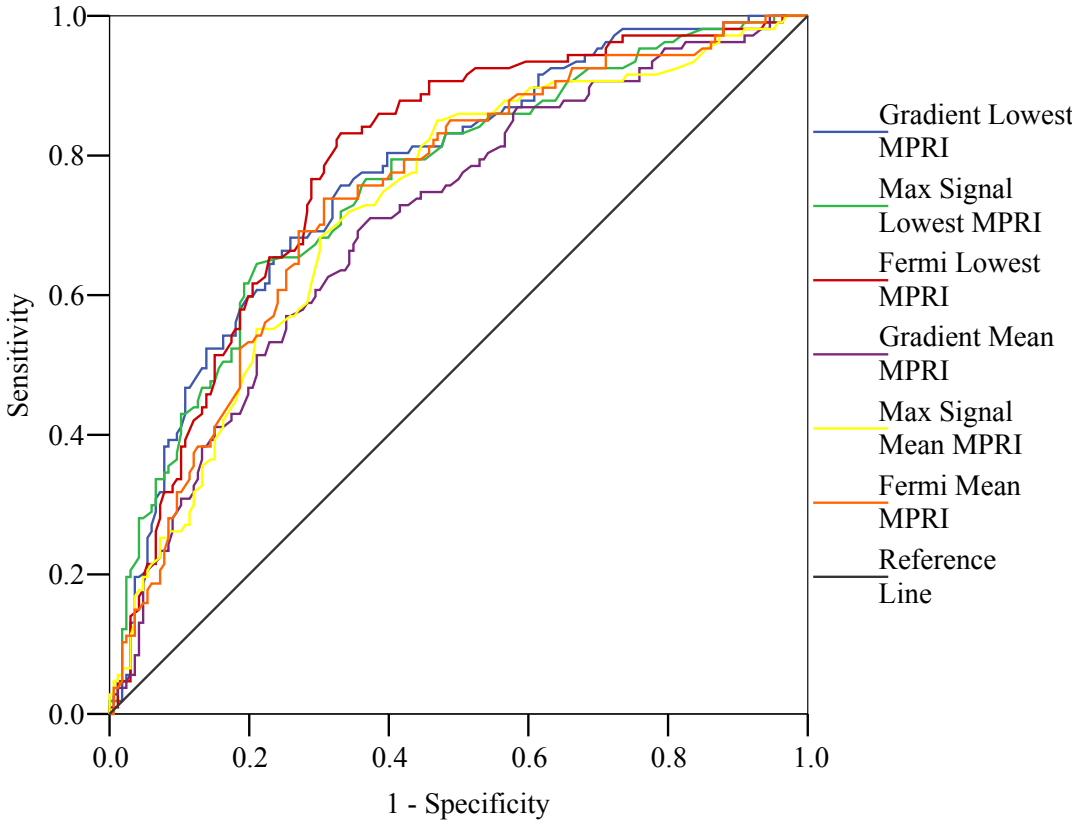

4.3.2.8 Post-Revascularisation Myocardial Perfusion Reserve Index (MPRI)

4.3.2.8.1 Post-PCI MPRI Results

The Fermi method with deconvolution was chosen for this analysis as this was shown in the preceeding data to have the largest area under the ROC curve. We measured the mean MPRI for all coronary artery territory segments, the lowest MPRI within in the coronary territories and a total mean MPRI for the whole heart (mean of all 16 segments per patient). This was recorded for the PCI patients pre-PCI, at 24 hours post-PCI and at 4 weeks post-PCI. Figure 4.43 shows the mean MPRI per coronary territory for the

three time points. The mean MPRI value pre-PCI was 1.88 (Median–1.71, SD=0.73, IQ range-1.36-2.42) at 24 hours post-PCI was 2.45 (Median-2.38, SD=0.93, IQ range-1.81-2.87) and at 4 weeks post-PCI was 2.5 (Median-2.42, SD=0.78, IQ range-2.00-2.97). The lowest MPRI value for each coronary territory which had PCI performed was also compared. The mean lowest MPRI value pre-PCI was 1.12 (Median-1.09, SD=0.54, IQ range 0.72-1.37) and at 24 hours had risen to 1.65 (Median-1.55, SD=0.76, IQ range 1.03-2.14) and at 4 weeks was 1.79 (Median-1.67, SD=0.66, IQ range 1.34-2.23).

Figure 4.43 - Boxplot showing the mean MPRI for those myocardial segments of the supplying coronary artery which has had PCI performed highlighting the median MPRI, the interquartile range, spread of data excluding outliers and the outliers.

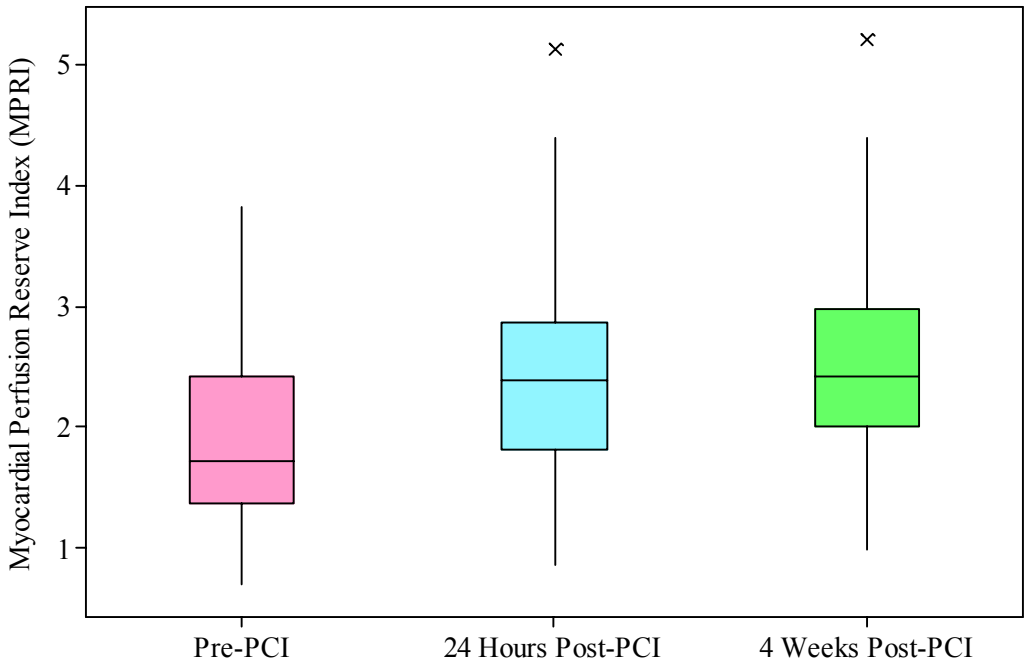

The data for these three time points was analysed using a one way analysis of variance (ANOVA) with multiple comparisons being made with the Tukey 95% simultaneous confidence intervals test. The one way ANOVA was significant with $p<0.0001$. When the pre-PCI scan MPRI is subtracted from the 24 hour post-PCI MPRI the difference is significant as the confidence interval for the combination of means excludes zero (0.23,

0.57, 0.91). In addition the difference between the pre-PCI and 4 weeks post-PCI scan is also significantly different (0.28, 0.62, 0.96). There was no significant difference between the 24 hour post-PCI and 4 week post-PCI scan as the confidence interval included zero (-0.30, 0.05, 0.40). Similar results were found using the lowest MPRI per coronary territory with statistically significant differences being noted between the pre-PCI scan and the 24 hour post-PCI scan and the pre-PCI and the 4 week post-PCI scan. We also looked at the mean total MPRI for the whole heart pre and post-PCI in order to perform comparisons with the CABG data. The mean total MPRI pre-PCI was 2.09 (Median-1.99, SD=0.75, IQ range 1.52-2.54). This increased to 2.43 (Median-2.31, SD=0.82, IQ range 1.83-2.98) at 24 hours and to 2.39 (Median-2.48, SD=0.78, IQ range 1.86-2.86) at 4 weeks post-PCI. These data are presented in figure 4.44.

Figure 4.44 - Boxplot showing the mean total MPRI for all myocardial segments in patients who have had PCI performed highlighting the median MPRI, the interquartile range, spread of data excluding outliers and the outliers.

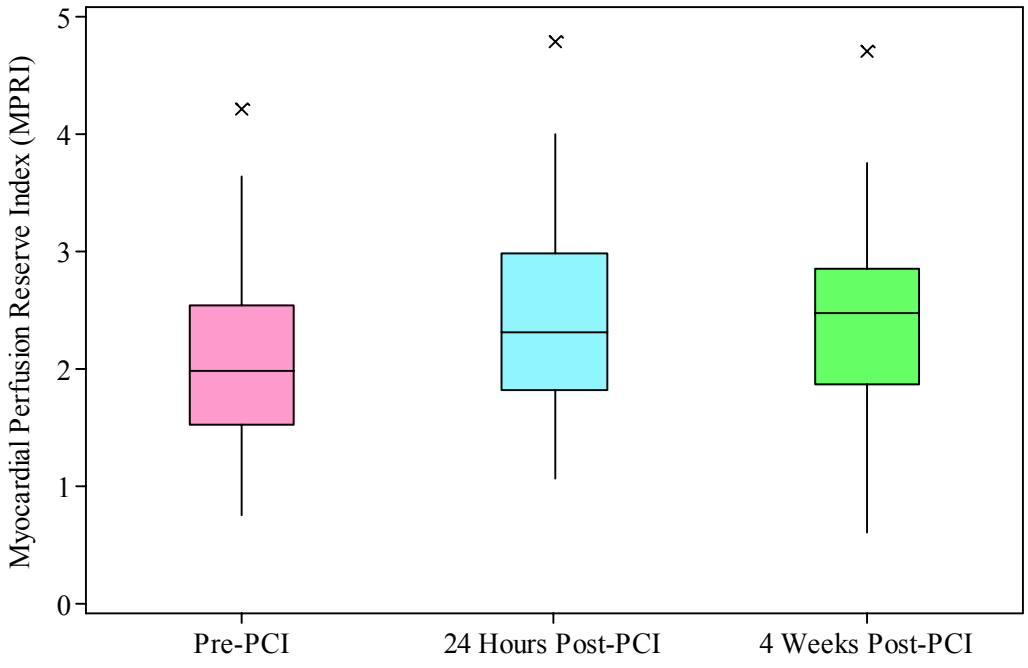

The mean total MPRI for the three time points was again compared using ANOVA however did not quite reach statistical significance with p=0.065. Using Tukey 95% simultaneous confidence intervals there was no significant difference between the pre-PCI scan and 24 hours post-PCI scan (-0.04, 0.33, 0.70), or the pre-PCI scan and the 4 weeks post-PCI scan (-0.07, 0.30, 0.66). However the lower confidence limit was very close to zero for both of these time points. Unsurprisingly there was therefore no significant difference between the 24 hour post-PCI and 4 weeks post-PCI scans (-0.41, -0.03, 0.35).

4.3.2.8.2 Post-CABG MPRI Results

The mean MPRI pre-CABG for the coronary territories revascularised was 1.65 (Median-1.57, SD=0.61, IQ range 1.16-2.25). This increased to 2.15 (Median-2.10, SD=0.50, IQ range 1.77-2.59) at 4 weeks post-CABG. The mean difference was 0.5. This increase was statistically significant ($p<0.0001$), with 95% confidence intervals for the mean difference being 0.28 and 0.72. These data are displayed graphically on figure 4.45.

Figure 4.45 - Boxplot showing the mean MPRI of revascularised coronary territories in patients who have had CABG performed highlighting the median MPRI, the interquartile range, spread of data excluding outliers and the outliers pre and post surgery.

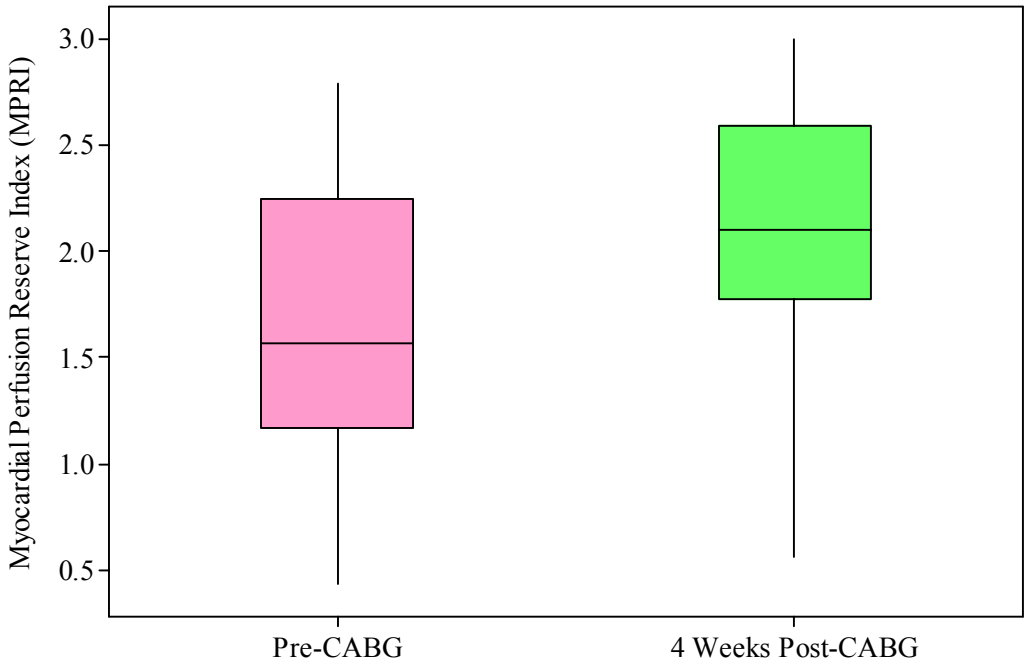

The lowest MPRI per coronary artery territory was also recorded as was done for the PCI results. The mean lowest MPRI pre-CABG was 0.99 (Median-0.85, SD=0.51, IQ range 0.61-1.39) and post-CABG was 1.54 (Median-1.51, SD=0.48, IQ range 1.21-1.94). The mean difference between pre and post-CABG was 0.55 which was significant with $p<0.0001$ and the 95% confidence intervals for the mean difference were 0.37 and 0.73. The mean total MPRI for all myocardial segments per patient was also recorded as was performed in the PCI patients. The mean total MPRI pre-CABG was 1.72 (Median-1.70, SD=0.51, IQ range 1.26 – 2.15) and 4 weeks post-CABG was 2.14 (Median-2.02, SD=0.43, IQ range 1.93-2.57). The mean difference was 0.43 which was significant with $p=0.013$ and the 95% confidence intervals for the mean difference were 0.11 and 0.74. These data are shown on figure 4.46.

Figure 4.46 - Boxplot showing the mean total MPRI for all myocardial segments in patients who have had CABG performed highlighting the median MPRI, the interquartile range, spread of data excluding outliers and the outliers pre and post surgery.

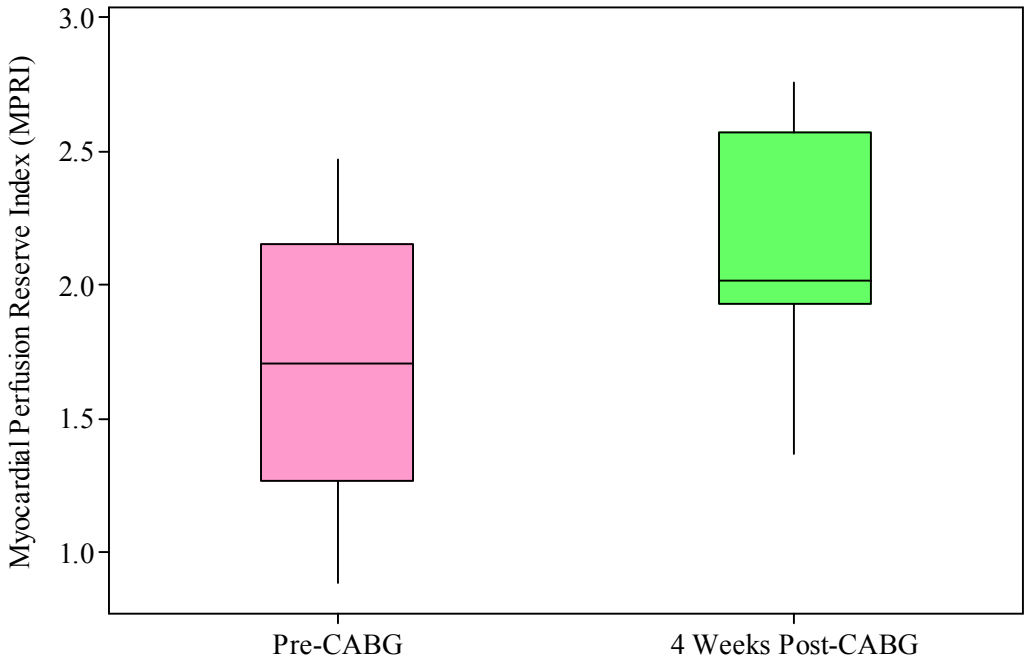

4.3.2.8.3 MPRI Pre and Post-Revascularisation – PCI vs CABG

As mentioned in the individual sections for PCI and CABG above, prior to revascularisation, the median MPRI for the CABG group was lower than that for the PCI group (1.57 vs 1.71) however this difference didn't reach statistical significance (p=0.21, 95% confidence intervals for difference were 0.05 and 0.55). As patients requiring CABG tend to have more extensive coronary disease we may have suspected more of a difference between these two groups. There was also a trend towards lower lowest MPRI values for coronary territories in the CABG group (Median 0.85 vs 1.09), however this was also not significant (p=0.28, 95% confidence intervals for difference -0.09 and 0.33). These data are displayed on figure 4.47.

Figure 4.47 - Boxplot showing the mean MPRI of coronary territories pre-PCI and CABG and the lowest MPRI value for both groups highlighting the median MPRI, the interquartile range, spread of data excluding outliers and the outliers.

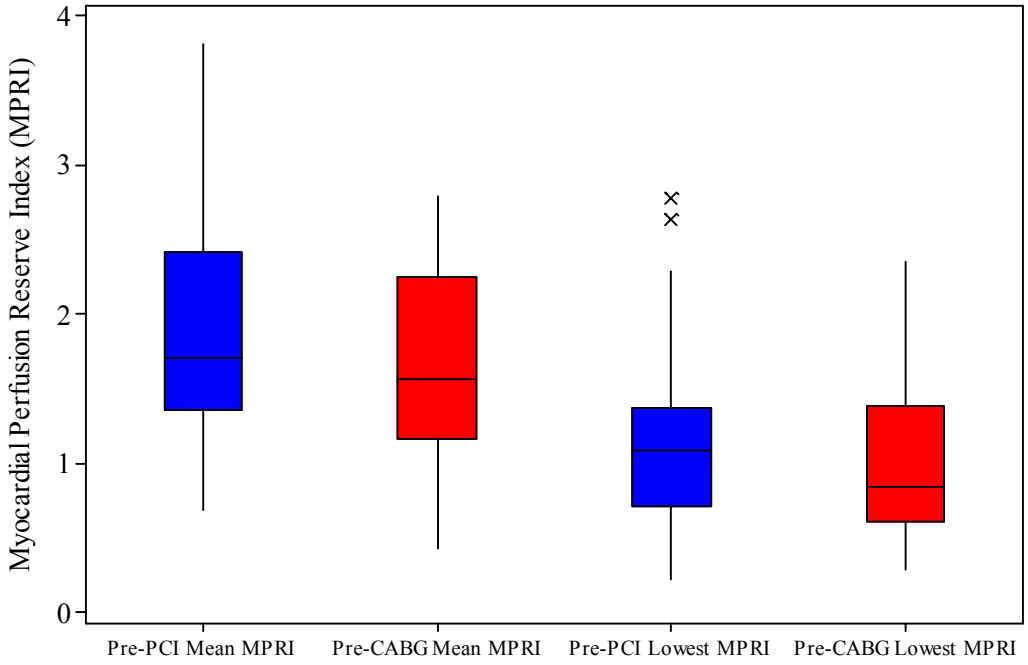

Both the CABG and PCI groups had MRI scans performed at 4 weeks post revascularisation in order to allow a like with like comparison. Examining the mean MPRI for each of the revascularised coronary territories post-revascularisation revealed a significantly better result in the PCI group with a median MPRI of 2.42 vs 2.10 (p=0.019, 95% confidence interval for the difference was 0.05 and 0.56). There was a trend to a higher lowest MPRI per revascularised coronary artery territory (Median 1.67 vs 1.51) however this difference failed to reach significance (p=0.08). These results are shown on figure 4.48.

Figure 4.48 - Boxplots showing the mean and lowest MPRI of coronary territories post-PCI and CABG highlighting the median MPRI, the interquartile range, spread of data excluding outliers and the outliers.

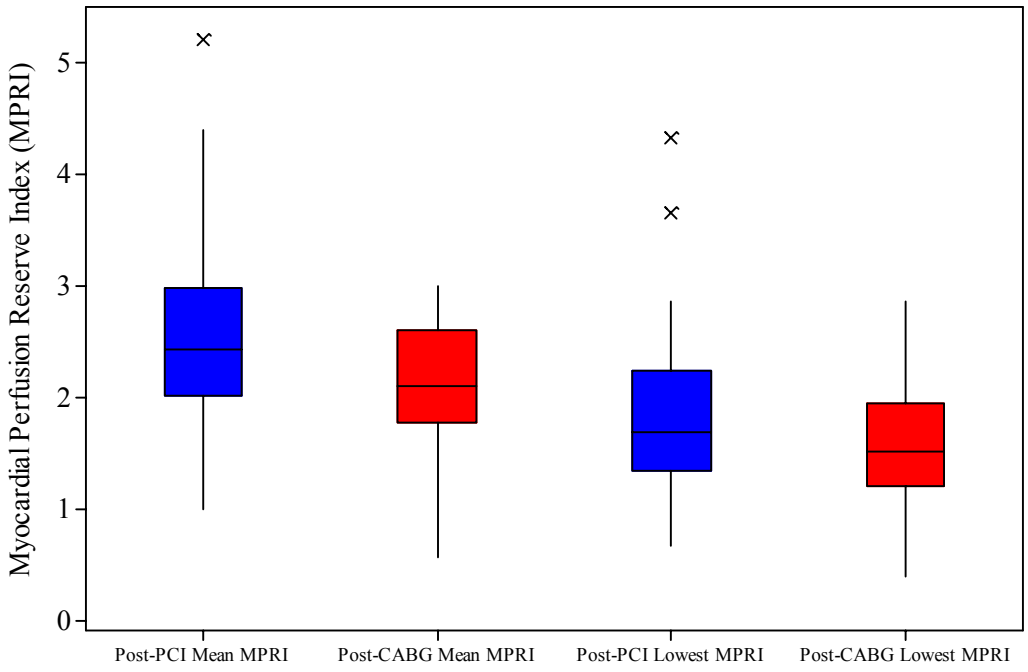

We also analysed the pre and post revascularisation mean MPRI for all 16 myocardial segments in both groups. Again there was a trend towards a higher MPRI value prior to revascularisation in the PCI group (Median 1.99 vs 1.70) with a p value of 0.1. This trend was also apparent post-revascularisation with the median MPRI post-PCI being 2.48 compared to 2.01 post-CABG (p=0.18). These data are displayed on figure 4.49.

Figure 4.49 - Boxplots showing the mean MPRI for all 16 myocardial segments per patient pre and post-PCI and CABG highlighting the median MPRI, the interquartile range, spread of data excluding outliers and the outliers.

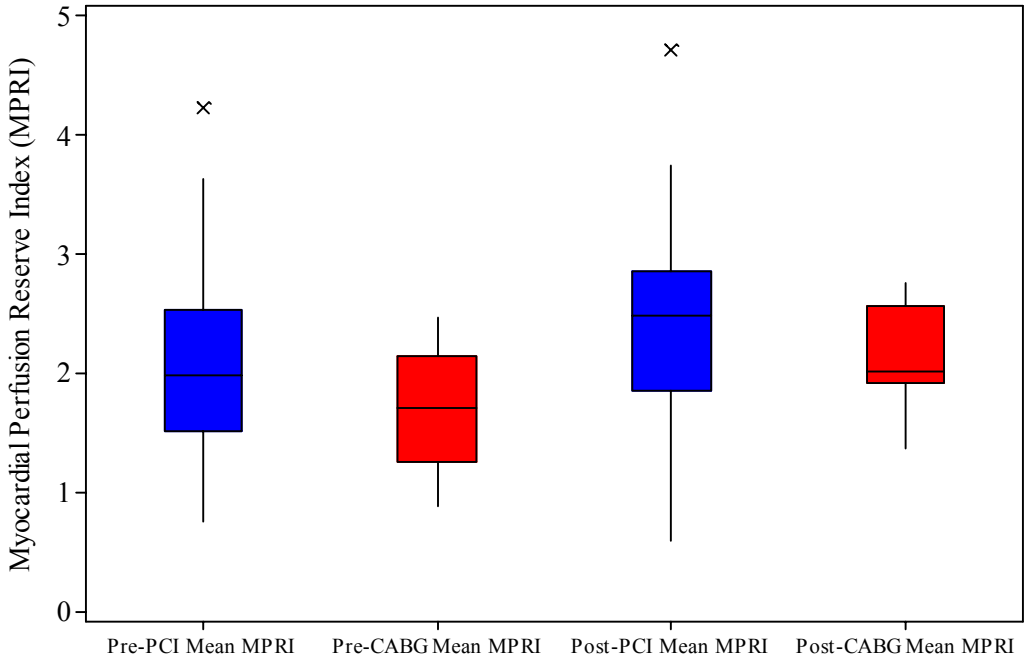

The final part of our comparison between PCI and CABG analysed the increase in MPRI pre and post-PCI, and pre and post-CABG. These data are presented in table 4.18. The difference in mean increase in MPRI per coronary artery territory between the two groups was 0.13 (95% Confidence Interval -0.17 and 0.43) which was not significant (p=0.39). The difference in mean increase in the lowest MPRI per coronary artery territory between the two groups was 0.09 (95% Confidence Interval -0.17 and 0.37) which was also not significant (p=0.48). Therefore as expected the difference in median increase in the mean total MPRI for the 16 coronary segments between the two groups was also not significant (p=0.92). The results of each of these analyses was insignificant, however perhaps one would expect a higher overall mean MPRI increase in the CABG group who would be expected to have achieved a greater rate of total arterial revascularisation.

Table 4.18 - The change in MPRI pre and post revascularisation for individual coronary territories (PCI mean and CABG mean), the lowest MPRI value for individual coronary artery territories (PCI lowest and CABG lowest) and the total mean for all 16 myocardial segments per patient (PCI total and CABG total).

	Number	Mean	Median	SD	Min	Max
PCI mean	61	0.63	0.58	0.78	-1.42	2.59
CABG mean	37	0.49	0.49	0.67	-0.9	1.93
PCI lowest	61	0.65	0.58	0.81	-1.24	3.45
CABG lowest	37	0.55	0.55	0.53	-0.38	2.01
PCI total	48	0.33	0.34	0.70	-1.19	2.01
CABG total	13	0.43	0.25	0.53	-0.46	1.61

4.4 LVEF, Mass and Volume Analysis

LVEF, mass and volume were calculated by two observers blinded to all patient details.

4.4.1 LVEF Analysis

The mean ejection fraction for the 226 MRI scans performed by observer 1 was 69.0% (Median=69.7, SD=7.6, Range 42.6-85.8) and observer 2 was 69.3% (Median=70.1, SD=8.0, Range 46.1-88.4). The Pearson correlation coefficient for observer 1 versus observer 2 was $r=0.83$ with $p<0.0001$ as expected when the same scans are analysed by two observers.

In order to examine the level of agreement between observers a Bland-Altman plot was created showing the difference between observers against their mean (Figure 4.50). This shows that there is no relationship between measurement error and the mean value which we take to be the true LVEF. In order to examine the bias in measurements we calculated the mean difference between observers which was 0.36% with a standard deviation of 4.5%. As shown in figure 4.50 most of the differences between observers lie between 0.36% and ±1.96xSD. Examining the limits of agreement between observers showed that observer 2 may be 9.2% below or 8.5% above observer 1.

Figure 4.50 - Difference in LVEF (%) against the mean LVEF with reference lines showing the mean±1.96SD within which 95% of the differences lie.

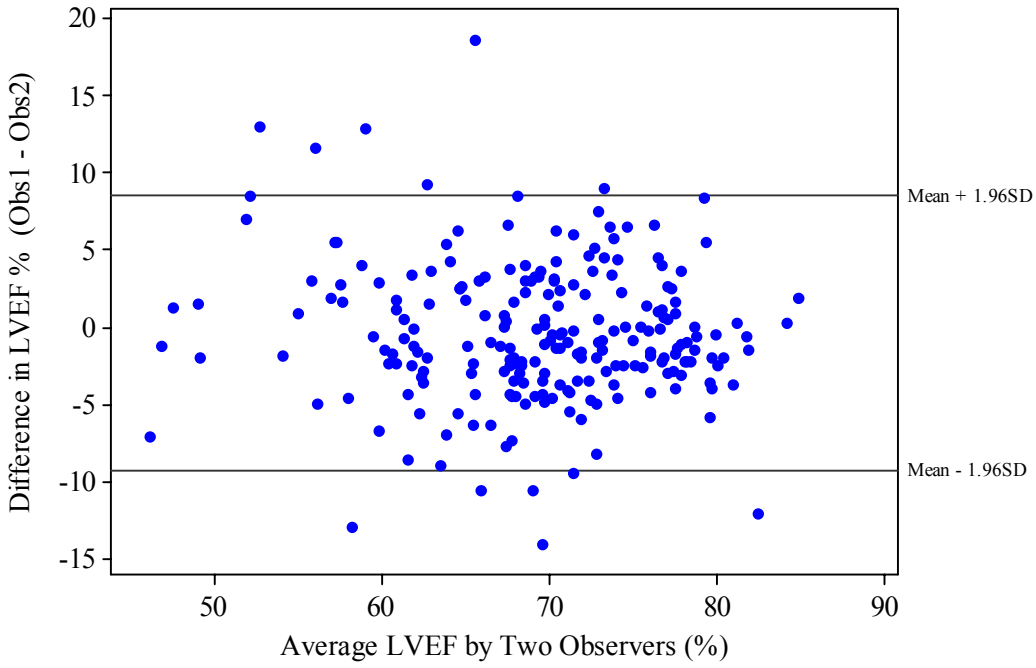

Examining the precision of the estimated limits of agreement the standard error of the mean difference was calculated to be 0.3 with 225 DF and a t=1.97. The 95% confidence interval of the bias was -0.95 to 0.23%. The standard error of the 95% limits of agreement was 0.51%, therefore the 95% confidence intervals for the lower limit of

agreement were narrow at -10.4 to -8.4% and for the upper limit of agreement were 7.7 to 9.7%.

4.4.2 Left Ventricular Myocardial Mass Analysis

The mean LV myocardial mass for the 226 MRI scans performed by observer 1 was 124.9g (Median=122, SD=31.3, Range 60.8-215.4) and observer 2 was 123.6g (Median=119.5, SD=31, Range 46.1-203.8). The Pearson correlation coefficient for observer 1 versus observer 2 was $r=0.79$ with $p<0.0001$.

The mean difference between observers was 1.3g with a standard deviation of 20.2g. Figure 4.51 shows a Bland Altman plot of LV mass difference against mean LV mass. The limits of agreement were between -38.3 and +40.9g. The 95% confidence interval for the bias was -1.4 to 3.9g and the standard error of the 95% limits of agreement was 2.3. The 95% confidence interval for the lower limit of agreement was -5.8 to 3.2g and the upper limit of agreement was -0.6 to 8.4g.

Figure 4.51 - Difference in LV mass against the mean LV mass with reference lines showing the mean±1.96SD within which 95% of the differences lie.

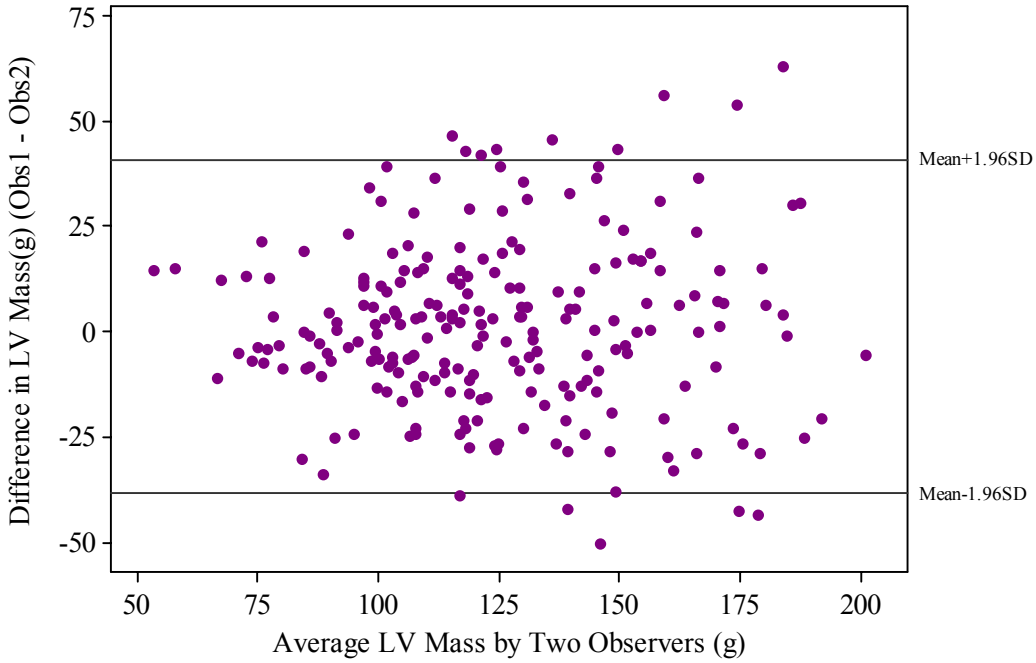

4.4.3 Left Ventricular End Diastolic Volume (LVEDV) Analysis

The mean LVEDV for the 226 MRI scans performed by observer 1 was 137.6ml (Median=137.8, SD=28.0, Range 74.8-212.7) and observer 2 was 126.2ml (Median=125.6, SD=27.8, Range 67-208). The Pearson correlation coefficient for observer 1 versus observer 2 was r=0.93 with p<0.0001.

The mean difference between observers was 11.4ml with a standard deviation of 10.5. Figure 4.52 shows a Bland Altman plot of LVEDV difference against mean LVEDV. The limits of agreement were between -9.2 and +32ml. The 95% confidence interval for the bias was 10.1 to 12.8ml and the standard error of the 95% limits of agreement was 1.2. The 95% confidence interval for the lower limit of agreement was 7.7 to 12.5ml and the upper limit of agreement was 10.4 to 15.2ml.

Figure 4.52 - Difference in LVEDV against the mean LVEDV with reference lines showing the mean±1.96SD within which 95% of the differences lie.

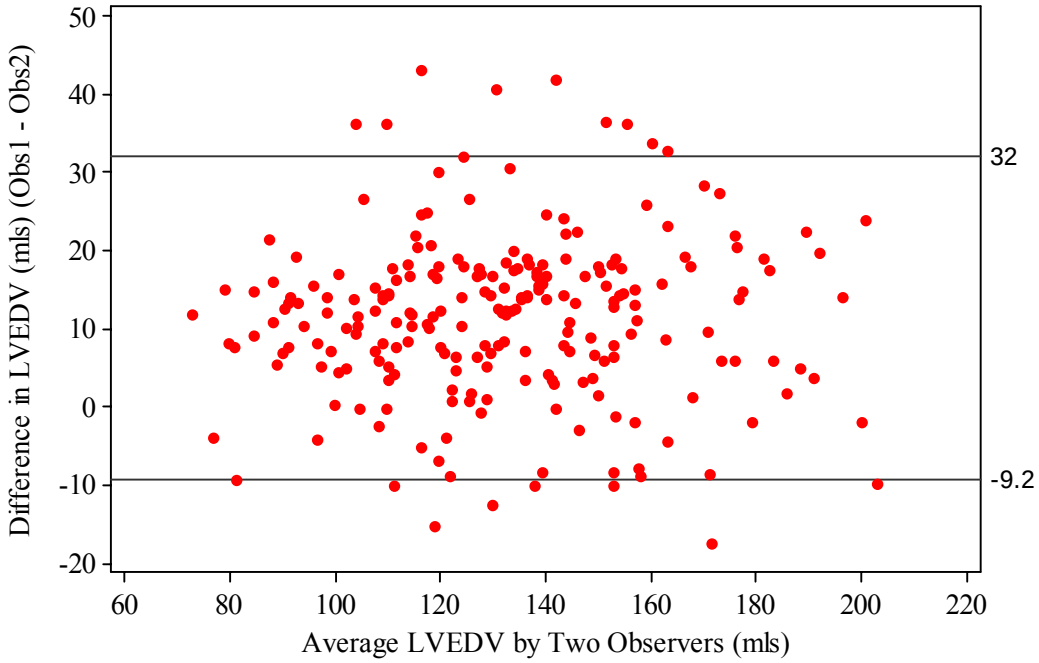

4.4.4 Left Ventricular End Systolic Volume (LVESV) Analysis

The mean LVESV for the 226 MRI scans performed by observer 1 was 43.3ml (Median=41.3, SD=15.5, Range 15.9-93.9) and observer 2 was 39.3ml (Median=36.5, SD=15.4, Range 11.3-83.6). The Pearson correlation coefficient for observer 1 versus observer 2 was r=0.91 with $p<0.0001$.

The mean difference between observers was 3.9ml with a standard deviation of 6.4. Figure 4.53 shows a Bland Altman plot of LVESV difference against mean LVESV. The limits of agreement were between -8.6 and +16.4ml. The 95% confidence interval for the bias was 3.1 to 4.8ml and the standard error of the 95% limits of agreement was 0.7. The 95% confidence interval for the lower limit of agreement was 1.6 to 4.6ml and the upper limit of agreement was 3.3 to 6.3ml.

Figure 4.53 - Difference in LVESV against the mean LVESV with reference lines showing the mean±1.96SD within which 95% of the differences lie.

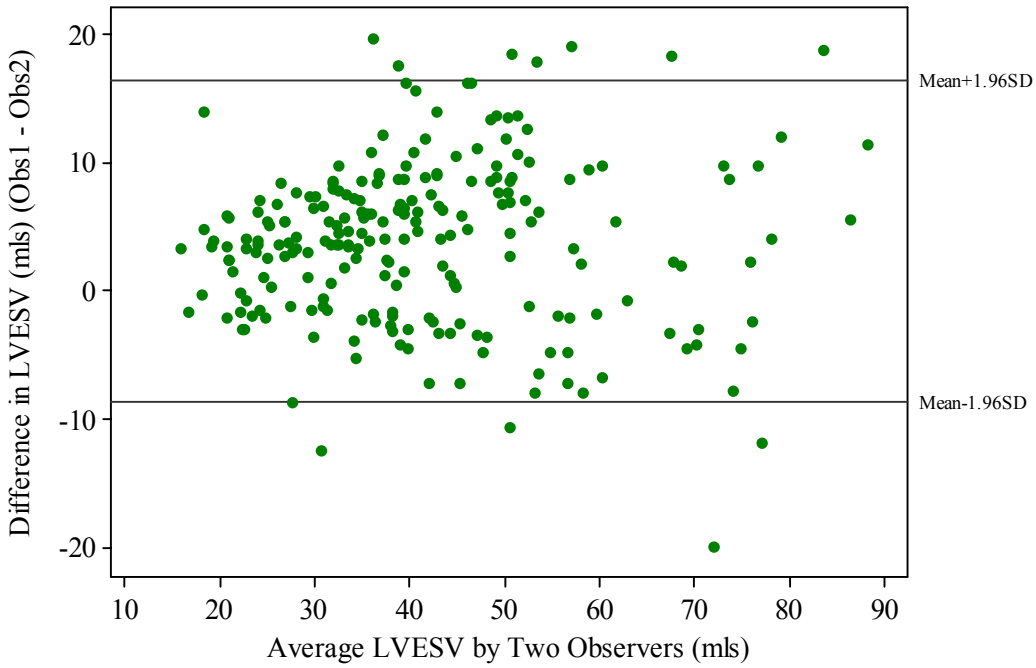

4.4.5 LV Volume Measurements in PCI, CABG, Medical and Normal Patients

For this analysis an average measurement was taken from observer 1 and observer 2. All patients had an MRI scan performed prior to the coronary angiogram. A boxplot of all 4 patient groups (normal, PCI, CABG and medical therapy) initial LV ejection fraction results are presented on Figure 4.54. The mean and standard deviation results are contained in table 4.19.

Figure 4.54 - Boxplot comparing initial ejection fractions (EF) in the normal, PCI, CABG and medical therapy groups highlighting the median EF, the interquartile range, spread of data excluding outliers and the outliers.

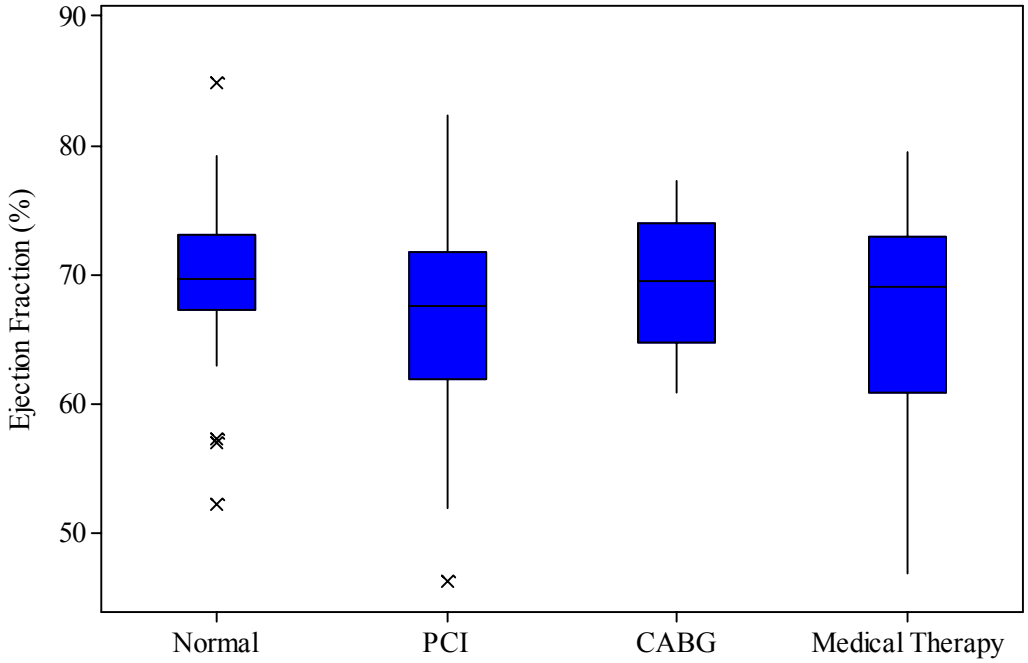

Those patients who had PCI performed had a repeat scan at 24 hours post-PCI and also at 4 weeks post PCI to examine the impact PCI had on ejection fraction, myocardial mass and LV volumes. Figure 4.55 shows the mean change in ejection fraction (EF) following PCI. 57 patients had PCI performed with 54 (95%) attending for the 24 hour scan and 52 (91%) attending for the 4 week scan. Of the 3 patients who declined the 24 hour scan, one had ongoing chest pain following his PCI, one had a migraine and a further patient declined due to claustrophobia. Of the 5 patients who refused the 4 week scan, 2 declined without giving reason, 2 complained of claustrophobia and one patient had substantial weight gain between scans and would have been unable to fit within the bore of the scanner.

Figure 4.55 - Boxplot showing change in ejection fraction (EF) pre and post-PCI highlighting the median EF, the interquartile range, spread of data excluding outliers and the outliers.

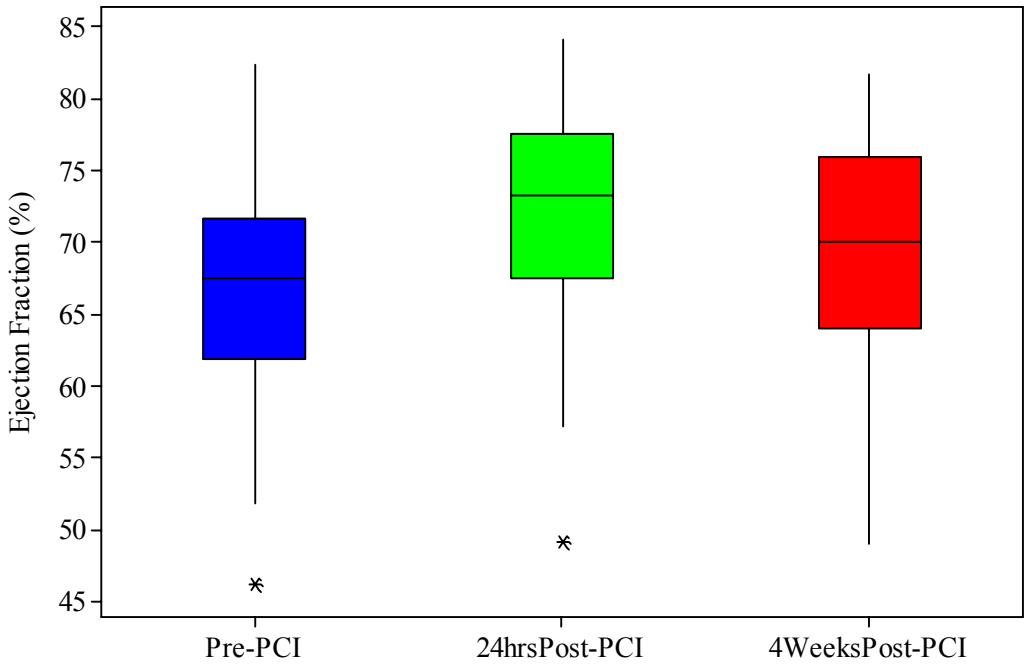

ANOVA was used to compare the mean ejection fraction between these three time points. The overall p value revealed a significant difference between the scans with p=0.003. Using Tukey 95% simultaneous confidence intervals revealed at significant difference between the pre-PCI scan and the 24 hour post-PCI scan with the confidence intervals excluding zero (1.6, 5.0, 8.4). The comparison between the pre-PCI scan and the 4 week scan was close to being significant however did include zero (-0.5, 2.9, 6.3). There was no significant difference between the 24 hour and 4 week post-PCI scans (-5.5, -2.1, 1.3). The mean and median ejection fractions are presented on table 4.19.

Table 4.19 - Descriptive data for ejection fraction (%) in normals, pre-PCI, 24 hours post-PCI, 4 weeks post-PCI, pre-CABG, 4 weeks post-CABG, pre-medical therapy and 3 months post medical therapy groups.

	No	**Mean**	**Median**	**SD**
Normal	20	69.1	69.6	7.5
Pre-PCI	57	66.7	67.5	7.3
24h Post-PCI	54	71.9	67.5	7.1
4 Weeks Post-PCI	52	69.6	67.5	7.1
Pre-CABG	15	69.6	69.5	5.3
4 Weeks Post-CABG	14	68.8	69.8	7.4
Pre-Med Rx	9	66.8	69.0	10.1
3 Months Post-Med Rx	5	65.8	69.6	10.4

The ejection fraction data for the CABG patients pre and 4 weeks post surgery are presented in figure 4.56. Of the 15 patients who underwent CABG only one patient declined to have the 4 week repeat cardiac MRI scan. This patient did not feel well enough following his CABG to consider this. As indicated in table 4.19 there is no significant difference in ejection fraction pre and post CABG.

Figure 4.56 - Boxplot showing change in ejection fraction (EF) pre and post-CABG highlighting the median EF, the interquartile range and spread of data.

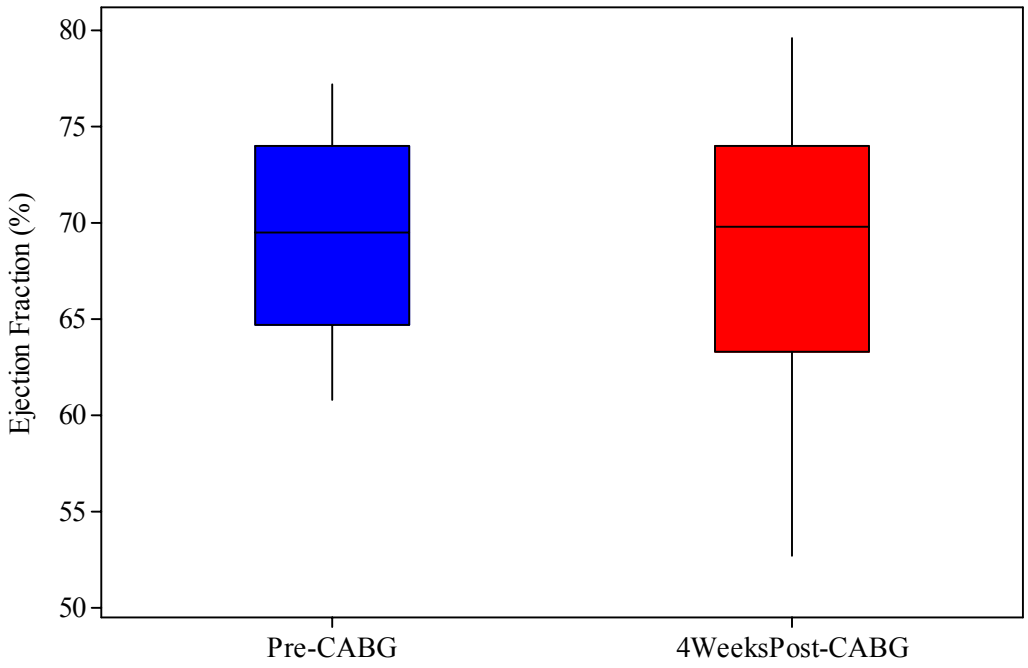

Of the 9 patients whose coronary artery disease was only felt to be suitable for treatment by medical therapy only 5 (56%) attended for a second MRI scan at 3 months post coronary angiography. Three patients refused without giving reason and one patient who tolerated his first scan developed claustrophobia at the start of the repeat scan. Figure 4.57 shows the change in ejection fraction between the two scans and table 4.19 confirms that there is no significant difference in ejection fraction pre and following three months of medical therapy.

Figure 4.57 - Boxplot showing change in ejection fraction (EF) pre and 3 months post-medical therapy highlighting the median EF, the interquartile range and spread of data.

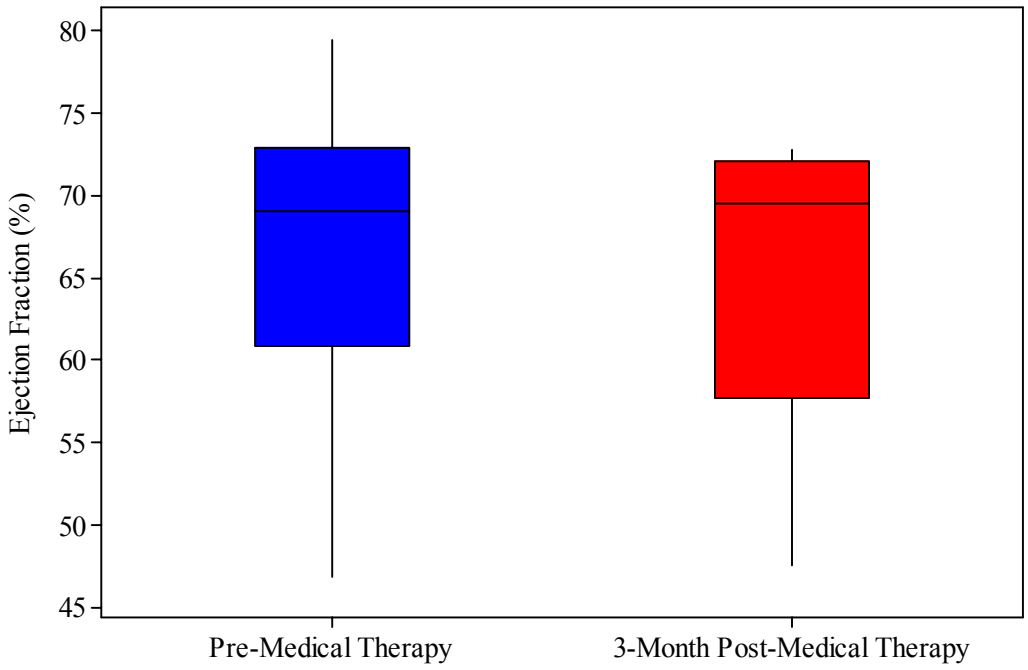

We then compared the ejection fractions of those patients who underwent PCI and those who had CABG. There was no significant difference between the two groups prior to revascularisation (T=-1.73, DF=29, p=0.09). In addition myocardial mass was not significantly different between groups (T=0.63, DF=32, p=0.5) as was end-diastolic volume (T=0.22, DF=18, p=0.8), end-systolic volume (T=0.86, DF=21, p=0.4) and cardiac output ((T=-0.22, DF=21, p=0.8). Descriptive Data showing myocardial mass, end diastolic volume, end systolic volume and cardiac output are presented in table 4.20.

Table 4.20 - Descriptive data of the myocardial mass, end diastolic volume, end systolic volume and cardiac output for the 4 groups of patients (normal, PCI, CABG and medical therapy).

	Number	Parameter	Mean	Median	SD	Min	Max
Normal	20	Mass	117.2	117.0	31.1	53.5	183.9
		EDV	137.3	130.8	37.2	76.8	203.0
		ESV	43.0	38.6	17.3	16.7	75.9
		CO	5.5	4.9	1.5	3.1	8.3
PCI	57	Mass	121.8	117.7	30.1	66.5	191.7
		EDV	135.8	139.1	27.1	87.3	185.8
		ESV	45.4	42.0	15.0	15.9	79.1
		CO	5.3	5.3	1.3	2.6	8.3
CABG	15	Mass	117.8	112.9	19.9	96.9	159.2
		EDV	133.6	136.0	36.7	79.6	200.8
		ESV	41.5	40.3	15.9	18.1	67.8
		CO	5.3	4.9	1.3	3.3	7.9
Medical	9	Mass	129.2	129.1	30.8	67.3	186.0
		EDV	149.1	149.8	29.9	104.7	196.1
		ESV	49.9	49.3	19.0	26.4	86.4
		CO	5.6	5.7	1.2	3.7	7.4

Interestingly there was no statistically significant difference in the ejection fractions at 4 weeks post PCI and 4 weeks post CABG as shown in figure 4.58 and table 4.21. In addition there were no differences in myocardial mass, end diastolic volume, end systolic volume and cardiac output as presented in table 4.21.

Figure 4.58 - Boxplot showing the ejection fraction (EF) 4 weeks post-PCI and CABG highlighting the median EF, the interquartile range and spread of data.

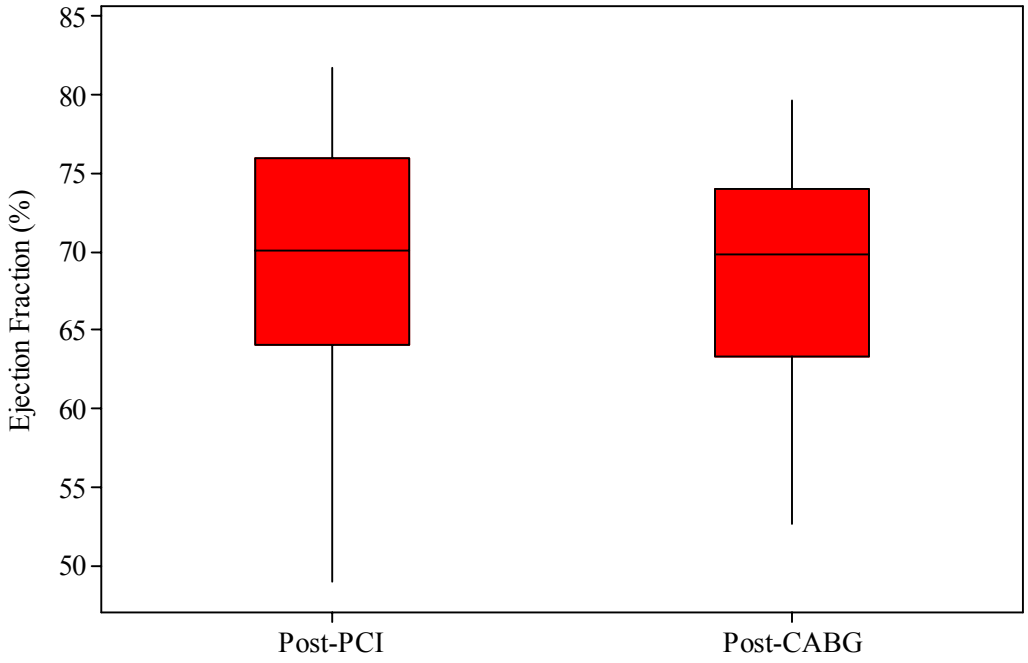

Table 4.21 - Comparision of LV parameters at 4 weeks post-PCI and CABG with corresponding two sample T-test results.

		Mean	**Median**	**SD**	**Min**	**Max**	**T/p value**
Ejection Fraction (%)	PCI	69.6	70.1	7.1	48.9	81.7	T=0.36 P=0.73
	CABG	68.8	69.8	7.4	52.7	79.6	
Myocardial Mass (g)	PCI	125.7	121.5	30.0	70.8	188.3	T=-0.02 P=0.99
	CABG	125.8	115.1	27.1	84.5	171.3	
End-Diastolic Volume (ml)	PCI	130.9	131.2	23.4	88.1	189.2	T=0.68 P=0.5
	CABG	125.8	122.5	25.6	84.6	177.1	
End-Systolic Volume (ml)	PCI	40.5	40.1	14.6	20.8	88.1	T=0.22 P=0.83
	CABG	39.6	34.2	13.8	20.7	67.6	
Cardiac Output (l/min)	PCI	5.29	5.25	0.94	3.32	7.76	T=-1.16 P=0.26
	CABG	5.63	5.58	1.02	4.03	7.72	

4.5 Late Gadolinium Enhancement Mass Analysis

The scans of 55 (96%) of the 57 patients who underwent PCI and 14 of 15 (93%) patients who had CABG were analysed for the mass of late gadolinium enhancement. Patients who didn't attend for any of the follow up scans were excluded from this analysis. Of the PCI group, 54 (98%) of 55 scans at 24 hours post PCI were interpretable as were 51 (93%) of 55 scans at 4 weeks post PCI. CABG patients only had one follow up scan to attend at 4 weeks which all 14 attended. Therefore in total 188 scans were analysed for the presence of late gadolinium enhancement by two blinded observers as documented in the methods section.

4.5.1 Late Gadolinium Enhancement Mass Interobserver Variability

The mean mass of late gadolinium enhancement in these 188 scans analysed by observer 1 was 2.45g (Median=0, SD=4.06, Interquartile Range 0.0-3.75) and observer 2 was 2.27g (Median=0, SD=3.85, Interquartile Range 0.0-3.12). The Pearson correlation coefficient for observer 1 versus observer 2 was $r=0.98$ with $p<0.0001$.

The mean difference between observers was 0.18g with a standard deviation of 0.83g. Figure 4.59 shows a Bland Altman plot of difference in LGE mass against mean LGE mass. The limits of agreement were between -1.45 and +1.81g. The 95% confidence interval for the bias was 0.06 to 0.3g and the standard error of the 95% limits of agreement was 0.1. The 95% confidence interval for the lower limit of agreement was -1.65 to -1.25g and the upper limit of agreement was 1.61 to 2.01g.

Figure 4.59 - Difference in mass of late gadolinium enhancement (LGE) against the mean mass of LGE with reference lines showing the mean±1.96SD within which 95% of the differences lie.

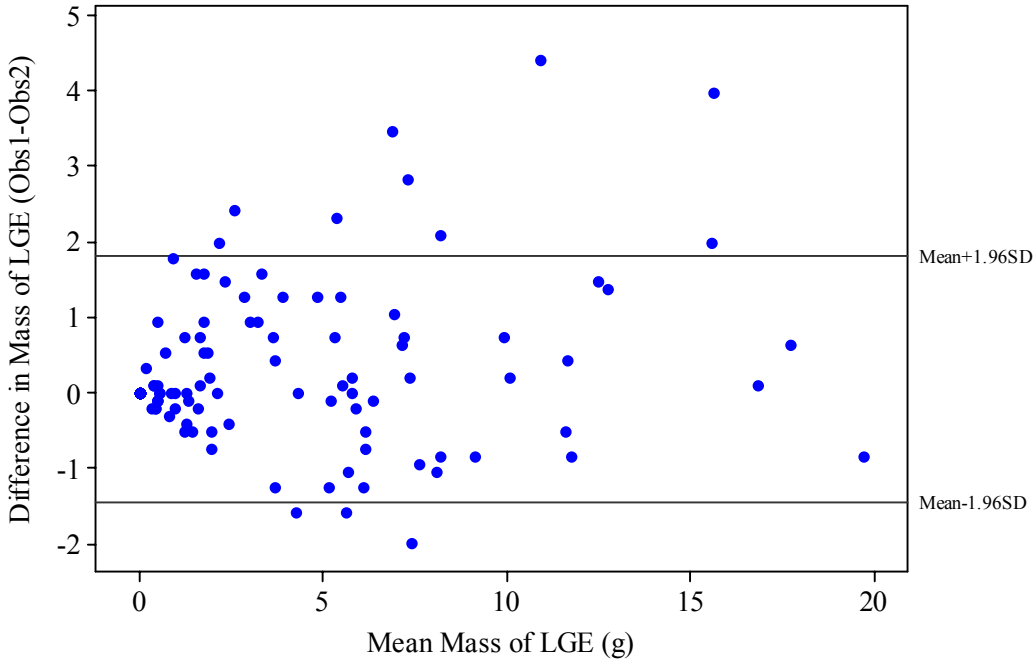

4.5.2 Mass of Late Gadolinium Enhancement – PCI v CABG group

Prior to revascularisation 26 (47%) of the 55 PCI patients had evidence of late gadolinium enhancement (LGE) compared to 6 (43%) of the 14 CABG patients (chi square=0.09, p=0.77). The mean mass of LGE in the PCI group was 2.55g (Median=0, SD=4.2, Interquartile Range 0 – 4.83) compared to 1.47g in the CABG group (Median=0, SD=2.3, Interquartile Range 0 – 1.99). At 4 weeks post PCI 23 (45%) of the 51 patients who attended for repeat MRI scanning had evidence of LGE compared to 10 (71%) of the 14 CABG patients (chi square=3.0, p=0.08). The mean mass of LGE at 4 weeks post PCI was 2.27g (Median=0, SD=3.9, Interquartile Range 0 – 3.68) and at 4 weeks post CABG was 2.55g (Median=1.37, SD=3.5, Interquartile Range 0 – 3.03). These data are presented along with the pre-revascularisation data in figure 4.60. The mass of LGE pre and post-revascularisation was compared using the Mann-Whitney U

test due to the dataset being positively skewed, however there were no significant differences between the groups (p=0.65 and p=0.20 respectively). A line plot of the change in mass of LGE pre and post CABG for all 14 patients is presented on figure 4.61 and for the 51 PCI patients is on figure 4.62.

Figure 4.60 - Boxplot showing mass of late gadolinium enhancement (g) pre and post PCI and CABG highlighting the median mass, the interquartile range, spread of data excluding outliers and the outliers.

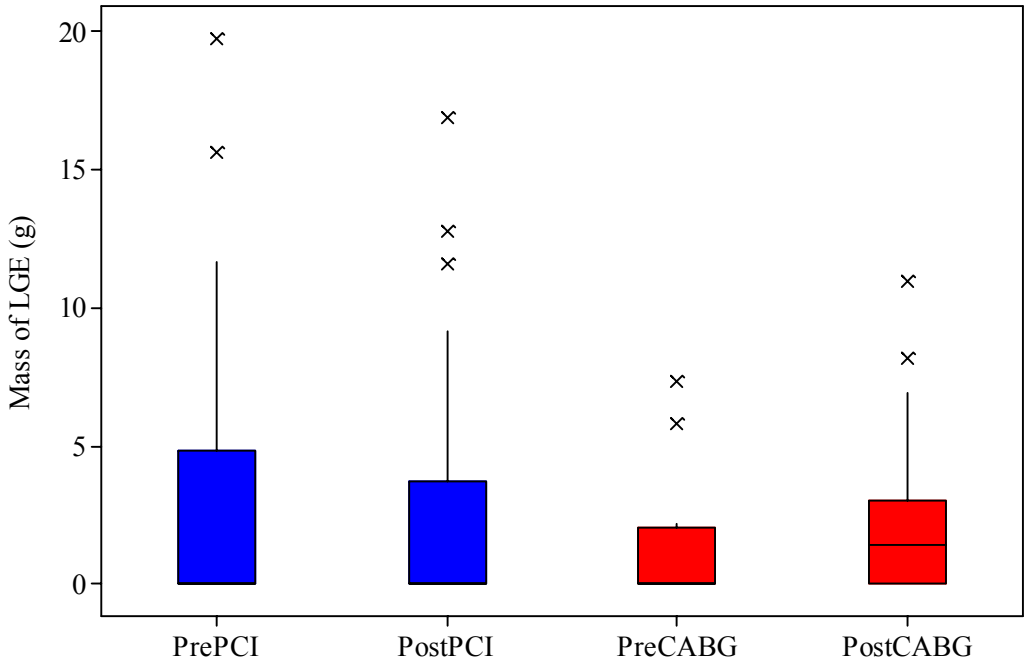

Figure 4.61 - Lineplot showing the change in mass of late gadolinium enhancement (LGE) pre and post CABG for each of the 14 patients who had a pre and post MRI scan performed.

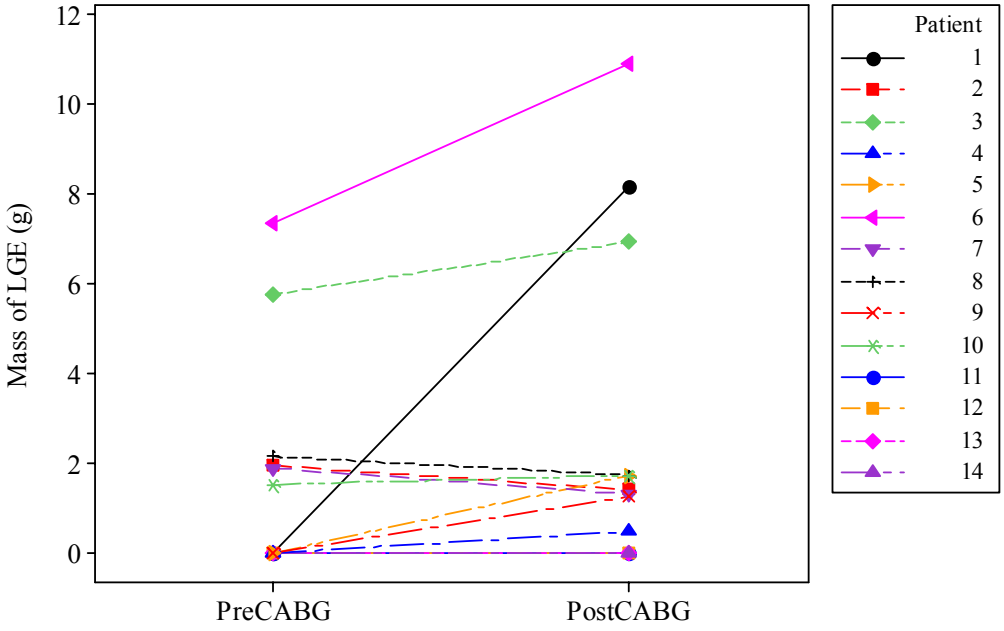

Figure 4.62 - Lineplot showing the change in mass of late gadolinium enhancement (LGE) pre and 4 weeks post-PCI for each of the 51 patients who had a pre and post MRI scan performed.

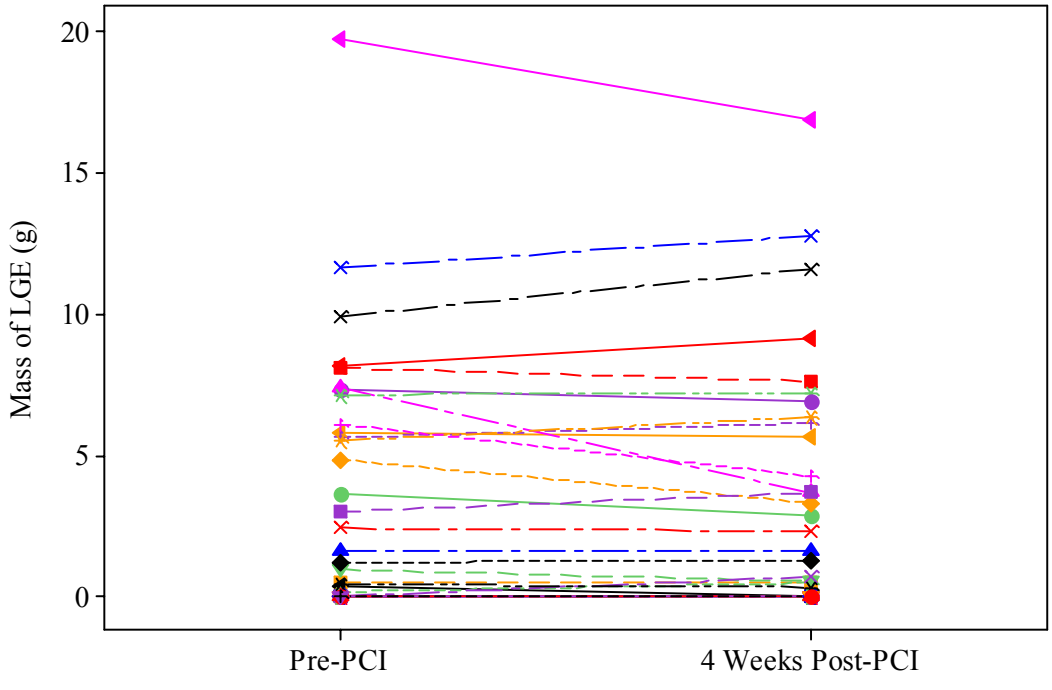

We also looked at the change in mass of LGE between both groups by subtracting the mass of LGE pre-revascularisation from the post-revascularisation value. The mean difference in the PCI group was -0.12g (Median=0, SD=0.8, Interquartile Range 0 – 0) and for the CABG group was 1.08g (Median=0.11, SD=2.3, Interquartile Range -0.11 – 1.38). There is a trend towards the development of more LGE following CABG than PCI however the difference between groups did not reach statistical significance (p=0.07).

4.5.3 Comparison of Mass of Late Gadolinium Enhancement with Troponin

We compared the measured change in mass of LGE between the 24 hour post-PCI scan and the pre-PCI scan and compared this with the measured 24 hour troponin measurement. No significant correlation was found to exist between these parameters for the 52 patients of 55 who had a troponin measurement performed (r=0.25, p=0.07). We found an even poorer correlation when we compared troponin with the change in mass of LGE from baseline to 4 weeks (r=-0.19, p=0.2). This may be due to thinning of recently infarcted myocardium due to myocyte necrosis, leading to a reduction in the measured mass of LGE. These data are presented on figure 4.63 with corresponding line of best fit. Comparisons were also made with the total mass of LGE measured at both 24 hours and 4 weeks and again no significant correlation was found when compared with troponin values (r=0.08 and 0.06 respectively). This confirms that no relationship was found between the biochemical marker of myocyte necrosis (troponin) and the measured amount of LGE which has a number of causes including myocyte necrosis.

Figure 4.63 - Scatterplot of change in mass of late gadolinium enhancement (LGE) between the 4 week post PCI MRI and the pre PCI scan and the measured troponin I value at 24 hours post PCI. A line of best fit is also drawn.

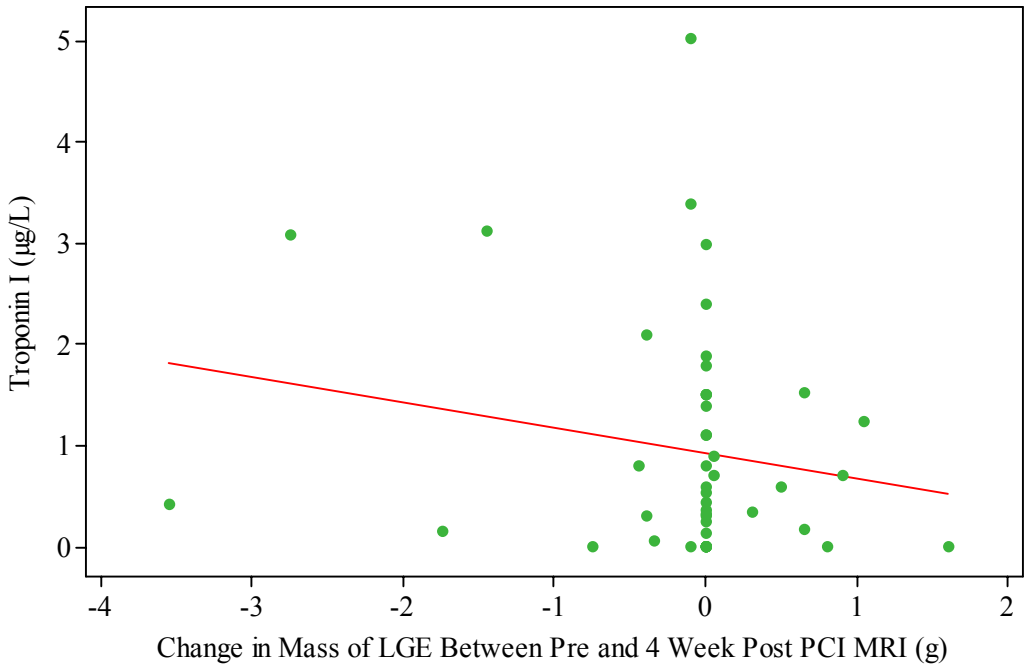

4.5.4 Comparison of Mass of Delayed Enhancement with Number of Arteries Treated During PCI

We then compared the change in measured mass of late gadolinium enhancement between the 4 week scan and baseline with the number of vessels to which PCI was performed using the Kruskal-Wallis test. This showed no significant change in the mass of LGE with increasing number of arteries being intervened upon at 24 hours post-PCI (H=2.1, p=0.35) and also at 4 weeks post-PCI (H=1.1, p=0.58). The number of patients who had 3 vessel PCI in this analysis was only 2 (4%) compared to 13 (25%) who had 2 vessel PCI and 36 (71%) who had single vessel PCI. These results should therefore be treated with caution as larger numbers in the 2 and 3 vessel groups would be required for a more robust analysis. The data relating to the change in mass of LGE at 24 hours and 4 weeks post PCI are presented in table 4.22.

Table 4.22 - Change in mass of late gadolinium enhancement (LGE) at 24 hours and 4 weeks depending on the number of arteries having undergone PCI.

Change in Mass of LGE with MRI	Number of Arteries Having PCI	Mean(g)	Median(g)	SD
24 Hours Post PCI	1	0.08	0	0.87
	2	-0.35	0	1.19
	3	0.18	0.18	0.25
4 Weeks Post PCI	1	-0.05	0	0.49
	2	-0.33	0	1.37
	3	0.15	0.15	0.21

4.5.5 New Late Gadolinium Enhancement at 24 Hours Post-PCI

At 24 hours post-PCI new late gadolinium enhancement (>0.1g) occurred in 10 (19%) of 54 patients who attended for follow-up MRI scanning. Late gadolinium enhancement (LGE) was present on 25 (46%) scans pre-PCI and 27 (50%) scans post-PCI. Of the 10 patients with new LGE, 8 (80%) had an increase from their pre-PCI scan and 2 (20%) developed new LGE having had none on their pre-PCI scan. The PCI patients were then divided into two groups according to whether or not they had new late gadolinium enhancement. The mean increase in LGE was 1.24g (95% Confidence Intervals 0.61 to 1.87) in the new LGE group compared to -0.31g (95% Confidence Intervals -0.53 to -0.09) in the group with no new LGE ($p<0.0001$). These data are represented in figure 4.64.

Figure 4.64 - Change in mass of late gadolinium enhancement (LGE) in grams from pre-PCI to 24 hours post-PCI in the new LGE and no new LGE groups.

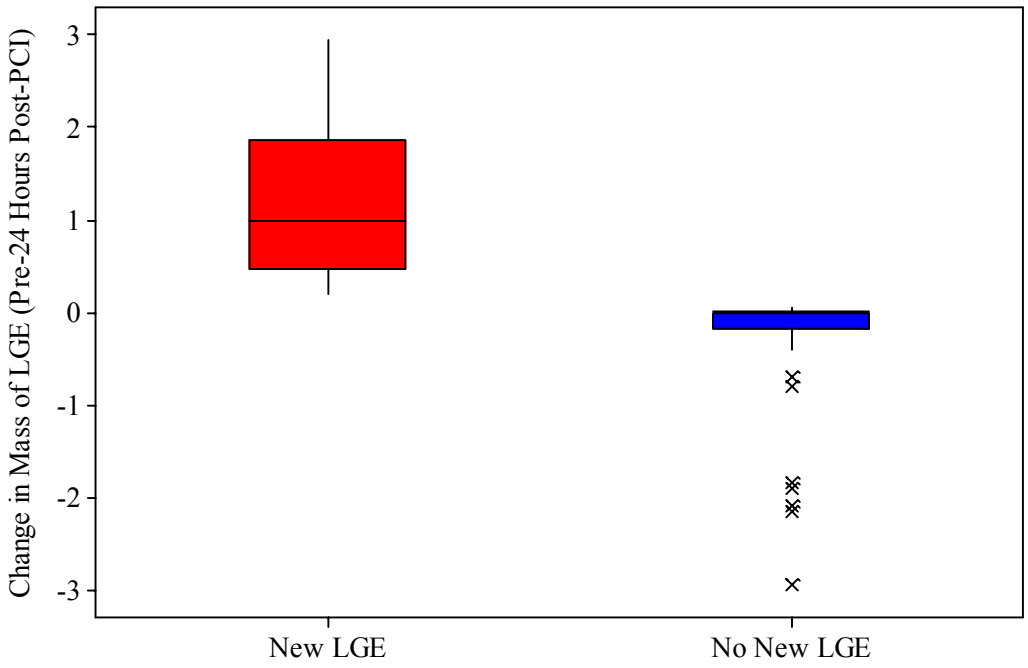

There was no significant difference in troponin levels between these two groups (p=0.5) with a median troponin level of 0.65 (SD=3.97) in the new LGE group compared to 0.57 (SD=1.2). These data are presented in the boxplot figure 4.65. The Spearman's rank correlation coefficient when comparing troponin with mass of new LGE was 0.03 indicating no correlation.

Figure 4.65 - Boxplot of troponin values in patients with and without new late gadolinium enhancement (LGE) showing the median troponin level, the interquartile range, spread of data excluding outliers and the outliers.

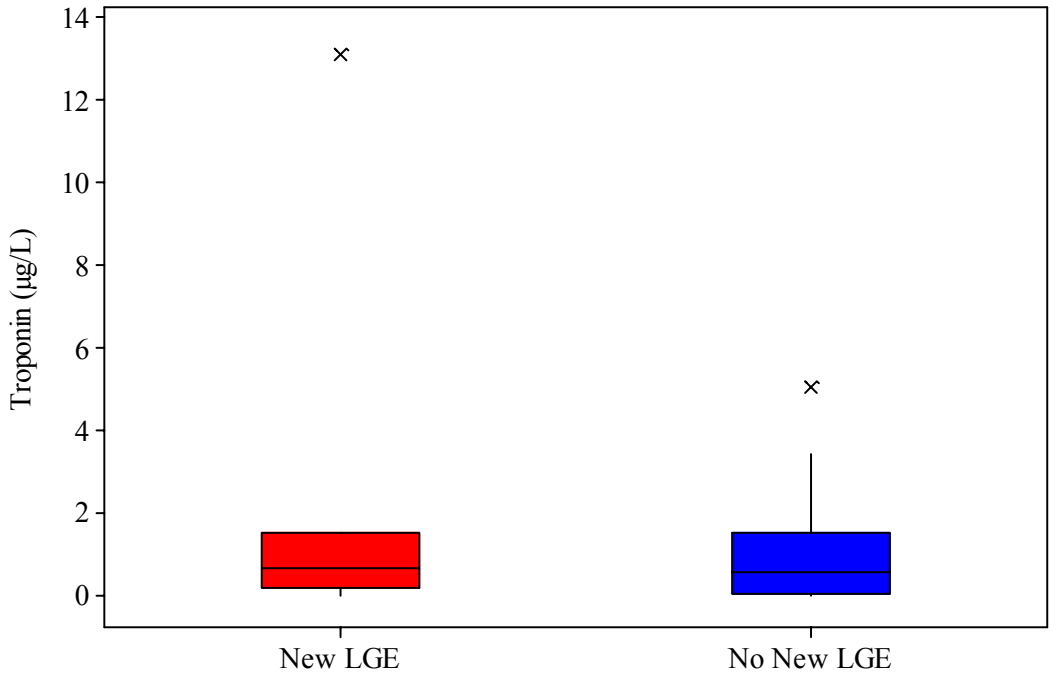

We then compared the length of the lesion being treated and the length of stent deployed to see if these measures played a role in the development of new LGE. These data are shown in figure 4.66. The median lesion length was 20.6mm (SD=16.5) in those patients with new LGE compared to 17.8mm (SD=10.2) in those without. This difference was not significant with p=0.49. Spearman's rho was 0.045 when comparing the mass of LGE with lesion length indicating no correlation. Stent length unsurprisingly produced similar results with a median length of 42.5mm (SD=22.9) in the new LGE group compared to 32mm (SD=32.3) in the no new LGE group. This difference was not significant with p=0.88. The Spearman's rho was 0.11 when comparing stent length with mass of new LGE.

Figure 4.66 - Boxplots comparing lesion lengths and stent lengths in patients with and without new late gadolinium enhancement (LGE) showing the median length, the interquartile range, spread of data excluding outliers and the outliers.

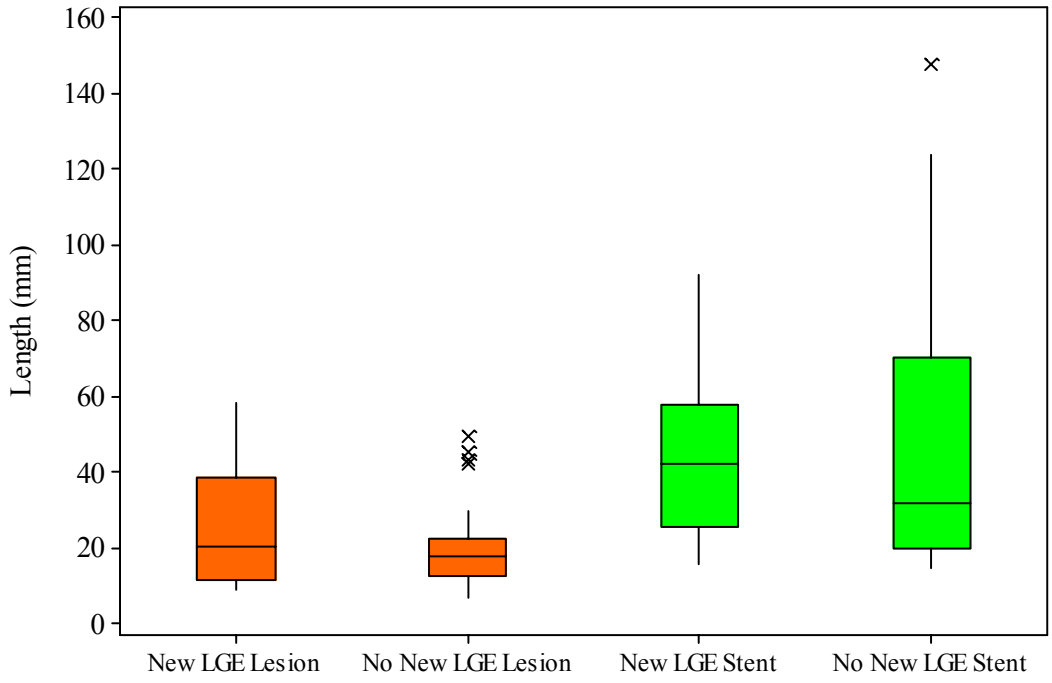

4.5.6 New Late Gadolinium Enhancement at 4 Weeks Post-PCI

Eight scans had evidence of new LGE at 4 weeks post-PCI. Only one of these patients did not have evidence of this on their 24 hour post-PCI scan. Two of the original 10 patients with new LGE at 24 hours refused to have a third MRI scan and one patient's mass of LGE returned to their pre-PCI level. Of these 8 patients with new LGE at 4 weeks the mean increase in mass of new LGE was 0.81g (0.48 to 1.14) compared to -0.28 (-0.51 to -0.05) in the no new LGE group. This difference was significant at $p<0.0001$ and is presented in figure 4.67.

Figure 4.67 - Boxplot of change in mass of late gadolinium enhancement (LGE) from pre-PCI to 4 weeks post-PCI in the new LGE and no new LGE groups.

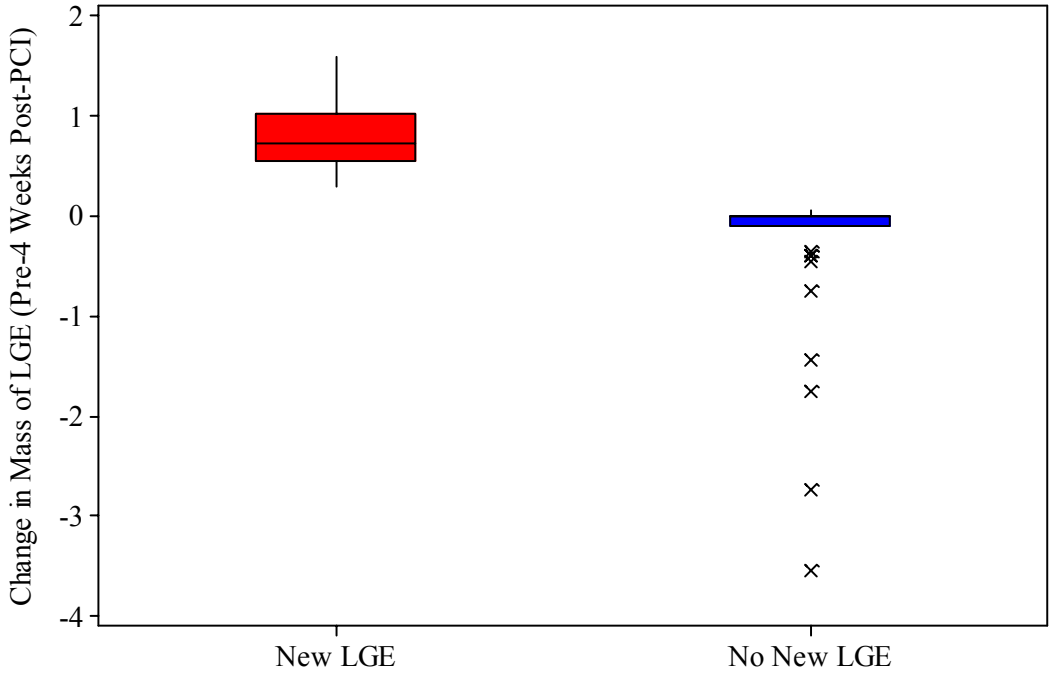

As was the case at 24 hours there was no significant difference in troponin levels between these two groups (p=0.53) with a median troponin level of 0.47 (SD=0.57) in the new LGE group compared to 0.57 (SD=1.19). These data are presented in the boxplot figure 4.68. The Spearman's rank correlation coefficient when comparing troponin with mass of new LGE was -0.12 indicating a very slight negative correlation which is unlikely to be relevant in this small group of patients.

Figure 4.68 - Boxplot of troponin values in patients with and without new late gadolinium enhancement (LGE) at 4 weeks post-PCI.

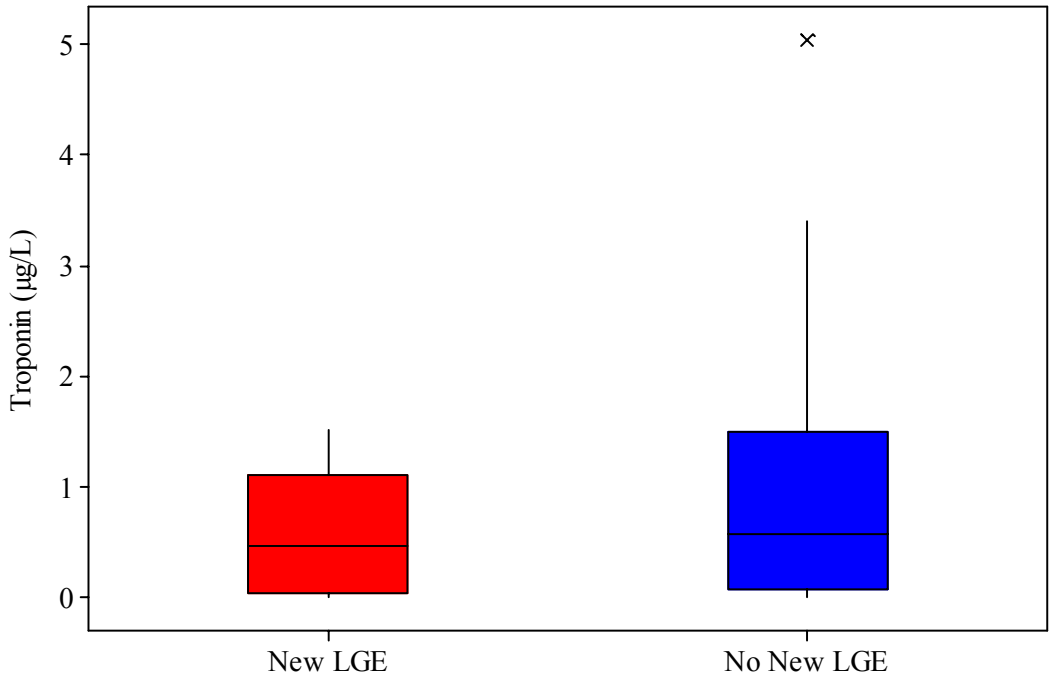

The length of lesion being treated and the length of stent deployed was then compared again to see if these parameters bore any relation to the development of new LGE. These data are shown in figure 4.69. The median lesion length was 24.7mm (SD=15.6) in those patients with new LGE compared to 17.5mm (SD=10.2) in those without. This difference did not quite reach statistical significance with p=0.07. Spearman's rho was -0.49 comparing the mass of LGE at 4 weeks with lesion length. This degree of correlation is surprising given that you would expect PCI of longer lesions to produce more LGE as opposed to the opposite. It is difficult to draw any meaningful conclusions from this small dataset. Stent length was longer in the new LGE group with a median length of 42.5mm (SD=22.3) compared to 32mm (SD=30.3) in the no new LGE group. This difference was not significant with p=0.62. The Spearman's rho was exactly 0.0 when comparing stent length with mass of new LGE indicating absolutely no correlation. This is therefore not in agreement with the lesion length correlation which in theory should be similar.

Figure 4.69 - A comparison of lesion lengths and stent lengths in patients with and without new late gadolinium enhancement (LGE) at 4 weeks post-PCI.

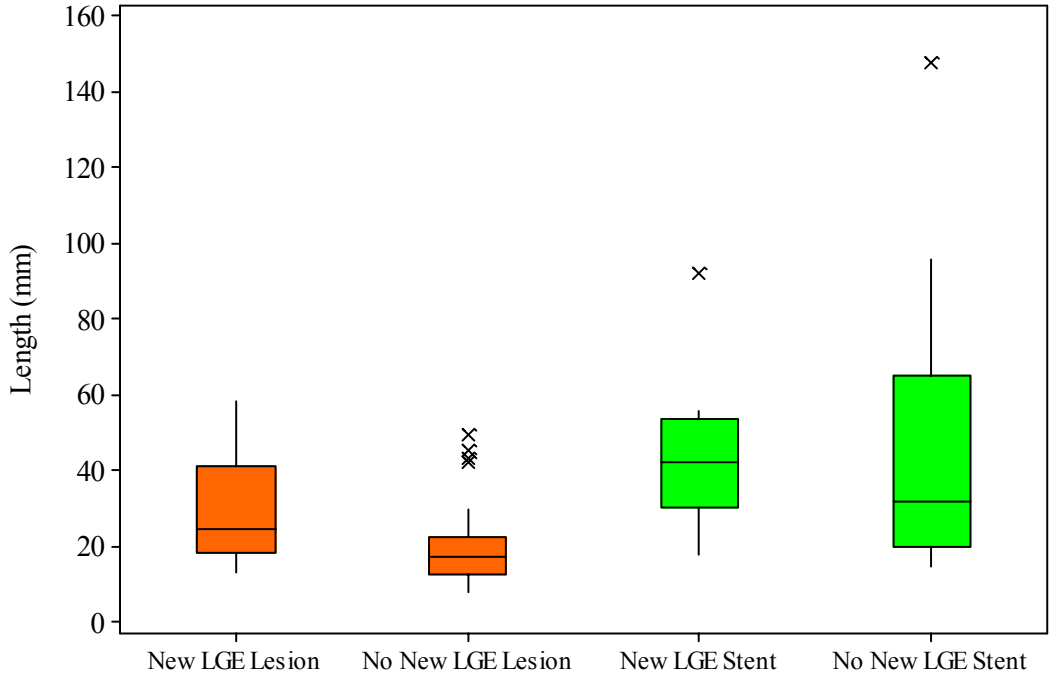

4.6 Quantitative Coronary Angiography

QCA was performed on 334 coronary arteries by 2 independent observers blinded to the MRMPI scan results, pressure wire haemodynamic data and procedural outcome ie PCI, CABG, medical therapy or non-flow limiting coronary disease. Degree of stenosis (%), area of stenosis (%), minimal luminal diameter (mm), ideal diameter of vessel at stenosis (mm), reference vessel diameter (mm) and lesion length (mm) were all measured by QCA. The results from both observers were combined to create a mean value used in the following results. The overall mean degree of stenosis for all coronary arteries was 44.3% (SD=32.0, IQ range=19.1-67.4). The mean area of stenosis was 58.6% (SD=35.2, IQ range=34.5-89.1). The overall mean reference vessel diameter was 2.91mm (SD=0.6, IQ range=2.44-3.27). The mean ideal diameter at a stenosis was 2.66mm (SD=0.54, IQ range=2.28-2.98). The mean minimal luminal diameter was 1.48mm (SD=0.73, IQ range=0.99-1.89). The mean lesion length was 12.34mm

(SD=8.99, IQ range=6.82-17.21). There were 35 totally occluded coronary arteries. Sixty-four arteries were felt by both observers to have no angiographic coronary disease. A histogram showing the range in coronary disease severity by degree of stenosis is shown on figure 4.70.

Figure 4.70 - Histogram of degree of stenosis for all 334 coronary arteries.

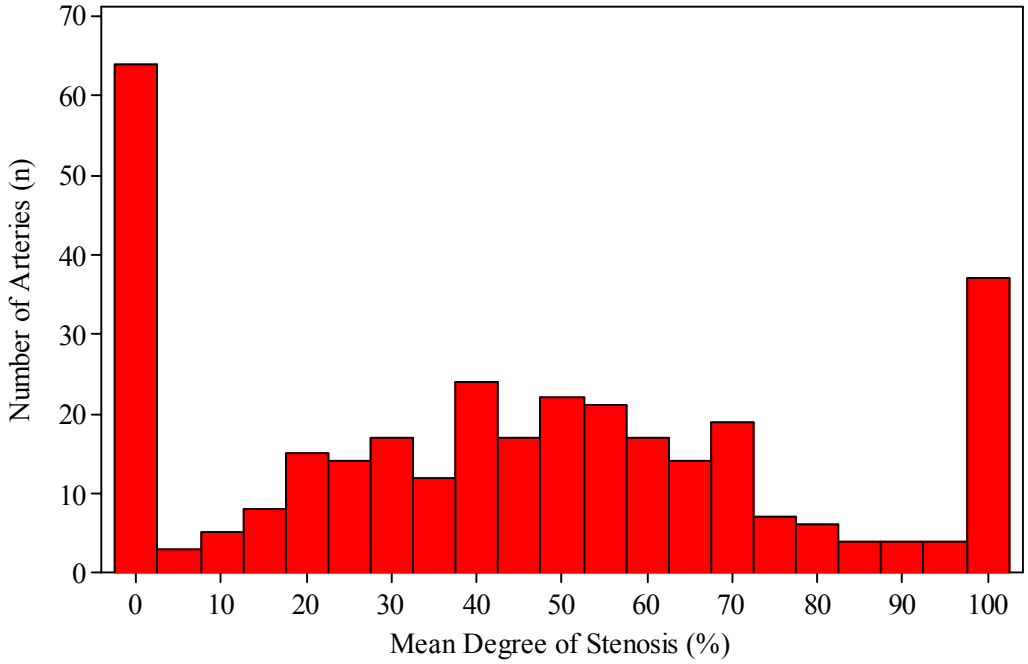

Interobserver variability of the measured degree of stenosis is highlighted on the Bland-Altman plot figure 4.71. There was excellent agreement between observers with a correlation coefficient of 0.95 and $p<0.0001$.

Figure 4.71 - Difference in degree os stenosis (%) between observers against the mean degree of stenosis with reference lines showing the mean±1.96SD within which 95% of the differences lie.

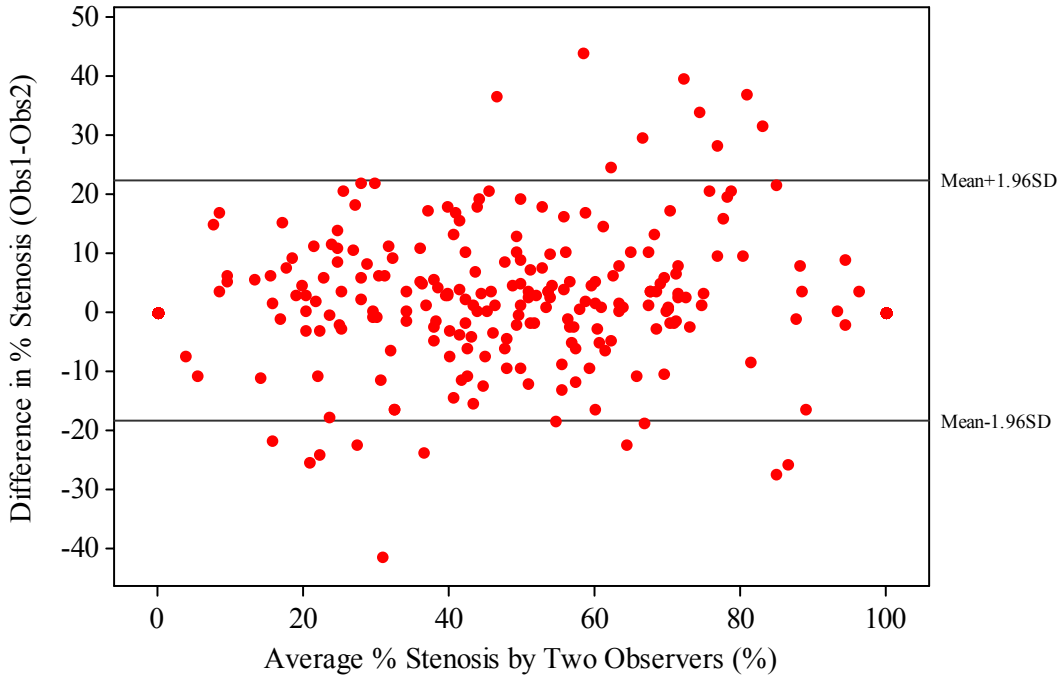

The area of stenosis was also calculated for each of the coronary arteries. The range in mean results is shown on figure 4.72. A significant correlation was found between observers with a correlation coefficient of 0.95 and $p<0.0001$.

Figure 4.72 - Histogram of area of stenosis for all 334 coronary arteries.

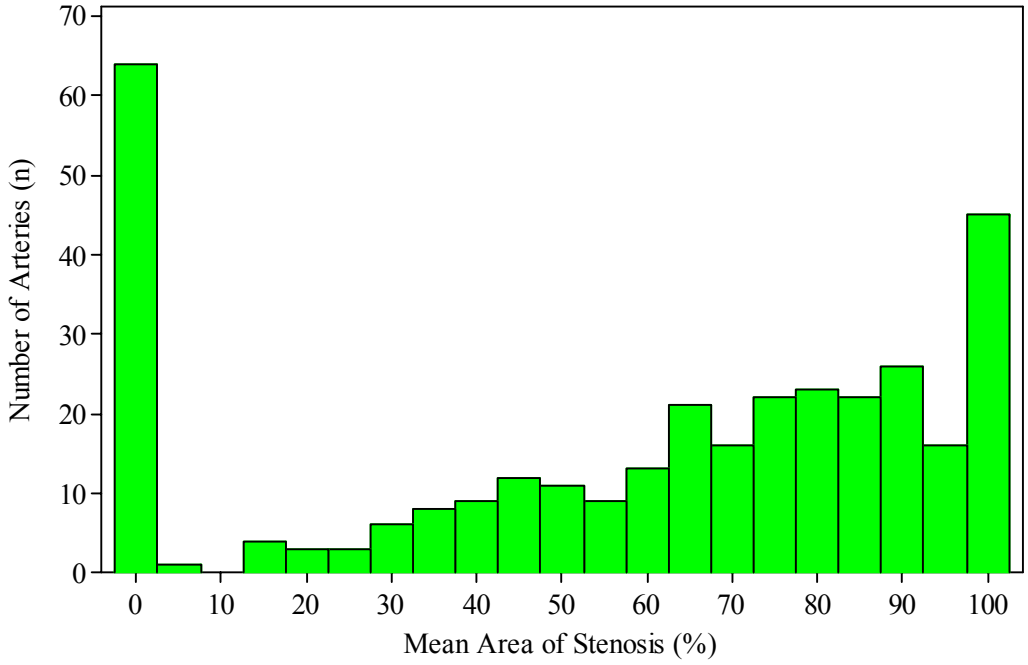

The mean lesion length is another important QCA variable which was recorded. The ranges of lesion lengths are presented on figure 4.73.

Figure 4.73 - Histogram of mean lesion length for all 334 coronary arteries.

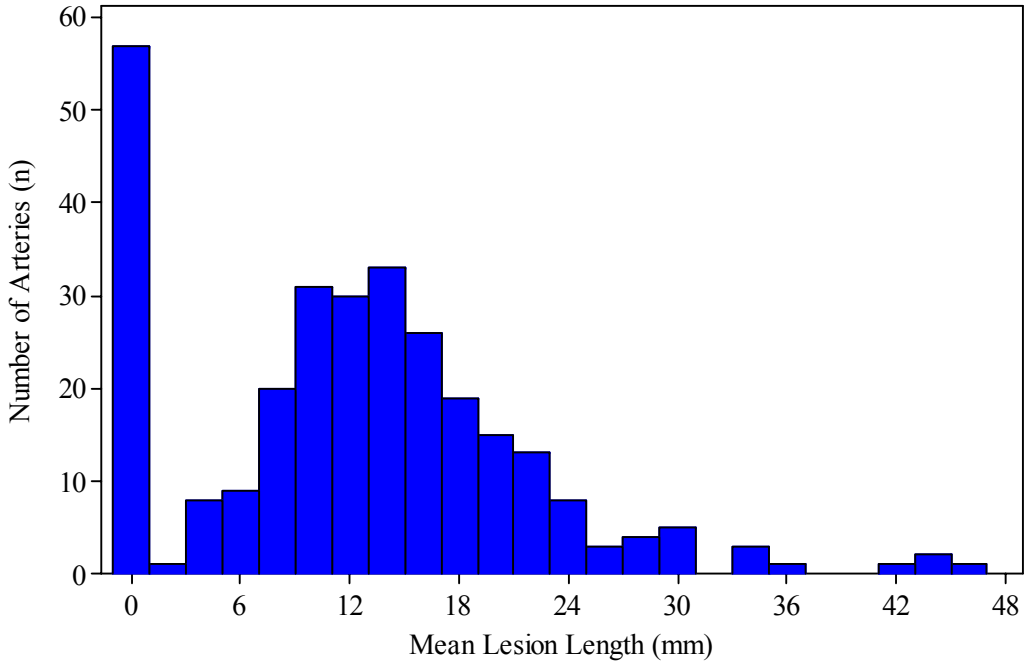

On this occasion there was less agreement between the observers on the lengths of coronary artery lesions as shown on figure 4.74. The correlation coefficient was 0.5 with $p<0.0001$ as before.

Figure 4.74 - Difference in lesion length (mm) between observers against the mean lesion length with reference lines showing the mean±1.96SD within which 95% of the differences lie.

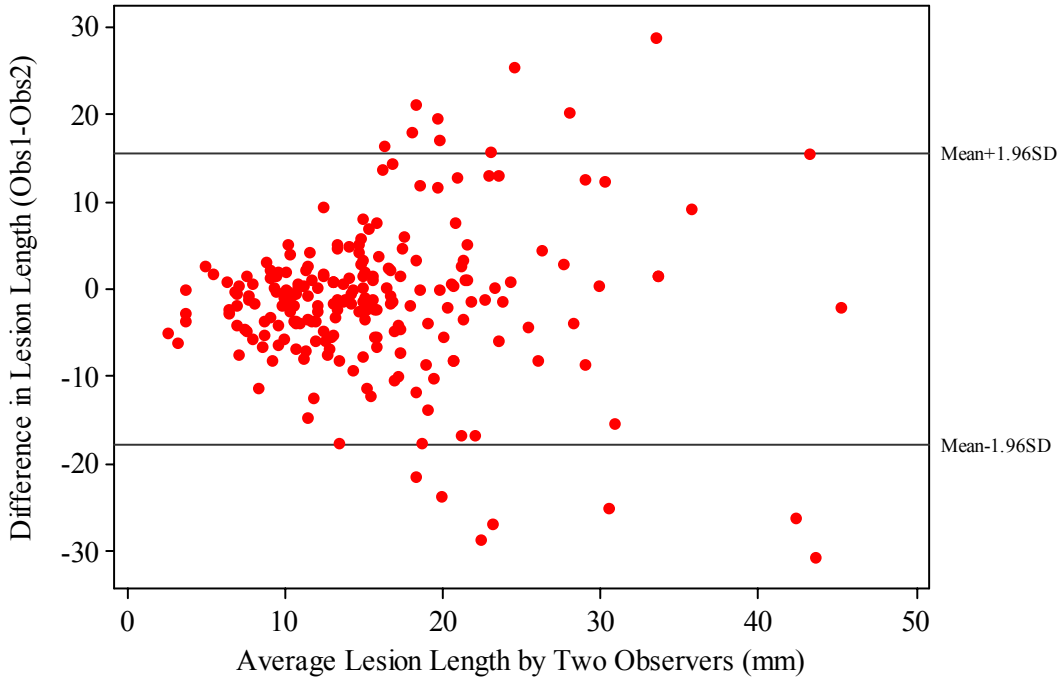

The reference vessel diameter of all coronaries was recorded where possible including occluded arteries. No reference vessel diameter was obtainable in arteries with an ostial occlusion. The differences in reference vessel diameters are presented in table 4.23.

Table 4.23 - Reference vessel diameters for each of the coronary arteries analysed by QCA.

	No	Mean	Median	SD	Min	Max
LMS	7	3.85	3.57	1.09	2.91	6.06
LAD	98	2.91	2.90	0.50	2.11	4.83
LCx	56	2.93	2.99	0.55	1.29	4.18
OM	44	2.51	2.41	0.43	1.72	3.43
RCA	94	3.06	3.08	0.63	1.87	4.78
D1	6	2.43	2.38	0.48	1.81	3.13
IM	8	2.48	2.43	0.32	2.14	2.93
LPDA	14	3.06	3.20	0.62	1.96	4.11

4.7 Coronary Pressure Wire Results

4.7.1 Fractional Flow Reserve (FFR)

The FFR was recorded in 260 coronary arteries. The spread of results are demonstrated in the histogram (Figure 4.75) below. This histogram does not include occluded arteries where the pressure wire was unable to cross the areas of occlusion.

Figure 4.75 - Histogram of FFR results in the 260 coronary arteries.

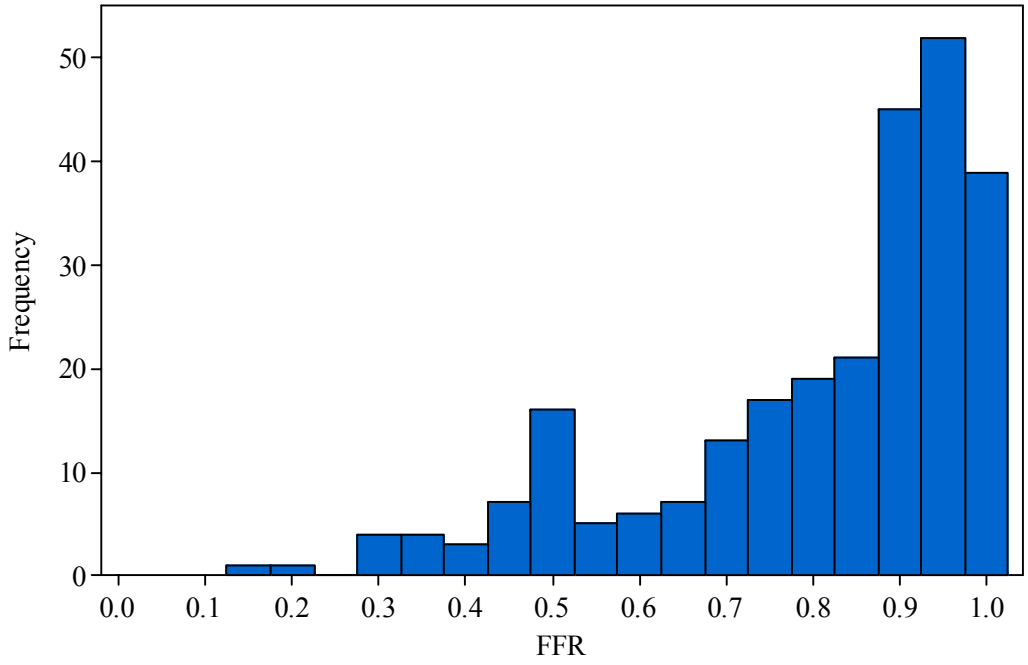

The median FFR was 0.88 with a mean of 0.81 (SD=0.19; Interquartile range 0.71-0.95). Sixty-nine arteries had a measured FFR<0.75 whereas 191 arteries had an FFR≥0.75. Of the 101 patients the FFR was obtained in 4 arteries per patient in 5 (5%) cases, 3 arteries in 63 (62%) cases, 2 arteries in 22 (22%) cases, 1 artery in 7 (7%) cases and no FFR values were obtained in 4 (4%) cases. FFR results were obtained from 90 (34.6%) left anterior descending coronary arteries, 45 (17.3%) left circumflex arteries, 38 (14.6%) obtuse marginal branches, 65 (25%) right coronary arteries, 6 (2.3%) 1st diagonal branches, 8 (3.1%) left posterior descending arteries and 8 (3.1%) intermediate

arteries. There were 35 completely occluded arteries including 18 right coronary arteries, 10 left circumflex / obtuse marginal coronary arteries, 5 left anterior descending coronary arteries and 2 left posterior descending arteries. Five arteries were sub-totally occluded including 3 right, 1 left anterior descending and 1 left circumflex coronary arteries. Three patients had severe left main stem disease and FFR was not measured to avoid any risk associated with crossing these lesions with a wire. A further 7 arteries had severe angiographically significant disease which was clearly significant but again not crossed with the pressure wire. One patient with angiographically normal coronary arteries did not have FFR measurements made due to a very abnormal take-off of both arteries making selective cannulation of the coronary ostia difficult. Only 2 data points were obtainable in three patients. In one patient the left circumflex artery was not identified but there was no lateral perfusion on the perfusion MRI. The other two patients had very small non-dominant RCA's which were not wired. In the final data analysis where only three coronary territories per patient were included, 121 arteries had a FFR <0.75 (including occluded and subtotally occluded arteries) and 179 arteries had FFR ≥0.75. A grey zone is known to exist between FFR values of ≥0.75 and ≤0.8 which may represent lesions capable of inducing myocardial ischaemia. In our study 26 coronary arteries fell into this group.

4.7.2 Relationship Between FFR and Resting Pd/Pa

There has been some debate relating to whether or not adenosine stress is necessary if the resting Pd/Pa is above or below a certain threshold. Table 4.24 presents our data with resting Pd/Pa in the left hand column and the chances of reaching either the FFR≤0.8 cut-off of the grey zone or the FFR<0.75 cut-off which was used in most of the original FFR studies. Interestingly if you have a resting Pd/Pa of between 0.95 and

1.0, none of the 158 arteries studied reached an FFR<0.75. As the resting Pd/Pa value decreases an increasing proportion of lesions exhibit an ischaemic FFR value.

Table 4.24 - Data relating to the achieved FFR depending on the pre-adenosine Pd/Pa measurement. This shows the absolute number and % of arteries that achieved an FFR≤0.8 and FFR<0.75 depending on the pre-adenosine Pd/Pa.

Resting Pd/Pa	**Arteries (n)**	**Arteries FFR ≤0.8**	**Arteries FFR >0.8**	**% Reaching ≤0.8**	**Arteries FFR <0.75**	**Arteries FFR ≥0.75**	**% Reaching <0.75**
0.95 – 1.0	158	4	154	**2.6**	0	158	**0**
0.9 – 0.94	57	12	45	**21.1**	3	54	**5.3**
0.85 – 0.89	24	16	8	**66.7**	9	15	**37.5**
0.81 – 0.84	10	8	2	**80**	7	3	**70**
0.75 – 0.8	10	-	-	**-**	8	2	**80**

4.7.3 Coronary Flow Reserve (CFR)

CFR was measured in 250 arteries during the initial microvascular function assessment. The mean CFR was 2.45 and the median was 2.2 (SD=1.32; Interquartile Range 1.49 – 3.16). A histogram of CFR measurements is shown in Figure 4.76.

Figure 4.76 - Histogram of CFR measurements.

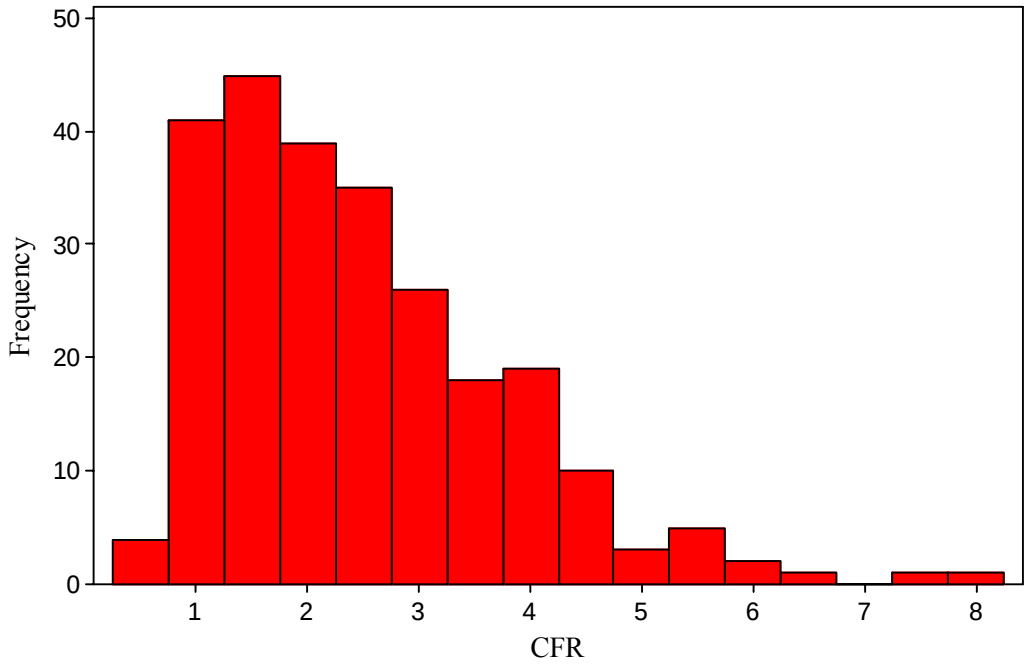

The CFR was recorded in 4 coronary arteries in 4 (4%) patients, 3 coronary arteries in 57 (56%) patients, 2 coronary arteries in 27 (27%) patients, 1 coronary artery in 9 (9%) patients and in none of the coronary arteries in 4 (4%) patients (three left main stem stenoses and one patient with poor guide catheter engagement). The location of the arteries in which CFR was measured is indicated in the pie chart figure 4.77. Interestingly the recorded CFR was less than 1 in 26 arteries which will be discussed later in the discussion (chapter 5.4).

Figure 4.77 - Pie chart demonstrating those arteries in which the CFR was measured (numbers and % of total arteries interrogated).

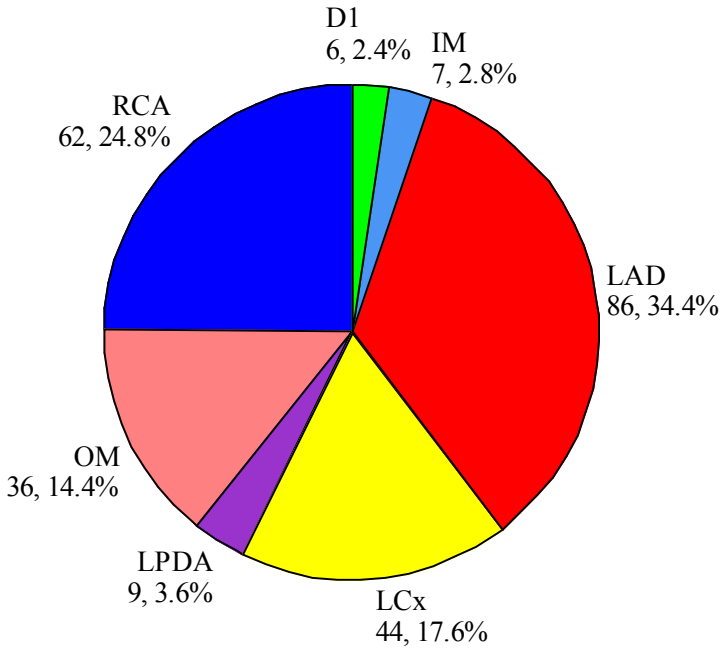

4.7.4 Index of Microcirculatory Resistance (IMR)

The IMR was recorded in 231 coronary arteries. These values were not corrected for contributions from collateral flow as coronary wedge pressure values were only obtained for those arteries which had PCI performed. A corrected IMR was obtained for 43 arteries in which distal coronary / wedge pressure was obtained. A histogram of uncorrected IMR measurements is shown in figure 4.78.

Figure 4.78 - Histogram showing the distribution of uncorrected IMR readings.

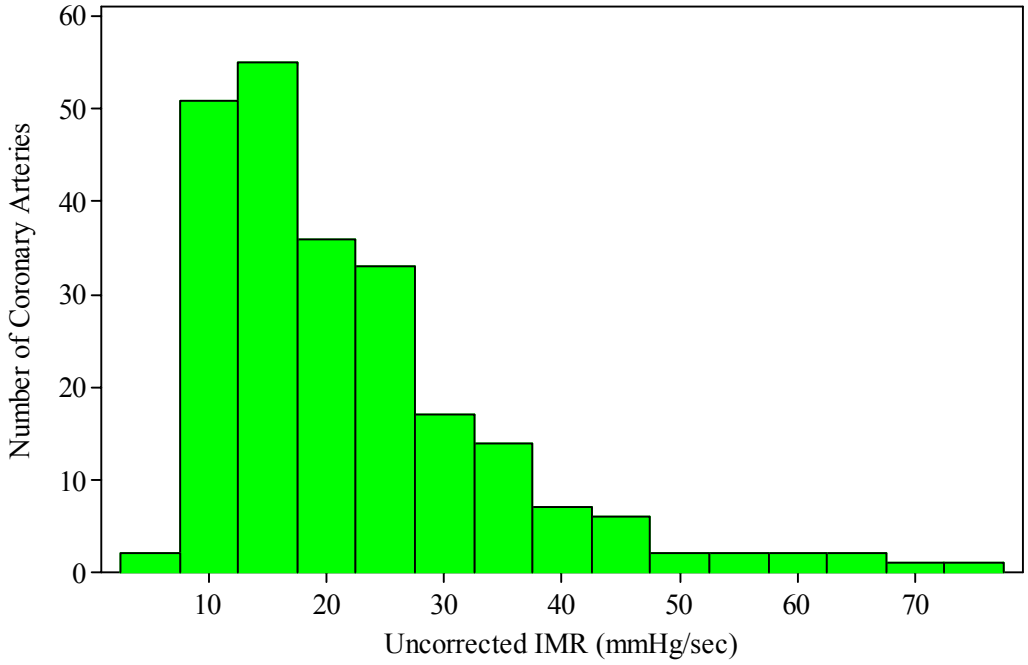

The mean uncorrected IMR was 21.8mmHgs^{-1} and the median was 18.4mmHgs^{-1} (SD=12.4, Interquartile Range 12.8 – 26.2). The distribution of the coronary arteries from which these results were obtained is shown on the pie chart Figure 4.79.

Figure 4.79 - Pie chart of arteries from which uncorrected IMR values were obtained.

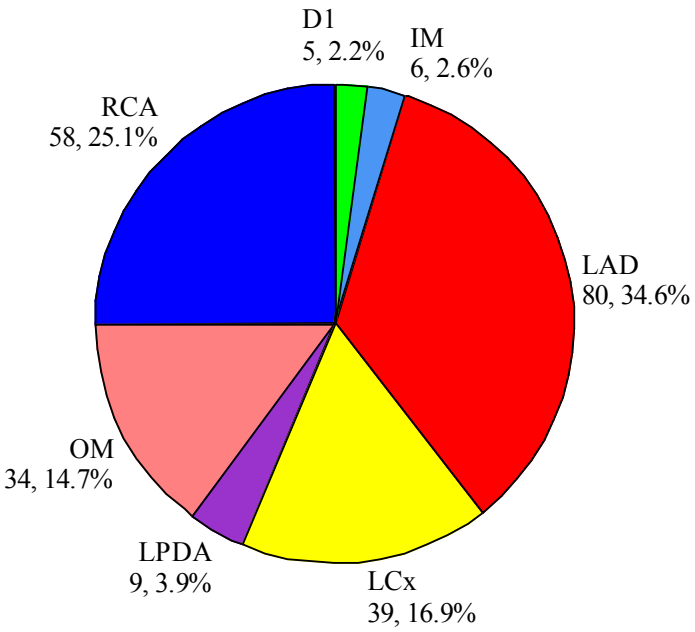

Uncorrected IMR results were obtained from 4 coronary arteries in 2 (2%) patients, 3 arteries in 54 (53%) patients, 2 arteries in 27 (27%) patients, 1 artery in 7 (7%) patients and from no arteries in 12 (12%) patients. A corrected IMR was obtained for 43 coronary arteries with a mean value of 15.5mmHgs^{-1} and a median of 13.5mmHgs^{-1} (SD=8.9, Interquartile range 9.6 – 20.8). Figure 4.80 shows the change in IMR when this is corrected for the wedge pressure. Following logarithmic transformation of this data the difference between uncorrected and corrected IMR results was significant (paired T=5.69, p<0.0001)

Figure 4.80 - Uncorrected and corrected IMRs when coronary wedge pressure is taken into account in individual arteries.

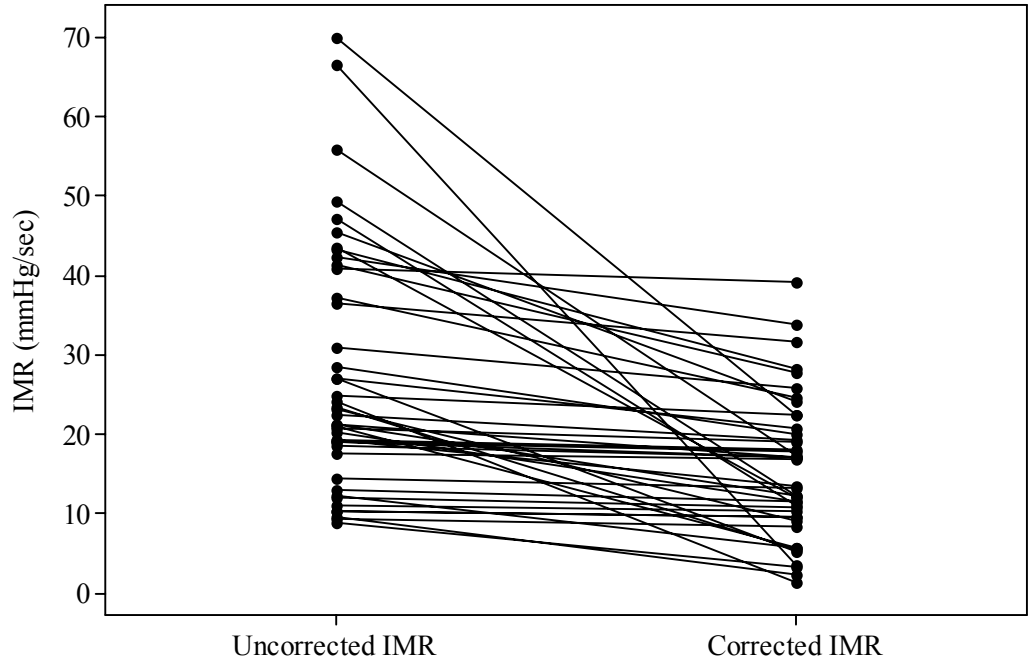

4.8 Troponin Levels Post-Percutaneous Coronary Intervention

Troponin I levels were measured 24 hours post-PCI in 53 out of the 57 (93%) patients who underwent PCI. The remaining samples were either lost or labelled incorrectly and therefore not processed. The distribution of measured troponin I levels are shown in the histogram below (Figure 4.81).

Figure 4.81 - A histogram of troponin I measurements 24 hours post-PCI.

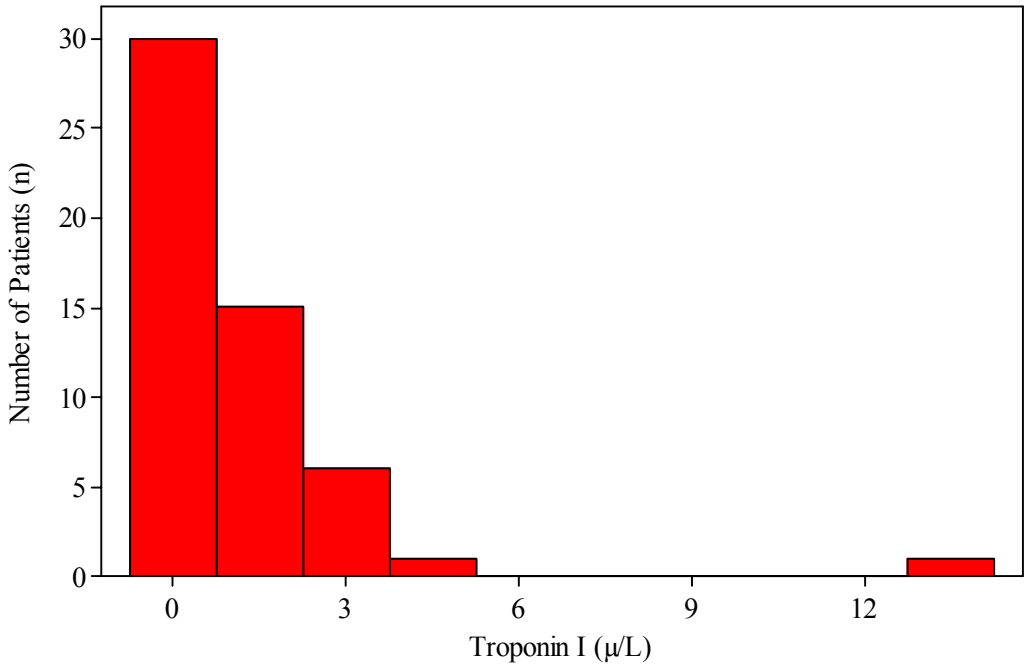

The mean troponin level was 1.18µg/L (Median 0.57, SD=2.0). One patient had an exceptionally high troponin of 13.1 following single vessel PCI however all other patients had levels less than 6µg/L. This data was then split into those patients who had received single, two or three vessel PCI. Table 4.25 summarises the troponin data depending on number of vessel intervened upon.

Table 4.25 - Troponin I data for single vessel, two or three vessel PCI.

PCI Arteries	Number (n)	Mean	Median	StD	Minimum	Maximum
1	39	1.17	0.37	2.25	Undetected	13.1
2	12	1.36	1.15	1.11	Undetected	3.1
3	2	0.39	0.39	0.07	0.34	0.44

There was no significant difference detected in comparing troponin results from patients having 1 or 2 vessel PCI ($p=0.16$), 1 or 3 vessel PCI ($p=1.0$) or 2 and 3 vessel PCI ($p=0.24$). However there were only 2 patients with troponin results who had 3 vessel PCI performed.

The only parameters found to correlate with troponin I levels post PCI were lesion length and total stent length. As shown on Figure 4.82, troponin I levels increase with increasing length of the lesion ($r=0.6$, $p<0.0001$).

Figure 4.82 - Scatterplot of lesion length pre-PCI and troponin I levels post-PCI.

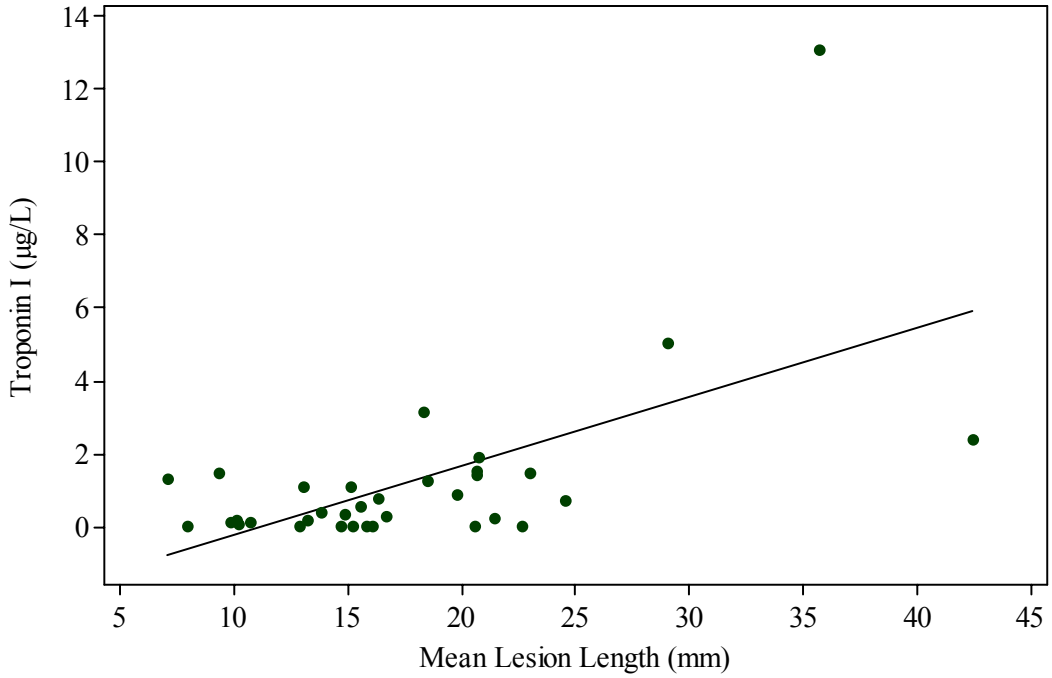

Given that lesion length was found to correlate with post PCI troponin I levels, unsurprisingly total stent length was also found to correlate with troponin I levels increasing with increasing total stent length (r=0.37, p=0.02). This data is shown on figure 4.83.

Figure 4.83 - Scatterplot of total stent length inserted and troponin I levels post-PCI.

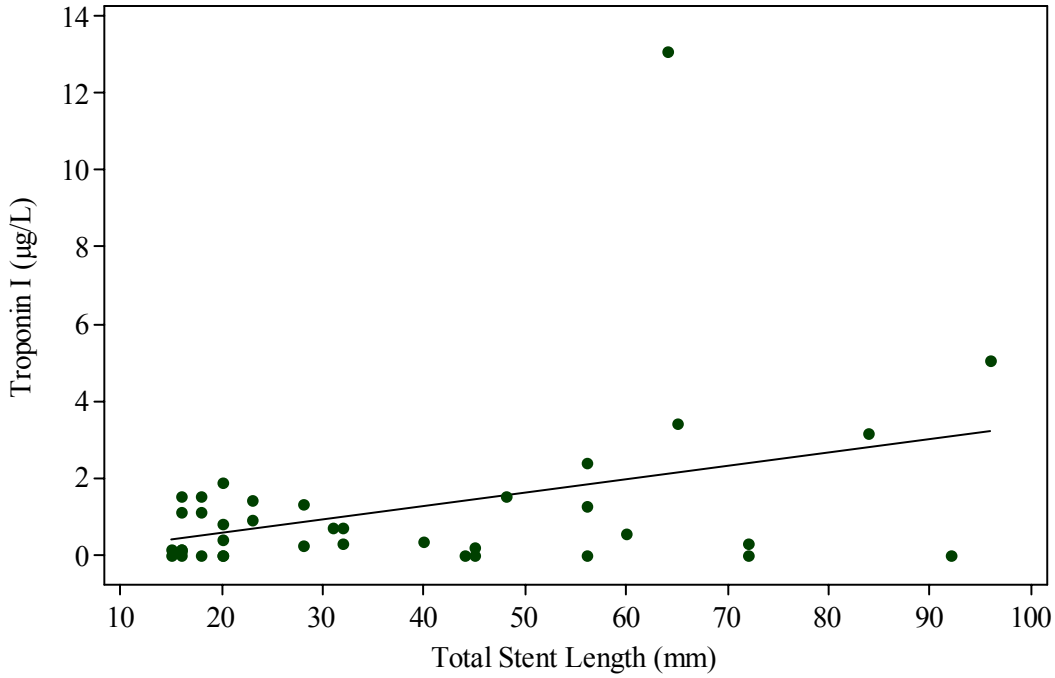

4.9 Haemodynamic and Symptomatic Effects of Adenosine

Pulse and blood pressure were closely monitored prior to and during the adenosine infusion whilst having the stress perfusion component of the MRI scan performed. Along with the symptoms experienced this helps tell if patients are adequately stressed by the vasodilating stress agent. The following box plots show the changes in pulse (figure 4.84), SBP (figure 4.85) and DBP (figure 4.86) from rest (prior to the adenosine infusion) and at least 2 minutes into the infusion with 140mcg/kg/min IV adenosine.

Figure 4.84 - Box plot showing pulse data at rest and stress highlighting the median pulse, the interquartile range, spread of data excluding outliers and the outliers.

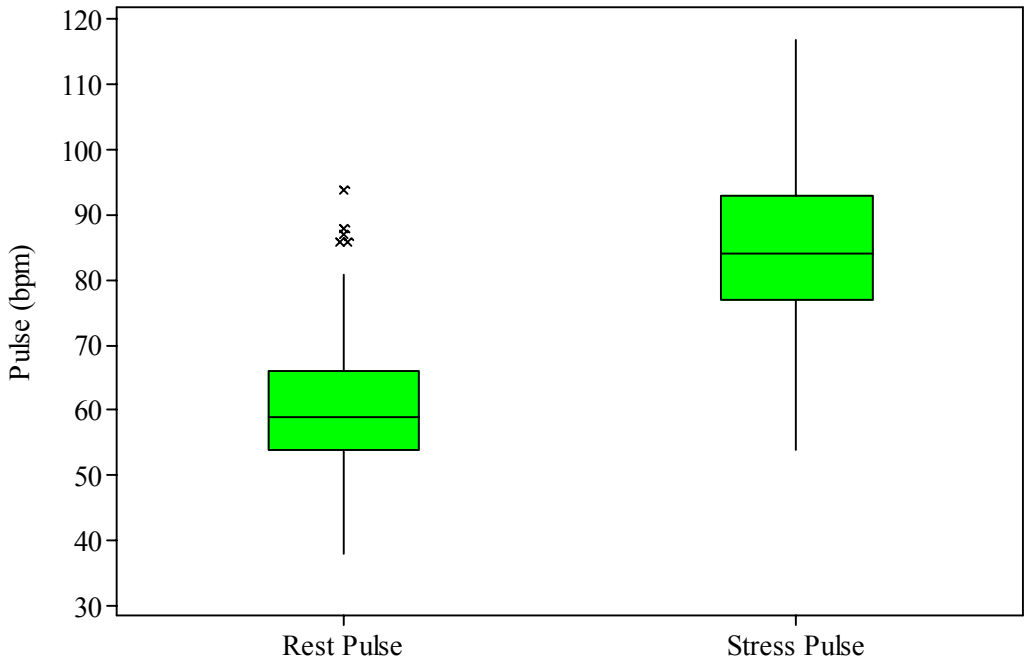

Figure 4.85 - Box plot showing SBP data at rest and stress highlighting the median SBP, the interquartile range, spread of data excluding outliers and the outliers.

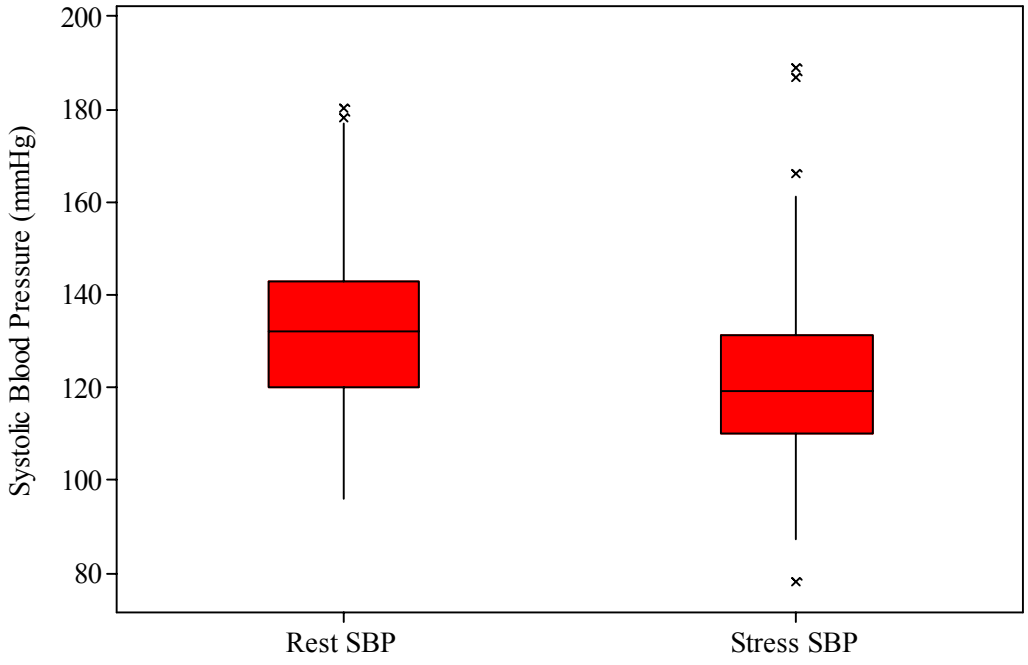

Figure 4.86 - Box plot showing DBP data at rest and stress highlighting the median DBP, the interquartile range, spread of data excluding outliers and the outliers.

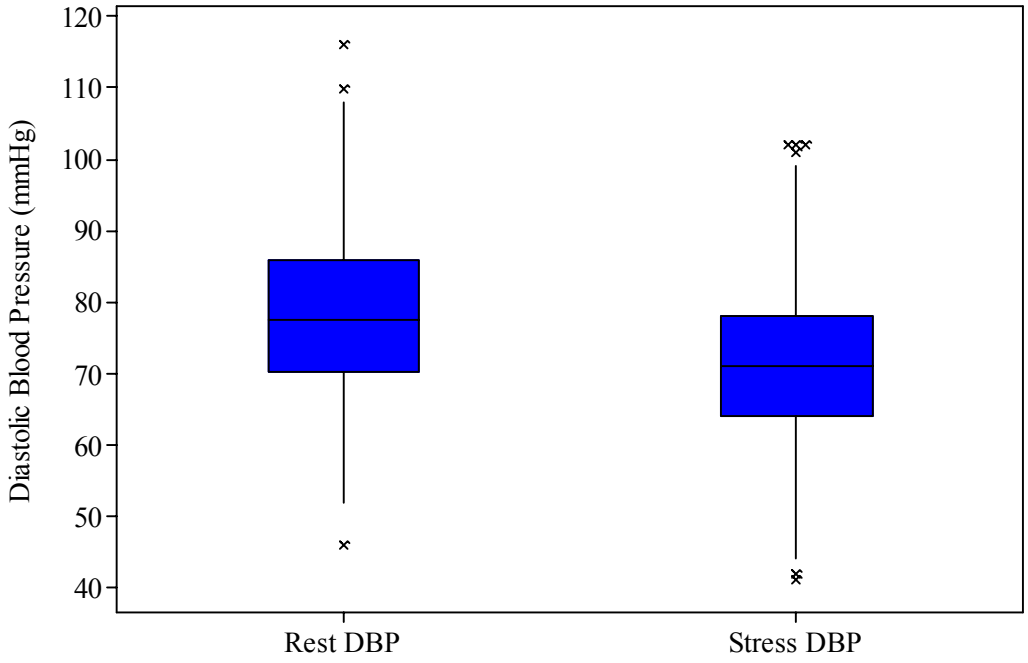

The haemodynamic response to adenosine during the stress phase of the perfusion MRI is summarised in table 4.26. This shows a significant increase in heart rate with a significant fall in both SBP and DBP as expected with this vasodilating stress agent. Of the 101 patients included in the final analysis 5 (5%) were felt to have not achieved haemodyanamic stress on the basis of the haemodynamic data and symptoms experienced. This was despite increasing the dose of administered adenosine above 140mcg/kg/min.

Table 4.26 - Changes in pulse, systolic BP and diastolic BP during adenosine stress MRMPI. Data were analysed using paired t-test comparing rest and stress data. * denotes skewed data where logarithmic transformation was performed.

	No	Mean	Median	SD	t-value	P value
Rest Pulse	225	61	59	9.3	43.3*	<0.0001
Stress Pulse	225	85	84	11.9		
Rest SBP	224	133	132	17.8	12.4*	<0.0001
Stress SBP	223	121	119	17.2		
Rest DBP	224	78	77.5	11.6	10.4	<0.0001
Stress DBP	223	71	71	11.7		

The symptoms experienced during the adenosine infusion are presented in figure 4.87. The most common symptom experienced was breathlessness which was noted in 162 (71.7%) scans. A warm flushing sensation was experienced in 120 (53.1%), chest pain in 119 (52.7%), headache in 41 (18.1%) and abdominal pain in 16 (7.1%). No patients experienced any wheeze and only one patient developed symptomatic AV block.

Figure 4.87 - Symptoms experienced by patients during the IV adenosine infusion of the MRMPI scan.

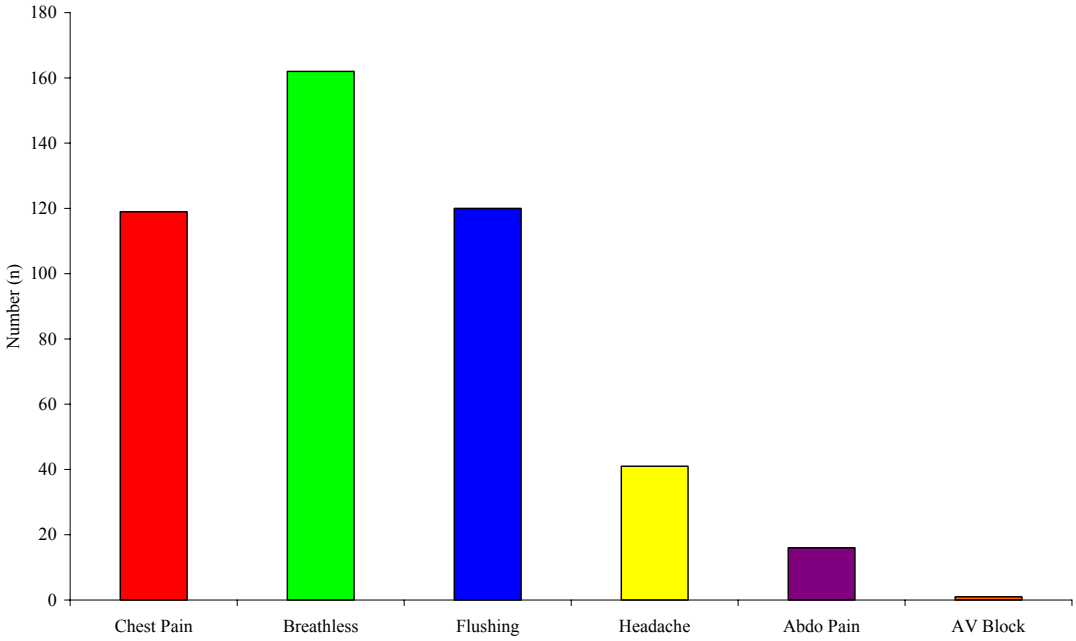

4.10 Serum Caffeine Measurements and Effects on Haemodynamics and Symptoms

Of the 226 MRMPI scans performed, caffeine levels were measured in 220 (97%). Significant caffeine levels (≥1mg/L) were only detected on 29 (13.2%) occasions. One patient had detectable caffeine levels on all 3 attendances for MRMPI, 3 patients had detectable caffeine levels on 2 occasions and 20 patients on only one occasion. The spread of detectable caffeine levels is presented in figure 4.88. The median caffeine level was 1.33mg/L and the mean was 1.84mg/L (SD=1.13, IQ range=1.19-2.13).

Figure 4.88 - Histogram of serum caffeine levels (mg/L).

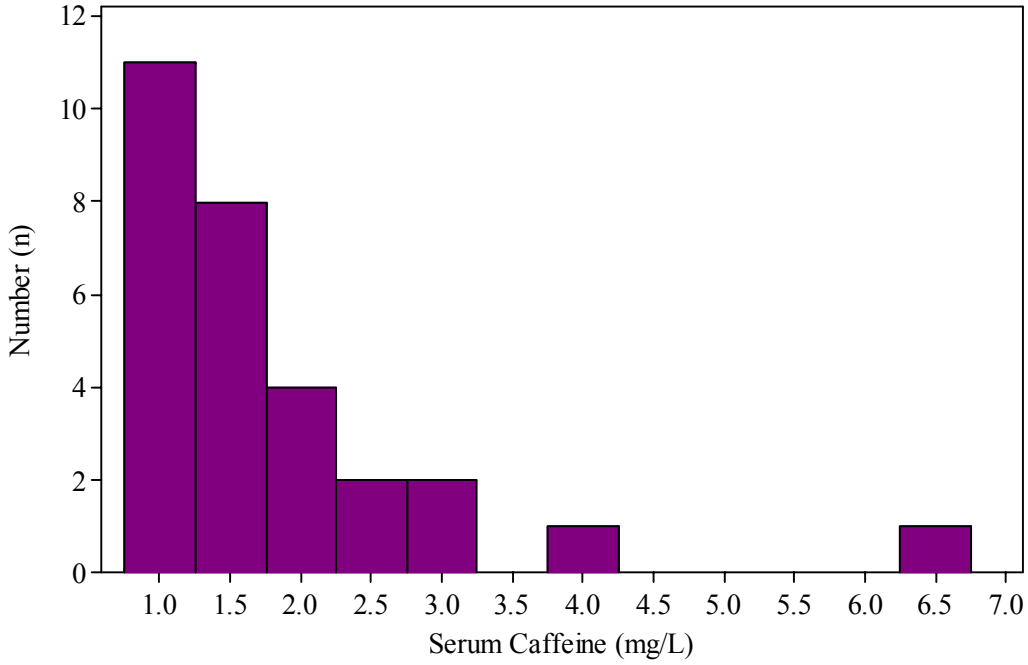

We then went on to compare the haemodynamic responses to the adenosine infusion (140mcg/kg/min) during the MRMPI scan between those patients with detectable caffeine levels (>1mg/l) and those patients with levels <1mg/l. Table 4.27 summarises the differences in pulse, SBP and DBP in those with and without detectable caffeine. The corresponding p values are given where comparisons have been made.

Table 4.27 - Table comparing pulse, systolic BP (SBP) and diastolic BP (DBP) at rest and stress in patients with and without detectable caffeine levels. Due to skewed dataset p values were obtained by first taking logarithmic transformations of the data and then using the two-sample T test.

	Rest/Stress	Caffeine	Mean	Median	SD	Min	Max	P value
Heart Rate	Rest	<1mg/l	61	60	9.1	38	94	0.05
		≥1mg/l	57	57	10.0	41	81	
	Stress	<1mg/l	86	84	11.6	60	117	0.02
		≥1mg/l	79	81	12.4	54	100	
SBP	Rest	<1mg/l	132	132	17.6	96	180	0.09
		≥1mg/l	138	141	19.0	111	178	
	Stress	<1mg/l	121	119	16.6	78	187	0.4
		≥1mg/l	125	121	21.2	98	189	
DBP	Rest	<1mg/l	78	86	11.4	46	108	0.4
		≥1mg/l	80	78	12.9	62	116	
	Stress	<1mg/l	71	78	11.1	41	102	0.97
		≥1mg/l	72	69	15.4	44	102	

This table shows that the maximum stress heart rate achieved was significantly greater in those patients without detectable caffeine levels. This is an important observation as peak heart rate is an indicator of the achieved maximal hyperaemia. The stress heart rate data are also displayed graphically in Figure 4.89. There was also a trend towards a lower resting SBP in the undetectable caffeine level group however this did not reach statistical significance. Interestingly there was also a non-significant trend towards the detectable caffeine level group having a lower resting heart rate.

Figure 4.89 - Box plot showing stress heart rate data in patients with and without detectable caffeine levels highlighting the median heart rate, the interquartile range and the spread of the data.

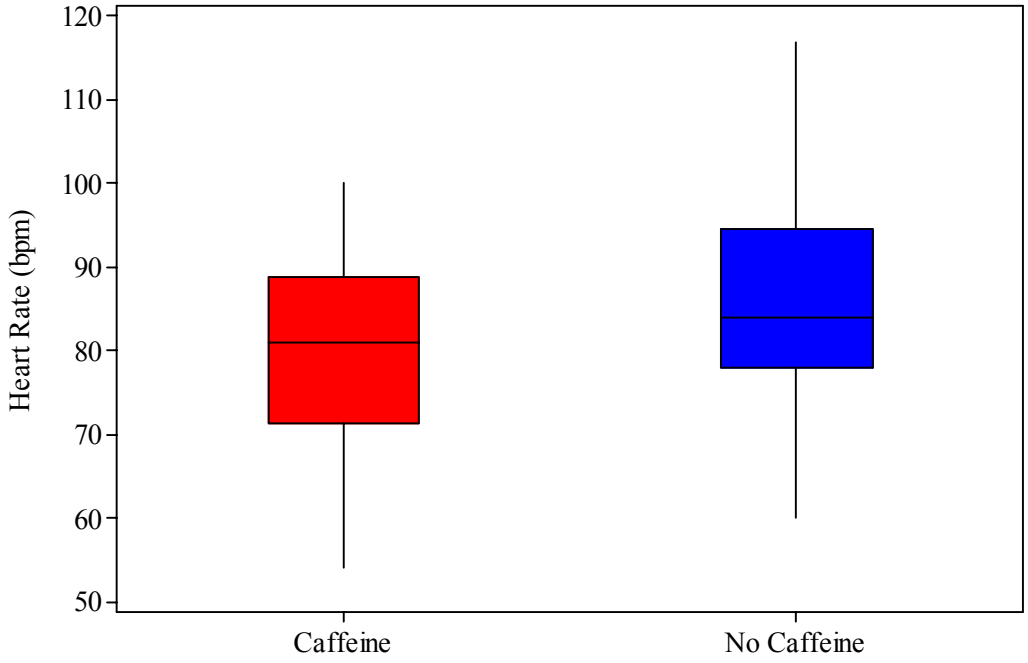

We also examined the differences in pulse, SBP and DBP at rest and stress in individual patients in the caffeine detected and not detected groups. These data are presented by means of boxplots in figures 4.90, 4.91 and 4.92. There was no significant difference between differences in heart rate (p=0.12), differences in SBP (p= 0.35) and differences in DBP (p=0.36) in the caffeine detected and not detected groups.

Figure 4.90 - Box plot showing difference in heart rate between rest and stress in patients with and without detectable caffeine levels highlighting the median difference, the interquartile range, the spread of the data without outliers and the outliers.

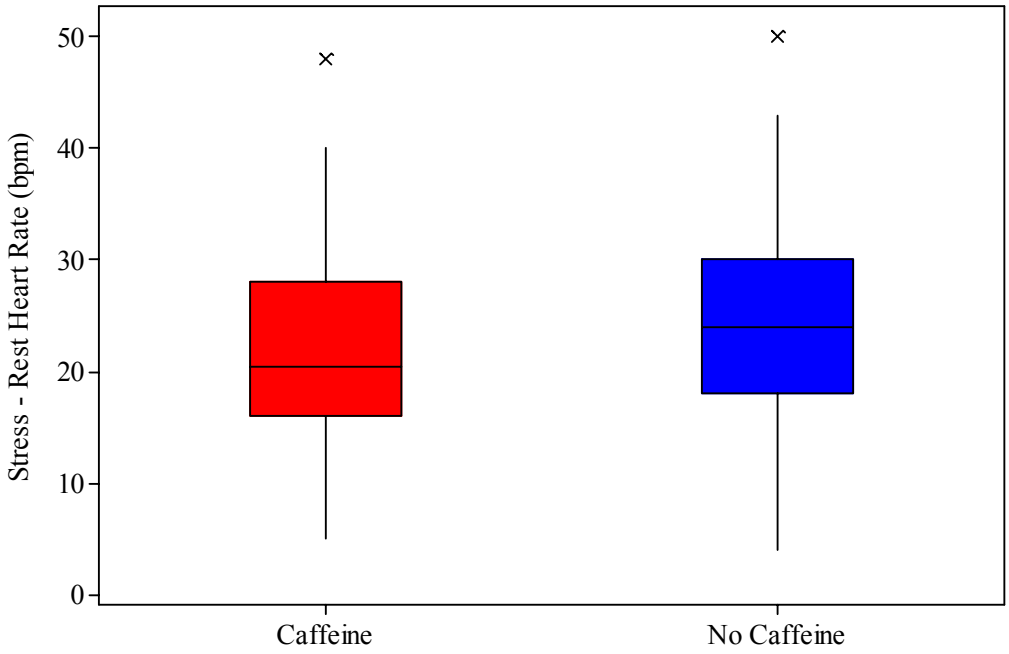

Figure 4.91 - Box plot showing difference in systolic BP between rest and stress in patients with and without detectable caffeine levels highlighting the median difference, the interquartile range, the spread of the data without outliers and the outliers.

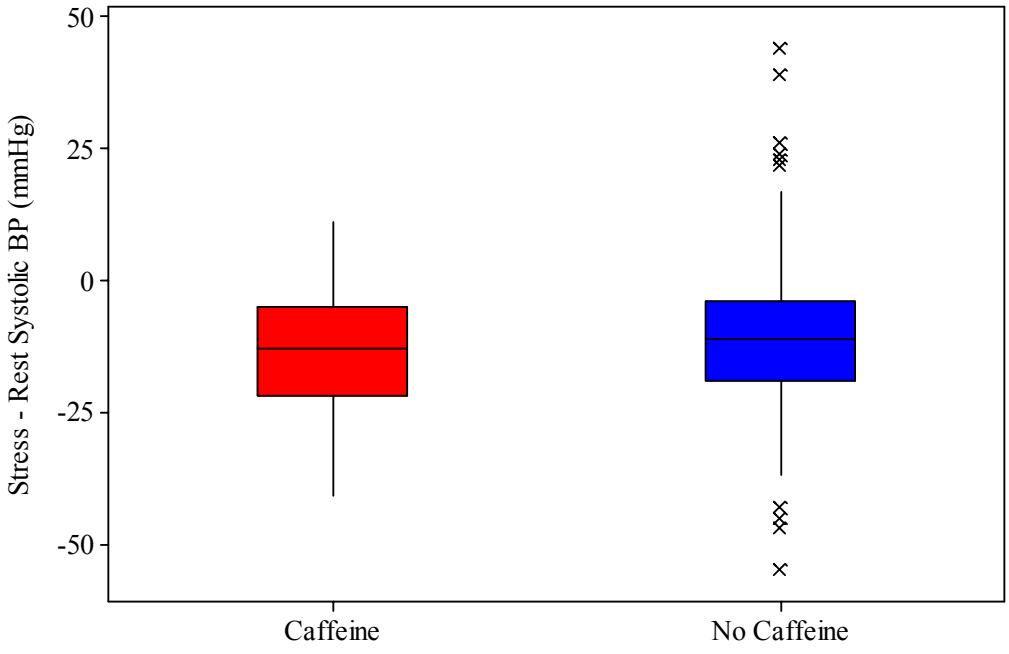

Figure 4.92 - Box plot showing difference in diastolic BP between rest and stress in patients with and without detectable caffeine levels highlighting the median difference, the interquartile range, the spread of the data without outliers and the outliers.

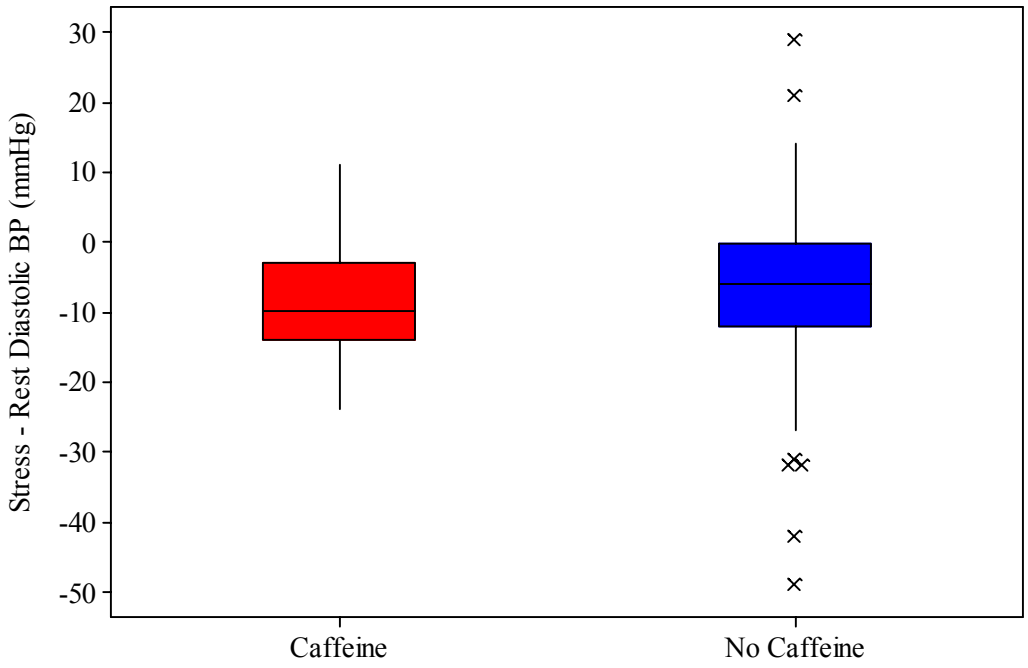

In those patients who were found to have a detectable caffeine level (≥1mg/l) we used Pearson's correlation coefficient to see if any relationship existed between the mean caffeine level (average of pre and post MRMPI caffeine levels) and the various parameters examined above. The results of this analysis are tabulated in table 4.28. As shown no significant correlation was found however the greatest correlation was found with resting SBP (p=0.08) and the difference in DBP between stress and rest (p=0.08). Scatterplots with a line of best fit are displayed for these two parameters in figures 4.93 and 4.94.

Table 4.28 - Pearson's correlation coefficient and p value for various measured haemodynamic parameters compared to mean caffeine levels (mg/l) during MRMPI scanning.

Haemodynamic Parameter	Correlation Coefficient (r)	P Value
Resting Heart Rate	-0.28	0.16
Stress Heart Rate	-0.12	0.55
Resting Systolic BP	0.35	0.08
Stress Systolic BP	0.26	0.18
Rest Diastolic BP	0.028	0.89
Stress Diastolic BP	0.23	0.24
Heart Rate Difference	0.14	0.49
Systolic BP Difference	-0.08	0.68
Diastolic BP Difference	0.34	0.08

Figure 4.93 - Scatterplot of resting systolic BP (mmHg) and mean caffeine levels (mg/l) with corresponding line of best fit equating to r=0.35.

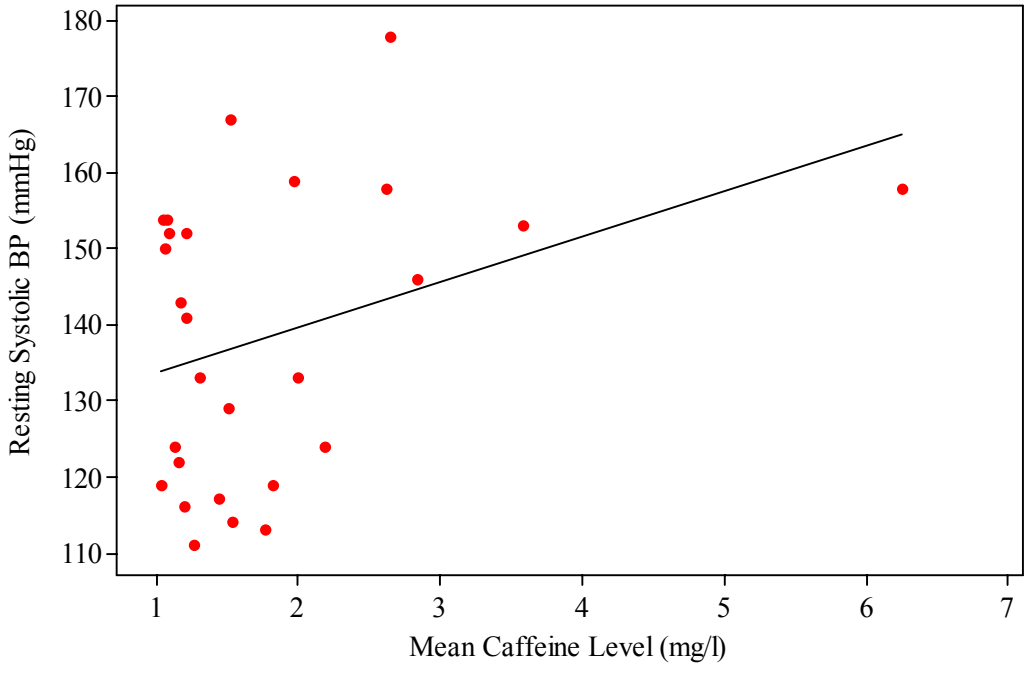

Figure 4.94 - Scatterplot of difference in stress and rest diastolic BP (mmHg) and mean caffeine levels (mg/l) with corresponding line of best fit equating to r=0.34.

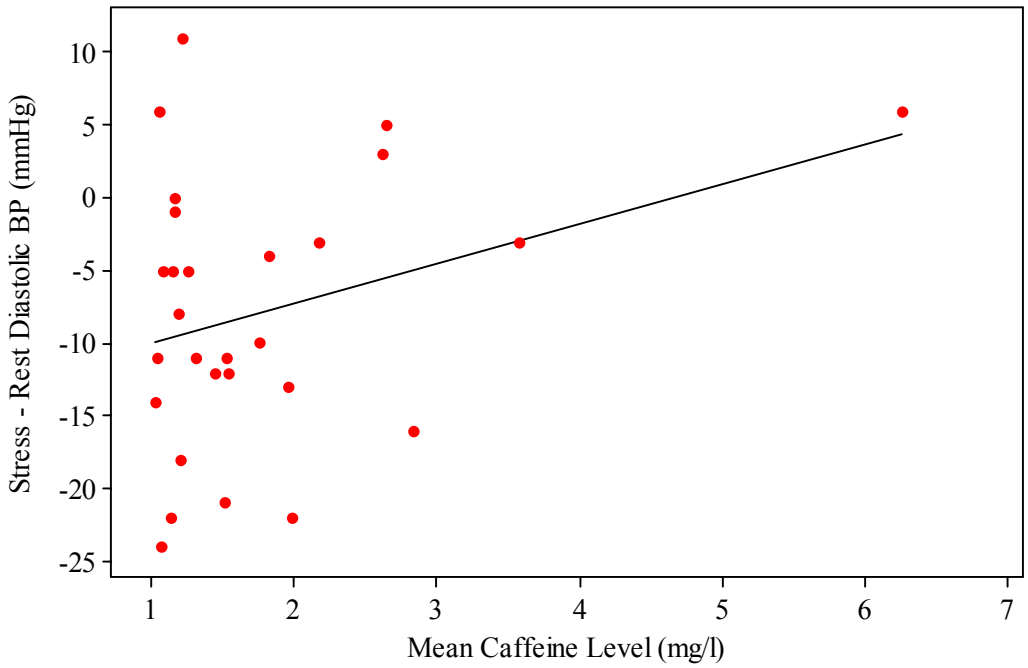

Another indicator of the effectiveness of pharmacological stress is the development of symptoms during the adenosine infusion. We compared the incidence of each of the common symptoms experienced. Chest pain was experienced in 13 (45%) of the 29 patients with detectable caffeine compared to 106 (54%) of the 196 patients with caffeine levels <1mg/l. This difference was not significant with p=0.35 using the chi-square test. Shortness of breath occurred in 20 (69%) patients with detectable caffeine compared to 142 (72%) without detectable caffeine (p=0.69). Flushing was encountered in 10 (34%) patients with detectable caffeine compared to 110 (56%) of those without. This difference was statistically significant with p=0.03. Headache occurred in 4 (14%) of those patients with detectable caffeine compared to 37 (19%) of those patients without (p=0.51). One patient (3%) in the caffeine group complained of abdominal pain compared to 15 (8%) without detectable caffeine (p=0.41). Taking both groups of patients collectively 4 (14%) patients in the caffeine group failed to experience any symptoms during the adenosine infusion compared to 11 (6%) in the group with

undetectable caffeine. The p value was 0.09 indicating a trend towards more symptoms in patients with lower caffeine levels however this does not quite reach statistical significance.

5 Discussion

5.1 Patient Characteristics

The patients recruited into the study demonstrated the typical risk factor profile that predisposes to coronary artery disease. The majority of our patients were male (74%) with a high body mass index. Hypercholesterolaemia was the most prevalent risk factor for coronary artery disease affecting 79% of our patients. Hypertension was also very common in our group, which is also of high prevalence in the West of Scotland. There were more ex-smokers than smokers in our study (40% vs 17%) which we hope will be a continuing trend in Scotland since smoking was banned in public places in March 2006. Certainly the number of admissions in Scotland with an acute coronary syndrome fell after the implementation of this.(127) Just over half (51%) of our patients also had a family history of premature ischaemic heart disease which highlights the genetic predisposition to this common disease. Two patients undergoing renal dialysis therapy for chronic kidney disease were recruited into the study before we knew of the concerns regarding nephrogenic systemic fibrosis (NSF). This condition carries a 30% risk of mortality and is thought to be due to free gadolinium ions separating from its chelation compound in uraemic patients and entering the extracellular space where fibrillogenesis is accelerated.(110;112;114) Gadolinium appears to stimulate a fibroblast reaction which can be found in skin biopsies and can lead to progressive thickening of the skin. The majority of cases that have been reported appear to been associated with the gadodiamide preparation of gadolinium (Omniscan, GE Healthcare) which was used in the current study.(111) It is now advised not to give gadolinium to patients with a glomerular filtration rate of less than 30ml/min/1.73m^2.(113) Twenty-four (23%) patients had experienced a previous MI and only a small number of patients had

evidence of vascular disease elsewhere with 2 patients having had a previous stroke and 2 patients with known peripheral vascular disease.

Interestingly, at the time of referral to the cardiology clinic almost all of the patients were taking aspirin, a beta blocker and a statin (almost 90%). Twenty-four of these patients would have been on these medications following their previous MI however the rest would have been commenced by the referring cardiologist or their general practitioner. Forty-four percent of patients had already been commenced on clopidogrel in anticipation of them requiring PCI or having had an acute coronary syndrome in the preceding 3 months. As far as antianginal therapy was concerned nicorandil and calcium channel blockers were slightly more popular than stand-alone nitrate preparations.9 (34% vs 30%). Angiotensin converting enzyme inhibitors and angiotensin receptor blockers had been prescribed in 55% of patients, probably as a result of the high prevalence of hypertension and previous MI.

5.2 Patient Outcome

As we had anticipated in our power calculation, the majority of patients (57) ended up having PCI as their method of revascularisation and only 15 patients had CABG. None of the 101 patients died during the study period. The PCI patients had significant improvements in FFR, CFR, Qcorr, resting Pd/Pa and a significant reduction in the uncorrected IMR. The mean post-PCI FFR was 0.90 which was our target value following intervention and has been shown to be associated with excellent outcomes in a large multicenter study.(56) All CABG patients received at least one arterial graft. Only 3 CABG patients had no post-operative complications however all but one attended for follow-up imaging. This showed significant reductions in the number of

hypoperfused coronary segments in both groups of patients with a non-significant trend towards fewer segments in the PCI group.

5.3 Magnetic Resonance Myocardial Perfusion Imaging v FFR and Quantitative Coronary Angiography

Several previous studies have assessed the ability of MRMPI to detect reversible myocardial ischaemia though this study is the largest to date. The majority chose to use quantitative coronary angiography as the gold standard for calculation of sensitivity and specificity.(13;15;17-25) Some used nuclear perfusion methods such as SPECT and PET.(11;12;14;16) We have compared MRMPI to a combined invasive gold standard of FFR and CFR. The most important finding in this study is the excellent sensitivity and specificity, and positive and negative predictive values of MRMPI when compared to our gold standard and to prior studies utilising MRMPI.(11-25) No previous study has employed both FFR and CFR together. Our findings suggest that the diagnostic utility of MRMPI has perhaps been underestimated. Of the 4 previous studies comparing MRMPI and FFR alone, two present the same data and the number of patients in these studies was small (n=43, 37 & 30) .(30;31;33;35) In the study by Rieber et al, the FFR was only measured in 1/3 of coronary territories.(30) Upslope derived MPRI was used to assess the accuracy of MRMPI with similar sensitivity and specificity values to our own of 88% and 90% respectively. The study by Costa et al, also reported by Futamatsu et al chose to use a fully quantitative method of measuring myocardial perfusion reserve (MPR) with the Fermi method and deconvolution.(31;33) These studies however only compared MPR and FFR in 44 segments equating to 40% of coronary territories. The sensitivity was good at 93% however the specificity was 57% with wide 95% confidence intervals. Kühl et al had chosen a similar method of analysis to Rieber et al where upslope derived MPR was calculated.(35) Similarly this study failed to measure

FFR in all coronary arteries with only 31% of potential measurements being made. This study found an excellent sensitivity and specificity at 92% which is similar to the findings of Rieber et al.

It is not surprising that MRMPI is superior to other non-invasive methods such as SPECT and stress echocardiography in that it provides superior spatial and temporal resolution over the nuclear perfusion methods and is not limited by imaging plane or inadequate ultrasonic windows. Our study highlights the well known limitations of using quantitative coronary angiography to assess the functional significance of coronary arterial disease.(2;3) The sensitivity and negative predictive values of QCA are excellent but the specificity and positive predictive values are poor. Our study also highlights the importance of ensuring that patients have demonstrated an adequate haemodynamic response to the vasodilating agent, in this case adenosine, before reporting a negative study. Even with a recommended 24 hours of abstention from caffeine we still observed that around 5% of patients failed to respond to adenosine. This aspect of perfusion imaging will be discussed later in the discussion.

The majority of centres use visual analysis for the assessment of myocardial perfusion scans (Table 1.2). Comparing the rest and stress scans together on a viewing platform enables recognition of perfusion defects and discrimination from artefacts.(43) As visual analysis remains the main method of assessing MRMPI clinically, we used this method in our study but also subjected the data to exhaustive further analysis using 3 different semi-automatic quantitative methods of measuring regional myocardial perfusion reserve index (MPRI).(22) The argument remains that patients with triple vessel disease and balanced hypoperfusion throughout the mycocardium would be missed by a purely visual based assessment. Nine patients in the present study had

proven functionally significant triple vessel disease by FFR assessment. In 3/9 visual analysis of the MRMPI scans correctly diagnosed hypoperfusion in all 3 vessel territories; in 4/9 patients 2 hypoperfused territories were diagnosed. In one patient hypoperfusion was diagnosed in one vessel and in one patient the MRMPI scan was interpreted as being normal. Interestingly these latter two patients were both non-responders to adenosine and inadequate pharmacological stress is likely to have contributed to the diagnostic error. Both of our blinded observers had been independently reporting the results of clinical and research MRMPI scans for at least 2 years prior to performing the analysis for this study. On a per patient basis the observers had excellent agreement and by individual coronary perfusion territories agreement was substantial. Experience and knowledge of potential artefacts is critical to the accurate visual analysis of MRMPI scans as the commonly encountered artefacts with rapid image acquisition usually manifest themselves as dark subendocardial rims and may mimic perfusion defects especially in the interventricular septum and lateral wall.(43)

Using pressure wire derived FFR has a number of advantages in the evaluation of a non-invasive technique for the detection of physiologically significant coronary artery disease. It can reliably identify a flow limiting stenosis in an epicardial coronary artery and has been previously validated against what is probably the current gold standard, namely PET.(36) It is independent of heart rate, blood pressure and contractility, and takes into account the contribution of collateral flow to myocardial perfusion.(37) An FFR value <0.75 confirms that the stenosis being interrogated has the potential to induce ischaemia at maximal hyperaemia.(38;39) Most of the published studies describing the predictive accuracy of FFR measurements have been in the setting of stable angina but the technique has been validated in the setting of unstable angina and recent (>5 days) MI.(52;56;128) The majority of our patients had stable angina however

25% had experienced recent unstable symptoms and 23% had a previous MI. There is unpredictable variability in all biological measurements and so any cut-off value cannot be expected to have absolute precision. Increasing the FFR cut-off to 0.8 led to a reduction in the number of false positive territories at the expense of a large increase in the number of false negative territories. A thermodilution derived CFR<2.5 used alone as a gold standard was associated with a large number of false negative results. This may be in part due to a high cut-off value. We chose a CFR <2.5 based on previous Doppler derived CFR studies however the thermodilution technique did produce higher values in a recent comparative study.(60) Thermodilution measurements have more potential than FFR for error. It can be difficult to establish a consistent baseline transit time, especially at rest. A number of technical factors can affect these recordings especially guide catheter engagement which if altered between measurements can produce large differences in transit times. Interestingly 60% of false positive scans had a low CFR raising the possibility that microvascular disease may have contributed to their perfusion defects on MRMPI. Eighty percent of these scans however had FFR values in the grey zone of 0.75-0.8 and may in fact have been true positive results.

There are some important limitations of the current study. FFR was only measured in 81% of major epicardial coronary arteries. Not all occluded vessels were crossed with the pressure wire and often when occlusions were crossed, other types of wire which are more suited for this purpose were used. However we inserted an FFR value of 0.40 in totally occluded arteries not crossed with the pressure wire and this increased the proportion of epicardial vessel FFR data points to 92%. The number of non-occluded lesions not crossed is documented in the results section and this was mainly because it was felt unacceptable to expose the patient to the risk of crossing an angiographically

severe lesion when their overall pattern of disease required surgical rather than percutaneous revascularisation.

Despite the excellent results of MRMPI for the accurate detection of physiologically significant coronary artery disease there are also some important limitations of this technique. Claustrophobia remains problematic with the majority of commercially available scanners, however new open or wide bore scanners are in development. Some patients have contraindications to adenosine such as asthmatics and patients with high degrees of AV block. Exercise within the magnetic field of the scanner is becoming a possibility with specially adapted non-ferromagnetic exercise bicycles and open scanners.(129;130) Another limitation of this work is that in any given patient we cannot be certain that we have correctly assigned all myocardial segments to the appropriate coronary artery. For example in a patient with a co-dominant circulation it can be difficult to know which vessel provides the majority of the blood supply to the inferior wall. Another area of difficulty is when the left anterior descending coronary artery wraps around the apex of the heart and supplies a substantial proportion of the inferior wall. According to the AHA coronary artery territory model this apical inferior wall is supplied by the right coronary artery.(10) If the right coronary artery was normal in this circumstance and there was an inferior perfusion defect as a result of a stenosis in the left anterior descending coronary artery then, in terms of localisation of ischaemia this would be classed as a false positive.

We chose to repeat the MRMPI scan at 4 weeks post-PCI and post-CABG in order to compare the success of revascularisation by these two methods at the same point in time. We were interested to see if patients having undergone PCI would have a return to

normal perfusion within 24 hours of revascularisation or if there was a lag period following distal embolisation of plaque debris. Four weeks was felt to be an optimal time as patient's post-CABG would have recovered from their surgery and we felt that all patients would be more likely to attend earlier rather than later after revascularisation provided this had been successful. The disadvantages of scanning at this time are that we may not have assessed the maximal improvement in LV systolic function following CABG by this stage where waiting until 6 months had elapsed would have been best. In addition patients are unlikely to develop problems within 4 weeks and waiting till a later date would have been advantageous to those patients who experienced a return of symptoms.

5.4 MRMPI and Pressure Wire in the Detection of Microcirculatory Disease

One of the aims of the present study was to determine if false positive MRMPI scans were due to microvascular coronary disease as assessed by CFR and the index of microcirculatory resistance (IMR). Or in other words assess if a qualitative assessment of MRMPI was able to diagnose isolated microcirulatory dysfunction in arteries with normal epicardial function. We defined arteries as having isolated microcirculatory dysfunction when the FFR was >0.8 and the CFR<2.5. Twelve arteries had to be excluded from this analysis due to late gadolinium enhancement in the downstream myocardium. Of the remaining 55 arteries only one corresponding territory had evidence of a perfusion defect therefore confirming that qualitative analysis of MRMPI scans cannot be used to diagnose isolated microcirculatory disease as defined by these pressure wire criteria. We then looked at 28 identified arteries with an FFR>0.8 and CFR<2.0 and no LGE on MRI which would have a greater likelihood of microvascular disease. No visually identified perfusion defects were found suggesting again that

qualitative assessment of MRMPI is unable to identify isolated microvascular disease. Microcirculatory dysfunction has been proposed as a cause of cardiac syndrome X.(131;132) In this condition patients complain of typical anginal sounding pain with an ischaemic ETT however normal epicardial coronary arteries at angiography. It has been shown that semiquantification of MRMPI using the myocardial perfusion reserve index (MPRI) can be used to identify subendocardial hypoperfusion compared to the subepicardium in patients with cardiac syndrome X.(133) In the present study we calculated the subendocardial MPRI for comparison with FFR in the diagnosis of ischaemia. Our Fermi deconvolution derived MPRI results for 26 coronary territories with an FFR>0.8 and CFR<2.0 found a mean of 2.2 which is less than the cut-off proposed in our FFR comparison of 2.41. We didn't draw regions of interest in the subepicardium for comparison with the subendocardium as this was beyond the scope of this study and would have added greatly to the time of the analysis of these scans. One limitation of using CFR for the identification of microvascular disease in the presence of a normal FFR is the variation that is encountered when measuring this parameter. It can be very difficult to obtain 3 identical thermodilution curves at rest which is the downside to this method.

We had 11 false positive coronary territories with hypoperfusion on MRMPI however an FFR≥0.75. On closer examination of these territories, 8 (73%) were likely to be true positives as their corresponding FFR was in the grey zone between 0.75 and 0.8. It is generally accepted that no biological measurement has an exact cut-off value representing normality and some centres now use 0.8 as their cut-off as has been used in the recent FAME study which reported its findings at the Trans-Catheter Therapeutics (TCT) Conference in Washington.(126)

As documented in the results section, a CFR measurement of less than 1 was encountered in 26 arteries. This suggests that during coronary vasodilation with adenosine, coronary flow is less than that encountered at rest thereby producing a result of less than one. A potential biological reason for this could be the coronary steal phenomenon whereby coronary blood flow falls in one collateralised coronary region in favour of another region.(134) In other words, the blood supply to a region of myocardium is diverted to an adjacent area which leads to hypoperfusion of the original region of myocardium.

5.5 Myocardial Perfusion Reserve Index (MPRI)

In addition to the visual analysis of the MRMPI scans, we also undertook a semi-quantitative analysis looking at the myocardial perfusion reserve index (MPRI) Absolute quantification of myocardial blood flow was not possible at the dose of gadolinium we used in this study. At a dose of 0.1mmol/kg gadolinium kinetics are non-linear with myocardial blood flow. Other studies have attempted quantification however these studies have chosen lower gadolinium doses.(31) We chose a 0.1mmol/kg dose of gadolinium as this was felt using the turboFLASH pulse sequence to give the best images for qualitative assessment, which was the primary measure of the study. In Glasgow we had a lot of experience of using this dose prior to commencing the study and were familiar with the dark rim artefacts encountered which is the main disadvantage of its use. We were still able to semi-quantitatively measure MPRI however were unable to perform absolute flow quantitation as explained above. Using 0.1mmol/kg also allowed us to perform our LGE imaging after the stress first pass images and therefore keep the total scan duration down and improve patient tolerability. The MPRI gives a semi-quantitative measure of coronary flow and can be assessed for

each of the coronary segments as defined in the AHA model.(10). There are some advantages in having a measure of perfusion rather than just eye-balling the scans for areas of hypoperfusion. As mentioned above there is a concern that in patients with triple vessel coronary artery disease balanced hypoperfusion may be missed by perfusion imaging techniques. Visual assessment relies on at least one area of the heart to appear normally perfused in order to distinguish areas of hypoperfusion. In clinical practice we have not found this to be much of an issue. In theory however, if all myocardial territories were to be hypoperfused to a similar extent then a semi-quantitative method such as measuring the MPRI should identify this. Calculating the MPRI has also allowed us to generate receiver operator curves (ROC) which are useful in determining the clinical utility of MRMPI. The disadvantage of this approach is primarily the length of time it takes to analyse one scan. This can take up to 30 minutes each, depending on the amount of motion artefact caused by patient breathing during the scan. Having each of the 50 images per first pass of gadolinium accurately spatially aligned such that the myocardial segments are exactly on top of one another is essential for the generation of signal intensity/time curves. From these curves we calculate MPRI values. The drawing of regions of interest involves drawing endocardial and epicardial lines between which we measure the signal intensity. At the time of this study and probably still now there is no perfect software package which can perform this task without error. We collaborated with Dr Murdoch Norton, physicist at Aberdeen Royal Infirmary, who has designed a programme which can calculate MPRI and this was modified for our purposes in this study. Nevertheless the analysis remained time-consuming. Some patients had great difficulty holding their breath, normally because they were very symptomatic during the adenosine infusion. There were also some patients who did not achieve an especially high heart rate during the infusion and therefore had to endure a longer breath hold. In these patients even our image

registration software could not cope with large movements of the heart. When each image per slice has to be aligned manually this increases time of analysis. In these cases it can take well over an hour to complete the analysis of one scan. Despite the time involved, myself and Dr Norton, the second observer analysed each of the MRI scans performed in this study. As documented in the results section, some of the scans had to be excluded form the analysis due to artefacts, including breathing artefact. Some scans had to be excluded where the most basal slice was too close to the left ventricular outflow tract. This caused the anterior and anteroseptal segments in the basal slice to have the same signal intensity/time curve as the AIF (LV blood pool). This led to MPRI values that were exceptionally high. In addition, if there were inaccuracies in determining the region of interest and it included epicardial fat, this would also lead to a very high MPRI value. Despite problems with the semiquantitative analysis in these patients both observers were still able to assess these scans qualitatively. Another consideration we had to make was determining any areas of dark rim artefact usually caused by susceptibility. This artefact usually occurs septally and laterally at the interface between myocardium and the LV blood pool and can mimic perfusion defects. Both observers were experienced in the analysis of MRMPI scans and visualised both the stress and rest scans before drawing the regions of interest. Generally where a dark rim occurs in both scans which is not an area of MI we took it to represent artefact, and therefore avoided this area. The dose of gadolinium we chose for our analysis was good for the analysis of scans visually and by upslope parameters however it does lead to more susceptibility artefact.(22;23) If areas of susceptibility artefact were included in the analysis this would give a false positive result with an artificially low MPRI.

We chose three of the most commonly used methods to assess MPRI, namely the Fermi method with deconvolution, maximum signal, and upslope gradient. In our analysis we

examined the lowest MPRI per coronary territory, and also the mean MPRI per coronary territory. As we only had 3 short axis slices and therefore only 16 segments of the 17 segment AHA model, we took the mean of the 6 left anterior descending artery segments, and the 5 left circumflex and 5 right coronary artery segments. In the final analysis a mean value was obtained from the 2 observers to improve the accuracy of our results. A greater difference in results between observers is noted with this type of analysis and probably reflects differences in selection of regions of interest. Observers also had to select the points of the curves for determination of the upslope gradient, and also the points of the maximum signal, which may introduce a degree of error. The calculation of the Fermi deconvolution derived MPRI was more of an automated process performed by the computer programme. The majority of differences between observers with any of the methods of assessing MPRI were around 0, however on some occasions observers have discrepancies of a MPRI of around 3. We chose to look at the lowest MPRI value in addition to the mean MPRI per coronary territory as we were concerned that a small perfusion defect with a low MPRI in one or two segments could be diluted with normal or high MPRI values in the other segments. Although we followed the AHA model for our analysis, it is generally accepted that there is individual variation in which arteries supply which coronary segments. One concern of ours was the blood supply to the inferior wall in the apical and mid ventricular slices. This would be supplied by the RCA in the majority of cases however there are patients in whom the left anterior descending coronary artery wraps around the LV apex to supply a substantial proportion of the inferior surface of the heart. Therefore patients with a severe stenosis in an LAD would have an inferior perfusion defect leading to inaccurate results. Similarly, we also found a number of patients in whom the basal inferior septum was supplied by the LAD as opposed to the RCA, as defined in the AHA model.(10) This problem may have lead to some inaccuracies in our

measurements. Our results show that the difference between observers generally exhibits a normal distribution, with the majority of differences being zero, which is reassuring. This was the same for each of the 3 methods of measuring MPRI using either the mean MPRI or the lowest MPRI per coronary territory. We then went on to compare MPRI with FFR, which was our gold standard invasive test. Each of the methods of assessing MPRI had a good correlation with FFR however this was consistently better when the lowest MPRI value was taken, as opposed to the mean value per coronary artery territory. This most likely reflects the dilution of results and overlapping coronary artery territories, as discussed above. The second best invasive pressure wire measurement to correlate with MPRI was CFR. This was not surprising as CFR takes into account both the flow within the epicardial coronary artery and also the microcirculation. Interestingly when we compared the uncorrected and corrected indices of microcirculatory resistance (IMR) the results were somewhat surprising. Unfortunately we do not have any literature to make any comparisons to in this field. With increasing degrees of IMR (uncorrected) there was a negative Pearson's correlation coefficient when compared with MPRI which would be expected as low microcirculatory resistance would lead to a greater measured MPRI. The degree of correlation was not strong, however was greatest with maximum signal derived MPRI where the Pearson's correlation coefficient was -0.29 for the mean MPRI per coronary territory and -0.27 for the lowest MPRI per coronary territory. A positive correlation was found between MPRI and corrected IMR for each of the methods. This was mainly a weakly positive correlation however was 0.32 for mean MPRI and 0.27 for lowest MPRI when assessed by upslope gradient. The difference between these 2 methods of assessing IMR is that we have taken the contribution to myocardial flow from collateral vessels into the equation. The number of results we have where a coronary artery wedge

pressure has been recorded was small compared to the other invasive parameters and perhaps this is a spurious result as we would expect an inverse relationship here.

All of our ROC curves showed that the lowest MPRI value per coronary artery territory was better than the mean MPRI value for each of the 3 methods used in assessing if an area was hypoperfused when using FFR as the gold standard. Our sensitivity and specificity results were slightly inferior to those produced in the two previously published comparisons with FFR. Using Fermi deconvolution derived MPRI and taking a MPRI cut-off of 1.7 and FFR<0.75 we obtained a sensitivity of 90% and specificity of 48%. Costa et al using an MPRI cut-off of 2.04 and the same FFR cut-off obtained a sensitivity of 92.9% and specificity of 56.7% with wide 95% confidence intervals.(33) Given that the authors of this study claim this is an absolute quantification of myocardial perfusion reserve and has been validated with radiolabelled microspheres then overall our method has not performed too badly.(46) Our sensitivities and specificities were also slightly lower than that achieved by Rieber et al who using a MPRI cut-off of 1.5 had a sensitivity of 88% and specificity of 90%.(30) Our study was never designed to be a comparison with MPRI. We set out to compare the most widely used method of assessing MRMPI scans in clinical practice which is qualitative visual analysis. When this is performed our results are better than that obtained by MPRI with a sensitivity and specificity of 91% and 94% respectively. It is perhaps not surprising that the MPRI results do not match this as the dose of gadolinium we chose was double that used in the previous MPRI studies for the reasons explained above (table 1.3).

The measurement of MPRI proved to be useful when assessing the success of coronary revascularisation. When using the lowest and the mean MPRI per coronary territory and

the total mean MPRI for all 16 segments per heart we found a significant increase in MPRI from pre-revascularisation to 24 hours post-revascularisation in the PCI group. There was also a significant increase in MPRI between the pre-revascularisation and 4 weeks post revascularisation in both the PCI and CABG groups. Interestingly there was no significant increase in MPRI between the 24 hours post-PCI and 4 weeks post-PCI MRMPI scan indicating that the majority of the benefit in coronary perfusion occurs within 24 hours of revascularisation. PCI was shown to result in a significantly better mean MPRI per coronary territory when compared with CABG (2.42 v. 2.1, p=0.019). In addition there was a trend towards a higher lowest MPRI values per coronary territory and total mean MPRI per heart in the PCI group. This result was surprising as CABG would be expected to result in a higher proportion of patients receiving complete revascularisation. In terms of the increase in mean MPRI per coronary territory there was a trend towards a greater increase in the PCI patients when compared to CABG.

5.6 Left Ventricular Function, Mass and Volume Analysis

The majority of previous studies looking at magnetic resonance myocardial perfusion imaging (MRMPI) did not provide information on the ejection fractions of the patients involved in their studies.(11-13;15;17;21;22;24;25;27;31;32;34) Compared to those studies which did include an MRI derived LVEF our study, with a mean LV ejection fraction of 67.7% with a standard deviation of 7.4% was at the higher end of the spectrum. The only study with a higher ejection fraction was Schwitter et al, 2001, where ejection fraction was 73% with a standard deviation of 4% however this was in patients with no coronary disease.(14) Interestingly their patients with coronary disease had an ejection fraction of 67% (S.D = 7%) which is almost exactly the same as in our patients. Cury et al 2006 had the lowest mean ejection fraction at 54.8% (S.D = 8.2%).

Two thirds of their patients had significant coronary artery disease as per coronary angiographic appearances and in our study 80% of patients had proven significant coronary disease. We therefore cannot put the difference in ejection fraction down to the severity of coronary artery disease. In each of the studies differing software packages had been used to analyse left ventricular volumes and ejection fractions and this may have contributed to a difference. Those studies who have recorded a mean ejection fraction have their data presented on table 5.1, including those already mentioned in this section.

Table 5.1 - Ejection fractions of patients who participated in previous first pass perfusion MRI studies.

Author	**Year**	**Patients**	**Ejection Fraction (%)**	**Standard Deviation (%)**
Schwitter J(14)	2001	66 (incl. 18 volunteers)	67 (CAD) 73 (no CAD)	7 4
Ibrahim T(16)	2002	59 (incl. 34 volunteers)	64	13.5
Ishida N(18)	2003	104	61.2	9.15
Paetsch I(20)	2004	79	58	6
Klem I(28)	2006	92	56	13
Cury RC(29)	2006	46	54.8	8.2
Costa MA(33)	2007	37	57	13
Rieber J(30)	2006	43	58	9

Interobserver variability was assessed for each of the parameters measured using Argus dynamic signal. Both observers were experienced in measuring myocardial mass, LV

ejection fraction, end diastolic and end systolic volumes.Differences in LV ejection fraction and myocardial mass between observers followed a normal distribution. Interestingly when we assessed differences in left ventricular end diastolic volume and left ventricular end systolic volume observer 1 had a tendency to higher values than that of observer 2. Variations in left ventricular volumes are usually due to differences in determining which slice represents the most basal segment that is taken into account when calculating volume. The majority of centres practise on the principle that if there is a circumference of myocardium greater than 50% then this should be included in the volume analysis. Some software packages have incorporated a tracking system for the mitral valve plane in order to determine the location of the most basal slice for more accurate measurements of left ventricular function and volumes. (CMR tools, Imperial College London).(135) This helps to ensure that left atrial volume is not included in the left ventricular volume. Another reason for differences in calculated volumes is due to partial volume of myocardium. In this circumstance where myocardium is not fully within the slice it can appear as being less dense or a lighter shade than other myocardium. There are different opinions on how much of this myocardium should be counted in the analysis and this becomes more difficult as you get towards the apex of the left ventricle where there are more trabeculations and more partial volume effects.

Analysis of the ejection fractions of our patients prior to coronary angiography when divided into their subsequent groups (normal, PCI, CABG, medical therapy) revealed no significant difference as shown on figure 4.54. PCI was associated with a significant increase in the LVEF at 24 hours post-PCI compared to the pre-PCI scan. These data were highly significant and are demonstrated in figure 4.55 and also on table 4.19. Interestingly there was a non-significant drop in ejection fraction between the 24 hour post PCI scan and the 4 week post PCI scan. It is difficult to know why this is, as

restenosis would be unlikely within 4 weeks and none of our patients complained of any significant chest pain when they attended for the scan. If anything one would have expected the same or a slightly better ejection fraction at 24 hours as the pre-PCI scan as hibernation may persist for some time in chronically ischaemic myocardium prior to an improvement in LV ejection fraction. We would have expected the 4 week scan to be better than the 24 hour scan. However when the pre PCI scan was compared with the 4 weeks post PCI scan there is still a non-significant increase. A recent study published in the European Heart Journal examined the time course of functional recovery of hibernating myocardium using contrast enhanced cardiac MRI.(136) This study included 35 patients who had contrast enhanced cardiac MRI performed 1 month prior to revacularisation and at 3, 6, and 24 ± 12 months post revascularisation. Of the 35 patients 25 (71%) were revascularised by CABG and 10 (29%) had PCI performed. Seven patients had a previous CABG and 3 had previous PCI prior to being recruited into the study. The cardiac MRI scans were analysed for LV ejection fraction and segmental hyperhancement by calculating the area of hyperenhancement within the myocardial segments. LV function improved at each of follow-up time points however only reached statistical significance at 6 months ($p=0.036$). Segmental functional improvement was inversely related to the segmental hyperenhancement as expected. By the end of the study period 93% of segments with no hyperenhancement demonstrated functional improvement compared to 70% of segments with 1-25% segment hyperenhancement, 66% with 26-50% segment hyperenhancement, 36% with 51-75% and 5% with 75-100%. The time course for this recovery was protracted with less than half (45%) of all segments which eventually improved showing some improvement by 3 months. The time course of recovery was significantly more delayed in segments with more hyperenhancement at baseline ($p<0.001$). Therefore the study concluded that the time course and likelihood of function recovery was dependent on the amount of

myocardial scar. (136) Prior to this study Zellweger et al published in 2004 a study of 38 patients who underwent myocardial perfusion SPECT 17 ± 22 days prior to and 177 ± 54 days post PCI. Eighty-two percent of patients had single vessel PCI performed and the remaining 18% had ≥2 vessel PCI. This resulted in a huge reduction in the symptoms of angina from 84% of patients to 5% ($p<0.001$). Despite a significant reduction in the signs of ischaemia by stress ECG and myocardial perfusion SPECT ($p<0.001$) there was no significant change in LV ejection fraction as defined by SPECT (55 ± 10% vs 57 ± 13% at 6 months) however there were significant reductions in LV end diastolic volume and end systolic volume ($p=0.006$ and 0.001 respectively) indicating a positive effect on LV remodelling.(137) These results show no significant improvement in LV ejection fraction whereas we found quite a significant increase. This study however used SPECT as opposed to cardiac MRI for the evaluation of left ventricular function which is known to be less accurate. Cardiac MRI is now widely regarded as the reference standard for evaluating cardiac function due to its excellent temporal and spatial resolution.(138-140) In addition a proportion of patients in this study were not completely revascularised with 26% having double vessel coronary disease and 5% with triple vessel disease whereas only 18% got ≥2 vessel PCI performed, leaving 13% of vessels without revascularisation. In our study there were 7 CTOs which were not opened. Two of these were small non-dominant vessels and not even attempted. Therefore in our study our percentage of vessels not revasularised was half of that in the study by Zellweger et al at 6%. This may also help account for the significant increase in LV ejection fraction post-PCI that we found in our study.

A more recent study of 50 patients from Oxford used cardiac MRI to evaluate left ventricular function pre and post-PCI.(105) This study also correlated post-PCI troponin elevations with new late gadolinium enhancement and has already been discussed in the

introduction section. As well as performing late gadolinium enhancement imaging, cine MRI sequences were also performed to evaluate left ventricular function. The pre-PCI LV ejection fraction was 67 ± 11% compared to 68 ± 11% post-PCI (p=0.8). In patients with no new late gadolinium enhancement there was no significant change (p=0.8) in LV ejection fraction (69 ± 12% vs 71 ± 11%). In addition there was no significant change (p=0.9) in those patients with new late gadolinium enhancement (65 ± 8% vs 64 ± 11%). Unfortunately this study does not specify if these ejection fraction values were at 24 hours or 7 to 8 months post-PCI. The pattern of coronary artery disease was different between our two studies in that 70% of our PCI patients had single vessel PCI, 26% had two vessel PCI and 4% had triple vessel PCI compared to 56% with single vessel PCI and 44% with 2 vessel PCI in the Selvanayagam study. However you would therefore expect the study with the more severe disease to gain the largest benefits in LVEF post-PCI. Our study does however include a complete physiological assessment of the severity of coronary artery disease whereas in the Oxford study coronary disease severity was assessed by visual assessment. This does raise the possibility that some lesions may have been revascularised inappropriately in which case no improvement in LV ejection fraction would be expected (105)

CABG in our study made no significant impact on ejection fraction at 4 weeks however, our bypass group was significantly smaller than our group of patients who underwent PCI. Perhaps we have scanned our CABG patients too early to detect a significant change in LV ejection fraction as in the Bondarenko study, which included a majority of CABG patients and only found a statistically significant increase in LV ejection fraction at 6 months post revascularisation.(136) All of our CABG patients had good LVEF to begin with and therefore perhaps not much improvement could have been expected (Figure 4.56). Improvements in left ventricular function in patients with markedly

impaired left ventricular function have been reported in various studies. A study of 75 patients with moderate to severely impaired LV dysfunction was reported this year (2008).(141) Left ventricular function as assessed by echocardiography improved from 0.32 ± 0.06 to 0.46 ± 0.02 which was a significant improvement ($p<0.001$). Selevanayagam et al published a study in 2004 comparing the effects of off and on-pump CABG in 60 patients (30 randomised to each arm).(142) Cardiac MRI examination was performed prior to CABG and a median follow-up of 6 days post surgery. The baseline ejection fraction for both groups was 62 ± 12%. Post-operatively this dropped to 59 ± 11% in the on-pump CABG group and increased to 65 ± 12% in the off-pump CABG group. The absolute difference between the surgical groups was significant ($p=0.03$) however the overall difference between pre and post-CABG ejection fractions was not significant. The study concluded that off-pump CABG led to significantly better LV function early after surgery. On-pump CABG can cause periods of ischaemia during aortic cross-clamping which can lead to myocardial damage. All of our patients had on-pump CABG with good pre-operative LV ejection fractions as was the case in this study, therefore our results are very similar. It is interesting that the less invasive approach led to a good early improvement in LV ejection fraction as was the case in our own PCI group who had a significant improvement at 24 hours compared to baseline. In this study by Selevanayagam et al troponin levels were also recorded as was the occurrence of new late gadolinium enhancement. Analysis of this data showed that the area-under-the-curve values for troponin were significantly higher in the on-pump CABG group. There was however no statistically significant difference in the amount of new late gadolinium enhancement post-CABG with 6.3 ± 3.6g in the on-pump group compared to 6.8 ± 4g in the off-pump group. Therefore despite an improvement in LV function in the off-pump group there was no reduction in the amount of late gadolinium enhancement and therefore no reduction in scar formation as a result of CABG. This is

despite a lower troponin release in this group.(142) Interestingly the same group from Oxford studied the effects of on and off-pump CABG on early and late right ventricular function. This study found an early reduction in RV function as measured by cardiac MRI in both groups which had recovered by 6 months.(143) RV function was not assessed as part of the present study. We also compared left ventricular end-systolic and end-diastolic volumes at 4 weeks post-CABG and PCI to see if there was any difference in remodelling however no statistically significant difference was found (Table 4.21).

Those patients who were found to have significant coronary disease with no revascularisation options and were treated with medical therapy also had no significant change in their LVEF. However it must be noted that this group was exceptionally small with only 5 patients returning for the repeat MRI scan at 3 months.

5.7 Post-PCI Troponin Levels

Fifty-three (93%) patients had troponin measurements pre and post PCI. The majority of troponin levels were less than 6µg/L however one patient had a substantial post-PCI infarction due to side vessel occlusion resulting in a troponin level of 13.1µg/L. Other than this patient all the other patients were discharged on the day following PCI. The median troponin release post-PCI was 0.57µg/L and the mean was1.18µg/L. This is substantially less than that found in the Selevanayagam study of 50 PCI patients where the mean post-procedure troponin was 3.7 ± 3.0µg/L.(105) Their study measured the post-PCI troponin at 24 hours post PCI as was performed in the present study. In our study we had less 2 vessel angioplasty (23% vs 44%) however 2 of our patients did have 3 vessel PCI compared to zero in the Selevanayagam study. In addition, the mean stent length in our study was longer at 34.9 vs 24mm. We did not specifically look into how many lesions were bifurcations and perhaps this may be significant. Apart from the

increased percentage of 2 vessel PCI there is no obvious reason for this discrepancy in measured troponin values. In our study 42 (79%) patients had a positive troponin post PCI compared to 14 (37%) in the Selevanayagam study. The immunoassay in our hospital had a lower limit of detectable troponin down to 0.04μg/L compared to 0.2μg/L which helps explain some of this difference however on closer analysis of the data this would only account for 3 cases in our study where the troponin I was less than 0.2 and greater than 0.04. Taking these patients out of the equation, we still had double the number of troponin releases post-PCI however our troponin elevations were far smaller than those obtained in Oxford. Our mean lesion length was 16.95mm (Median 15.22mm) compared to 15mm which may have contributed to the greater number of troponin releases and also our mean stent length was far higher (34.92 vs 24mm) which is also a significant difference. With longer lesions one may have expected our troponin elevations to be higher than that in the Selevanayagam study. Both laboratories used an immunoassay technique in estimating troponin levels however different analyzers were used. Our stented segment lengths greatly exceeded the lesion length with a median lesion length of 15.2mm and median stent length of 28mm. Reasons for this may included operator caution, plaque shift requiring further stenting and under estimating the lesion length using QCA.

We looked at a variety of QCA and haemodynamic parameters to see if any of them correlated with troponin levels. Interestingly degree of stenosis, area of stenosis and minimal lumen diameter provided no significant correlation. Number of stents and stent diameter did not provide significant correlations with troponin levels. Lesion length had the best correlation with post-PCI troponin levels ($r=0.6$, $p<0.0001$) and unsurprisingly therefore stent length was also significant in this regard ($r=0.37$, $p=0.02$). Surprisingly

only stent length was significantly related to the likelihood of procedure related irreversible injury in the Selevanayagam study while lesion length was not.(105)

5.8 Late Gadolinium Enhancement Post-PCI

We obtained a good level of agreement between our two observers on the mass of late gadolinium enhancement. The mass of LGE was measured in order to verify the findings of the aforementioned study by Selevanayagam et al. In addition we also measured the occurrence of new late gadolinium enhancement following CABG. We chose to use a similar gradient echo sequence on the same make and model of scanner and also administered the same dose of gadolinium to our patients as was done previously.(105) It has been known for some time that minor elevations in troponin and CK following PCI are common.(90-92;105) The mechanisms of this have already been discussed in detail in the introduction however minor side branch occlusion and distal embolisation are thought to be the main causes. Selevanayagam et al found a strong correlation between troponin I measurements and the mean mass of new LGE on their 24 hour and 7-8 month scans ($r=0.84$ and $r=0.71$ respectively). We failed to reproduce this at both 24 hours and 4 weeks post PCI. The r value at 24 hours was 0.25 with $p=0.07$ suggesting a non-significant trend with no apparent relationship at 4 weeks ($r=-0.19$, $p=0.2$). Potential explantations for this could be that some PCI's result in myocyte necrosis which is below the detection limits of LGE imaging. Alternatively there may be some troponin release following PCI which is due to reversible ischaemia rather than infarction. In this regard it is interesting to note that the troponin release we did see in our patients had no deleterious effects on ejection fraction which significantly increased following PCI. In the 4 week scans there may be a reduction in myocyte numbers due to necrosis leading to myocardial thinning. Finally our absolute troponin levels were much lower than that of the previous study and this may have obscured any relationship

between troponin and the extent of LGE. Selevanayagam et al did select a cohort of patients with particularly complex disease with over two thirds of lesions being graded B2 or higher by the AHA/ACC lesion criteria. In addition a higher percentage of their patients underwent two vessel PCI. We failed to find any correlation between the mass of LGE post-PCI and the number of vessels treated by PCI at either 24 hours or 4 weeks but the numbers of patients having 2 and 3 vessel angioplasty were small in comparison to the single vessel PCI group making it difficult to draw firm conclusions from this analysis.

A closer analysis of the PCI group showed that 10 patients at 24 hours had new LGE with a mean increase in mass of LGE of 1.24g. There was no difference in troponin I levels between those patients with new LGE and those without and no correlation was found between lesion length / stent length and new LGE. Similar results were also found at 4 weeks post-PCI. In our study the mean increase in mass of LGE was far less than that found in the previous study by Selvanayagam et al (6g compared to 1.24g) as was our troponin I levels as has already been discussed which may account for the differences in findings.

The mean difference in mass of LGE from pre-PCI to 4 weeks post PCI was -0.12g. This was thought to be due to myocardial thinning following previous infarction causing the appearance of less LGE. The standard deviation for this measurement was small at 0.8 and part of this result may be secondary measurement error.

5.9 Late Gadolinium Enhancement Post-CABG

Prior to CABG, 6 patients had evidence of LGE on their initial MRI scan however the mean mass of this was small at 1.47 ± 2.3g. Following CABG 10 patients had LGE with

a mean mass of 2.55 ± 3.5g with no significant reduction in ejection fraction. The median change in mass of LGE was only 0.11g following CABG. There was a trend towards developing more LGE post-CABG compared to post-PCI however the results did not reach statistical significance (p=0.07). This may be a reflection of the relatively small numbers of patients who required CABG in this study compared to those who had PCI performed. Steuer et al found late gadolinium enhancement in 18 (78%) of their 23 patients post CABG however no pre CABG contrast enhanced MRI scan had been performed.(95) Their patients did however have normal pre CABG ECG's and left ventricular function. It is difficult to be sure however that all of these patients requiring CABG did not have any undiagnosed areas of infarction. In our study 43% of subjects had LGE on their initial pre CABG MRI scan and 50% of patients in a larger study (n=60) comparing the occurrence of LGE pre and post on-pump and off-pump CABG had LGE pre-surgery.(142) All three of our studies show that new LGE develops following CABG. In the Selevanayagam study 40% of patients in total had evidence of new LGE post-CABG which is more in keeping with the results of our own smaller CABG subgroup where new LGE was confirmed in 43%. As shown on figure 4.90 two of our patients had quite significant increases in the mass of LGE with confirmed perioperative MIs. Unfortunately post-operative troponin measurements were not made as part of this study. Overall there is a trend towards the development of more LGE following CABG than PCI.

5.10 Resolution of Perfusion Defects Post-Revascularisation

One of the more interesting findings of the present study was that patients who achieved complete resolution of a pre-revascularisation perfusion defect had a significantly higher (but still <0.75) FFR value in the corresponding coronary artery pre-revascularisation compared to those patients who only achieved partial resolution of

their pre-revascularisation perfusion defect (p=0.01). There was no significant difference in FFR value between those patients who had partial or complete resolution of a perfusion defect post-PCI suggesting that perhaps residual perfusion defects could be due to either microcirculatory obstruction due to plaque embolisation or occlusion of small side braches as has been suggested in the previous literature.(94;106;109) Unfortunately we had very few patients with persistence of their perfusion defect post-revascularisation to gain any significant insight into this phenomenon. However, ultimately from a patient's perspective this was a good outcome.

5.11 Serum Caffeine Measurements and the Effects on Haemodynamics and Symptoms

Caffeine measurement in the setting of MRMPI imaging has not previously been reported. As documented in the introduction the majority of our knowledge in this area stems from nuclear perfusion imaging research. Some recent work has contradicted the belief that caffeine may affect the results of tests looking for reversible myocardial ischaemia.(79;80) There is good evidence from the nuclear perfusion work that a period of abstention from caffeine prior to stress testing with adenosine / dipyridamole is wise. Some research has suggested that 12 hours was too short a period and perhaps 24 hours would be more appropriate.(81;82;84) In our study we asked patients to abstain from all methylxanthines for 24 hours prior to MRMPI on the basis of this preceding work. This was reinforced by a telephone call on the day prior to scanning to remind patients of this rule. This was in an attempt to reduce the number of false negative scans in our study to determine the true accuracy of MRMPI for the diagnosis of reversible myocardial ischaemia. Of the 220 scans performed in 101 patients in our study, 29 (13.2%) had detectable caffeine levels >1mg/L. This is a higher proportion than that found by Zheng et al in which their 36 patients all had levels less than 0.8mg/L.(84) This study

contained only a fraction of the number of analyses that was performed in our research. Jacobson et al found detectable caffeine levels in the range of 0.1 to 5.0mg/L in 40% of their 86 patients undergoing thallium-201 myocardial perfusion scintigraphy.(81) Their immunoassay technique was more sensitive than the one used in our study accounting for the higher number of detectable levels. Our median level was 1.33mg/L however one patient's level was exceptionally high at 6.49mg/L despite claiming to have adhered to the period of abstinence. In those patients with detectable caffeine levels the maximum stress heart rate achieved during the adenosine infusion was significantly lower than those with undetectable levels (p=0.02) There was also a trend to a higher resting systolic BP in the caffeine detectable group (p=0.09). There was however no significant difference in the change in heart rate, systolic BP and diastolic BP between those patients with and without detectable caffeine. This is similar to the findings of Jacobson et al who also chose a 1.0mg/L cut-off for their analysis.(81) Majd-Ardekani et al in 2000 also failed to find significant differences in haemodynamic parameters after 12 hours of abstention. This study chose to use a higher cut-off of 2.9mg/L to compare their haemodynamic measurements.(82) We also looked at the occurrence of symptoms during the adenosine stress as a marker of hyperaemia. A higher proportion of patients in the caffeine detected group experienced absolutely no symptoms with the adenosine infusion however this did not reach statistical significance (14% vs 6%, p=0.09). Examining individual symptoms revealed significantly less flushing in the caffeine detected group (p=0.03) and a non-significant trend to less chest pain and headache. A significant difference in the occurrence of symptoms was found in the Majd-Ardekani study where only 12 hours of abstention was adhered to and higher caffeine levels were recorded. Interestingly the 5 patients who were labelled as non-responders to the intravenous adenosine infusion as on the basis of symptoms experienced and haemodynamic response all had serum caffeine levels less than 1mg/L.

This interesting finding raises the possibility of these patients having not been given enough adenosine to induce maximal hyperaemia or having high levels of another methylxanthine which was not measured in this study. This section of the study complements the nuclear perfusion literature that already exists in that a 24 hour abstention from caffeine is necessary as a minimum in order to achieve low caffeine levels in a high proportion of patients (<1mg/L). The significantly lower stress heart rate in those caffeine detected patients and the trend towards less symptoms is suggestive of less complete maximal hyperaemia and therefore perhaps we should consider a slightly longer period of caffeine abstention. However our non-responders all had levels less than 1mg/L and therefore other compounds may be responsible. Perhaps further research should be conducted measuring levels of theobromine and theophyline which are also commonly found in our diets as well.

6 Conclusion

In conclusion, this is one of the largest studies performed to assess the clinical utility of MRMPI in the diagnosis of significant coronary artery disease and is certainly the largest study which has chosen FFR as a physiological gold standard. Our data suggest that previous studies have underestimated the diagnostic accuracy of MRMPI where a non-invasive gold standard, mainly QCA, has been used. MRMPI using gadolinium is a very accurate technique for the non-invasive diagnosis of significant coronary artery disease.

The interobserver variability is good between observers for both qualitative and semi-quantitative analysis of MPRI.

False positive MRMPI scans are not due to microvascular disease as assessed by the invasive measurements of CFR and the index of microcirculatory resistance (IMR). In our study a substantial proportion of our false positive may in fact have been true positives with FFR values in the grey zone.

Qualitative analysis of MRMPI is unable to detect isolated microcirculatory disease as defined by an FFR>0.8 and a CFR<2.0.

A small troponin release is common post PCI and is related to the length of the lesion being treated and the length of stent deployed to treat the lesion. Small troponin values

do not accurately correlate with the occurrence of new late gadolinium enhancement as has been shown in previous studies of more complex coronary disease and larger troponin values. The troponin elevations in the present study had no adverse effects on left ventricular function. In fact there was a significant increase in ejection fraction at 24 hours.

CABG did result in a trend towards more new late gadolinium enhancement and no significant improvement in left ventricular function was noted when comparing pre and post operative MRI scans. Post-operative complications were common in the CABG group of patients.

Abstaining from caffeine for 24 hours pre-adenosine stress MRI resulted in the majority of patients having undetectable caffeine levels. However some of the symptoms associated with adenosine are less in those with detectable caffeine and less tachycardia is experienced, suggesting that perhaps a longer period of abstention should be considered. Interestingly our 5 patients who failed to develop the usual symptoms and haemodynamics during the adenosine infusion (non-responders) all had undetectable caffeine levels making the relationship between adenosine stress physiology and caffeine levels a complex one. This raises the possibility that other methylxanthines play a role in this process.

Further research is required in the development of faster MRMPI pulse sequences with better spatial resolution. In order to expand the availability of use of MRMPI the development of larger bore and open topped scanners will minimise claustrophobia

which remains a limitation. New stress agents are being developed and need tested in MRMPI imaging. Follow-up data on patients with new late gadolinium enhancement post-PCI needs to be obtained to ensure that this is not relevant in causing future arrhythmias. Measurements of the other methylxanthines in studies using adenosine stress would be useful in trying to determine the cause of adenosine non-responders in patients with undetectable caffeine. Good semi quantitative analysis remains time consuming and further development of reliable software would be welcomed by the cardiac MR community. This would lead to more patients having this method of assessment performed as opposed to a purely qualitative assessment. Work is currently ongoing in many of these areas which will expand the appeal and use of MRMPI. This technique may eventually replace nuclear perfusion imaging for the diagnosis of myocardial ischaemia.

7 References

(1) Nandalur KR, Dwamena BA, Choudhri AF, Nandalur MR, Carlos RC. Diagnostic performance of stress cardiac magnetic resonance imaging in the detection of coronary artery disease: a meta-analysis. J Am Coll Cardiol 2007; 50(14):1343-1353.

(2) White CW, Wright CB, Doty DB. Does visual interpretation of the coronary arteriogram predict the physiologic importance of a coronary stenosis? New Eng J Med 1984; 310(13):819-824.

(3) Bech GJ, De Bruyne B, Pijls NH, de Muinck ED, Hoorntje JC, Escaned J et al. Fractional flow reserve to determine the appropriateness of angioplasty in moderate coronary stenosis: a randomized trial. Circ 2001; 103(24):2928-2934.

(4) NHS National Services Scotland.Information and Statistics Division. Coronary Heart Disease. 30-10-2007.

(5) Leal J, Luengo-Fernandez R, Gray A, Petersen S, Rayner M. Economic burden of cardiovascular diseases in the enlarged European Union. Eur Heart J 2006; 27(13):1610-1619.

(6) Ashley EA, Myers J, Froelicher V. Exercise testing in clinical medicine. Lancet 2000; 356(9241):1592-1597.

(7) Underwood SR, Anagnostopoulos C, Cerqueira M, Ell PJ, Flint EJ, Harbinson M et al. Myocardial perfusion scintigraphy: the evidence. Eur J Nucl Med Mol Imaging 2004; 31(2):261-291.

(8) Moir S, Haluska BA, Jenkins C, Fathi R, Marwick TH. Incremental benefit of myocardial contrast to combined dipyridamole- exercise stress echocardiography for the assessment of coronary artery disease. 2004; 110(9):1108-1113.

(9) Donnelly PM, Higginson JD, Hanley PD. Multidetector CT coronary angiography: have we found the holy grail of non-invasive coronary imaging? Heart 2005; 91(11):1385-1388.

(10) Cerqueira MD, Weissman NJ, Dilsizian V, Jacobs AK, Kaul S, Laskey WK et al. Standardized myocardial sementation and nomenclature for tomographic imaging of the heart: A Statement for Healthcare Professionals from the Cardiac Imaging Committee of the Council on Clinical Cardiology of the American Heart Association. Circ 2002; 105(4):539-542.

(11) Eichenberger AC, Schuiki E, Kochli VD, Amann FW, McKinnon GC, Von Schulthess GK. Ischemic heart disease: assessment with gadolinium-enhanced ultrafast MR imaging and dipyridamole stress. J Magn Reson Imaging 1994; 4(3):425-431.

(12) Keijer JT, Van Rossum AC, Van Eenige MJ, Bax JJ, Visser FC, Teule JJ et al. Magnetic resonance imaging of regional myocardial perfusion in patients with single-vessel coronary artery disease: Quantitative comparison with 201Thallium-SPECT and coronary angiography. J Magn Res Imag 2000; 11(6):607-615.

(13) Al Saadi N, Nagel E, Gross M, Bornstedt A, Schnackenburg B, Klein C et al. Noninvasive detection of myocardial ischemia from perfusion reserve based on cardiovascular magnetic resonance. Circ 2000; 101(12):1379-1383.

(14) Schwitter J, Nanz D, Kneifel S, Bertschinger K, Buchi M, Knusel PR et al. Assessment of myocardial perfusion in coronary artery disease by magnetic resonance: A comparison with positron emission tomography and coronary angiography. Circ 2001; 103(18):2230-2235.

(15) Bertschinger KM, Nanz D, Buechi M, Luescher TF, Marincek B, Von Schulthess GK et al. Magnetic resonance myocardial first-pass perfusion imaging: Parameter optimization for signal response and cardiac coverage. J Magn Res Imag 2001; 14(5):556-562.

(16) Ibrahim T, Nekolla SG, Schreiber K, Odaka K, Volz S, Mehilli J et al. Assessment of coronary flow reserve: Comparison between contrast-enhanced magnetic resonance imaging and positron emission tomography. J Am Coll Cardiol 2002; 39(5):864-870.

(17) Nagel E, Klein C, Paetsch I, Hettwer S, Schnackenburg B, Wegscheider K et al. Magnetic resonance perfusion measurements for the noninvasive detection of coronary artery disease. Circ 2003; 108(4):432-437.

(18) Ishida N, Sakuma H, Motoyasu M, Okinaka T, Isaka N, Nakano T et al. Noninfarcted myocardium: Correlation between dynamic first-pass contrast-enhanced

myocardial MR imaging and quantitative coronary angiography. Radiol 2003; 229(1):209-216.

(19) Plein S, Greenwood JP, Ridgway JP, Cranny G, Ball SG, Sivananthan MU. Assessment of non-ST-segment elevation acute coronary syndromes with cardiac magnetic resonance imaging. J Am Coll Cardiol 2004; 44(11):2173-2181.

(20) Paetsch I, Jahnke C, Wahl A, Gebker R, Neuss M, Fleck E et al. Comparison of dobutamine stress magnetic resonance, adenosine stress magnetic resonance, and adenosine stress magnetic resonance perfusion. Circ 2004; 110(7):835-842.

(21) Takase B, Nagata M, Kihara T, Kameyawa A, Noya K, Matsui T et al. Whole-heart dipyridamole stress first-pass myocardial perfusion MRI for the detection of coronary artery disease. Jpn Heart J 2004; 45(3):475-486.

(22) Wolff SD, Schwitter J, Coulden R, Friedrich MG, Bluemke DA, Biederman RW et al. Myocardial first-pass perfusion magnetic resonance imaging: A multicenter dose-ranging study. Circ 2004; 110(6):732-737.

(23) Giang TH, Nanz D, Coulden R, Friedrich M, Graves M, Al Saadi N et al. Detection of coronary artery disease by magnetic resonance myocardial perfusion imaging with various contrast medium doses: First european multi-centre experience. Eur Heart J 2004; 25(18):1657-1665.

(24) Ishida M, Sakuma H, Kato N, Ishida N, Kitagawa K, Shimono T et al. Contrast-enhanced MR Imaging for evaluation of coronary artery disease before elective repair of aortic aneurysm. Radiol 2005; 237(2):458-464.

(25) Plein S, Radjenovic A, Ridgway JP, Barmby D, Greenwood JP, Ball SG et al. Coronary artery disease: myocardial perfusion MR imaging with sensitivity encoding versus conventional angiography. Radiol 2005; 235(2):423-430.

(26) Sakuma H, Suzawa N, Ichikawa Y, Makino K, Hirano T, Kitagawa K et al. Diagnostic accuracy of stress first-pass contrast-enhanced myocardial perfusion MRI compared with stress myocardial perfusion scintigraphy. Am J Roentgenol 2005; 185(1):95-102.

(27) Fenchel M, Helber U, Kramer U, Stauder NI, Franow A, Claussen CD et al. Detection of regional myocardial perfusion deficit using rest and stress perfusion MRI: a feasibility study. Am J Roentgenol 2005; 185(3):627-635.

(28) Klem I, Heitner JF, Shah DJ, Sketch MH, Jr., Behar V, Weinsaft J et al. Improved detection of coronary artery disease by stress perfusion cardiovascular magnetic resonance with the use of delayed enhancement infarction imaging. J Am Coll Cardiol 2006; 47(8):1630-1638.

(29) Cury RC, Cattani CA, Gabure LA, Racy DJ, de Gois JM, Siebert U et al. Diagnostic performance of stress perfusion and delayed-enhancement MR imaging in patients with coronary artery disease. Radiol 2006; 240(1):39-45.

(30) Rieber J, Huber A, Erhard I, Mueller S, Schweyer M, Koenig A et al. Cardiac magnetic resonance perfusion imaging for the functional assessment of coronary artery disease: a comparison with coronary angiography and fractional flow reserve. Eur Heart J 2006; 27(12):1465-1471.

(31) Futamatsu H, Wilke N, Klassen C, Shoemaker S, Angiolillo DJ, Siuciak A et al. Evaluation of cardiac magnetic resonance imaging parameters to detect anatomically and hemodynamically significant coronary artery disease. Am Heart J 2007; 154(2):298-305.

(32) Merkle N, Wohrle J, Grebe O, Nusser T, Kunze M, Kestler HA et al. Assessment of myocardial perfusion for detection of coronary artery stenoses by steady-state, free-precession magnetic resonance first-pass imaging. Heart 2007; 93(11):1381-1385.

(33) Costa MA, Shoemaker S, Futamatsu H, Klassen C, Angiolillo DJ, Nguyen M et al. Quantitative magnetic resonance perfusion imaging detects anatomic and physiologic coronary artery disease as measured by coronary angiography and fractional flow reserve. J Am Coll Cardiol 2007; 50(6):514-522.

(34) Barmeyer AA, Stork A, Muellerleile K, Tiburtius C, Schofer AK, Heitzer TA et al. Contrast-enhanced cardiac MR imaging in the detection of reduced coronary flow velocity reserve. Radiol 2007; 243(2):377-385.

(35) Kuhl HP, Katoh M, Buhr C, Krombach GA, Hoffmann R, Rassaf T et al. Comparison of magnetic resonance perfusion imaging versus invasive fractional flow

reserve for assessment of the hemodynamic significance of epicardial coronary artery stenosis. Am J Cardiol 2007; 99(8):1090-1095.

(36) De Bruyne B, Baudhuin T, Melin JA, Pijls NHJ, Sys SU, Bol A et al. Coronary flow reserve calculated from pressure measurements in humans: Validation with positron emission tomography. Circ 1994; 89(3):1013-1022.

(37) Balachandran KP, Berry C, Norrie J, Vallance BD, Malekian M, Gilbert TJ et al. Relation between coronary pressure derived collateral flow, TIMI myocardial perfusion grade and outcome in left ventricular function following rescue percutaneous coronary intervention for failed thrombolysis in acute myocardial infarction. Heart 2004; 90(12):1450-1454.

(38) Pijls NHJ, Van Gelder BM, Van der Voort PM, Peels KM, Bracke FALE, Bonnier HJRM et al. Fractional Flow Reserve: A Useful Index to Evaluate the Influence of an Epicardial Coronary Stenosis on Myocardial Blood Flow. Circ 1995; 92(11):3183-3193.

(39) Pijls NHJ, De Bruyne B, Peels K, Van Der Voort PH, Bonner HJRM, Bartunek J et al. Measurement of fractional flow reserve to assess the functional severity of coronary-artery stenoses. New Eng J Med 1996; 334(26):1703-1708.

(40) Koenig SH, Spiller M, Brown RD, III, Wolf GL. Relaxation of water protons in the intra- and extracellular regions of blood containing Gd(DTPA). Magn Reson Med 1986; 3(5):791-795.

(41) Gatehouse PD, Elkington AG, Ablitt NA, Yang G-Z, Pennell DJ, Firmin DN. Accurate assessment of the arterial input function during high-dose myocardial perfusion cardiovascular magnetic resonance. J Magn Res Imag 2004; 20(1):39-45.

(42) Pennell DJ. Cardiovascular magnetic resonance and the role of adenosine pharmacologic stress. Am J Cardiol 2004; 94(2 SUPPL. 1):26D-32D.

(43) Di Bella EV, Parker DL, Sinusas AJ. On the dark rim artifact in dynamic contrast-enhanced MRI myocardial perfusion studies. Magn Reson Med 2005; 54(5):1295-1299.

(44) Kraitchman DL, Wilke N, Hexeberg E, Jerosch-Herold M, Wang Y, Parrish TB et al. Myocardial perfusion and function in dogs with moderate coronary stenosis. Magn Reson Med 1996; 35(5):771-780.

(45) Keijer JT, Van Rossum AC, Van Eenige MJ, Karreman AJP, Hofman MBM, Valk J et al. Semiquantitation of regional myocardial blood flow in normal human subjects by first-pass magnetic resonance imaging. Am Heart J 1995; 130(4):893-901.

(46) Wilke N, Jerosch-Herold M, Wang Y, Huang Y, Christensen BV, Stillman AE et al. Myocardial perfusion reserve: Assessment with multisection, quantitative, first-pass MR imaging. Radiol 1997; 204(2):373-384.

(47) Jerosch-Herold M, Wilke N, Stillman AE, Wilson RF. Magnetic resonance quantification of the myocardial perfusion reserve with a Fermi function model for constrained deconvolution. Med Phys 1998; 25(1):73-84.

(48) McGeoch RJ, Oldroyd KG. Pharmacological options for inducing maximal hyperaemia during studies of coronary physiology. Catheter Cardiovasc Interv 2008; 71(2):198-204.

(49) Pijls NHJ, Van Gelder B, Van d, V, Peels K, Bracke FALE, Bonnier HJRM et al. Fractional flow reserve: A useful index to evaluate the influence of an epicardial coronary stenosis on myocardial blood flow. Circ 1995; 92(11):3183-3193.

(50) Pijls NH, De Bruyne B, Bech GJ, Liistro F, Heyndrickx GR, Bonnier HJ et al. Coronary pressure measurement to assess the hemodynamic significance of serial stenoses within one coronary artery: validation in humans. Circ 2000; 102(19):2371-2377.

(51) De Bruyne B, Bartunek J, Sys SU, Pijls NHJ, Heyndrickx GR, Wijns W. Simultaneous coronary pressure and flow velocity measurements in humans: Feasibility, reproducibility, and hemodynamic dependence of coronary flow velocity reserve, hyperemic flow versus pressure slope index, and fractional flow reserve. Circ 1996; 94(8):1842-1849.

(52) De Bruyne B, Pijls NHJ, Bartunek J, Kulecki K, Bech J-W, De Winter H et al. Fractional flow reserve in patients with prior myocardial infarction. Circ 2001; 104(2):157-162.

(53) Bech GJW, Pijls NHJ, De Bruyne B, Peels KH, Michels HR, Bonnier HJRM et al. Usefulness of fractional flow reserve to predict clinical outcome after balloon angioplasty. Circ 1999; 99(7):883-888.

(54) Bech GJW, De Bruyne B, Bonnier HJRM, Bartunek J, Wijns W, Peels K et al. Long-term follow-up after deferral of percutaneous transluminal coronary angioplasty of intermediate stenosis on the basis of coronary pressure measurement. J Am Coll Cardiol 1998; 31(4):841-847.

(55) Pijls NH, van Schaardenburgh P, Manoharan G, Boersma E, Bech JW, van't Veer M et al. Percutaneous coronary intervention of functionally nonsignificant stenosis: 5-year follow-up of the DEFER Study. J Am Coll Cardiol 2007; 49(21):2105-2111.

(56) Pijls NHJ, Klauss V, Siebert U, Powers E, Takazawa K, Fearon WF et al. Coronary pressure measurement after stenting predicts adverse events at follow-up: A multicenter registry. Circ 2002; 105(25):2950-2954.

(57) Pijls NH. Optimum guidance of complex PCI by coronary pressure measurement. Heart 2004; 90(9):1085-1093.

(58) De Bruyne B, Pijls NHJ, Smith L, Wievegg M, Heyndrickx GR. Coronary thermodilution to assess flow reserve experimental validation. Circ 2001; 104(17):2003-2006.

(59) Pijls NHJ, De Bruyne B, Smith L, Aarnoudse W, Barbato E, Bartunek J et al. Coronary thermodilution to assess flow reserve: Validation in humans. Circ 2002; 105(21):2482-2486.

(60) Barbato E, Aarnoudse W, Aengevaeren WR, Werner G, Klauss V, Bojara W et al. Validation of coronary flow reserve measurements by thermodilution in clinical practice. Eur Heart J 2004; 25(3):219-223.

(61) Akasaka T, Yamamuro A, Kamiyama N, Koyama Y, Akiyama M, Watanabe N et al. Assessment of coronary flow reserve by coronary pressure measurement: comparison with flow- or velocity-derived coronary flow reserve. J Am Coll Cardiol 2003; 41(9):1554-1560.

(62) Fearon WF, Farouque HMO, Balsam LB, Cooke DT, Robbins RC, Fitzgerald PJ et al. Comparison of Coronary Thermodilution and Doppler Velocity for Assessing Coronary Flow Reserve. Circ 2003; 108(18):2198-2200.

(63) Albertal M, Voskuil M, Piek JJ, De Bruyne B, Van Langenhove G, Kay PI et al. Coronary flow velocity reserve after percutaneous interventions is predictive of periprocedural outcome. Circulation 2002; 105(13):1573-1578.

(64) Zbinden R, Zbinden S, Billinger M, Windecker S, Meier B, Seiler C. Influence of diabetes mellitus on coronary collateral flow: an answer to an old controversy. Heart 2005; 91(10):1289-1293.

(65) Fearon WF, Balsam LB, Farouque HM, Caffarelli AD, Robbins RC, Fitzgerald PJ et al. Novel index for invasively assessing the coronary microcirculation. Circ 2003; 107(25):3129-3132.

(66) Aarnoudse W, van den BP, Van D, V, Geven M, Rutten M, Van Turnhout M et al. Myocardial resistance assessed by guidewire-based pressure-temperature measurement: in vitro validation. Catheter Cardiovasc Interv 2004; 62(1):56-63.

(67) Fearon WF, Aarnoudse W, Pijls NHJ, De Bruyne B, Balsam LB, Cooke DT et al. Microvascular resistance is not influenced by epicardial coronary artery stenosis severity: Experimental validation. Circ 2004; 109(19):2269-2272.

(68) Aarnoudse W, Fearon WF, Manoharan G, Geven M, Van D, V, Rutten M et al. Epicardial stenosis severity does not affect minimal microcirculatory resistance. Circ 2004; 110(15):2137-2142.

(69) Fearon WF, Shah M, Ng M, Brinton T, Wilson A, Tremmel JA et al. Predictive value of the index of microcirculatory resistance in patients with ST-segment elevation myocardial infarction. J Am Coll Cardiol 2008; 51(5):560-565.

(70) Murry CE, Jennings RB, Reimer KA. Preconditioning with ischemia: a delay of lethal cell injury in ischemic myocardium. Circ 1986; 74(5):1124-1136.

(71) Marzilli M, Orsini E, Marraccini P, Testa R. Beneficial effects of intracoronary adenosine as an adjunct to primary angioplasty in acute myocardial infarction. Circ 2000; 101(18):2154-2159.

(72) Mahaffey KW, Puma JA, Barbagelata NA, DiCarli MF, Leesar MA, Browne KF et al. Adenosine as an adjunct to thrombolytic therapy for acute myocardial infarction: results of a multicenter, randomized, placebo-controlled trial: the Acute Myocardial

Infarction STudy of ADenosine (AMISTAD) trial. J Am Coll Cardiol 1999; 34(6):1711-1720.

(73) Simonetti O, Cirioni O, Goteri G, Ghiselli R, Kamysz W, Kamysz E et al. Temporin A is effective in MRSA-infected wounds through bactericidal activity and acceleration of wound repair in a murine model. Peptides 2008; 29(4):520-528.

(74) Cerqueira MD. The future of pharmacologic stress: Selective A2a adenosine receptor agonists. Am J Cardiol 2004; 94(2 SUPPL. 1):33D-42D.

(75) Lieu HD, Shryock JC, von Mering GO, Gordi T, Blackburn B, Olmsted AW et al. Regadenoson, a selective A2A adenosine receptor agonist, causes dose-dependent increases in coronary blood flow velocity in humans. J Nucl Cardiol 2007; 14(4):514-520.

(76) Smits P, Aengevaeren WRM, Corstens FHM, Thien T. Caffeine reduces dipyridamole-induced myocardial ischemia. J Nucl Med 1989; 30(10):1723-1726.

(77) Bottcher M, Czernin J, Sun KT, Phelps ME, Schelbert HR. Effect of caffeine on myocardial blood flow at rest and during pharmacological vasodilation. J Nucl Med 1995; 36(11):2016-2021.

(78) Kubo S, Tadamura E, Toyoda H, Mamede M, Yamamuro M, Magata Y et al. Effect of caffeine intake on myocardial hyperemic flow induced by adenosine triphosphate and dipyridamole. J Nucl Med 2004; 45(5):730-738.

(79) Aqel RA, Zoghbi GJ, Trimm JR, Baldwin SA, Iskandrian AE. Effect of caffeine administered intravenously on intracoronary- administered adenosine-induced coronary hemodynamics in patients with coronary artery disease. Am J Cardiol 2004; 93(3):343-346.

(80) Zoghbi GJ, Htay T, Aqel R, Blackmon L, Heo J, Iskandrian AE. Effect of caffeine on ischemia detection by adenosine single-photon emission computed tomography perfusion imaging. J Am Coll Cardiol 2006; 47(11):2296-2302.

(81) Jacobson AF, Cerqueira MD, Raisys V, Shattuc S. Serum caffeine levels after 24 hours of caffeine abstention: observations on clinical patients undergoing myocardial perfusion imaging with dipyridamole or adenosine. Eur J Nucl Med 1994; 21(1):23-26.

(82) Majd-Ardekani J, Clowes P, Menash-Bonsu V, Nunan TO. Time for abstention from caffeine before an adenosine myocardial perfusion scan. Nucl Med Commun 2000; 21(4):361-364.

(83) Smits P, Lenders JW, Thien T. Caffeine and theophylline attenuate adenosine-induced vasodilation in humans. Clin Pharmacol Ther 1990; 48(4):410-418.

(84) Zheng XM, Williams RC. Serum caffeine levels after 24-hour abstention: clinical implications on dipyridamole (201)Tl myocardial perfusion imaging. J Nucl Med Technol 2002; 30(3):123-127.

(85) Hurwitz R, Lyons K, Taketa R. Adenosine challenge and boost protocols: new tools for myocardial perfusion imaging. Clin Nucl Med 1999; 24(2):92-93.

(86) Lopez-Garcia E, van Dam RM, Willett WC, Rimm EB, Manson JE, Stampfer MJ et al. Coffee consumption and coronary heart disease in men and women: a prospective cohort study. Circ 2006; 113(17):2045-2053.

(87) Kim RJ, Judd RM, Chen EL, Fieno DS, Parrish TB, Lima JA. Relationship of elevated 23Na magnetic resonance image intensity to infarct size after acute reperfused myocardial infarction. Circ 1999; 100(2):185-192.

(88) Kim RJ, Fieno DS, Parrish TB, Harris K, Chen EL, Simonetti O et al. Relationship of MRI delayed contrast enhancement to irreversible injury, infarct age, and contractile function. Circ 1999; 100(19):1992-2002.

(89) Kim RJ, Wu E, Rafael A, Chen EL, Parker MA, Simonetti O et al. The use of contrast-enhanced magnetic resonance imaging to identify reversible myocardial dysfunction. N Engl J Med 2000; 343(20):1445-1453.

(90) Oh JK, Shub C, Ilstrup DM, Reeder GS. Creatine kinase release after successful percutaneous transluminal coronary angioplasty. Am Heart J 1985; 109(6):1225-1231.

(91) Pauletto P, Piccolo D, Scannapieco G, Vescovo G, Zaninotto M, Corbara F et al. Changes in myoglobin, creatine kinase and creatine kinase-MB after percutaneous transluminal coronary angioplasty for stable angina pectoris. Am J Cardiol 1987; 59(9):999-1000.

(92) Harrington RA, Lincoff AM, Califf RM, Holmes DR, Jr., Berdan LG, O'Hanesian MA et al. Characteristics and consequences of myocardial infarction after

percutaneous coronary intervention: insights from the Coronary Angioplasty Versus Excisional Atherectomy Trial (CAVEAT). J Am Coll Cardiol 1995; 25(7):1693-1699.

(93) Ricciardi MJ, Wu E, Davidson CJ, Choi KM, Klocke FJ, Bonow RO et al. Visualization of discrete microinfarction after percutaneous coronary intervention associated with mild creatine kinase-MB elevation. Circ 2001; 103(23):2780-2783.

(94) Choi JW, Gibson CM, Murphy SA, Davidson CJ, Kim RJ, Ricciardi MJ. Myonecrosis following stent placement: association between impaired TIMI myocardial perfusion grade and MRI visualization of microinfarction. Catheter Cardiovasc Interv 2004; 61(4):472-476.

(95) Steuer J, Bjerner T, Duvernoy O, Jideus L, Johansson L, Ahlstrom H et al. Visualisation and quantification of peri-operative myocardial infarction after coronary artery bypass surgery with contrast-enhanced magnetic resonance imaging. Eur Heart J 2004; 25(15):1293-1299.

(96) Costa MA, Carere RG, Lichtenstein SV, Foley DP, de V, V, Lindenboom W et al. Incidence, predictors, and significance of abnormal cardiac enzyme rise in patients treated with bypass surgery in the arterial revascularization therapies study (ARTS). Circ 2001; 104(22):2689-2693.

(97) Brener SJ, Lytle BW, Schneider JP, Ellis SG, Topol EJ. Association between CK-MB elevation after percutaneous or surgical revascularization and three-year mortality. J Am Coll Cardiol 2002; 40(11):1961-1967.

(98) Januzzi JL, Lewandrowski K, MacGillivray TE, Newell JB, Kathiresan S, Servoss SJ et al. A comparison of cardiac troponin T and creatine kinase-MB for patient evaluation after cardiac surgery. J Am Coll Cardiol 2002; 39(9):1518-1523.

(99) Steuer J, Horte LG, Lindahl B, Stahle E. Impact of perioperative myocardial injury on early and long-term outcome after coronary artery bypass grafting. Eur Heart J 2002; 23(15):1219-1227.

(100) Califf RM, Abdelmeguid AE, Kuntz RE, Popma JJ, Davidson CJ, Cohen EA et al. Myonecrosis after revascularization procedures. J Am Coll Cardiol 1998; 31(2):241-251.

(101) Ravkilde J, Nissen H, Mickley H, Andersen PE, Thayssen P, Horder M. Cardiac troponin T and CK-MB mass release after visually successful percutaneous transluminal coronary angioplasty in stable angina pectoris. Am Heart J 1994; 127(1):13-20.

(102) Johansen O, Brekke M, Stromme JH, Valen V, Seljeflot I, Skjaeggestad O et al. Myocardial damage during percutaneous transluminal coronary angioplasty as evidenced by troponin T measurements. Eur Heart J 1998; 19(1):112-117.

(103) Nageh T, Sherwood RA, Harris BM, Byrne JA, Thomas MR. Cardiac troponin T and I and creatine kinase-MB as markers of myocardial injury and predictors of outcome following percutaneous coronary intervention. Int J Cardiol 2003; 92(2-3):285-293.

(104) Cantor WJ, Newby LK, Christenson RH, Tuttle RH, Hasselblad V, Armstrong PW et al. Prognostic significance of elevated troponin I after percutaneous coronary intervention. J Am Coll Cardiol 2002; 39(11):1738-1744.

(105) Selvanayagam JB, Porto I, Channon K, Petersen SE, Francis JM, Neubauer S et al. Troponin elevation after percutaneous coronary intervention directly represents the extent of irreversible myocardial injury: insights from cardiovascular magnetic resonance imaging. Circ 2005; 111(8):1027-1032.

(106) Porto I, Selvanayagam JB, Van Gaal WJ, Prati F, Cheng A, Channon K et al. Plaque volume and occurrence and location of periprocedural myocardial necrosis after percutaneous coronary intervention: insights from delayed-enhancement magnetic resonance imaging, thrombolysis in myocardial infarction myocardial perfusion grade analysis, and intravascular ultrasound. Circ 2006; 114(7):662-669.

(107) Kwong RY, Chan AK, Brown KA, Chan CW, Reynolds HG, Tsang S et al. Impact of unrecognized myocardial scar detected by cardiac magnetic resonance imaging on event-free survival in patients presenting with signs or symptoms of coronary artery disease. Circ 2006; 113(23):2733-2743.

(108) Larose E. Below radar: contributions of cardiac magnetic resonance to the understanding of myonecrosis after percutaneous coronary intervention. Circ 2006; 114(7):620-622.

(109) Selvanayagam JB, Cheng AS, Jerosch-Herold M, Rahimi K, Porto I, van Gaal W et al. Effect of distal embolization on myocardial perfusion reserve after

percutaneous coronary intervention: a quantitative magnetic resonance perfusion study. Circ 2007; 116(13):1458-1464.

(110) Moreno-Romero JA, Segura S, Mascaro JM, Jr., Cowper SE, Julia M, Poch E et al. Nephrogenic systemic fibrosis: a case series suggesting gadolinium as a possible aetiological factor. Br J Dermatol 2007; 157(4):783-787.

(111) Broome DR. Nephrogenic systemic fibrosis associated with gadolinium based contrast agents: a summary of the medical literature reporting. Eur J Radiol 2008; 66(2):230-234.

(112) Canavese C, Mereu MC, Aime S, Lazzarich E, Fenoglio R, Quaglia M et al. Gadolinium-associated nephrogenic systemic fibrosis: the need for nephrologists' awareness. J Nephrol 2008; 21(3):324-336.

(113) Kurtkoti J, Snow T, Hiremagalur B. Gadolinium and nephrogenic systemic fibrosis: association or causation. Nephrology (Carlton) 2008; 13(3):235-241.

(114) Stratta P, Canavese C, Aime S. Gadolinium-enhanced magnetic resonance imaging, renal failure and nephrogenic systemic fibrosis/nephrogenic fibrosing dermopathy. Curr Med Chem 2008; 15(12):1229-1235.

(115) Barboriak DP, Padua AO, York GE, Macfall JR. Creation of DICOM--aware applications using ImageJ. J Digit Imaging 2005; 18(2):91-99.

(116) Jerosch-Herold M, Seethamraju RT, Swingen CM, Wilke NM, Stillman AE. Analysis of myocardial perfusion MRI. J Magn Reson Imag 2004; 19(6):758-770.

(117) Van Herck PL, Gavit L, Gorissen P, Wuyts FL, Claeys MJ, Bosmans JM et al. Quantitative coronary arteriography on digital flat-panel system. Catheter Cardiovasc Interv 2004; 63(2):192-200.

(118) Vanoverschelde JL, Wijns W, Depre C, Essamri B, Heyndrickx GR, Borgers M et al. Mechanisms of chronic regional postischemic dysfunction in humans. New insights from the study of noninfarcted collateral-dependent myocardium. Circ 1993; 87(5):1513-1523.

(119) Werner GS, Surber R, Ferrari M, Fritzenwanger M, Figulla HR. The functional reserve of collaterals supplying long-term chronic total coronary occlusions in patients without prior myocardial infarction. Eur Heart J 2006; 27(20):2406-2412.

(120) Werner GS, Fritzenwanger M, Prochnau D, Schwarz G, Ferrari M, Aarnoudse W et al. Determinants of coronary steal in chronic total coronary occlusions donor artery, collateral, and microvascular resistance. J Am Coll Cardiol 2006; 48(1):51-58.

(121) Tonino PA, De Bruyne B, Pijls NH, Siebert U, Ikeno F, Veer M et al. Fractional flow reserve versus angiography for guiding percutaneous coronary intervention. N Engl J Med 2009; 360(3):213-224.

(122) Lapeyre III AC, Goraya TY, Johnston DL, Gibbons RJ. The impact of caffeine on vasodilator stress perfusion studies. J Nucl Cardiol 2004; 11(4):506-511.

(123) Ou CN, Frawley VL, Ellis JM. Evaluation of the EMIT reagent system for measurement of caffeine with the EMIT Lab 5000 System and a centrifugal analyzer. Clin Chem 1984; 30(6):887-889.

(124) Miceli JN, Aravind MK, Ferrell WJ. Analysis of caffeine: comparison of the manual enzyme multiplied immunoassay (EMIT), automated EMIT, and high-performance liquid chromatography procedures. Ther Drug Monit 1984; 6(3):344-347.

(125) Zysset T, Wahllander A, Preisig R. Evaluation of caffeine plasma levels by an automated enzyme immunoassay (EMIT) in comparison with a high-performance liquid chromatographic method. Ther Drug Monit 1984; 6(3):348-354.

(126) Fearon WF, Tonino PA, De Bruyne B, Siebert U, Pijls NH. Rationale and design of the Fractional Flow Reserve versus Angiography for Multivessel Evaluation (FAME) study. Am Heart J 2007; 154(4):632-636.

(127) Pell JP, Haw S, Cobbe S, Newby DE, Pell AC, Fischbacher C et al. Smoke-free legislation and hospitalizations for acute coronary syndrome. N Engl J Med 2008; 359(5):482-491.

(128) Leesar MA, Abdul-Baki T, Akkus NI, Sharma A, Kannan T, Bolli R. Use of fractional flow reserve versus stress perfusion scintigraphy after unstable angina: Effect on duration of hospitalization, cost, procedural characteristics, and clinical outcome. J Am Coll Cardiol 2003; 41(7):1115-1121.

(129) Hjortdal VE, Emmertsen K, Stenbog E, Frund T, Schmidt MR, Kromann O et al. Effects of exercise and respiration on blood flow in total cavopulmonary connection: a real-time magnetic resonance flow study. Circ 2003; 108(10):1227-1231.

(130) Cheng CP, Herfkens RJ, Taylor CA. Abdominal aortic hemodynamic conditions in healthy subjects aged 50-70 at rest and during lower limb exercise: in vivo quantification using MRI. Atherosclerosis 2003; 168(2):323-331.

(131) Bellamy MF, Goodfellow J, Tweddel AC, Dunstan FD, Lewis MJ, Henderson AH. Syndrome X and endothelial dysfunction. Cardiovasc Res 1998; 40(2):410-417.

(132) Cannon RO, III, Epstein SE. "Microvascular angina" as a cause of chest pain with angiographically normal coronary arteries. Am J Cardiol 1988; 61(15):1338-1343.

(133) Panting JR, Gatehouse PD, Yang GZ, Grothues F, Firmin DN, Collins P et al. Abnormal subendocardial perfusion in cardiac syndrome X detected by cardiovascular magnetic resonance imaging. N Engl J Med 2002; 346(25):1948-1953.

(134) Berry C, Balachandran KP, L'Allier PL, Lesperance J, Bonan R, Oldroyd KG. Importance of collateral circulation in coronary heart disease. Eur Heart J 2007; 28(3):278-291.

(135) Maceira AM, Prasad SK, Khan M, Pennell DJ. Normalized left ventricular systolic and diastolic function by steady state free precession cardiovascular magnetic resonance. J Cardiovasc Magn Reson 2006; 8(3):417-426.

(136) Bondarenko O, Beek AM, Twisk JW, Visser CA, Van Rossum AC. Time course of functional recovery after revascularization of hibernating myocardium: a contrast-enhanced cardiovascular magnetic resonance study. Eur Heart J 2008; 29(16):2000-2005.

(137) Zellweger MJ, Tabacek G, Zutter AW, Weinbacher M, Cron TA, Muller-Brand J et al. Evidence for left ventricular remodeling after percutaneous coronary intervention: effect of percutaneous coronary intervention on left ventricular ejection fraction and volumes. Int J Cardiol 2004; 96(2):197-201.

(138) Semelka RC, Tomei E, Wagner S, Mayo J, Caputo G, O'Sullivan M et al. Interstudy reproducibility of dimensional and functional measurements between cine magnetic resonance studies in the morphologically abnormal left ventricle. Am Heart J 1990; 119(6):1367-1373.

(139) Semelka RC, Tomei E, Wagner S, Mayo J, Kondo C, Suzuki J et al. Normal left ventricular dimensions and function: interstudy reproducibility of measurements with cine MR imaging. Radiol 1990; 174(3 Pt 1):763-768.

(140) Finn JP, Nael K, Deshpande V, Ratib O, Laub G. Cardiac MR imaging: state of the technology. Radiol 2006; 241(2):338-354.

(141) Soliman Hamad MA, Tan ME, van Straten AH, van Zundert AA, Schonberger JP. Long-term results of coronary artery bypass grafting in patients with left ventricular dysfunction. Ann Thorac Surg 2008; 85(2):488-493.

(142) Selvanayagam JB, Petersen SE, Francis JM, Robson MD, Kardos A, Neubauer S et al. Effects of off-pump versus on-pump coronary surgery on reversible and irreversible myocardial injury: a randomized trial using cardiovascular magnetic resonance imaging and biochemical markers. Circ 2004; 109(3):345-350.

(143) Pegg TJ, Selvanayagam JB, Karamitsos TD, Arnold RJ, Francis JM, Neubauer S et al. Effects of off-pump versus on-pump coronary artery bypass grafting on early and late right ventricular function. Circ 2008; 117(17):2202-2210.

8 Appendices

8.1 Appendix 1 - Coronary Angiography and Perfusion MRI Caffeine Instructions

During your coronary angiogram and MRI scan we will be administering a medicine called adenosine which increases the blood flow to your heart. Adenosine is a naturally occurring substance and is already present in different forms in our bodies. Caffeine, which is present in a number of foods and beverages, can block the effects of adenosine and potentially lead to false results. We would therefore be grateful if you could abstain from caffeine containing foods and beverages for 24 hours before you attend for your tests. Things to avoid include:-

Coffee including decaffeinated

Tea including decaffeinated

Soft Drinks especially carbonated soda's eg. Coca-cola, Irn-Bru etc

High Energy Drinks containing guarana

Chocolate

Cocoa containing foods eg. Cake

Kola nuts

Over the counter drugs eg. Anadin, anadin extra

Cold and Flu Remedies

In you are unsure about the caffeine content of items please read the ingredients on the back of the packaging.

8.2 Appendix 2 – Technical Parameters of MRI Pulse Sequences

1. **Sagital, Coronal and Transaxial Localising Images**

   [TrueFISP; TE 1.7; TR 3.4; Flip Angle 60^{o}; Slice Thickness 6mm; FOV 276x340; Matrix 83x128]

2. **Transaxial HASTE Sequence – No Breath-hold**

   [TE 26; TR 700; Flip Angle 160^{o}; Slice Thickness 6mm; Slices 20; FOV 340x340; Matrix 151x256]

3. **2 Chamber Scout View**

   [TrueFISP; TE 1.7; TR 3.4; Flip Angle 60^{o}; Slice Thickness 6mm; FOV 276x340; Matrix 83x128; Slices 3]

4. **4 Chamber Scout View**

   [TrueFISP; TE 1.7; TR 3.4; Flip Angle 60^{o}; Slice Thickness 6mm; FOV 276x340; Matrix 83x128; Slices 3]

5. **Short Axis Scout Views**

   [TrueFISP; TE 1.7; TR 3.4; Flip Angle 60^{o}; Slice Thickness 6mm; FOV 276x340; Matrix 83x128; Slices 3]

6. **Vertical Long Axis Cine for 2 Chamber View**

   [TrueFISP; TE 1.57; TR 47.1(15 Segments); Flip Angle 60^{o}; Slice Thickness 8mm; FOV 276x340; Matrix 135x256; Distance Factor 20%; Phases 35]

7. **Horizontal Long Axis Cine for 4 Chamber View**

   [TrueFISP; TE 1.57; TR 47.1(15 Segments); Flip Angle 60^{o}; Slice Thickness 8mm; FOV 276x340; Matrix 135x256; Distance Factor 20%; Phases 35]

8. **Left Ventricular Outflow Tract Cine**

   [TrueFISP; TE 1.57; TR 47.1(15 Segments); Flip Angle 60^{o}; Slice Thickness 8mm; FOV 276x340; Matrix 135x256; Distance Factor 20%; Phases 35]

9. **Short Axis Cine Stack of LV Cavity from Base to Apex**

   [TrueFISP; TE 1.57; TR 47.1(15 Segments); Flip Angle 60^{o}; Slice Thickness 8mm; FOV 276x340; Matrix 135x256; Distance Factor 20%; Phases 35]

10. **1^{st} Pass Stress Perfusion Imaging**

    [TurboFLASH; TE 0.99; TR 173; TI 90; Flip Angle 8^{o}; Slice Thickness 8mm; Slices 3; FOV 213x340; Matrix 80x128; Spatial Resolution 2.7x2.7mm^2; Bandwidth 780Hz/pixel]

11. **Early Gadolinium Enhancement for Microvascular Obstruction**

    [Segmented TrueFISP; TE 15; TR 700; TI 440; Flip Angle 60^{o}; Slice Thickness 8mm; Slices 9; Distance Factor 25%; FOV 255x340; Matrix 96x256]

12. **Late Gadolinium for Delayed Enhancement Images**

    [TurboFLASH; TE 43; TR 1000; TI 320 (initially); Flip Angle 20^{o}; Slice Thickness 8mm; Slices 1; FOV 276x340; Matrix 125x256]

13. **1^{st} Pass Resting Perfusion Imaging**

    [TurboFLASH; TE 0.99; TR 173; TI 90; Flip Angle 8^{o}; Slice Thickness 8mm; Slices 3; FOV 213x340; Matrix 80x128; Spatial Resolution 2.7x2.7mm^2; Bandwidth 780Hz/pixel]

8.3 Appendix 3 – Adenosine Iinfusion Rate for MRMPI Scanning

120ML BAG OF ADENOSINE IN 0.9% SALINE (1MG/ML) INFUSION DURATION – 4 MINS

Weight (Kg)	**Infusion Rate (ml/min)**
40	5.6
50	7
60	8.4
70	9.8
80	11.2
90	12.6
100	14
110	15.4
120	16.8
130	18.2